Production of Seabird and Marine Mammal Distribution Models for the East of Scotland

November 2022

Scottish Government
Riaghaltas na h-Alba

Production of Seabird and Marine Mammal Distribution Models for the East of Scotland

Authors:

Paxton, C.G.M.[1], Waggitt, J.J.[2], Evans, P.G.H.[2,3], Miller, D.L.1, Burt, L[1]. and Chudzinska, M.E.[1]

Affiliations:

[1]Centre for Research into Ecological & Environmental Modelling, School of Mathematics & Statistics, University of St Andrews, St Andrews, Fife KY16 9LZ, Scotland

[2]School of Ocean Sciences, Bangor University, Menai Bridge, Isle of Anglesey LL59 5AB, Wales

[3]Sea Watch Foundation, Ewyn y Don, Bull Bay, Amlwch, Isle of Anglesey LL68 9SD, Wales

Report Code:CREEM-2021.06

Date: July 2022

Document Control

Please consider this document as uncontrolled copy when printed

Rev.	Date.	Reason for Issue.	Prepared by	Checked by
1	1/07/2022	Draft 1	CP	
2	25/07/2022	Draft 2	CP, PE	JW, MC
3	02/09/2022	Final 1	CP, PE, JW	MC
4	01/11/2022	Final 2	CP, PE, JW	MC

1. Executive Summary

The Scottish Government has an interest in monitoring the status of mobile marine megafauna especially with regard to the Marine Protected Area (MPA) network and offshore wind farm development. Knowledge of the spatial and temporal distribution and abundance of marine species is important in order for the Government to make evidence-based decisions regarding the status of these species and management of marine activities. This report describes temporal and spatial patterns of density for seabird and marine mammal species in the eastern waters of Scotland from digital aerial surveys undertaken by APEM Ltd. for Marine Scotland between February 2020 and March 2021.

Eleven bird species recorded sufficiently regularly within the surveys for modelling and abundance estimation included northern fulmar (*Fulmarus glacialis*), northern gannet (*Morus bassanus)*, great skua (*Stercorarius skua*), common gull (*Larus canus*), herring gull (*Larus argentatus*), great black-backed gull (*Larus marinus*), black-legged kittiwake (*Rissa tridactyla)*, common guillemot (*Uria aalge*), razorbill (*Alca torda)*, and Atlantic puffin (*Fratercula arctica*). Design-based estimates were obtained for abundance only for lesser black-backed gull (*Larus fuscus*) where a model could not be fitted.

There are four cetacean species of particular interest in this study due to their regular occurrence: minke whale (*Balaenoptera acutorostrata*), common dolphin (Delphinus delphis), white beaked dolphin (*Lagenorhynchus albirostris*) and harbour porpoise (*Phocoena phocoena)*. One species, common dolphin (*Delphinus delphis*) could not be modelled but designed based estimated were made. Other species such as killer whale (*Orcinus orca*), long-finned pilot whale (Globicephala melas), Atlantic white-sided dolphin (*Lagenorhynchus acutus*), Risso's dolphin (*Grampus griseus*), and humpback whale (*Megaptera novaeangliae*) do occur in the region on a regular basis but were identified too few times during the digital aerial surveys for their density distributions to be modelled. The number of individuals recorded within each species or species group per survey is given in Table 1.

Species/species group identifications were checked from a sample totalling c. 300 digital images, with emphasis on species with uncertain identification, species outside their normal range, and ones of similar appearance (see Appendix 1). Since many images could not be identified to species level, whilst some others were ascribed to a particular species when image resolution in our opinion was too poor for confident identification, in order to allocate species groups to individual species, and to improve the precision of estimates for some species with low sample sizes, an updated version of the MERP (Marine Ecosystems Research Programme) database was utilised in certain cases.

General additive mixed models were fitted separately to each species of interest. The response variable for these models was the number of animals detected on the surveys. The candidate explanatory variables associated with digital photos were location and environmental features (e.g. depth, seabed roughness, sea surface temperature (both mean and range), salinity (both mean and range), and stratification index).

For those seabird species with reasonable sample sizes, density and abundance estimates generally aligned well with estimates from previous published findings of earlier survey collations, taking account of recent status changes, where applicable. Estimates of abundance and density for cetacean species, on the other hand, tend to be much larger than from the SCANS survey. The reasons for the differences are not clear but may be partly due to corrections made for availability bias in this study.

The selected models were used to estimate abundance throughout the region of interest and to derive maps of estimated densities (numbers of individuals per km2) from each survey. Overall abundance estimates, and spatial and seasonal patterns of densities were compared with previously published results from analyses of larger survey datasets. For breeding seabirds, comparisons were made with colony counts, taking account of status changes recorded since the last published census (Seabird 2000) conducted between 1998-2002.

The limitations of using only digital aerial survey data are discussed. Recommendations for future monitoring include use of visual survey data, greater survey effort east of the Northern Isles, particularly Shetland, and during some critical periods, for example April to June when circumstances prevented coverage. The analysis is also based on data collected largely in a single calendar year (2020) and so may not be applicable to the longer term. With respect to seabirds, two

significant mortality events have occurred after the survey work was completed. The first of these was a large seabird wreck (affecting primarily Auk spp.) in late summer of 2021, and the second, an outbreak of highly pathogenic avian influenza during the seabird breeding season of 2022. These could lead to significant changes in the at-sea densities of some species.

Contents

2. List of figures and tables

3. Glossary

Term	Description
a_i	Area of the ith photo
Autocorrelation	Successive items in a sequence are more similar to each other than more distant items in the sequence
Covariate	Explanatory variable which is continuous (e.g. distance to event)
$\widehat{D}$ surface	Provides a summary of the relevant input data for the prediction both in terms of adjusted observed densities but also shows where there was actually survey effort (albeit not necessarily from the year in question) in that season. Predictions in regions of low survey effort should be treated with caution.
Factor	Explanatory variable which has a small number of discrete levels (e.g. period before or after event)
GAM	Generalized Additive Model - a generalized linear model in which explanatory variables take the form of smooth functions
GAMM	Generalized Additive Mixed Model - an extension to the generalized additive model (GAM) in which the linear predictor contains random effects in addition to the usual fixed effects.
$\widehat{N}_{ci}$	Estimated number of individuals in each ith covered segment (corrected where necessary for availability bias) of area ai.
Point estimate surfaces	The predicted densities for the conditions given.
Overdispersion	Presence of more variability than would be expected under the assumed mean-variance relationship.
2.5% and 97.5% percentile surfaces	The densities of the 2.5% and 97.5% quantiles for each cell of the surface, a measure of uncertainty encompassing the range of values that the model predicts there is a 95% probability of the true mean response lying within'
CV	Coefficient of variation – measure of a dispersion of a frequency distribution calculated as the ratio of the standard deviation to the mean, expressed in percentage.

4. INTRODUCTION

4.1 Context

Information on the abundance and distribution of seabirds and cetaceans at sea is required to assist in the management of internationally protected populations, for developing sectoral marine plans and their associated Strategic Environmental Assessments, and assessing sensitivity to human pressures including, for seabirds, oil spills via the Oil Sensitivity Index.

During the 1980s and 1990s, in response to concerns over possible impacts from developments by the oil and gas industry within the North Sea, European Seabirds at Sea (ESAS) surveys were undertaken by the UK Nature Conservancy Council (later becoming the Joint Nature Conservation Committee, JNCC) and other bodies (e.g. Ornis Consult from Denmark). Analyses of those data were published in a series of reports (Blake et al., 1984; Tasker et al. 1987, Carter et al. 1993, Stone et al. 1995, Pollock et al. 2000). Since then, there has been a review of at-sea surveys within the UK Exclusive Economic Zone to identify possible marine Special Protection Areas (SPAs) (Kober et al. 2010), and a wider collation of surveys (vessel based, aerial visual and aerial digital) analysed for both seabirds and cetaceans as part of the 5-year NERC-Defra funded Marine Ecosystems Research Programme (MERP) (Waggitt et al. 2020, Donovan et al. 2020). Three large-scale surveys of cetaceans (SCANS, SCANS-II, and SCANS-III) have been undertaken in the North Sea in 1994, 2005, and 2016, during the month of July (Hammond et al. 2002, 2013, 2021). In addition to the distribution maps produced by Waggitt et al. (2020), several reviews of the status and distribution of cetaceans in UK waters have been undertaken (Evans 1980, Evans et al. 1986, Evans 1992, Evans & Wang 2003, Evans et al. 2003, Reid et al. 2003, Paxton et al. 2016) as well as focused upon Scottish waters (Hague et al. 2020).

During the 1980s and 1990s, most surveys were vessel-based but over the last twenty years, aerial surveys have increasingly been used, with several now employing digital photography in place of visual recording (Thaxter & Burton 2009, Buckland et al. 2012). Aerial surveys have the advantage of providing more accurate representations of the perpendicular distance of detections to the track-line, and are less likely to be susceptible to responsive movement. Digital photography either by video or still images provides the opportunity for a permanent record of the strip covered by the survey. Although there have been few direct comparisons between aerial visual and aerial digital surveys, the latter appear to be better at estimating abundance for birds that form aggregations, for example common scoter, resulting in higher abundance estimates (Buckland et al. 2012, Zydelis et al. 2019).

On the other hand, it is more difficult to digitally detect and identify some taxa to species, and notable examples include auks such as razorbill and guillemot, and various gull species (Zydelis et al. 2019, Waggitt et al. 2020). The height at which the plane flies is another consideration. Visual aerial surveys tend to be undertaken at lower altitudes (e.g. 76m) than digital aerial surveys (e.g. 460+m) in order to better enable species identification (Zydelis et al. 2019). Flying at greater heights has the advantage of improved safety, less chance of disturbance of sensitive species, and a broader survey strip allowing larger sample sizes of detections, but species identification becomes more challenging. Improvements in camera technology have made this less critical but it remains an issue compared with vessel surveys where there is often much closer proximity to species. A comparison between digital aerial and vessel surveys found that the former could identify only 23% of birds to species level compared with 95% for the latter (Johnston et al. 2017). Vessel surveys also operate at much slower speeds than planes so there is more opportunity to detect animals at the surface. All forms of survey, however, require corrections to account for availability bias, particularly for cetaceans that spend a high proportion of their lives underwater, out of sight of observer or camera. Although less significant an issue, the same applies to diving seabirds such as auks, cormorants and shags, divers, grebes and sea ducks. The fact that digital aerial surveys can detect marine mammals just below the surface complicates corrections for availability bias and will be dependent upon the turbidity at the time.

Twenty-four seabird species regularly breed in Scottish waters, of which eleven were recorded in sufficient numbers within the study area to be considered for modelling: northern fulmar (*Fulmarus glacialis*), northern gannet (*Morus bassanus*), great skua (*Stercorarius skua*), common gull (*Larus canus)*, lesser black-backed gull (*Larus fuscus)*, herring gull (*Larus argentatus)*, great black-backed gull (*Larus marinus*), black-legged kittiwake (*Rissa tridactyla*), common guillemot (*Uria aalge*), razorbill

(*Alca torda*), and Atlantic puffin (*Fratercula arctica*). Other species of seabirds occurring in the region that were recorded but too few times during the surveys for their density distributions to be modelled, are listed in Table 1.

All 25 species of cetaceans recorded in Scottish territorial waters are classed as European protected species and are protected under the Conservation (Natural Habitats, &c.) Regulations 1994 (as amended) and the Offshore Marine Conservation (Natural Habitats, &c.) Regulations 2017. Knowledge of the spatial and temporal distribution and abundance of marine species is important in order for the Government to make evidence-based decisions regarding their status. There are four cetacean species of particular interest in this study due to their regular occurrence: minke whale (*Balaenoptera acutorostrata*), common dolphin (*Delphinus delphis)*, white beaked dolphin (*Lagenorhynchus albirostris)* and harbour porpoise (*Phocoena phocoena*). Other species such as killer whale (*Orcinus orca*), long-finned pilot whale (*Globicephala melas*), Atlantic white-sided dolphin (*Lagenorhynchus acutus*), Risso's dolphin (*Grampus griseus*), and humpback whale (Megaptera novaeangliae) do occur in the region on a regular basis but were identified too few times during the digital aerial surveys for their density distributions to be modelled. The number of individuals recorded within each species or species group per survey is given in Table 1.

4.2 Aims of the project

The aims of this project were 1) to produce seabird and marine mammal distribution models from which density surface and abundance estimates could be obtained, for offshore waters east of Scotland. These would be derived from data collected from strategic digital aerial surveys undertaken in 2020-21 in the northern North Sea beyond 12nm from the coast; 2) to summarise the modelling methods applied and the resulting distributions, species by species (for those species with sufficient sample sizes for modelling), and then relate these to previous studies of at-sea distributions; and 3) to identify any limitations in the methodology and make recommendations for how these could be addressed in the future.

Table 1. Species recorded during the eight digital aerial surveys, Feb 2020 – Mar 2021.

Species	Number of Individuals	Totals	Survey No. in which recorded
Seabird species			
Red-throated diver	0+0+1+3+11+2+1+1	19	3,4,5,6,7,8
Great northern diver	0+1+1+0+1+1+0+0	4	2,3,5,6
Diver sp.	0+0+0+2+7+2+3+3	17	4,5,6,7,8
Storm Petrel sp.	0+0+4+2+0+0+0+0	6	3,4
Northern fulmar	1838+1300+2056+2908+8003+5384+3284+2440	27,213	1,2,3,4,5,6,7,8
Manx shearwater	0+0+3+9+22+0+0	34	3,4,5
Northern gannet	377+720+1773+1582+3012+2146+1088+828	11,526	1,2,3,4,5,6,7,8
Cormorant/Shag	0+0+1+0+0+0+0+0	1	3
European Shag	0+0+0+0+0+1+0+0	1	6
Velvet scoter	0+0+0+0+0+0+1+0	1	7
Long-tailed duck	0+0+0+0+0+0+3+0	3	7
Red-breasted merganser	0+0+0+0+0+0+1+0	1	7
Grebe sp.	0+0+0+0+0+0+1+0	1	7
Common eider	0+0+0+0+1+0+0+0	1	5
Glaucous gull	0+0+0+0+0+0+2	2	7
Iceland gull	0+0+0+0+0+0+1	1	7
Lesser black-backed gull	3+1+17+10+0+0+2+0	33	1,2,3,4,7
Herring gull	271+14+301+148+20+378+705+57	1,894	1,2,3,4,5,6,7,8
Great black-backed gull	184+21+4+11+223+532+483+92	1,550	1,2,3,4,5,6,7,8
Black-backed gull sp.	2+0+2+1+3125+27+7	3,164	1,3,4,5,6,7,8
Common gull	13+2+0+3+8+35+29+6	96	1,2,4,5,6,7,8
Black-headed gull	0+0+0+0+0+1+0+0	1	6
Black-legged kittiwake	794+1356+3718+2802+9178+903+982+1203	20,936	1,2,3,4,5,6,7,8
Large gull sp.	411+21+44+67+170+449+224+65	1,451	1,2,3,4,5,6,7,8
Small gull sp.	245+31+59+40+119+81+35+56	666	1,2,3,4,5,6,7,8
Gull sp.	1+2+7+17+18+168+11+19	243	1,2,3,4,5,6,7,8
Common tern	0+0+2+0+0+0+0+0	2	3
Common/Arctic tern	0+0+13+384+3+0+0+0	400	3,4,5
Tern sp.	0+0+2+0+0+0+0+0	2	3
Great skua	0+1+28+33+31+5+2+0	100	2,3,4,5,6,7
Arctic skua	0+0+3+1+2+0+0+0	6	3,4,5
Skua sp.	0+0+1+5+7+2+0+0	15	3,4,5,6
Common guillemot	0+701+4371+2713+3311+469+246+675	12,486	2,3,4,5,6,7,8
Razorbill	1+1043+2843+1397+996+455+0+131	6,866	1, 2,3,4,5,6,8
Guillemot/Razorbill	5720+4230+2370+1694+38482+8434+7246+6922	75,098	1,2,3,4,5,6,7,8
Black Guillemot	0+1+6+0+0+0+1+6	14	2,3,7,8
Atlantic Puffin	29+74+251+65+12+6+0+0	437	1,2,3,4,5,6
Auk sp.	393+87+254+243+365+65+142+392	1,941	1,2,3,4,5,6,7,8

Marine Mammals			
Grey seal	6+1+11+7+2+0+0+0	27	1,2,3,4,5
Seal sp.	3+3+29+16+4+4+0+2	61	1,2,3,4,5,6,8
Minke whale	1+3+12+3+8+4+0+0	31	1,2,3,4,5,6
Common dolphin	5+0+22+0+0+0+0	27	1,3
White-beaked dolphin	3+0+10+71+12+20+2+12	130	1,3,4,5,6,7,8
Risso's dolphin	0+0+0+0+0+0+5+0	5	7
Dolphin sp.	27+2+24+17+5+0+1+0	76	1,2,3,4,5,7
Dolphin/Porpoise	51+13+249+293+18+18+9+22	673	1,2,3,4,5,6,7,8
Harbour porpoise	0+0+128+250+8+34+0+17	437	3,4,5,6,8
Whale sp.	0+0+3+0+0+1+1+0	5	3,6,7
Marine Mammal sp.	0+0+29+3+1+3+2+6	44	3,4,5,6,7,8

5. METHODS

5.1 Overview of Methods

Here we present a brief summary of the statistical methods and the general approach undertaken to produce the density surfaces, prior to a more detailed description in the later sections. Note that the primary consideration here was to obtain distribution and abundances from the digital aerial survey data. The data under consideration (see below) consisted of counts of animals from digitally referenced images from the survey. We modelled the numbers based on the number of animals detected in photos of known area ("the count method"; see Hedley 2000, Hedley & Buckland 2004, Hedley et al. 2004).

The first stage of the analysis consisted of correcting the observed numbers seen for imperfect identification. The second stage of the analysis involved modelling the resultant estimated densities as a function of space, time and other explanatory variables. The predictions were made from the models over the survey region (see Figure 1). In the case of marine mammals, the resulting predictions were then corrected for surface availability. Thus, monthly indices of abundance could be obtained. Associated with both of the processes is the estimation of the relevant uncertainty. Availability and recognition uncertainty were not incorporated at this stage. All analysis was undertaken in R (R Core Team. 2013).

5.2 Overview of the Data Collection Procedure

The data were collected in the form of temporally and spatially indexed photos from planes collected between February 2020 and March 2021 by APEM Ltd (Figure 1).

APEM's camera system was fitted into a twin-engine P68 Ravenair aircraft. The plane surveyed at a height of 2,000 feet and a ground speed of 120 knots (138 mph). The aerial digital surveys captured images along ten transects spaced in a saw tooth pattern to achieve full coverage across the targeted area east of Scotland. Data collected approximately two-centimetre ground sample distance (GSD) digital still images. The transect swathe was 960 metres, images were collected continuously (abutting digital still imagery) along the ten transects. The image sea surface area covered was 194 km^2, representing 1.5% coverage of the wider surface area. Flights were made in sea states less than 4 on the Beaufort scale.

Typically, several images were taken and processed at the same time. With a total of 242,550 images. However, the counts from simultaneous deployments of the camera were amalgamated if the precise time could be identified to make the data more tractable, creating a dataset of 97,090 location datums each with counts of a variety of species. Figure 1 gives the survey coverage by month.

Survey transects targeted offshore areas beyond 12 nautical miles.

5.3 Predictor Variables

At the spatial modelling stage of the project, animal numbers were modelled considering environmental and biological inputs of potential relevance. Only

predictors that can be assigned to all the relevant effort and sightings data were used.

The variables considered are given in Table 2 along with their temporal range. To be of use, the variables must cover the temporal and spatial range of the survey data. Further details are given below.

Variation in depth in the prediction region is shown in Figure 2 and highlights how the majority of the southern part of the study area is at depths of less than 100 metres whereas further north except for the Moray Firth and nearer the coast of east Orkney, depths usually exceeded 100 metres.

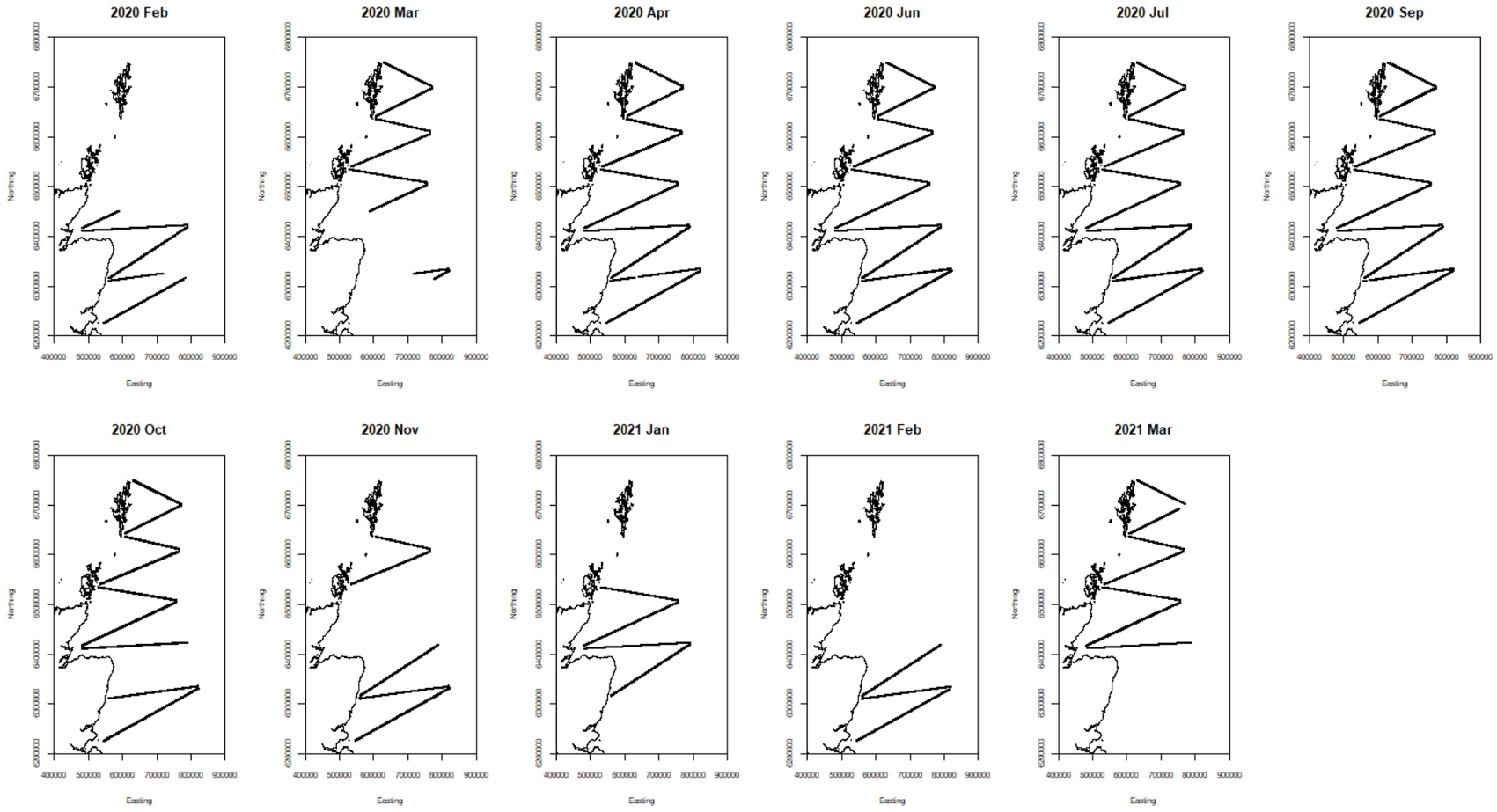

Figure 1. The graph shows flown transects for each surveyed month between by month February 2020 to March 2021

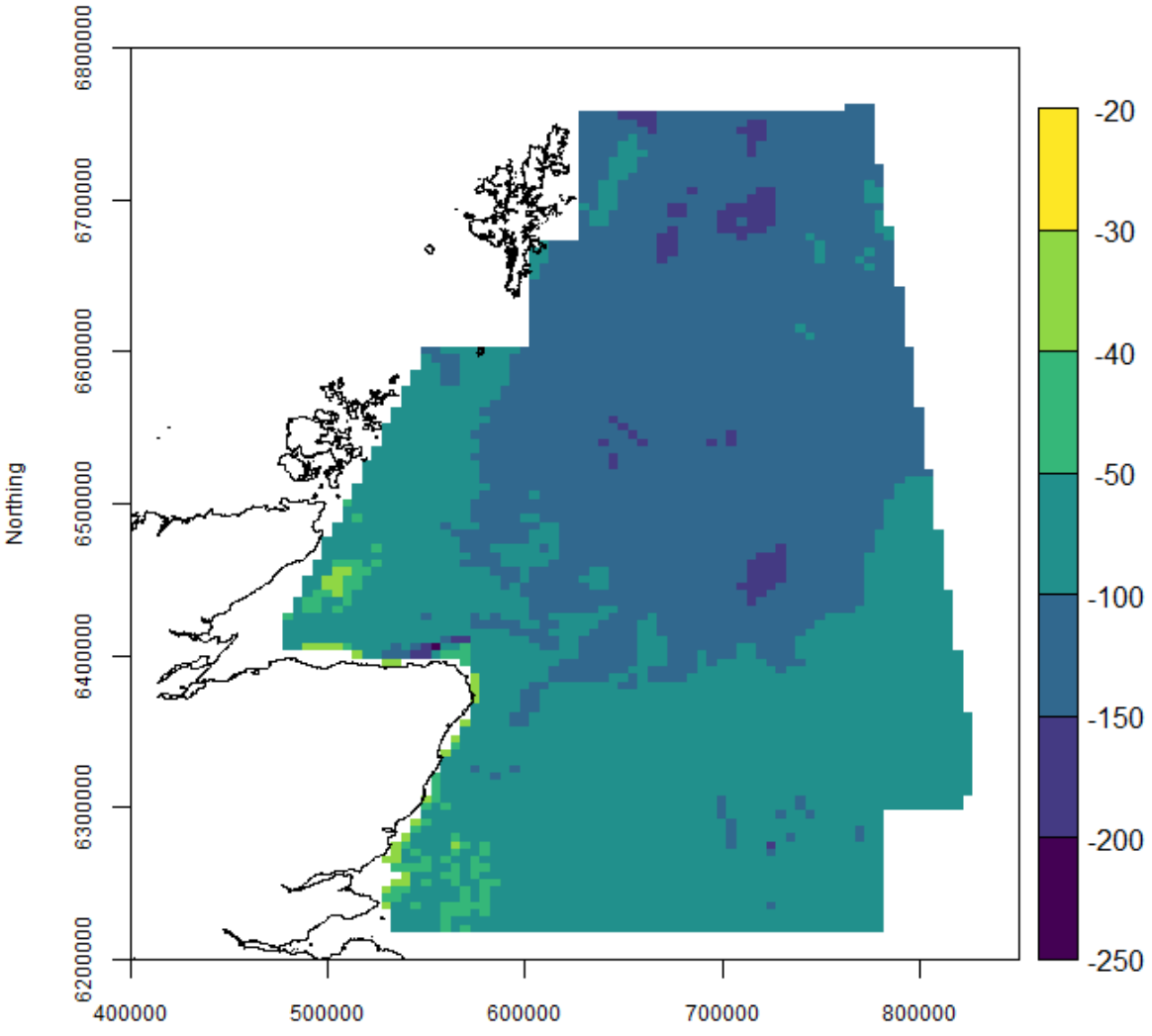

Figure 2. The graph showing variation in depths (in metres) across the survey region. The study area is deepest in the central and northern part.

Table 2. Spatial predictors for consideration in modelling.

Predictor	Description	Resolution	Temporal range	Reference/ link
Position	Easting, Northing assuming UTM30V zone.	1 m	Collected on survey	Position
Day of Year	Either from 1st Jan for breeding season only data or from end of breading season for non-breeding season analyses			Day of Year
Depth	The depth of the seabed. Different depths may support different prey assemblages (i.e., species or age-classes). Benthic prey is also more accessible on shallower seabeds.	Available at ~1m but resampled and processed at 1.5km	Static	EMODNet Bathymetry Portal (https://www.emodnet-bathymetry.eu/)
Monthly Sea Surface Temperature	The mean sea surface temperature (o C) in the calendar month for the survey. Temperature identifies different water-masses, which may support different prey assemblages (i.e species or age-classes).	1.5km	Monthly	From AMM15 FOAM Models, available at the Copernicus Monitoring Service (https://marine.copernicus.eu/)
Seabed roughness	Derived from 'Depth' using a terrain ruggedness index (TRI) which represents the mean difference between a focal cell and the 8 surrounding cells. This index identifies areas of rough and uneven seabed including banks, troughs, and complex coastal topography. Such features may promote hydrodynamic features that increase primary productivity and/or aggregate prey (see Cox et al 2018)	Available at ~1m but resampled and processed at 1.5km.	Static	EMODNet Bathymetry Portal (https://www.emodnet-bathymetry.eu/)

Simpson Hudson Stratification Index	Derived from 'Depth' and 'Mean Surface Current Speed' (log10 (h/u3), whereby h = depth in meters and u = speed in m/s). This index identifies areas likely to remain mixed (<1.9) or become stratified (>1.9) in summer. However, it also describes water column dynamics across the annuals cycle i.e., shallow and turbulent versus deep and non-turbulent. Note that calculations should strictly use depth-averaged current speeds rather than surface current speeds. However, the latter provided comparable measurements, and are sufficient to identify mixed and stratified water in the study area. Prey behaviour may be influenced by water column dynamics, influencing their exploitability. See Scott et al 2010.	1.5km	Static	From AMM15 FOAM Models, available at the Copernicus Monitoring Service (https://marine.copernicus.eu/) and EMODNet Bathymetry Portal (https://www.emodnet-bathymetry.eu/).
Monthly Mean Sea Surface Temperature Range	The range of sea surface temperature (o C) in the calendar month of the survey. High values identify regions of freshwater influence (ROFI) associated with higher productivity (See Cox et al 2018).		Monthly	From AMM15 FOAM Models, available at the Copernicus Monitoring Service (https://marine.copernicus.eu/)
Monthly Mean Salinity	The mean sea surface salinity (ppt) in the calendar month of the survey. Low values identify mouths of estuaries associated with migratory routes of some prey (See Cox et al 2018).		Monthly	From AMM15 FOAM Models, available at the Copernicus Monitoring Service (https://marine.copernicus.eu/)
Monthly Mean Salinity Range	The range of sea surface salinities (ppt) in the calendar month of the survey. High values identify mouths of estuaries associated with migratory routes of some prey (See Cox et al 2018).		Monthly	From AMM15 FOAM Models, available at the Copernicus Monitoring Service (https://marine.copernicus.eu/)
Mean Surface Current Speed	The mean sea surface current speeds (m/s) across a typical spring-neap cycle. Areas of high current speeds generally contain hydrodynamic features suspected to aggregate prey items and/or increase encounters with prey (See Benjamins et al 2015).		Static	From AMM15 FOAM Models, available at the Copernicus Monitoring Service (https://marine.copernicus.eu/)
Colony indices for each seabird species	Colony Index is an index (0-1) representing the distance to colonies weighted by the relative size of that colony. It assumes an exponential decay in animal densities with distance from colony, linked to a homogeneous dispersal across all directions.		Static	

5.4 Adjustments for Non-recognition

Some individual animals were not identified to species in the photo survey although they were identified to family (birds) and order (marine mammals). Such individuals were allocated to species as follows by using, where possible, species ratios obtained from the MERP database (see Waggitt et al. 2020). The MERP database included vessel, visual aerial and digital aerial data collected across the region by a much larger set of data providers and spanning a much longer time period (1980-2018). Vessel surveys in particular are better at identifying animals to species (Johnston et al. 2015, Waggitt et al. 2020). Ratios of abundance between similar species (e.g. razorbill and guillemot) have not changed very much over those years (Stone et al. 1995, Mitchell et al. 2004, JNCC 2016, Potiek et al. 2019, Waggitt et al. 2020), and so this was considered a valid procedure.

For each locality with an unidentified animal, all observations within 50 km of the locality were extracted from the MERP database. The ratio of species in the relevant group (e.g. skuas, auks, “dolphins”, “dolphin or porpoise” etc.) was used to allocate the vaguely identified images to species for that location.

5.5 Density Surface Modelling

Model selection proceeded as follows. The data were counts and contained large numbers of zeros, therefore the response data were likely to be more variable (i.e. overdispersed) than assumed under some distributions. This variability needed to be accommodated under the selected model. Furthermore, the observations were close together in space/time and these observations were likely to be more similar than observations distant in space/time. Covariate data can potentially explain part of the correlation in the counts; however, it is unlikely that the correlation will be explained in full. In the case of marine mammals, the data were initially considered as a complete set. Backwards model selection initially proceeded assuming the datums were independent. Model selection was by automatic smoothing with mgcv (Wood 2017) using restricted maximum likelihood (REML). Then, after the model was reduced, the residuals were tested for autocorrelation (by examination of partial and full autocorrelation plots of the residuals) to identify the interval at which datums became independent. Further variables were then removed on a wholly independent reduced data set after several models were fitted with different subsets of data (i.e. different reduced datasets were created by taking the nth datapoints from different start points). Finally, the full dataset (n = 97,090) was fitted using the reduced variable set within a mixed-model GAM (GAMM, Wood 2017) with an appropriate correlation error structure. More model reduction was allowed. The use of GAMMs allowed smoothed responses to be fitted to the predictors. Family error structure in this high zero frequency data set was considered to follow a negative binomial or Tweedie distribution. Diagnostic plots were examined to evaluate the best model.

If the model had a negative binomial error structure, it typically had the following form:

$$y_i = \exp(\beta_0 + s(Easting_j, Northing_i) + s(X_{1i}) + s(X_{2i}) + \varepsilon_i$$

where s($Easting_j$, $Northing_i$) is the 2D smooth of Easting and Northing for the ith point and X1 and X2 represent smooths of single predictors (see below for details) of which thre could be a large number (see below).

In the case of birds, the data were first split into breeding and non-breeding season (see Table 3) and then analysed as above for each season (although the candidate variable set was different, see Table 7).

Table 3. Bird seasons used in this analysis (following Searle et al. 2022).

Species	Breeding season	Non -breading season
Northern fulmar	April - August	September - March
Northern gannet	April - October	November - March
Great skua	April - July	August - March
Common gull	April - July	August - March
Lesser black-backed gull	April - July	August – March
Herring gull	April - July	August – March
Great black-backed gull	April - July	August - March
Black-legged kittiwake	April - August	September - March
Common guillemot	April - July	August - March
Razorbill	April - July	August - March
Atlantic puffin	April - August	September - March

For some species, model fitting on the reduced dataset (n = 97,090) proved impossible, so the data were further reduced to 5,093 by binning the data into 3 min bins (based on the number of photos taken). This reduced but did not eliminate the autocorrelation but made modelling more tractable. In the case of bird species, a Season factor variable was added to the models to allow different relationships across seasons in these models that considered all the data at the same time.

5.5.1.1 Predictions

Predictions from the models were made on a 5 km by 5 km resolution easting and northing grid with confidence intervals directly calculated from the estimated cell standard errors. The results were then corrected for availability (see below).

5.5.1.2 Availability adjustments

The proportion of animals available at the surface has to be considered. For marine mammals, an index of availability at the surface for each sighting was made by considering the reported proportion of time the animals spend at the surface. The probability of a mammal being available at the surface was given by

$$Proportion(Avail) = \frac{E[s]}{(E[s] + E[d])}$$

where s = surface time, d = dive time. The process in the context of this survey is instantaneous so no correction for observation time is necessary. No correction for availability was made for seabirds. The sources for species availability at the surface for diving marine mammals are summarised in Table 4.

Table 4. Mean surface and dive times used for individuals of target species.

Species	**Mean surface time (mins)**	**Mean dive time (mins)**
Minke whale	0.067 (Anderwald 2009) 0.044 (Gunnlaugsson 1989) 0.053 (Joyce et al. 1989 off Svalbard)	1.311(Joyce et al. 1989)
White-beaked dolphin	0.058 (P.G.H. Evans, unpublished data)	0.917 (M. Rasmussen pers. comm.)
Common dolphin	0.058 (P.G.H. Evans, unpublished data)	1.0 (Lockyer & Morris 1986, Lockyer & Morris 1987, Mate et al. 1995)
Harbour porpoise	Overall availability in 0 – 2m band 0.615 from Teilman et al. 2013	

6. RESULTS

Distribution models were produced for ten out of eleven seabird species and three out of four marine mammals. The list of covariates used in the initial models for each species in given in Table 7 and the selected covariates are listen in Table 8 for seabirds and Table 9 for marine mammals.

For seabirds for which it was possible to fit a separate model for breeding and non-breeding season, the model for non-breeding season retained more environmental variables than for breeding season. There was no single environmental covariate which would characterise distribution and density of all seabirds or all marine mammals.

Below we present the results each species: distribution patterns with point estimates and associated uncertainties (confidence intervals and coefficient of variation, CV)

6.1 Adjustments for non-recognition

Table 5 gives the adjustments made for each species due to non-recognition or species grouping. For species such as guillemot, 94% of observed numbers were assigned to species group, rather than species. For a small review of species grouping see Appendix 1.

Table 5. Allocation of vaguely identified animals.

Species	Adjustments	Non-recognised animals allocated	Proportion of total* numbers recorded
Northern fulmar	No adjustments made	0	0%
Northern gannet	No adjustment made	0	0%
Great skua	No adjustment made	0	0%
Common gull	Adjusted based on MERP database	41	30%
Lesser black-backed gull	Adjusted based on MERP database	57	63%
Herring gull	Adjusted based on MERP database	1347	42%
Great black-backed gull	Adjusted based on MERP database	603	28%
Black-legged kittiwake	No adjustment made	0	0%
Common guillemot	Adjusted based on MERP database	1583	94%
Razorbill	Adjusted based on MERP database	30	0.04%

Atlantic puffin	Adjusted based on MERP database	104	19%
Minke whale	Adjusted based on MERP database	6	16%
Common dolphin	Adjusted based on MERP database	0	0%
White-beaked dolphin	Adjusted based on MERP database	306	58%
Harbour porpoise	Adjusted based on MERP database	545	56%

*Knowns and estimated unknowns

6.2 Realised effort

The total effort (as areas) per year and per month is given in Figure 3. The total area surveyed was 16,882.47 km^2. The distribution of effort by survey is shown in Table 6 and Figure 6. The was no surveys taking place in May, August and December and February and March were surveyed both in 2020 and 2021.

.

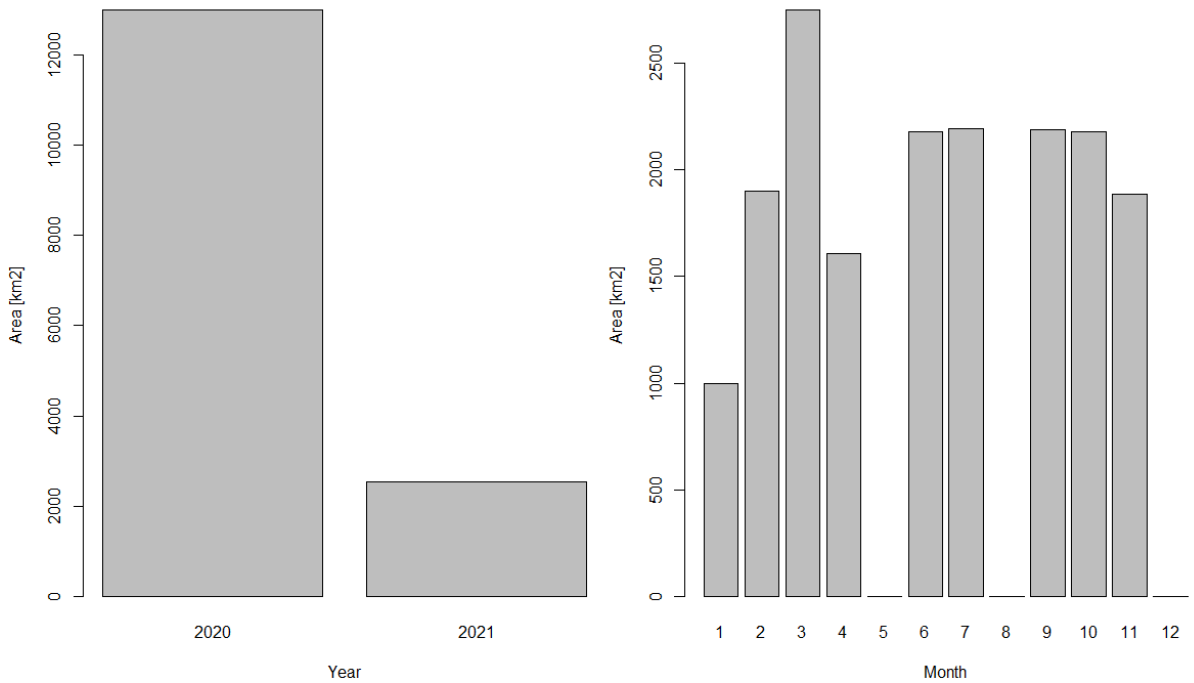

Figure 3. Total area covered (in km^2) by (left) surveyed year (2020 and 2021) and (right) by calendar month (numbered, Jan. = 1 etc.), including months when survey did not occur. March had the largest cover but January the lowest but note that March was included in 2020 and 2021 survey. N.B no data for May, August or December were recorded.

Table 6. Total area covered (in km^2) by each survey.

Survey	Time period	Covered area, as (km^2)
1	February/March 2020	2181
2	April 2020	1608
3	June 2020	2180
4	July 2020	2192
5	September 2020	2185
6	October 2020	2176
7	November 2020	1884
8	February/March 2021	2534
Total		16940

Table 7. Initial models including list of environmental covariates for each species. All covariates were fitted as continuous variables (indicated by s()).

Species	Initial Model (on scale of link function)
Most Birds breeding season	*s(Easting, Northing) + s(MeanSSTbymonth) + s(MeanRangeSSTbyMonth) + s(MeanSalinitybyMonth) + s(MeanRangeofSalinitybyMonth) + s(Current) + s(Depth) + s(Seabed Roughness) + s(Simpson Hudson Stratification Index)+s(Colony Index) + offset(log(Km^2)),*
Non-breeding season	*s(Easting, Northing) + s(MeanSSTbymonth) + s(MeanRangeSSTbyMonth) + s(MeanSalinitybyMonth) + s(MeanRangeofSalinitybyMonth) + s(Current) + s(Depth) + s(Seabed Roughness) + s(Simpson Hudson Stratification Index) + offset(log(Km^2)),*
Birds (reduced dataset (n = 5093)	*s(Easting, Northing by Season) + s(MeanSSTbymonth by Season) + s(MeanRangeSSTbyMonth by Season) + s(MeanSalinitybyMonth by Season) + s(MeanRangeofSalinitybyMonth by Season) + s(Current by Season) + s(Depth by Season) + s(Seabed Roughness by Season) + s(Simpson Hudson Stratification Index by Season)+s(Colony Index by Season) + offset(log(Km^2)),*
Minke whale	*s(Easting, Northing) + s(Dayofyear) + offset(log(Km^2))**
Common dolphin	*s(Easting, Northing) + offset(log(Km^2))*
White-beaked dolphin	*s(Easting, Northing) + s(MeanSSTbymonth) + s(MeanRangeSSTbyMonth) + s(MeanSalinitybyMonth) + s(MeanRangeofSalinitybyMonth) + s(Current) + s(Depth) + s(Seabed Roughness) + s(Simpson Hudson Stratification Index) + offset(log(Km^2)),*
Harbour porpoise	*s(Easting, Northing) + s(MeanSSTbymonth) + s(MeanRangeSSTbyMonth) + s(MeanSalinitybyMonth) + s(MeanRangeofSalinitybyMonth) + s(Current) + s(Depth) + s(Seabed Roughness) + s(Simpson Hudson Stratification Index) + offset(log(Km^2))*

**s(Depth)* was subsequently tried.

Table 8. Selected models for seabirds.

Species	Season	Final Model (on log scale, offset not shown)	No of segments	Correlation structure*	Assumed error
Northern fulmar	Breeding Non-breeding	*s(Easting, Northing) + MeanMonthlySST + MonthlySalinityRange* *s(Easting, Northing) + MeanMonthlySST + SSTMonthlyRange + MeanMonthlySalinity*	29291 67799	AR1 AR1	Negative binomial Negative binomial
Northern gannet	All year	*s(Easting) + s(MeanMonthlySST)*	5093	ARMA(1,1)	Negative binomial
Great skua	All year	*s(Easting, Northing by Season) + s(SSTMonthlyRange by Season)*	5093	ARMA(1,1)	Negative binomial
Common gull	Breeding Non-breeding	*s(Depth)* *None*	2723 2370	ARMA(1,1) ARMA(1,1)	Negative binomial Negative binomial
Lesser black-backed gull	Breeding Non-breeding	None None	29291 67799	AR1 AR1	Negative binomial Negative binomial
Herring gull	All year	*s(Easting, Northing by Season) + SSTmonthlyRange + s(Dayofyear) + s(Depth by Season)*	5093	AR1	Negative binomial
Great black-backed gull	Breeding	*MeanMonthlySalinity + Seabed roughness*	29291	AR1	Negative binomial

	Non-breeding	*s(Easting, Northing) + MeanMonthlySST + Depth*	67799	AR1	Negative binomial
Black-legged kittiwake	All year	*s(Easting, Northing by Season) + s(MeanMonthlySalinity by Season)*	5093	AR1	Negative binomial
Common guillemot	All year	*s(MeanMonthlySST) + s(Depth) + s(Dayofyear) + Seabed roughness*	5093	ARMA(0,1)	Negative binomial
Razorbill	Breeding Non-breeding	*s(Easting, Northing) + s(SSTMonthlyRange)* *s(Easting, Northing) + MeanMonthlySST + MeanSSTMonthlyRange + MeanMonthly Salinity*	29291 67799	AR1 AR1	Negative binomial Negative binomial
Atlantic puffin	Breeding Non-breeding	*s(Easting, Northing) + s(MeanMonthlySST) + MeanSSTMonthlyRange + MeanMonthly Salinity* *Current*	29291 67799	AR1 AR1	Negative binomial Negative binomial

*The assumed structure of the correlation in the error ARn: autoregressive of lag n, ARMA Autoregressive (of lag n) and moving average (m)

Table 9. Selected models for marine mammals (offsets not given).

Species	Final Model (on scale of link function)	No of segments	Correlation structure*	Assumed error
Minke whale	*s(Easting, Northing) +s(Dayofyear)*	5093	AR1	Logistic
Common dolphin	*None*	52549	AR1	Negative binomial
White-beaked dolphin	*s(Easting, Northing) + Month*	5093	ARMA(1,1)	Negative binomial
Harbour porpoise	*S(Easting, Northing) + MeanMonthlySalinity*	5093	ARMA(1,1)	Negative binomial

*The assumed structure of the correlation in the error. ARn: autoregressive of lag n, ARMA Autoregressive (of lag n) and moving average (m)

6.3 Seabird Species

6.3.1 Northern Fulmar

The separate fitted models for breading and non-breeding season are given in Table 8. The estimates of numbers of fulmars during the survey period is given in Figure 4. They indicate peak abundance after the end of the breeding season, in September declining thereafter.

Point estimates of fulmar density for the sampling months along with the confidence bounds are given in Figure 5, Figure 6, and Figure 7. They show highest densities offshore in the northernmost part of the North Sea east of Shetland and Orkney south to the Moray Firth. The CVs are shown in Figure 8 and are largest at the southern areas of the study site. The mean point estimates for breeding and non-breeding season in shown in Figure 9. The breeding distribution is closer to the shore than in the non-breeding season.

The effect of the non-location variables, sea surface temperature (SST) and salinity, in the breeding season model, is given in Figure 10. They indicate a general increase in fulmar densities with increasing SST and decreasing salinity during this season.

The effect of the same non-location variables as well as salinity range in the non-breeding season model, is given in Figure 11. They showed positive relationships of fulmar density with both SST and salinity during the non-breeding season.

Note that these are the effects of these variables given the presence of location in the model, so they may be very different from the actual biological effect.

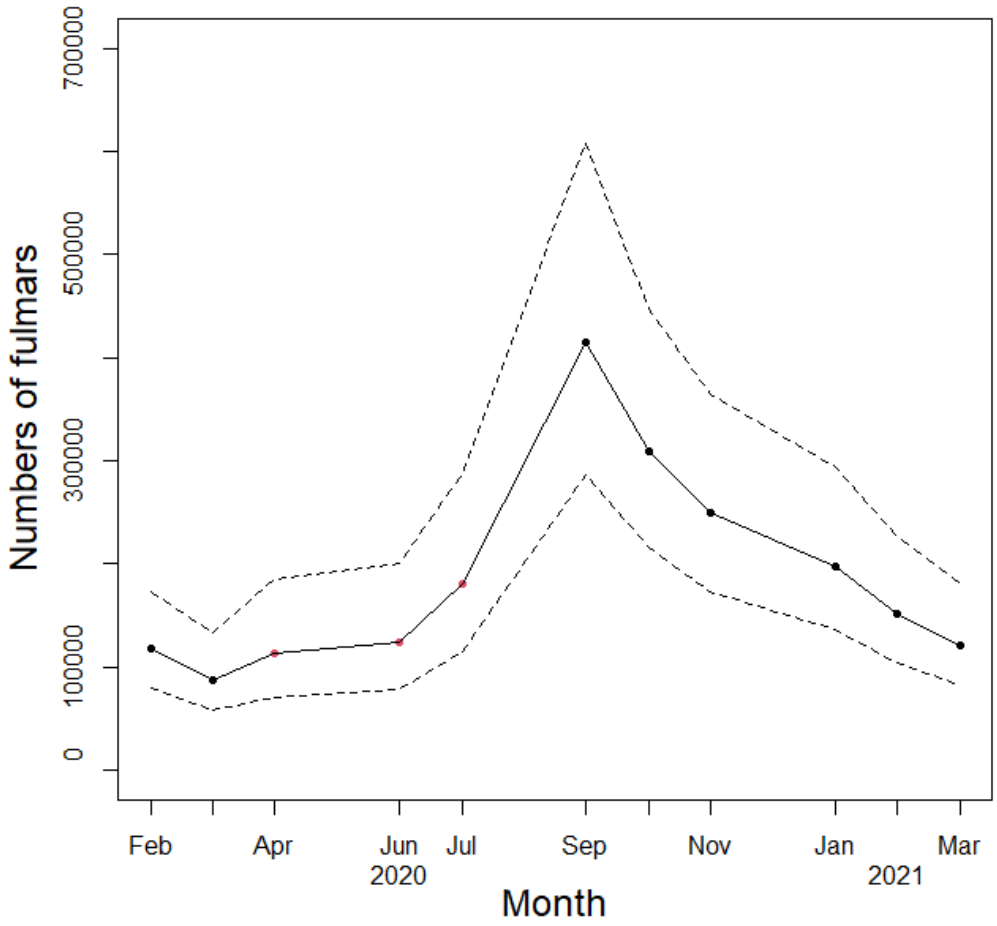

Figure 4. A graph showing estimated numbers of northern fulmars over the duration of the study from February 2020 to March 2021. Red points indicate the breeding season (April to July) and the dashed lines represent upper and lower bounds of the 95% confidence intervals. Numbers of fulmars peaked in September and had lowest values in winter months (January to April).

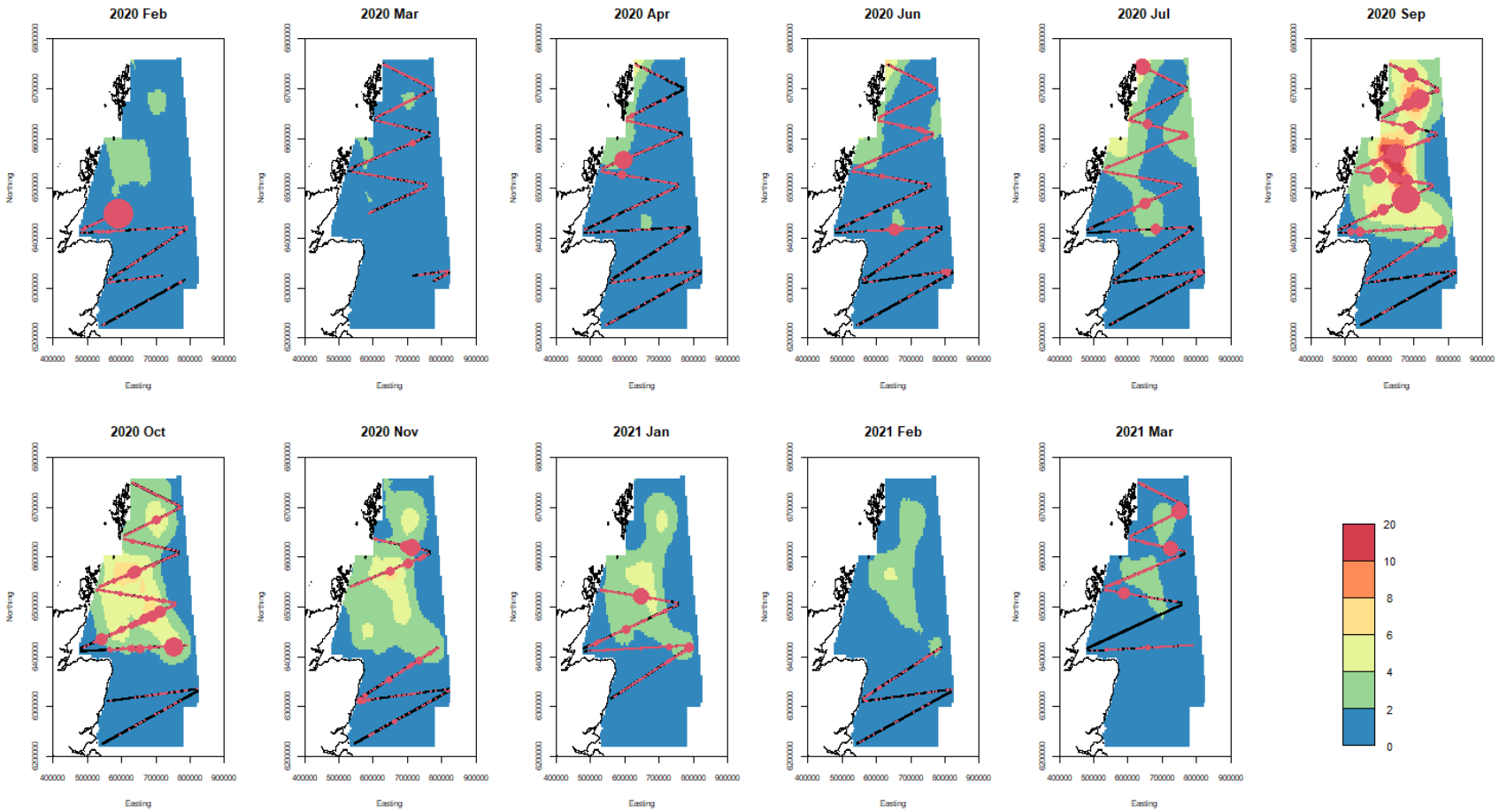

Figure 5. A graph showing point estimates of northern fulmar densities for each surveyed month from February 2020 to March 2021. Colours represent estimated densities per km^2. Black lines indicate sampling locations in that month. Red dots indicate observed numbers of birds with size proportional to observed number. Note that scale is matching the following graphs depicting lower and upper confidence intervals.

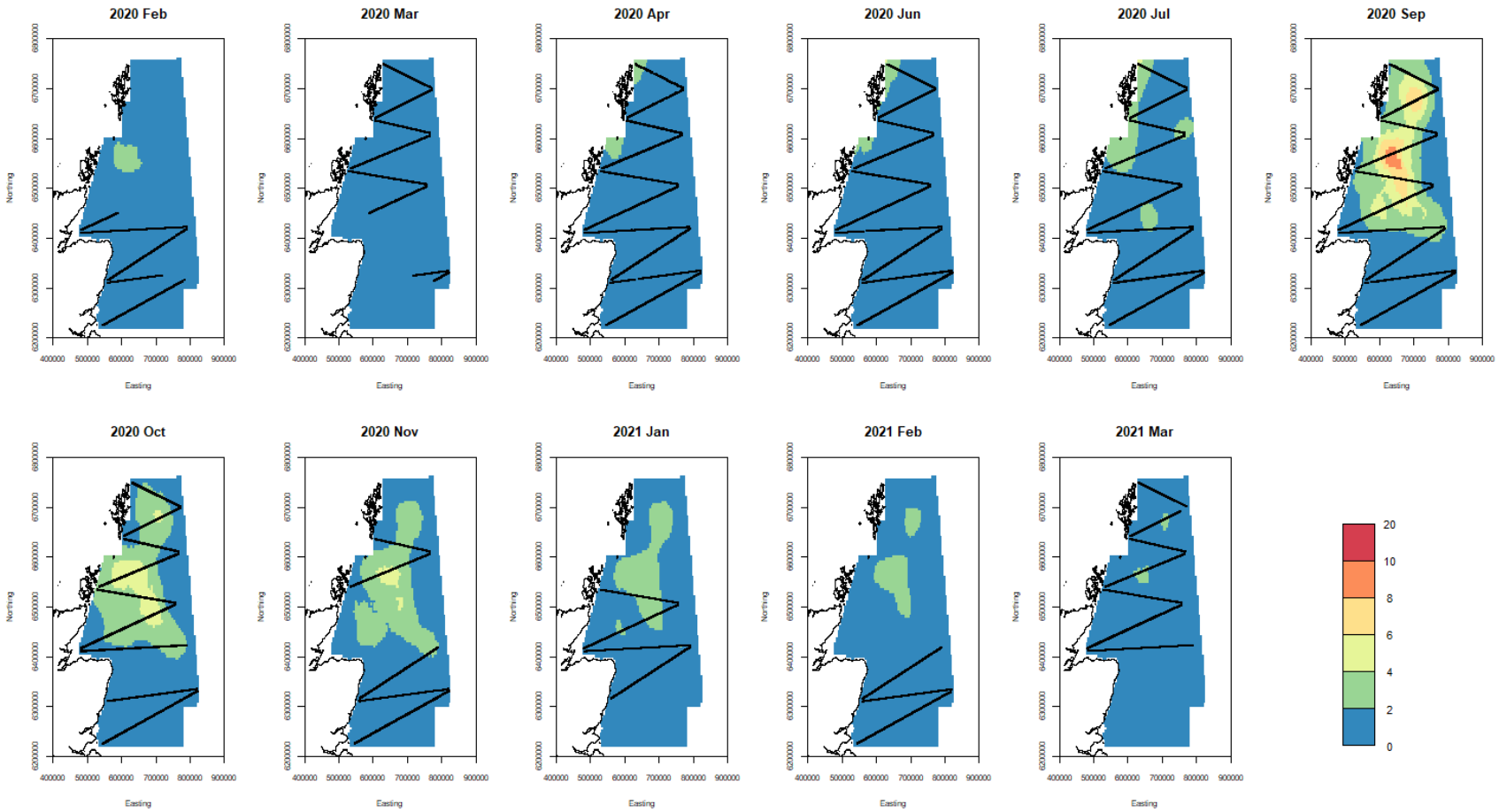

Figure 6. A graph showing lower confidence bound estimates (2.5%) of northern fulmar densities for each surveyed month from February 2020 to March 2021. Colours represent estimated densities per km^2. Black lines indicate sampling locations in that month.

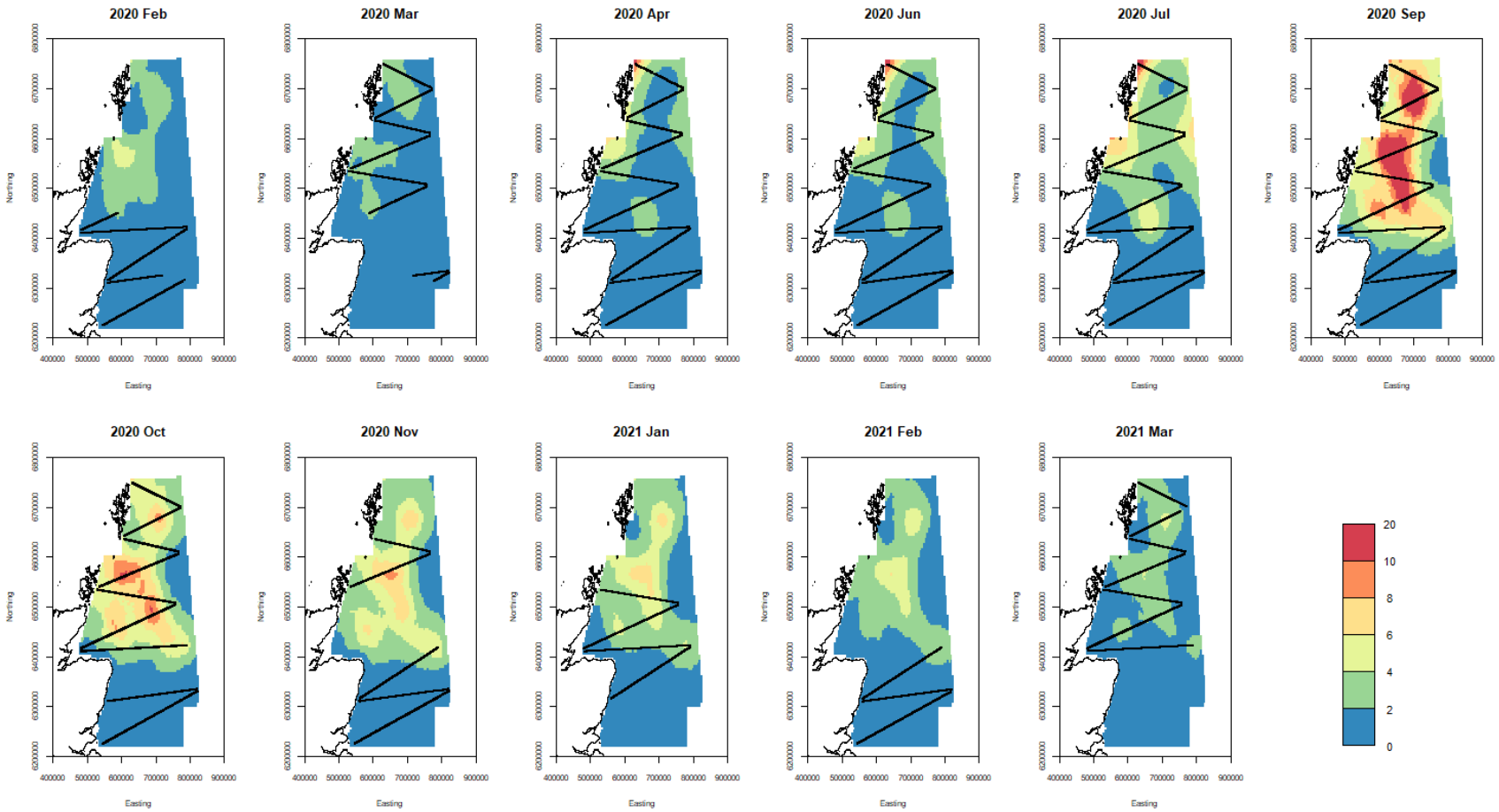

Figure 7. A graph showing upper confidence bound estimates (97.5%) of northern fulmar densities for each surveyed month from February 2020 to March 2021. Colours represent estimated densities per km^2. Black lines indicate sampling locations in that month.

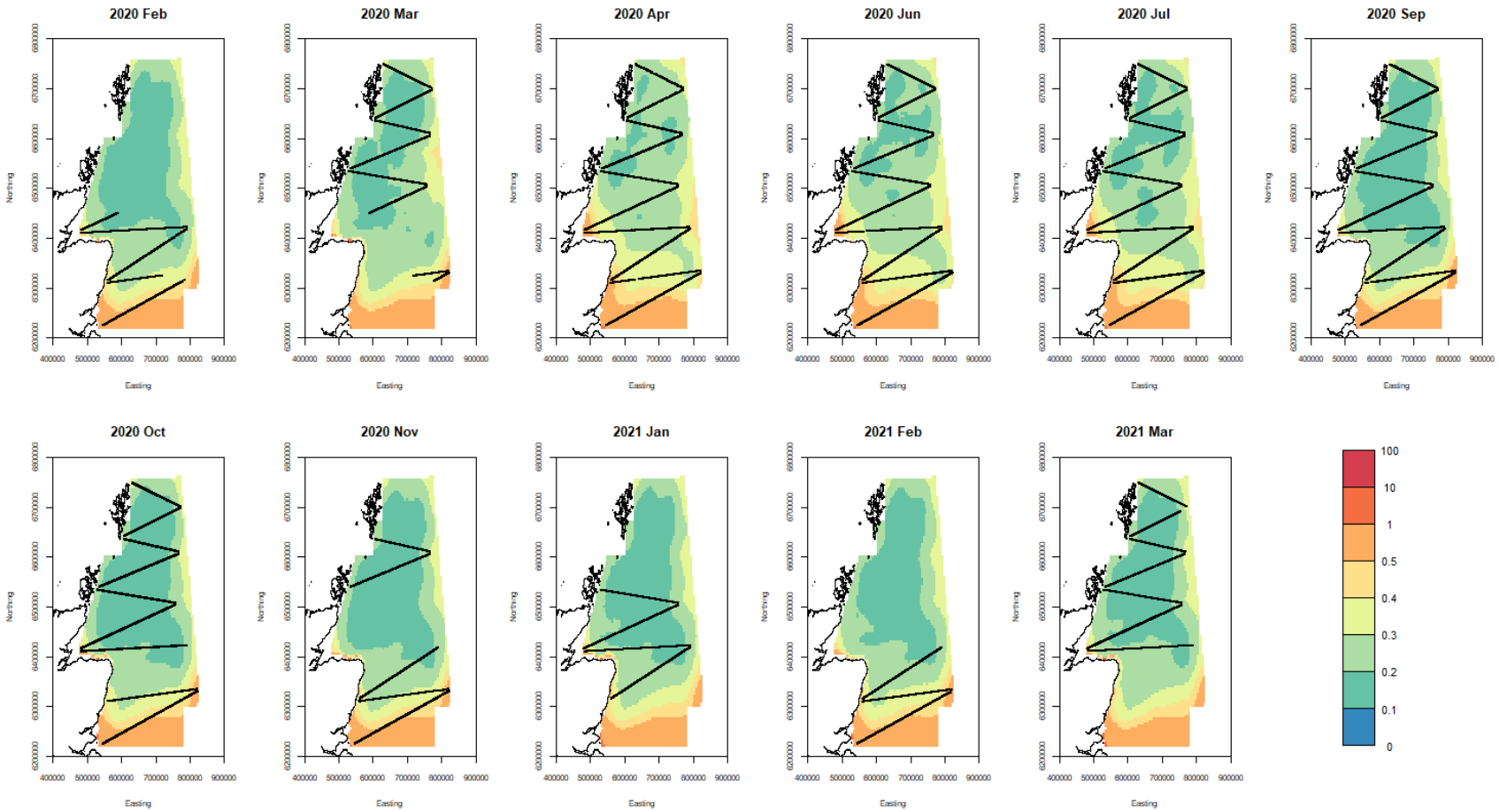

Figure 8. A graph showing coefficients of variation (CV, in %) in estimated densities of northern fulmars for each surveyed month from February 2020 to March 2021. Black lines indicate sampling locations in that month. The largest CVs are at the peripheries of the study area, especially in the south.

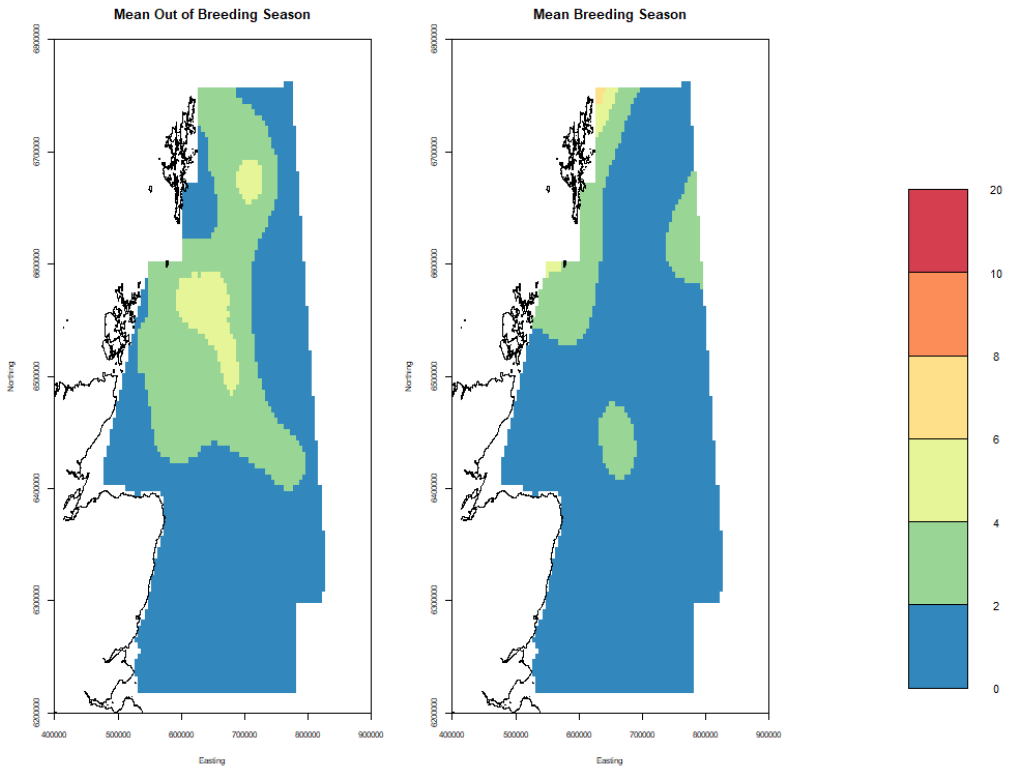

Figure 9. A graph showing mean fulmar density surfaces for breeding (April – August) and non-breeding (September – March) seasons.

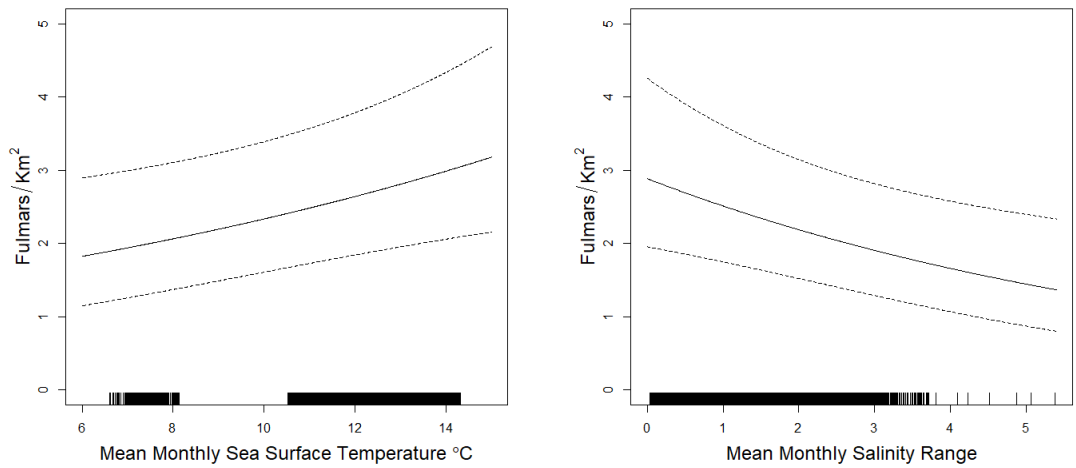

Figure 10. Graphs showing effect of (left) monthly sea surface temperature and (right) mean monthly salinity range on northern fulmar observed density assuming the middle of the survey area during the breeding season.

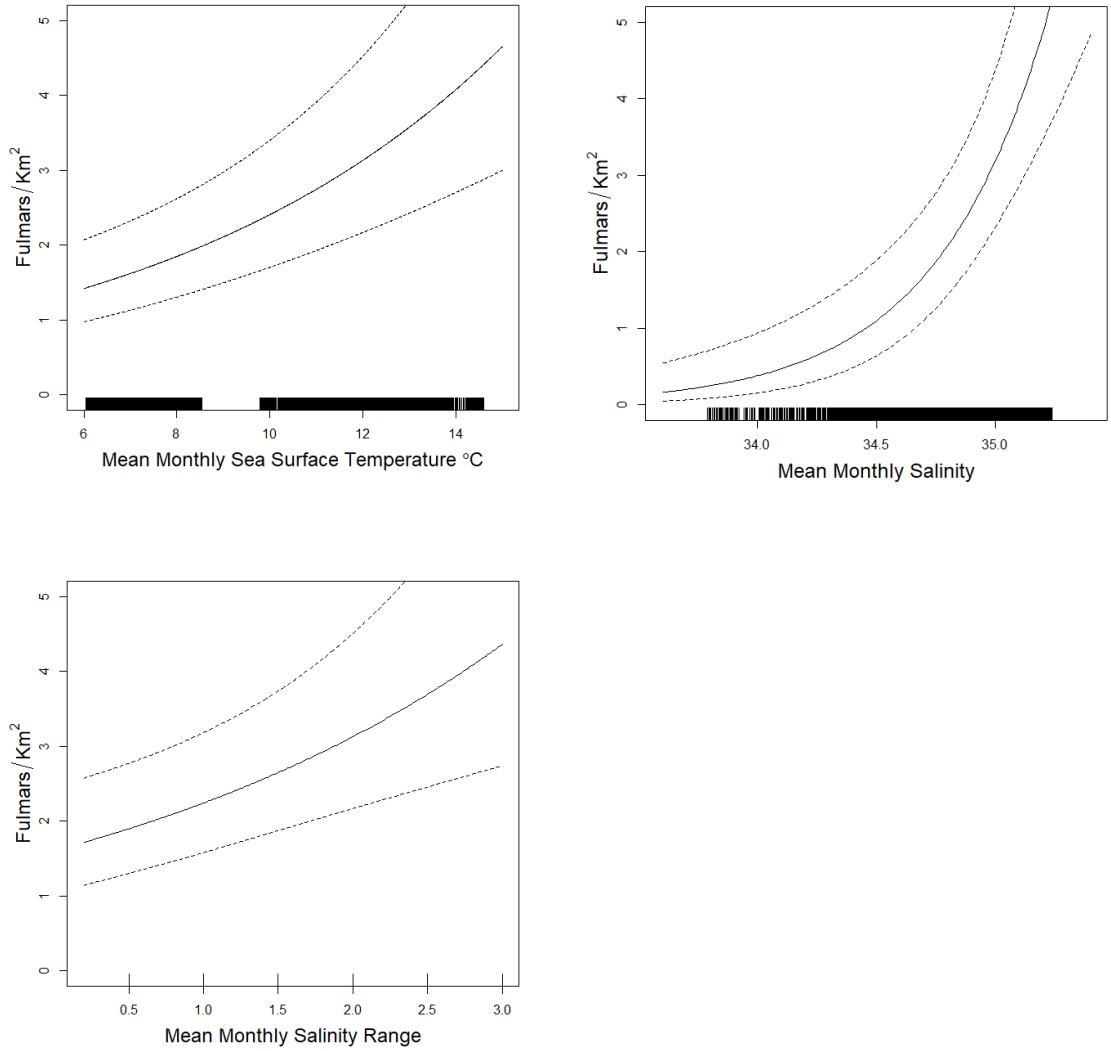

Figure 11. Graphs showing effect of (upper left) monthly sea surface temperature, (upper right) mean monthly salinity and (lower left) mean monthly salinity range on northern fulmar observed density assuming in the middle of survey area outside of the breeding season.

6.3.2 Northern Gannet

The best fit single model for the whole year is given in Table 8. Estimated numbers during the study period are depicted in Figure 12. They show a strong peak during the main breeding season between June and October.

Point estimates of gannet density for the sampling months along with the confidence bounds are given in Figures Figure 13, Figure 14 and Figure 15. They indicate a wide offshore distribution between June and October, with smaller numbers between

November and March occurring closer inshore in areas such as the Moray Firth. The CVs are shown in Figure 16 and are largest along the east and west border of the study area. The mean point estimates for breeding and non-breeding season in shown in Figure 17. The breeding distribution of birds is closer to the shore than in the non-breeding season.

The effect of sea surface temperature range on density is given in Figure 18 , and shows a general positive trend.

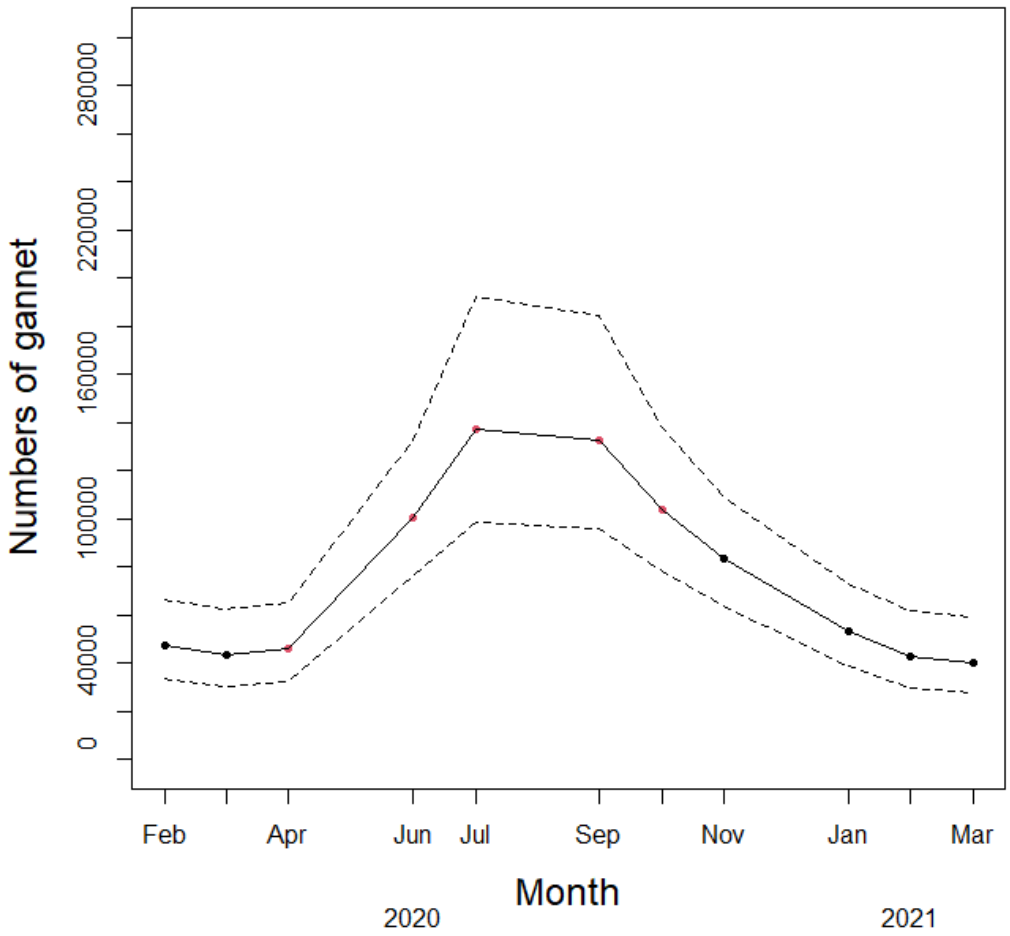

Figure 12. A graph showing estimated numbers of northern gannets over the duration of the study from February 2020 to March 2021. Red points indicate the breeding season (April to October) and the dashed lines represent upper and lower bounds of the 95% confidence intervals. Numbers of gannets peaked in July and September and had lowest values in winter months (January to April).

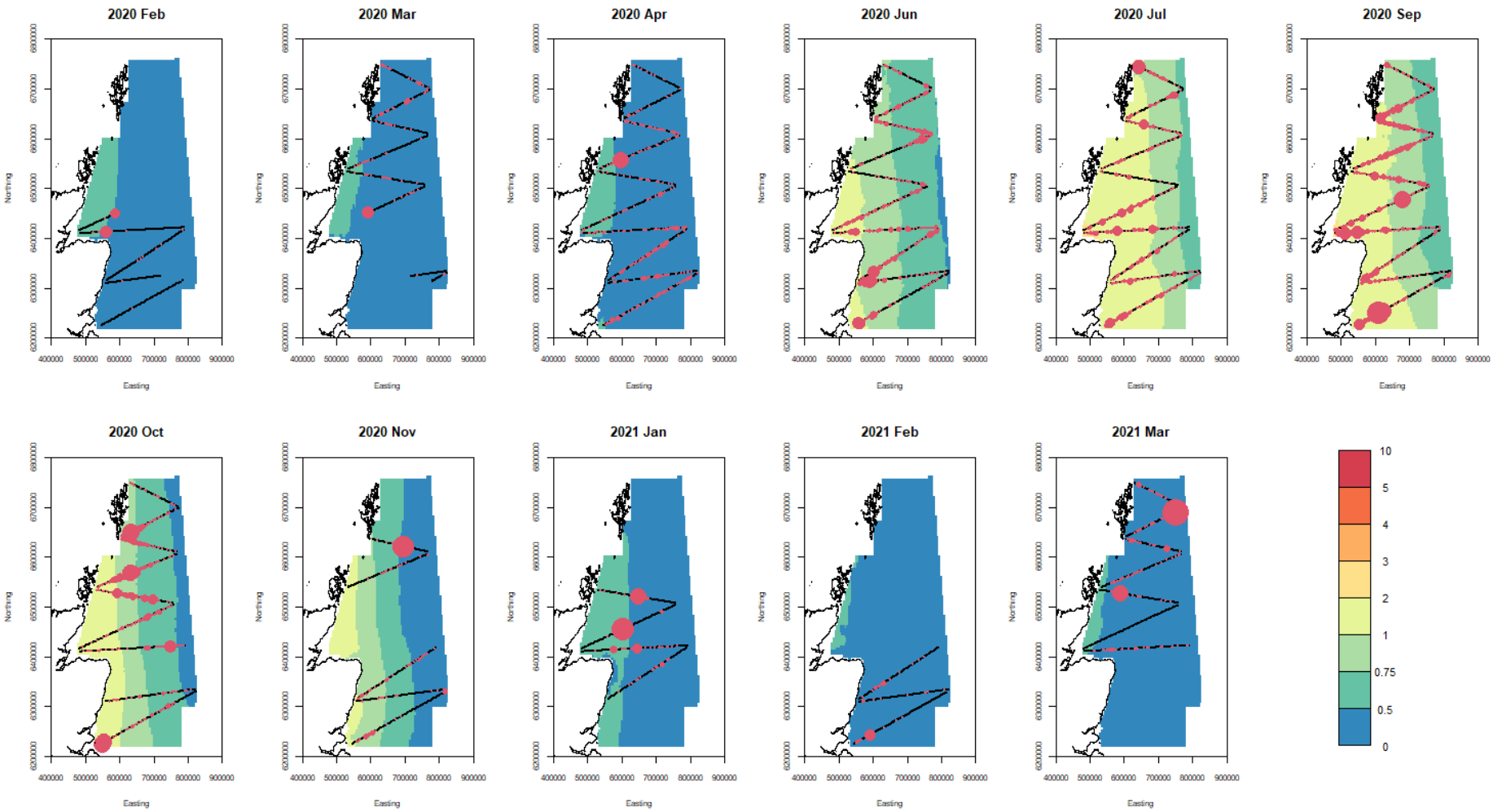

Figure 13. A graph showing point estimates of northern gannet densities for each surveyed month from February 2020 to March 2021. Colours represent estimated densities per km^2. Black lines indicate sampling locations in that month. Red dots indicate observed numbers of birds with size proportional to observed number. Note that scale is matching the following graphs depicting lower and upper confidence intervals.

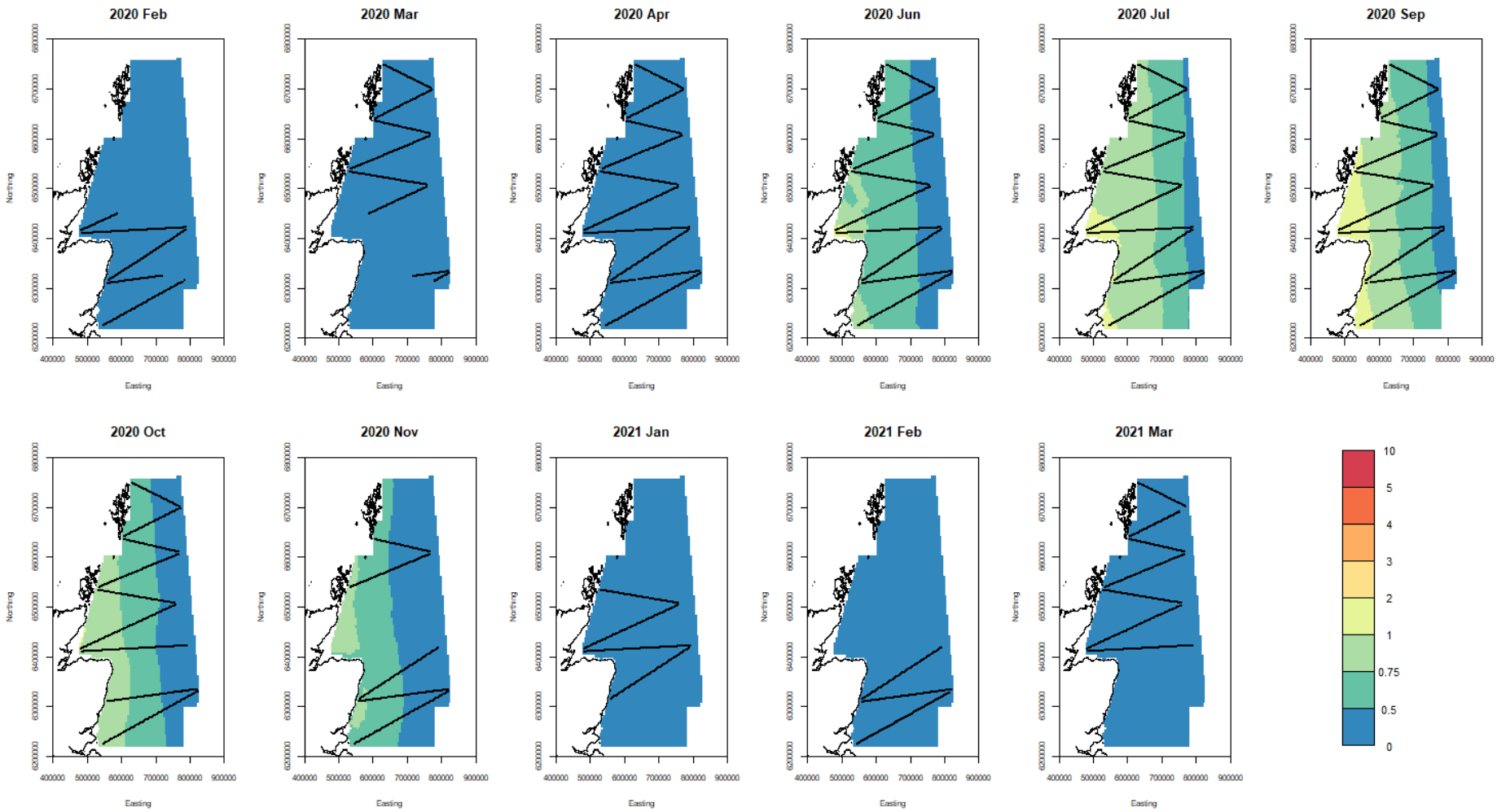

Figure 14. A graph showing lower confidence bound estimates (2.5%) of northern gannet densities for each surveyed month from February 2020 to March 2021. Colours represent estimated densities per km^2. Black lines indicate sampling locations in that month.

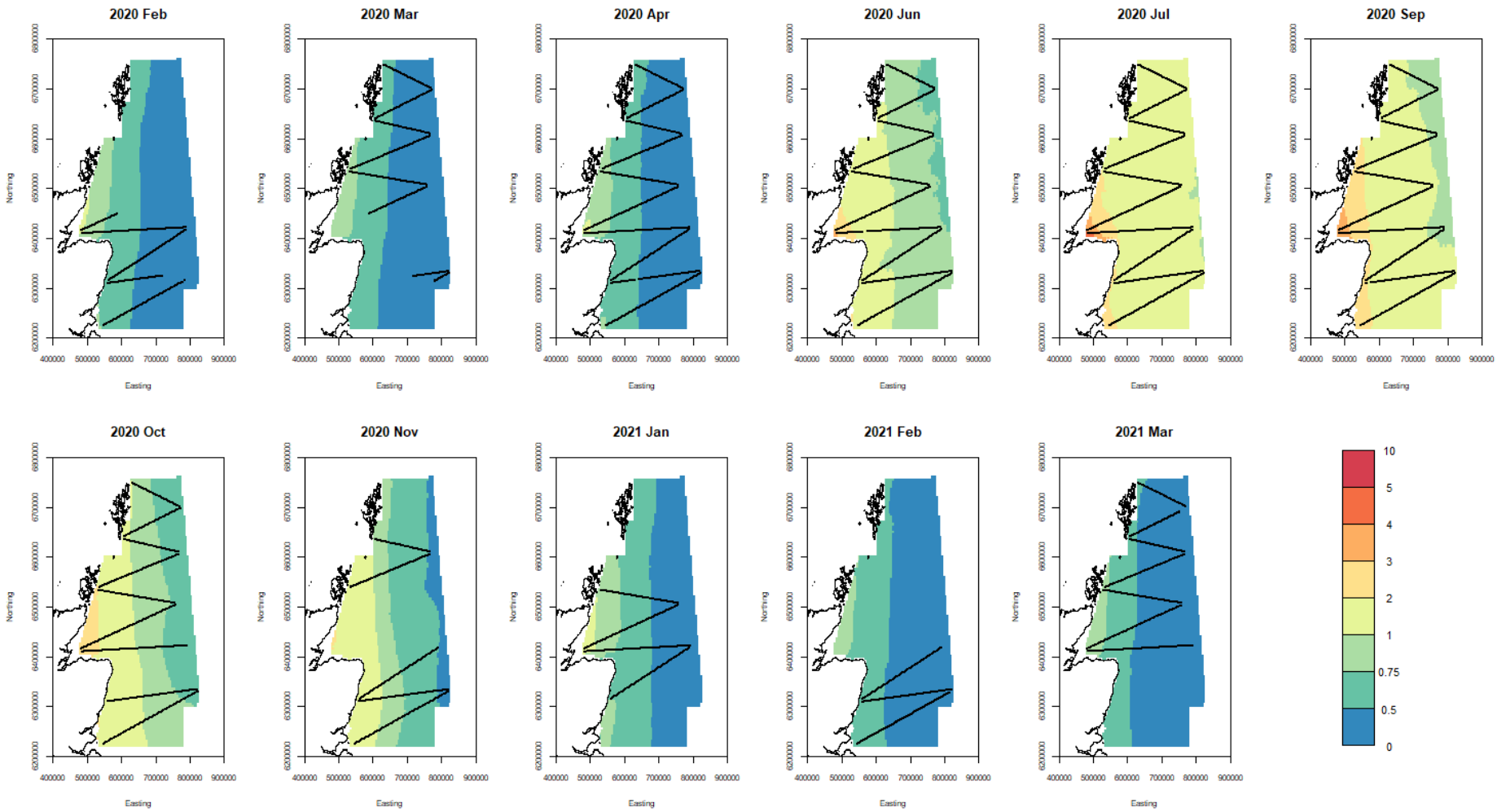

Figure 15. A graph showing upper confidence bound estimates (97.5%) of northern gannet densities for each surveyed month from February 2020 to March 2021. Colours represent estimated densities per km^2. Black lines indicate sampling locations in that month.

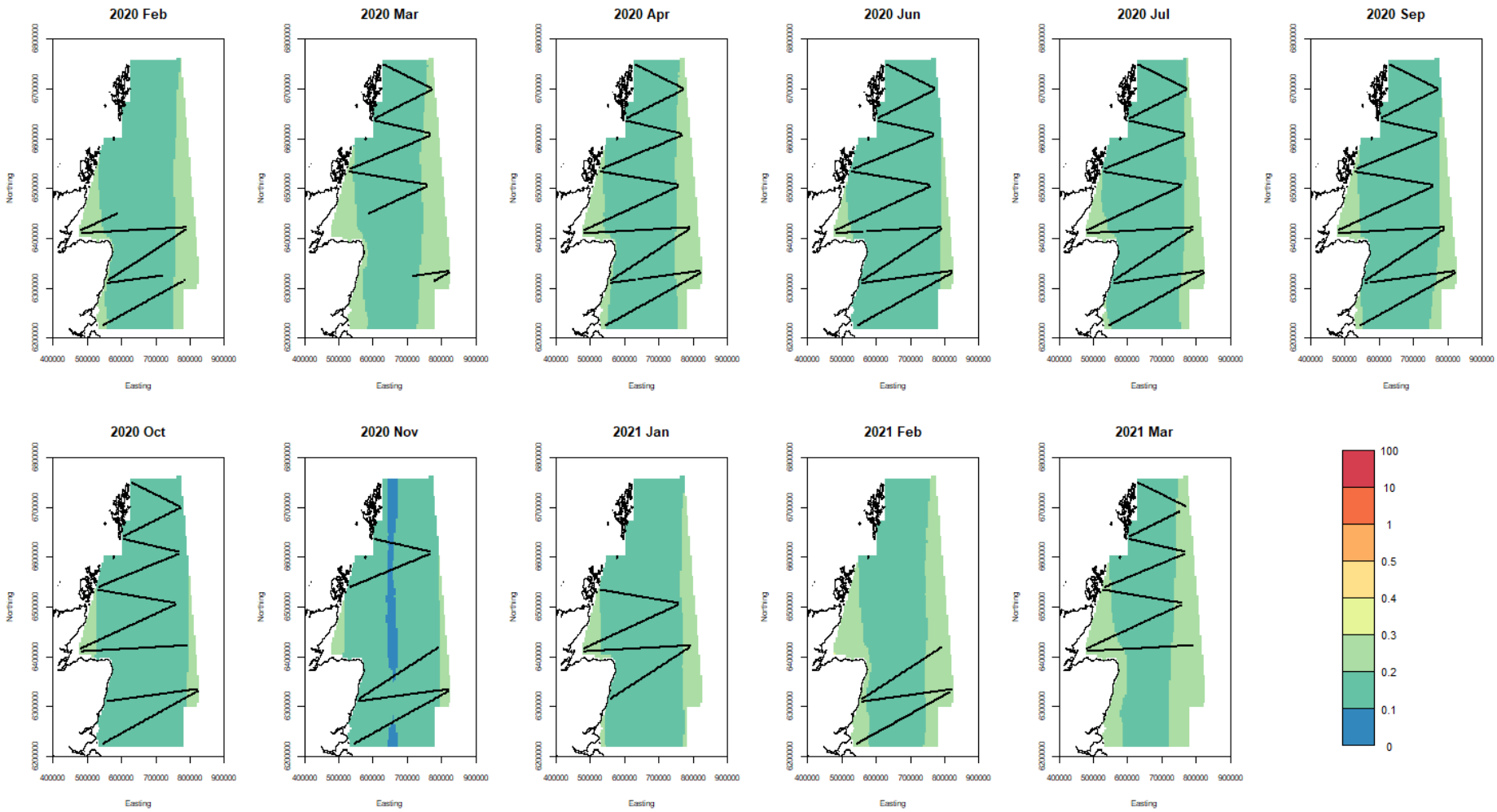

Figure 16. A graph showing northern gannet coefficients of variation (CV, in %) in estimated densities of birds for each surveyed month from February 2020 to March 2021. Black lines indicate sampling locations in that month. The largest CVs are at the eastern and western part of the study area.

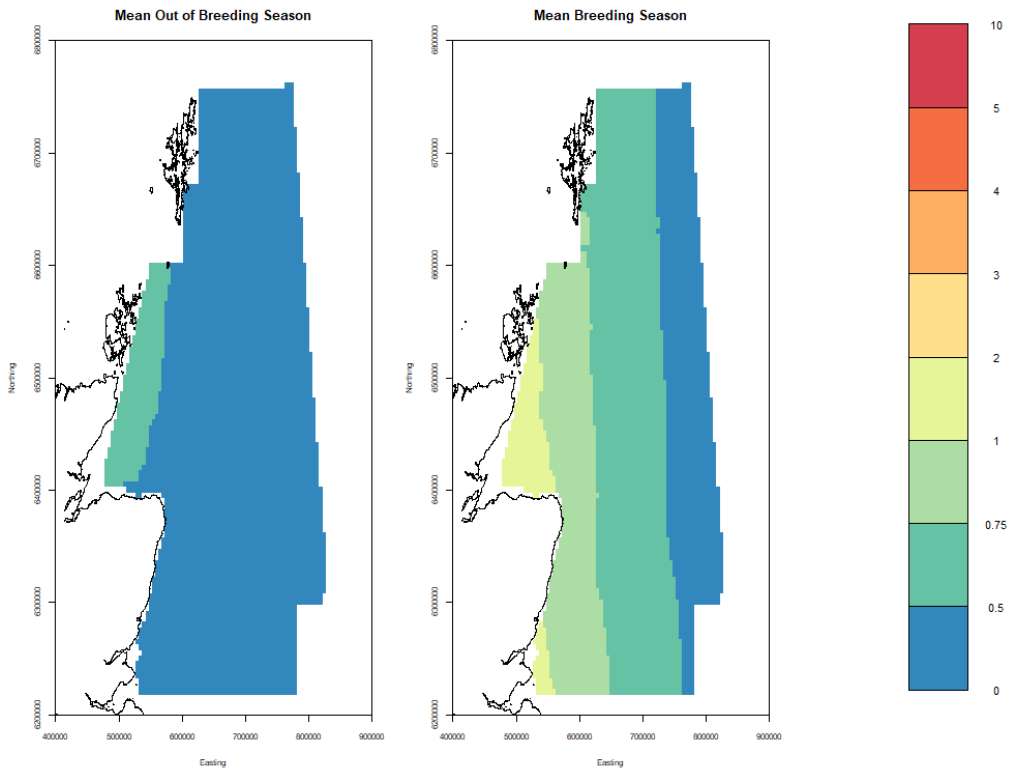

Figure 17. A graph showing mean northern gannet density (birds/km^2) surfaces for breeding (April – October) and non-breeding (November – March) seasons.

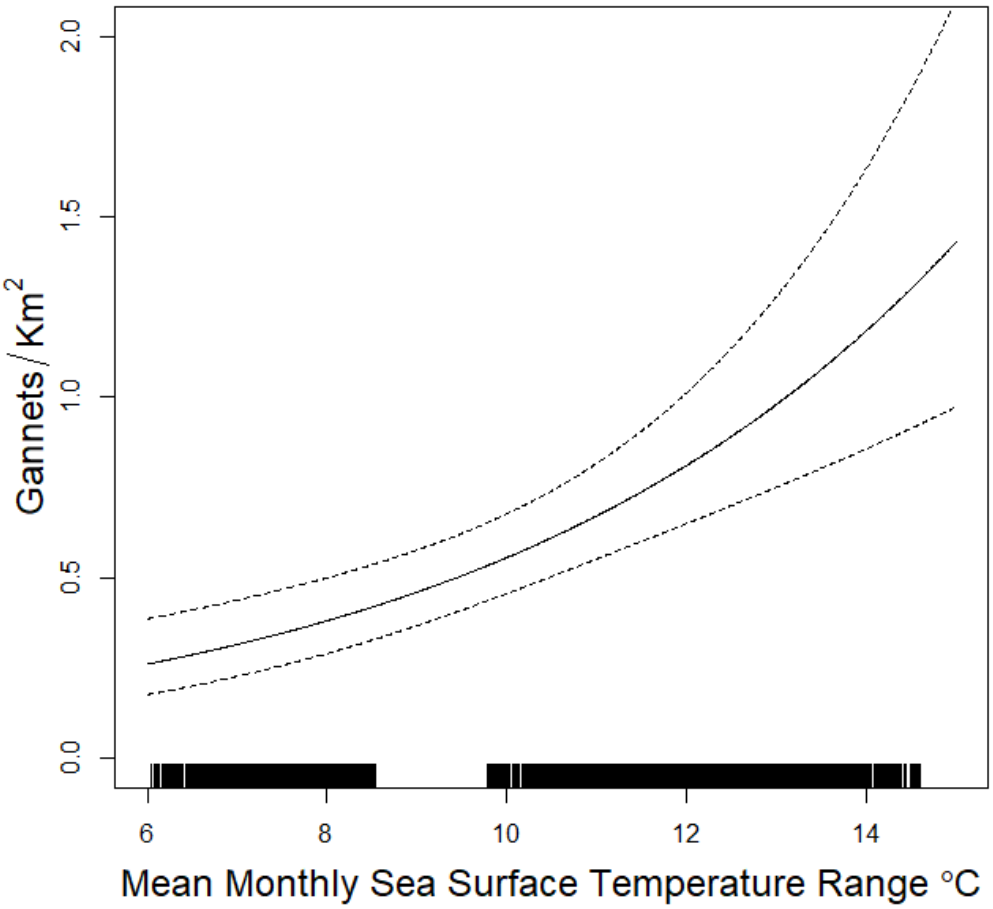

Figure 18. A graph showing effect of mean monthly sea surface temperature on northern gannet observed density assuming the middle of the survey area during the breeding season.

6.3.3 Great Skua

The model based on the amalgamated data set is given in Table 8. The estimates of numbers of great skuas during the survey period is given in Figure 19. They indicate peak abundance during the breeding season. The results of this model should be treated with caution as the diagnostics of the model were not ideal.

Point estimates of great skua density for the sampling months along with the confidence bounds are given in Figures Figure 20, Figure 21 and Figure 22. They show highest densities in the far north-western part of the survey region east of Shetland. The CVs are shown in Figure 23 and are largest at the southern areas of the study site during the breeding season and at the peripheral areas of the study site outside the breeding season. The mean point estimates for breeding and non-

breeding season in shown in Figure 24 The breeding distribution is concentrated at the northern site of the study area.

The effect of the non-location variable, sea surface temperature monthly range, in (red) and outside (black) the breeding season, is given in Figure 25.

Note that these are the effects given the presence of location in the model, so they may be very different from the actual biological effect.

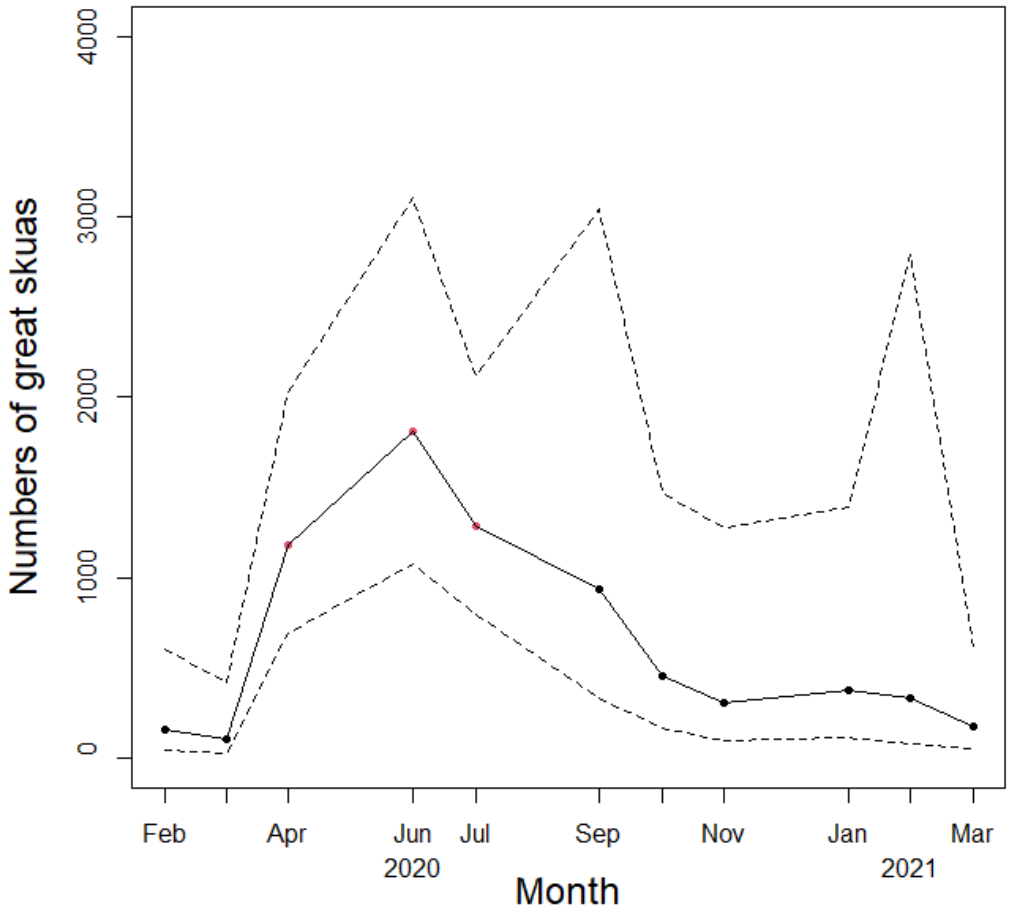

Figure 19. A graph showing estimated numbers of great skuas over the duration of the study from February 2020 to March 2021. Red points indicate the breeding season (April to July) and the dashed lines represent upper and lower bounds of the 95% confidence intervals. Numbers of great skuas peaked in June and had lowest values in late autumn and winter months (November to March). The results of this model should be treated with caution as not all model assumptions were met.

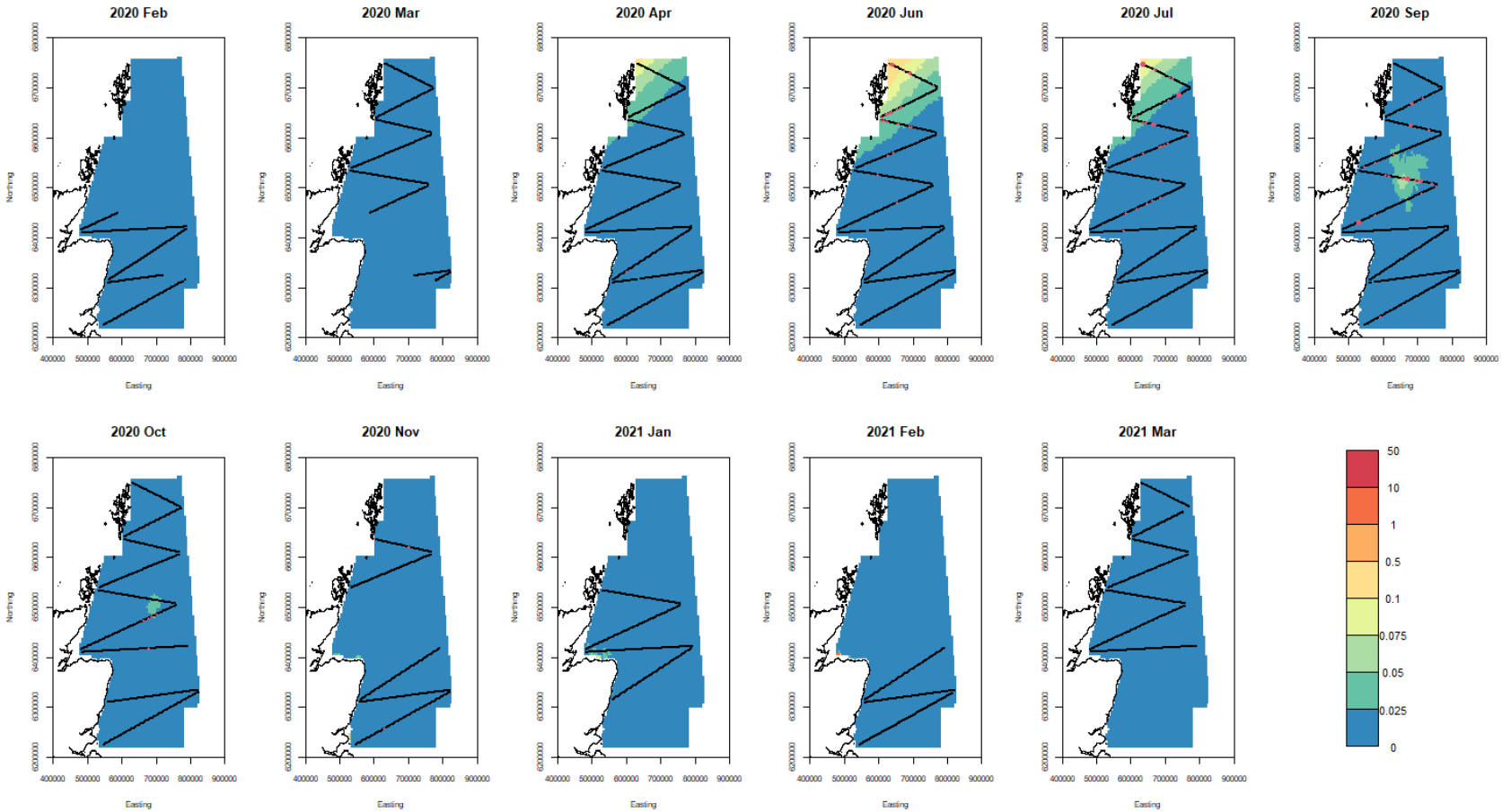

Figure 20. A graph showing point estimates of great skua densities for each surveyed month from February 2020 to March 2021. Colours represent estimated densities per km^2. Black lines indicate sampling locations in that month. Red dots indicate observed numbers of birds with size proportional to observed number. Note that scale is matching the following graphs depicting lower and upper confidence intervals. *The results of this model should be treated with caution as not all model assumptions were met.*

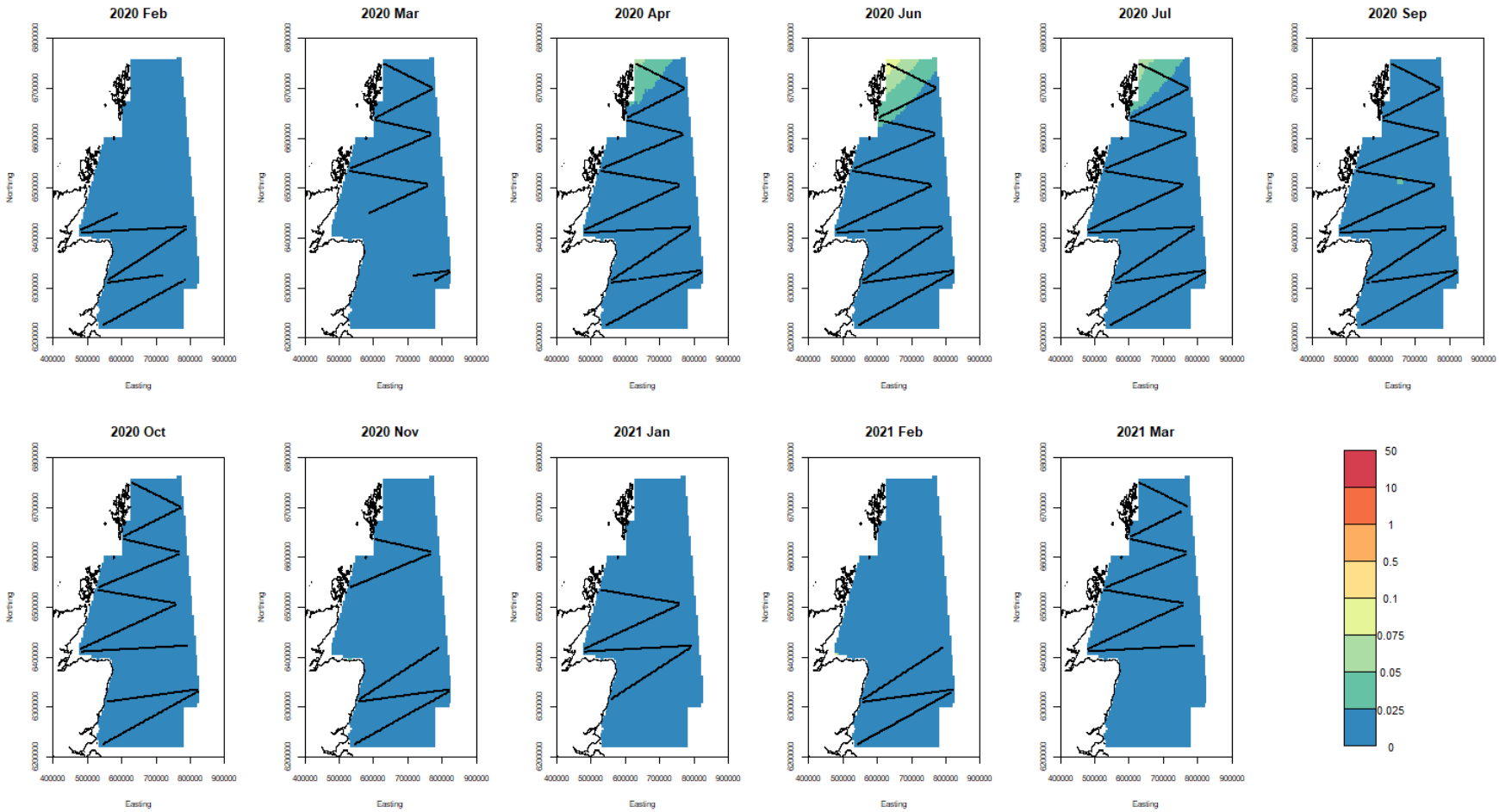

Figure 21. A graph showing lower confidence bound estimates (2.5%) of great skua densities for each surveyed month from February 2020 to March 2021. Colours represent estimated densities per km^2. Black lines indicate sampling locations in that month. The results of this model should be treated with caution as not all model assumptions were met.

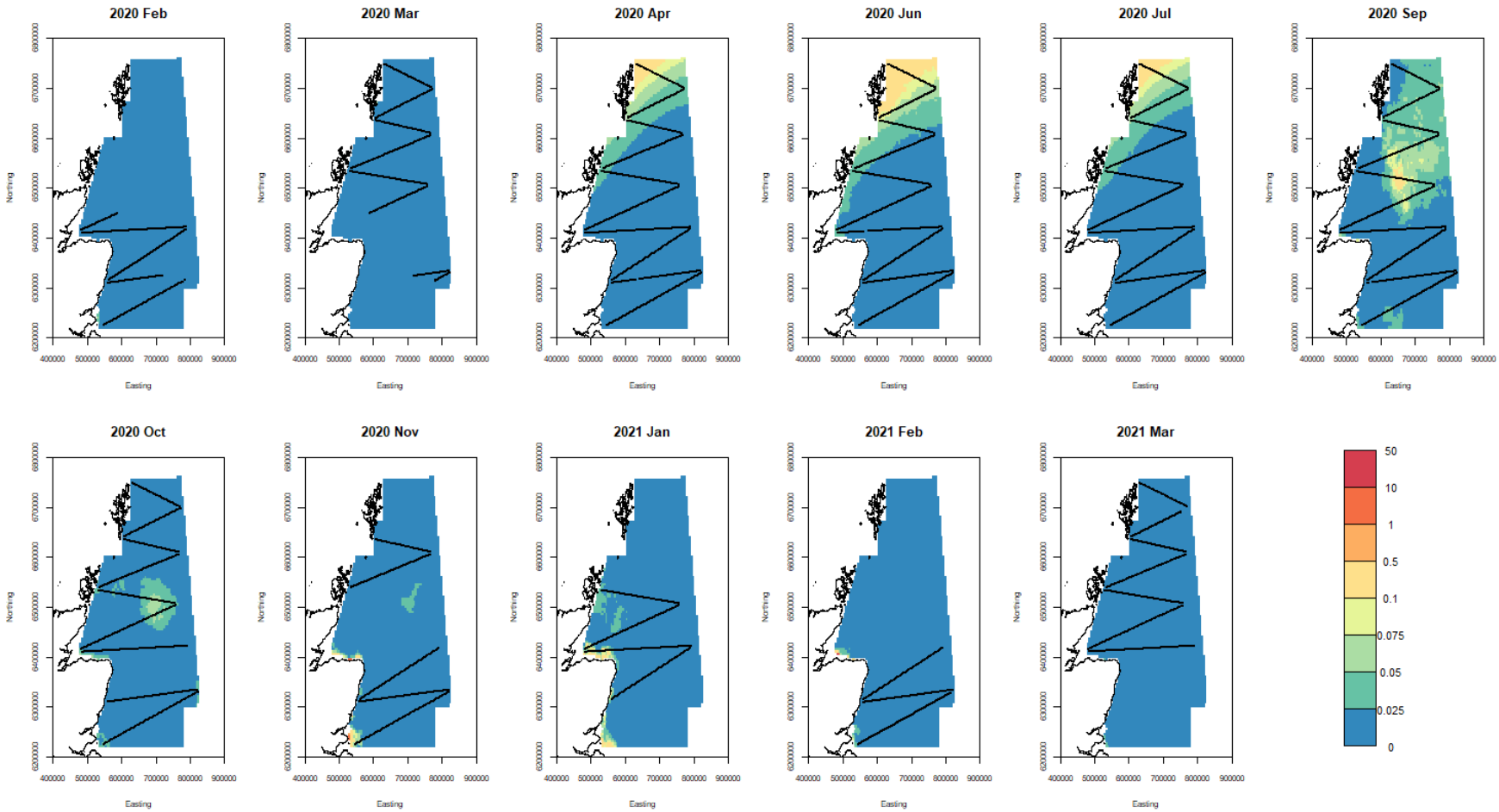

Figure 22. A graph showing upper confidence bound estimates (97.5%) of great skua densities for each surveyed month from February 2020 to March 2021. Colours represent estimated densities per km^2. Black lines indicate sampling locations in that month. The results of this model should be treated with caution as not all model assumptions were met.

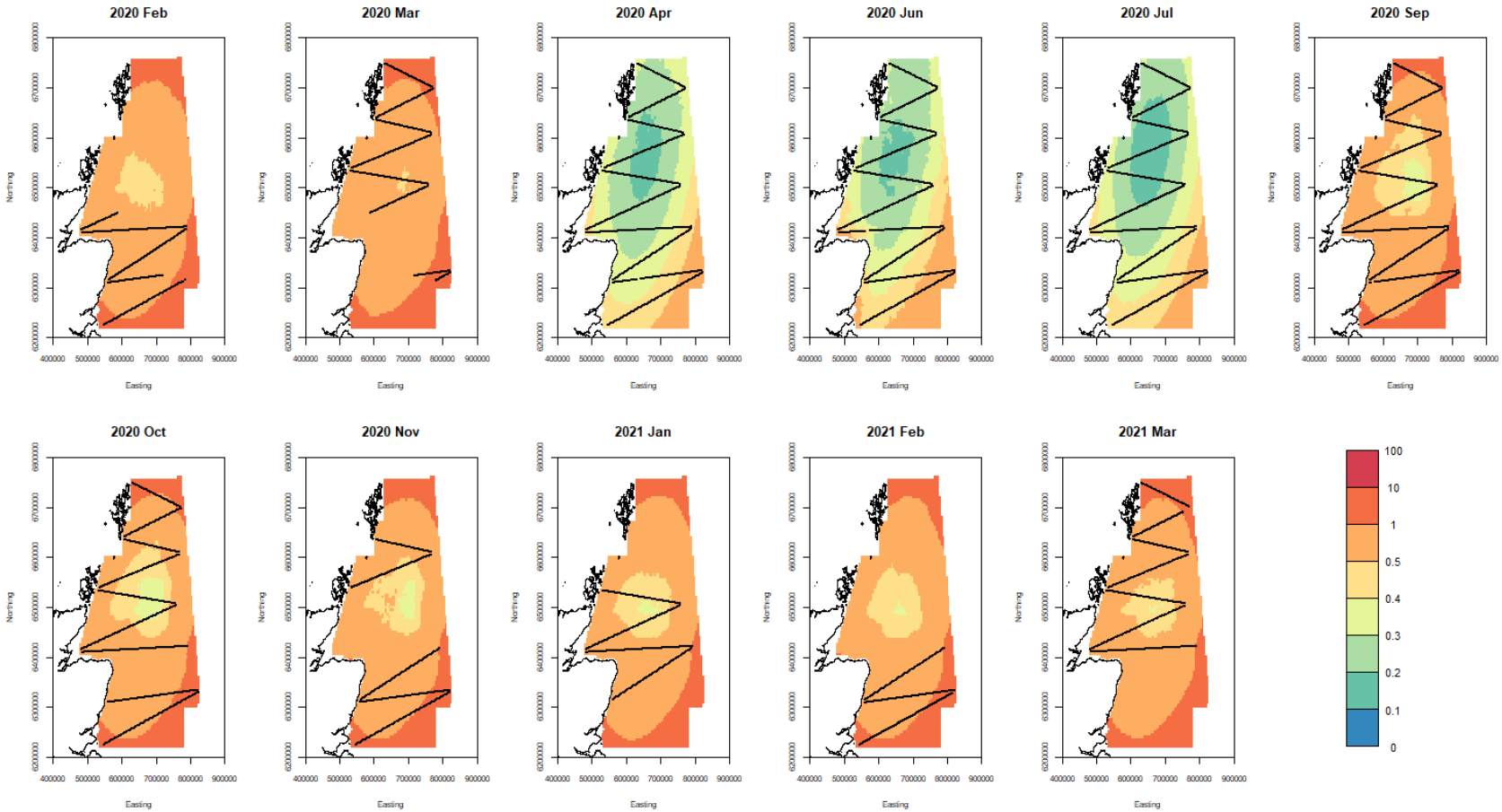

Figure 23. A graph showing great skua coefficients of variation (CV, in %) in estimated densities of birds for each surveyed month from February 2020 to March 2021. Black lines indicate sampling locations in that month. The largest CVs are at the peripheries of he study area outside the breeding season and in the southern art during the breeding season. The results of this model should be treated with caution as not all model assumptions were met.

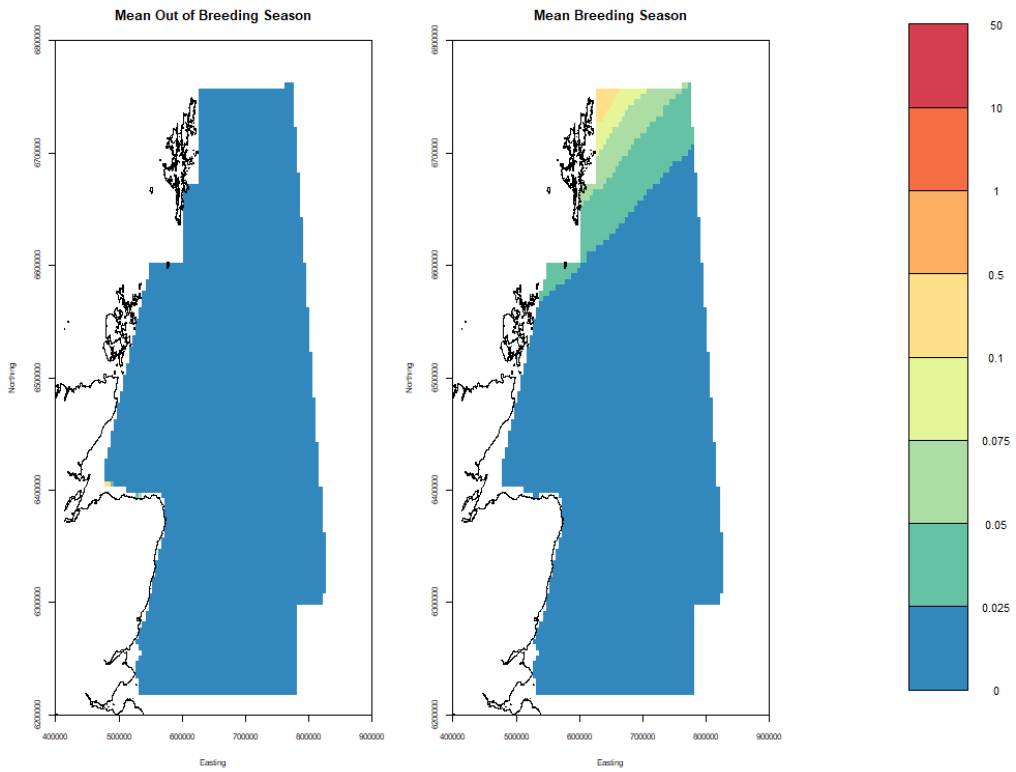

Figure 24. A graph showing mean great skua density (birds/km^2) surfaces for breeding (April – July) and non-breeding (August – March) seasons. The results of this model should be treated with caution as not all model assumptions were met.

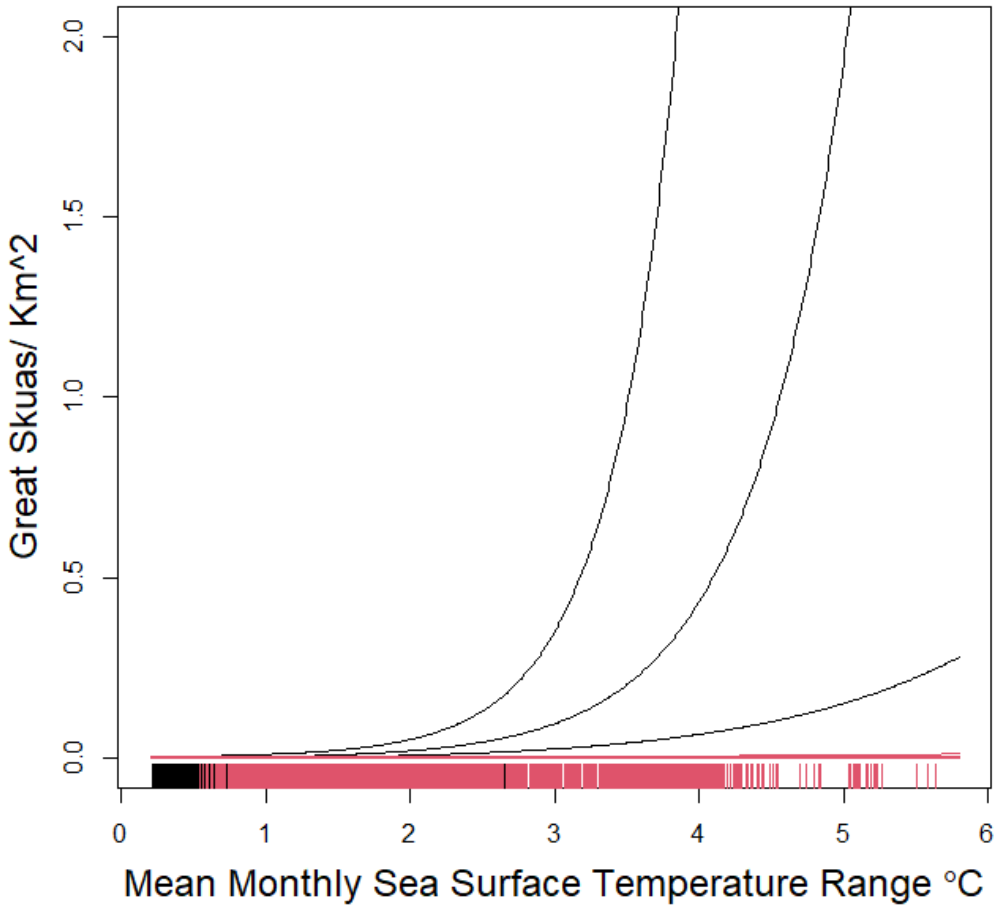

Figure 25. A graph showing effect of (mean monthly sea surface temperature range in (red) and out (black) the breeding season on great skua observed density assuming the middle of the survey area during respective season.

6.3.4 Common Gull

Predictions based a breeding season model is given in Table 8. No model was fitted to non-breeding season. Estimates of numbers in the area over the survey period are given in Figure 26. They show a general increase in abundance in the study area in the autumn. Results are constant within season.

Point estimates of common gull density for the sampling months along with the confidence bounds are given in Figure 27, Figure 28, and Figure 29. They indicate higher densities mainly off the coast during the breeding season. As the spatial pattern was uniform and consistent over the survey month for both breeding and non-breeding season, seasonal spatial patterns are not presented for this species as it can be deduced from Figure 27, Figure 28, Figure 29. The CVs are shown in Figure 30 and are largest at the central and norther part of the study site.

The effect of depth during the breeding season is shown in Figure 31.

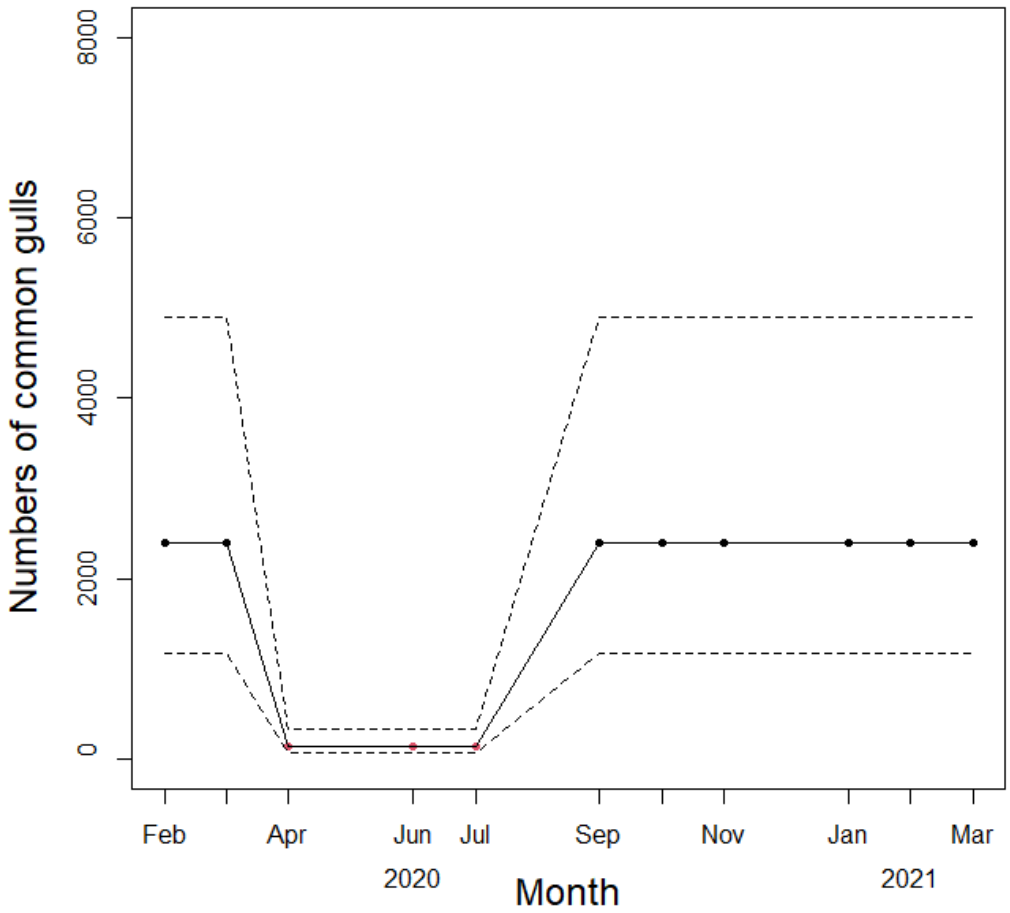

Figure 26. A graph showing estimated numbers of common gulls over the duration of the study from February 2020 to March 2021. Red points indicate the breeding season (April to July) and the dashed lines represent upper and lower bounds of the

95% confidence intervals. Numbers of common gulls was lowest during the breeding season.

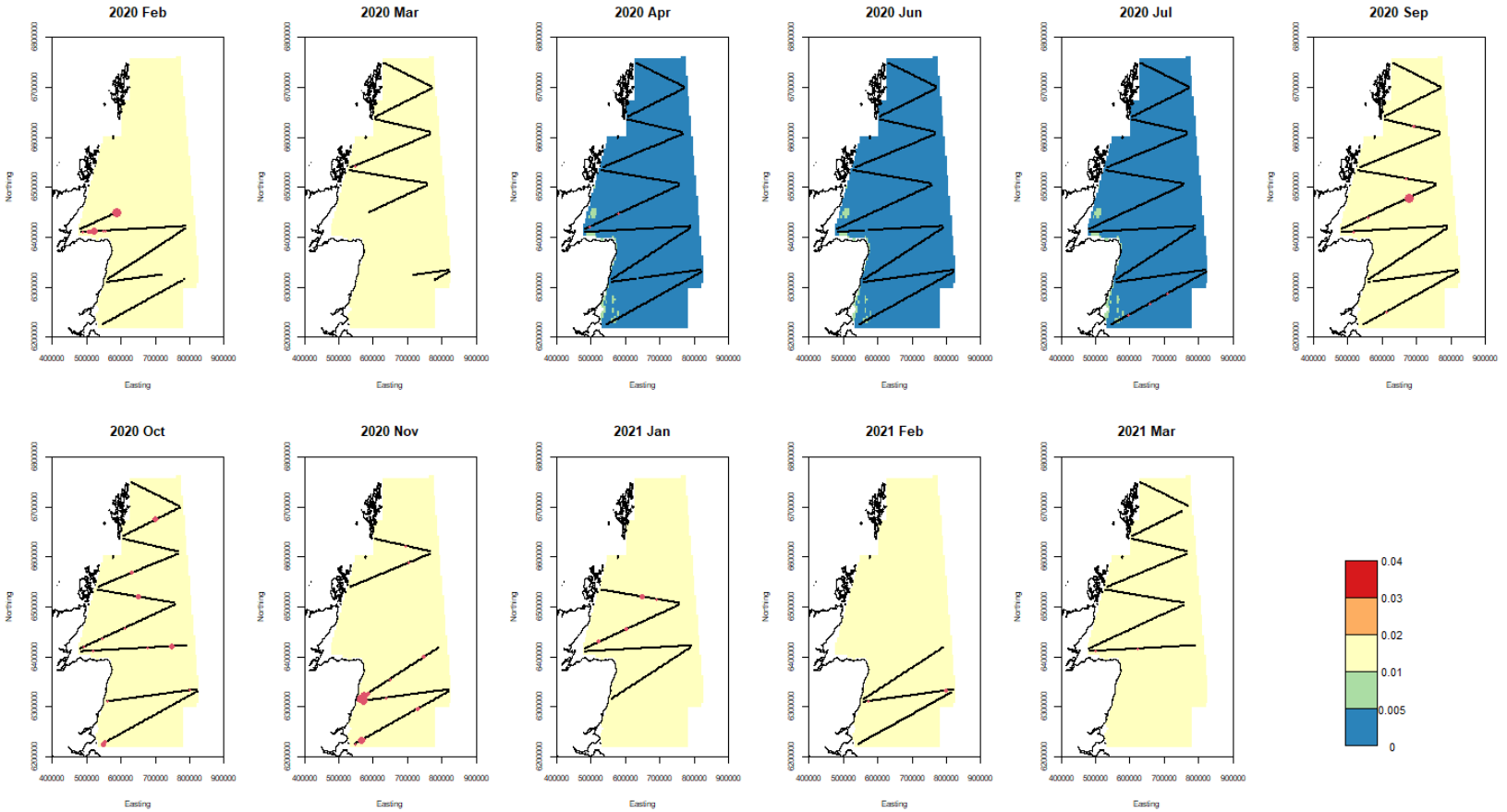

Figure 27. A graph showing point estimates of common gull densities for each surveyed month from February 2020 to March 2021. Colours represent estimated densities per km^2. Black lines indicate sampling locations in that month. Red dots indicate observed numbers of birds with size proportional to observed number. Note that scale is matching the following graphs depicting lower and upper confidence intervals. As the spatial pattern in density was consistent and uniform outside the breeding season, the graphs show mean estimates for non-breeding season for each surveyed month within this season.

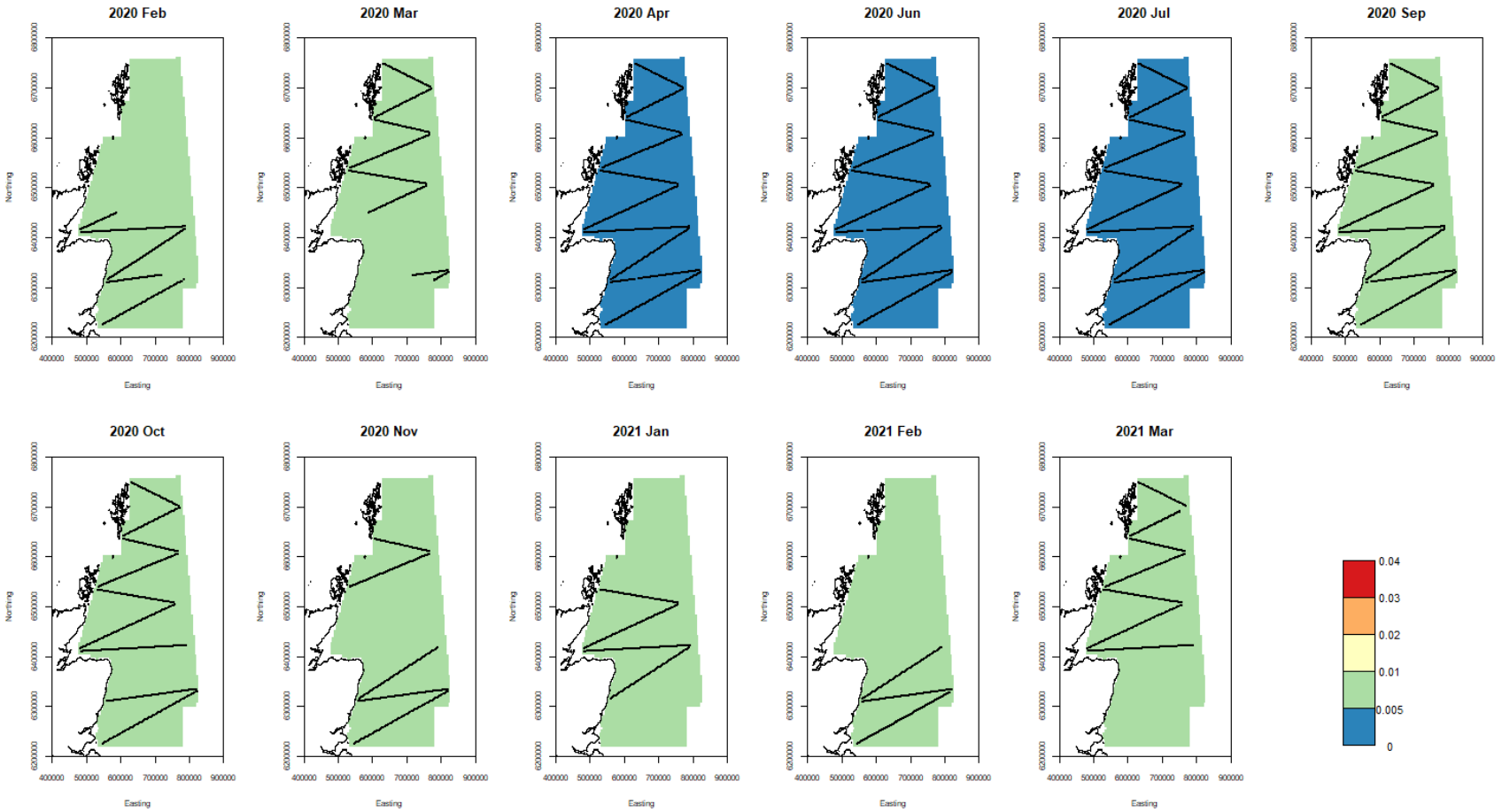

Figure 28. A graph showing lower confidence bound estimates (2.5%) of common gull densities for each surveyed month from February 2020 to March 2021. Colours represent estimated densities per km^2. Black lines indicate sampling locations in that month. As the spatial pattern in density was consistent and uniform outside the breeding season, the graphs show mean estimates for non-breeding season for each surveyed month within this season.

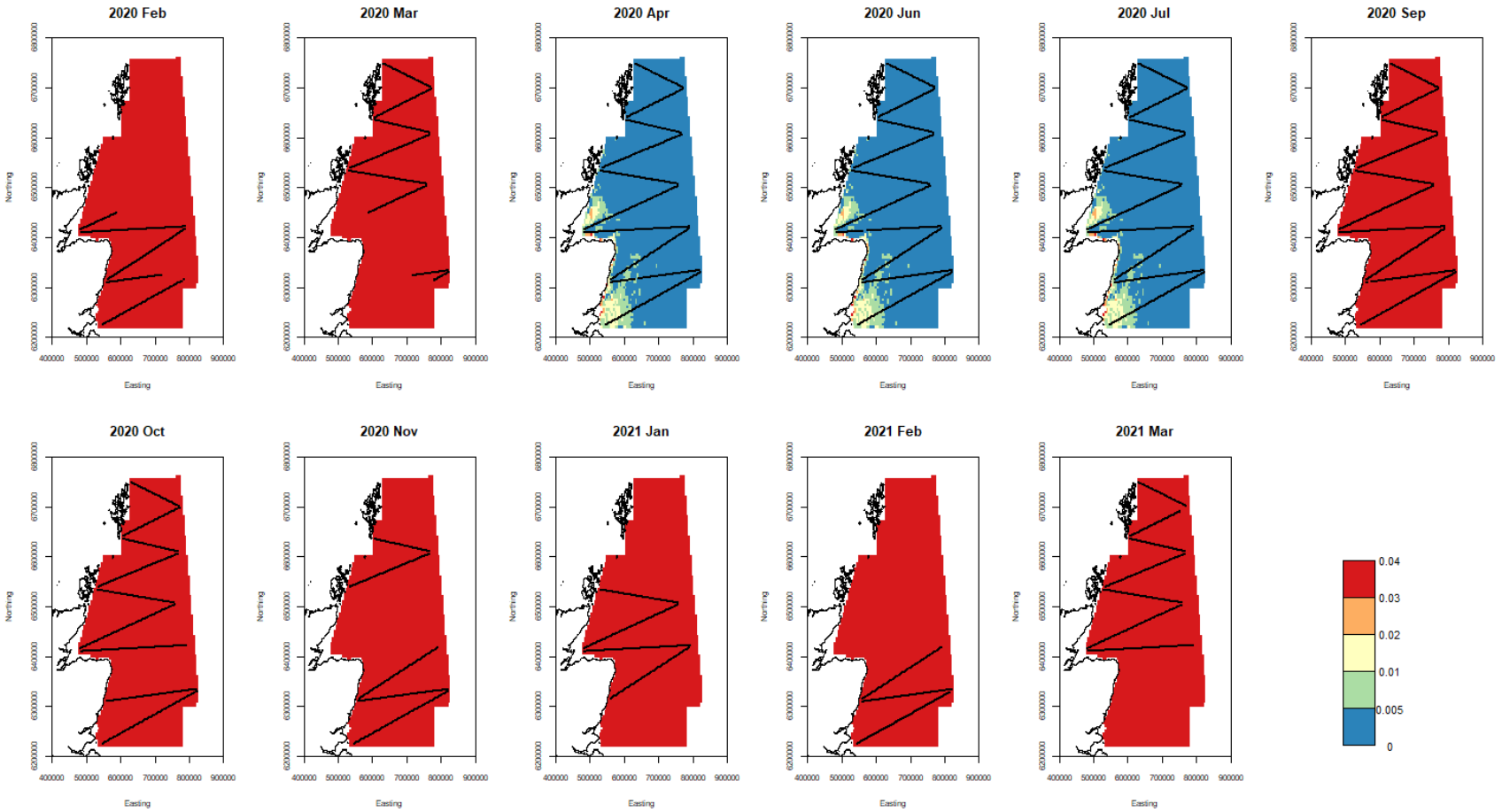

Figure 29. A graph showing upper confidence bound estimates (97.5%) of common gull densities for each surveyed month from February 2020 to March 2021. Colours represent estimated densities per km^2. Black lines indicate sampling locations in that month. As the spatial pattern in density was consistent and uniform outside the breeding season, the graphs show mean estimates for non-breeding season for each surveyed month within this season.

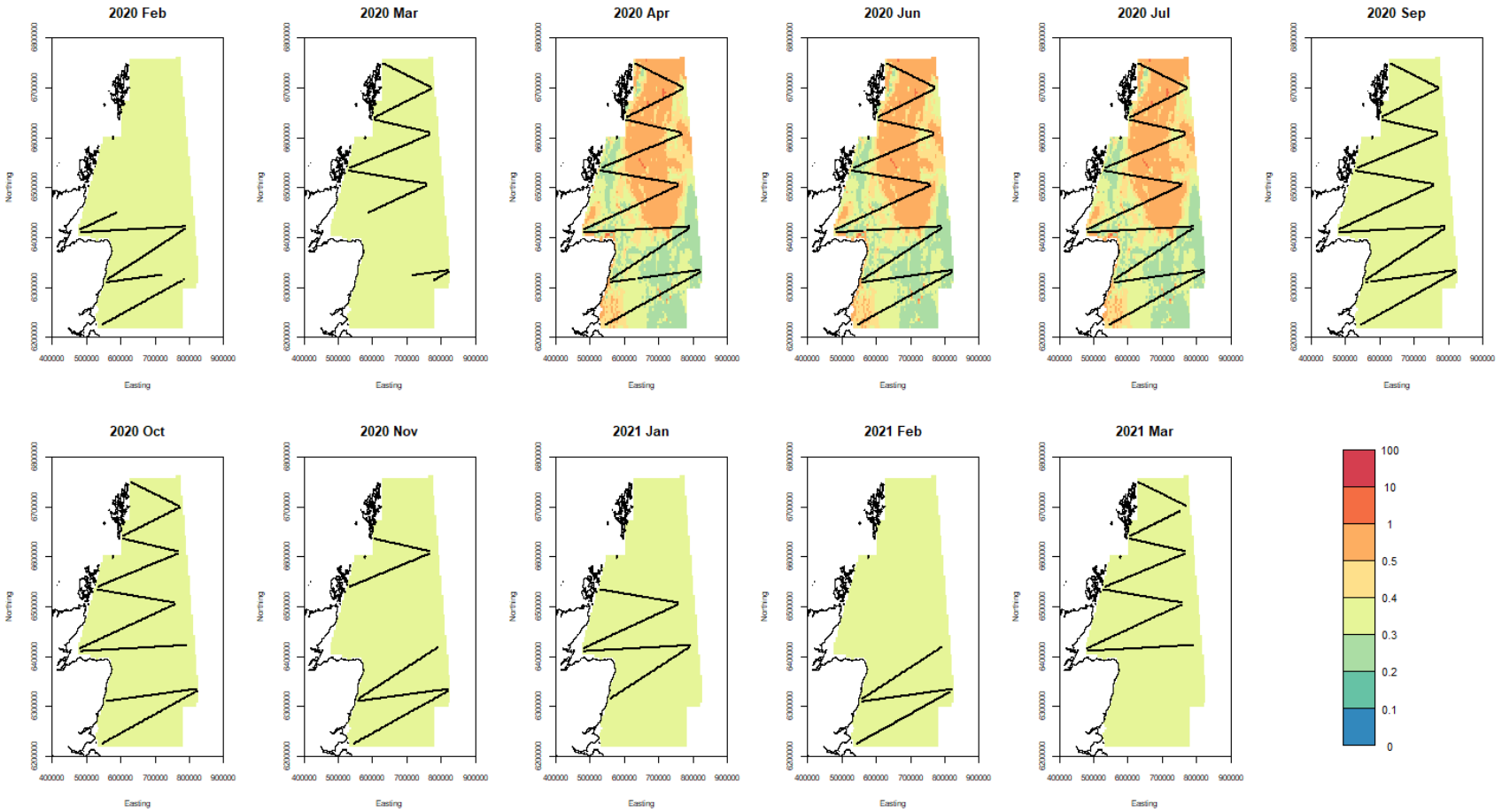

Figure 30. A graph showing common gull coefficients of variation (CV, in %) in estimated densities of birds for each surveyed month from February 2020 to March 2021. Black lines indicate sampling locations in that month. As the spatial pattern in density was consistent and uniform outside the breeding season, the graphs show mean estimates for non-breeding season for each surveyed month within this season.

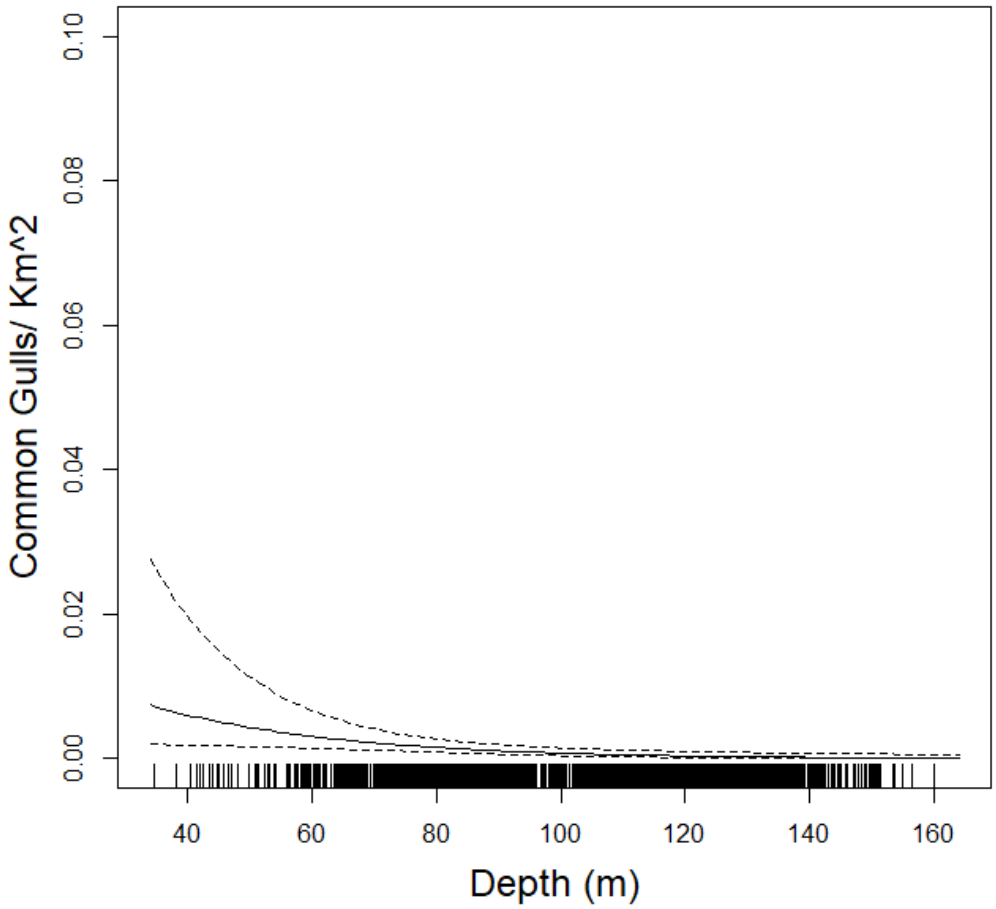

Figure 31. A graph showing the effect of depth on common gull observed densities assuming the middle of survey area. The effect of depth is estimated breeding season only.

6.3.5 Lesser Black-backed Gull

No variables were found that could predict the density of lesser black-backed gulls when the autocorrelation in the data was considered. The best estimate for abundance was 640 (95% CI: 280-1490). This species was only observed during five surveys and in very low numbers.

6.3.6 Herring Gull

The single (all year) fitted model is given in Table 8. Estimates of numbers in the area over the survey period are given in Figure 32. They show a general increase in abundance in the study area between September and March.

Point estimates of herring gull density for the sampling months along with the confidence bounds are given in Figure 33, Figure 34, and Figure 35. They indicate higher densities in the vicinity of the Moray Firth in October and November. The CVs are shown in Figure 36 and are largest at the peripheries of the study area. The mean point estimates for breeding and non-breeding season in shown in

Figure 37. The breeding distribution is closer to the shore in the non-breeding season.

The non-location spatial effects in all year model for herring gull are given below. They show greater densities in winter, and at greater depths during the breeding season but no relationship in the non-breeding season (Figure 38).

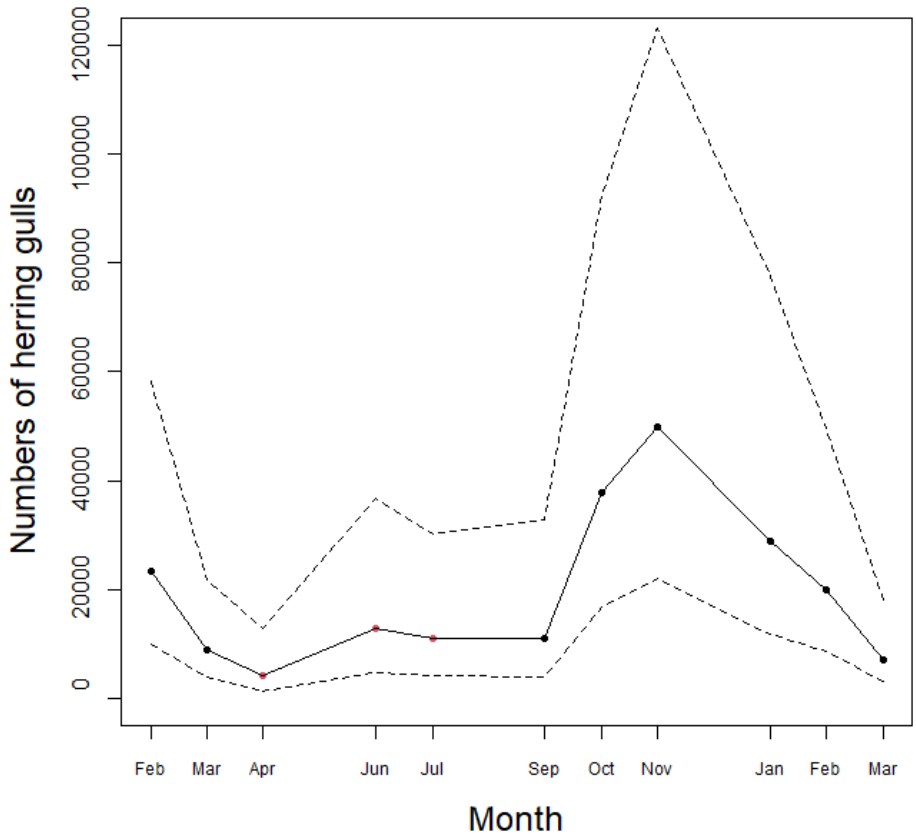

Figure 32. A graph showing estimated numbers of herring gull over the duration of the study from February 2020 to March 2021. Red points indicate the breeding season (April to July) and the dashed lines represent upper and lower bounds of the 95% confidence intervals. Numbers of herring gulls peaked in November.

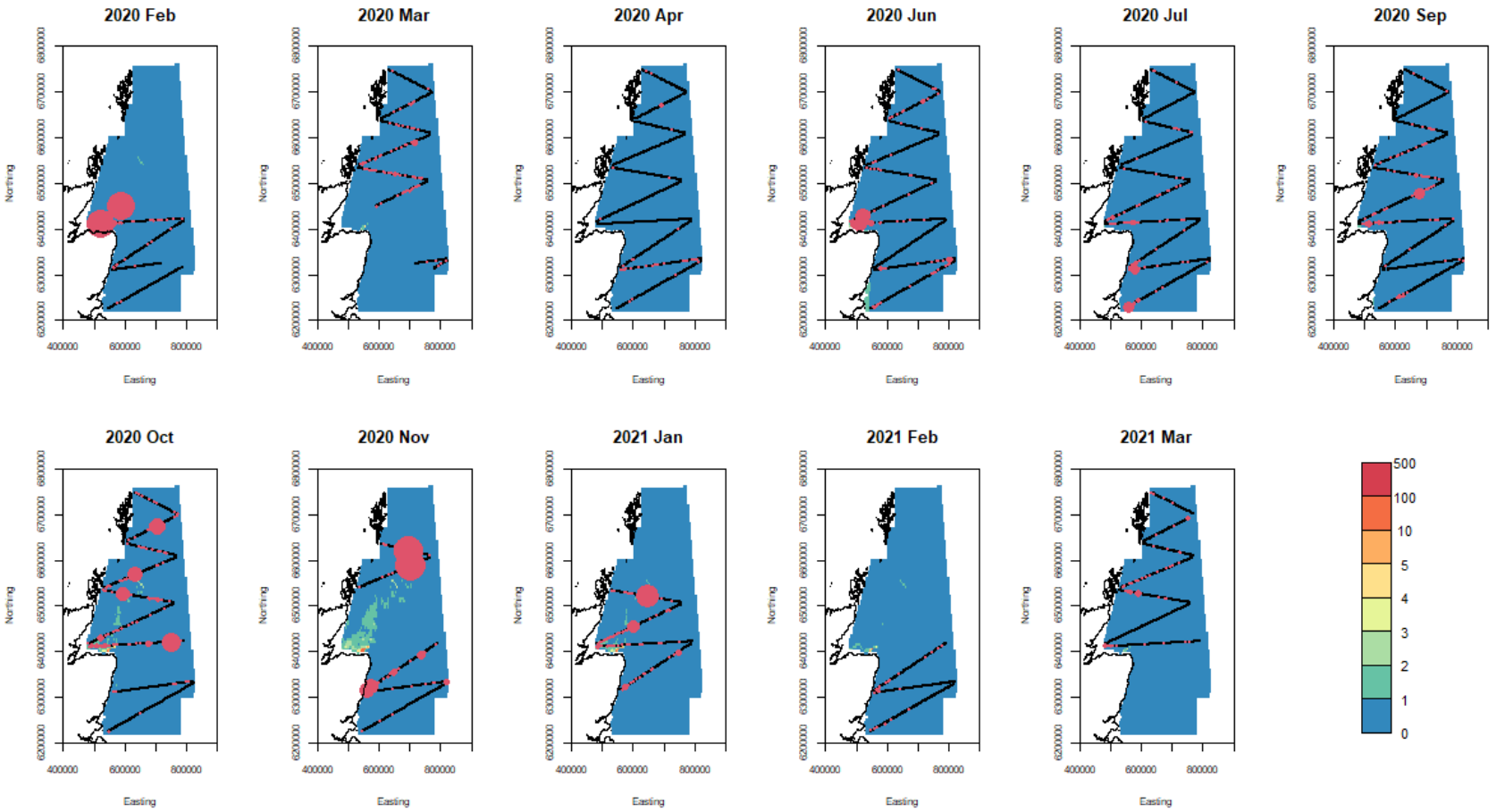

Figure 33. A graph showing point estimates of herring gull densities for each surveyed month from February 2020 to March 2021. Colours represent estimated densities per km^2. Black lines indicate sampling locations in that month. Red dots indicate observed numbers of birds with size proportional to observed number. Note that scale is matching the following graphs depicting lower and upper confidence intervals.

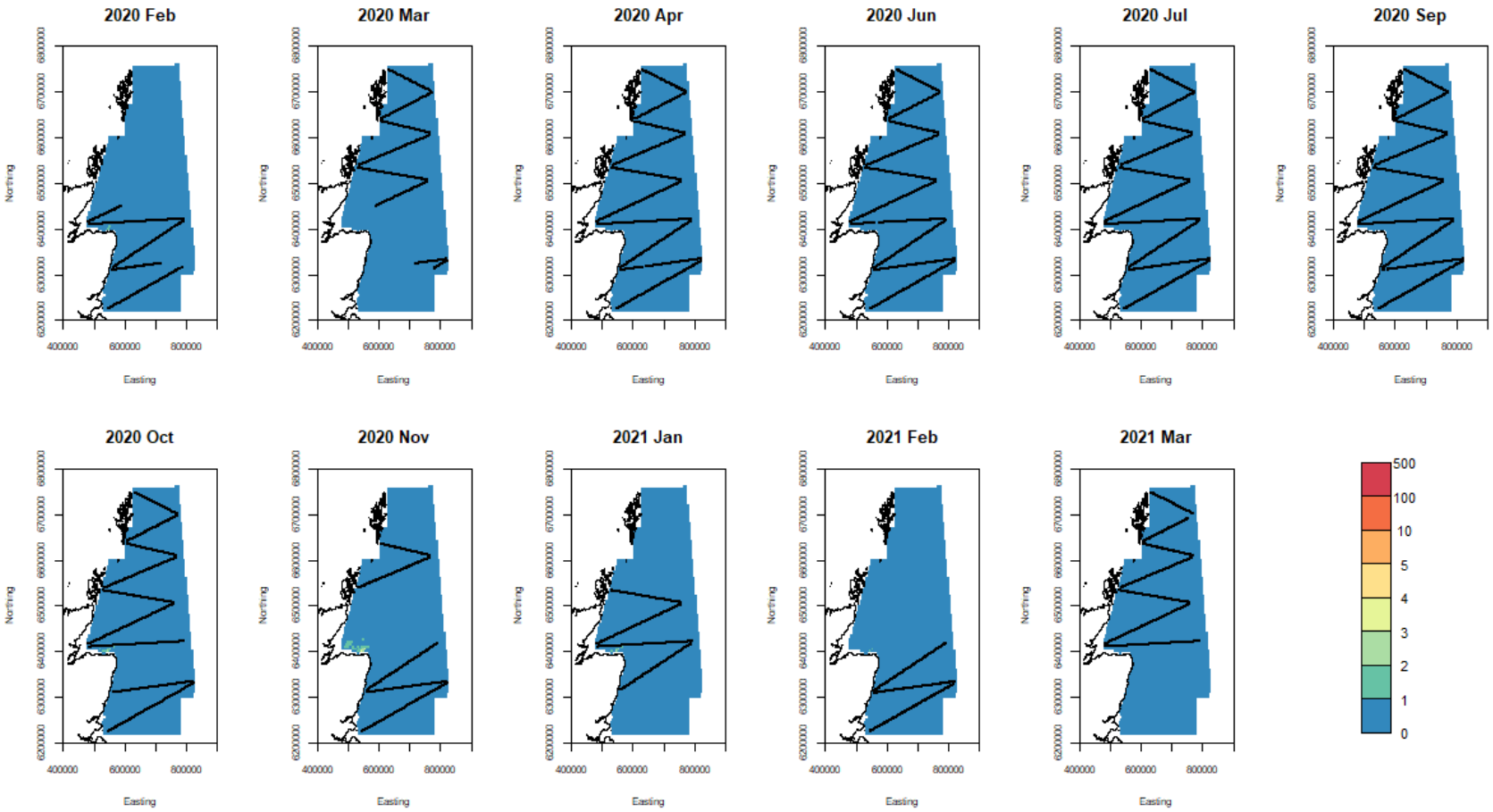

Figure 34. A graph showing lower confidence bound estimates (2.5%) of herring gull densities for each surveyed month from February 2020 to March 2021. Colours represent estimated densities per km^2. Black lines indicate sampling locations in that month

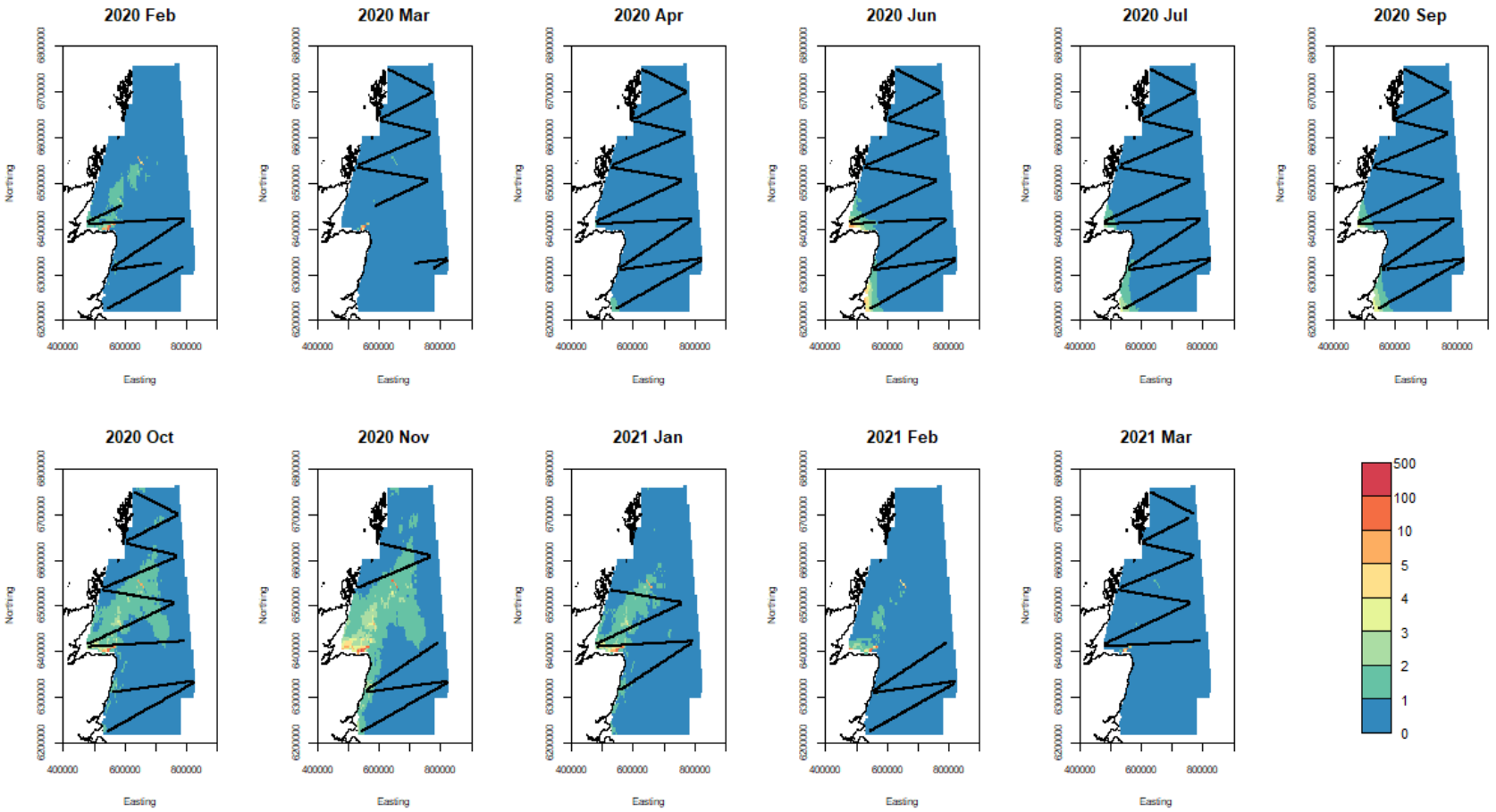

Figure 35. A graph showing upper confidence bound estimates (97.5%) of herring gull densities for each surveyed month from February 2020 to March 2021. Colours represent estimated densities per km^2. Black lines indicate sampling locations in that month.

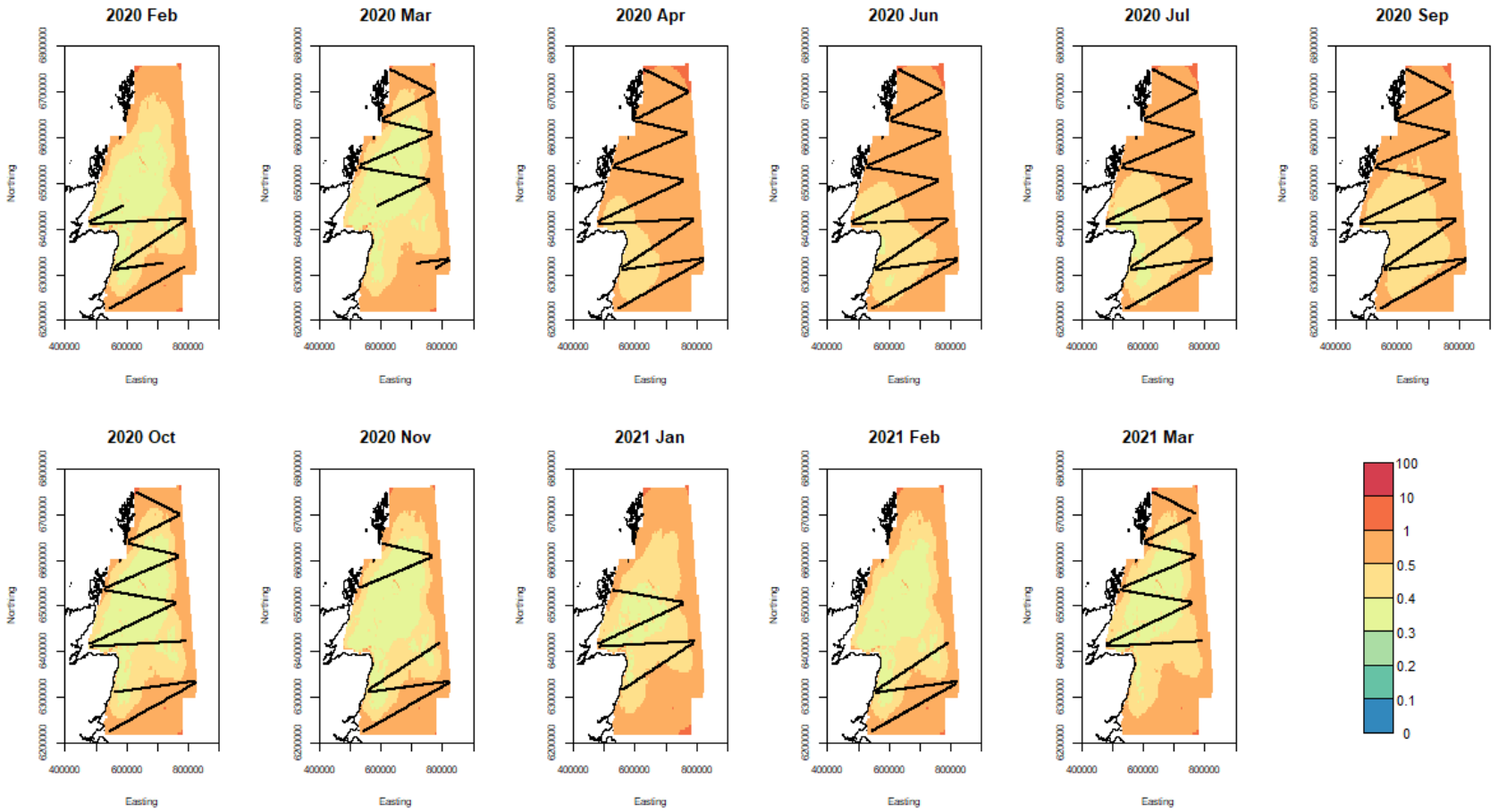

Figure 36. A graph showing herring gull coefficients of variation (CV, in %) in estimated densities of birds for each surveyed month from February 2020 to March 2021. Black lines indicate sampling locations in that month. The largest CVs are at the peripheries of the study area.

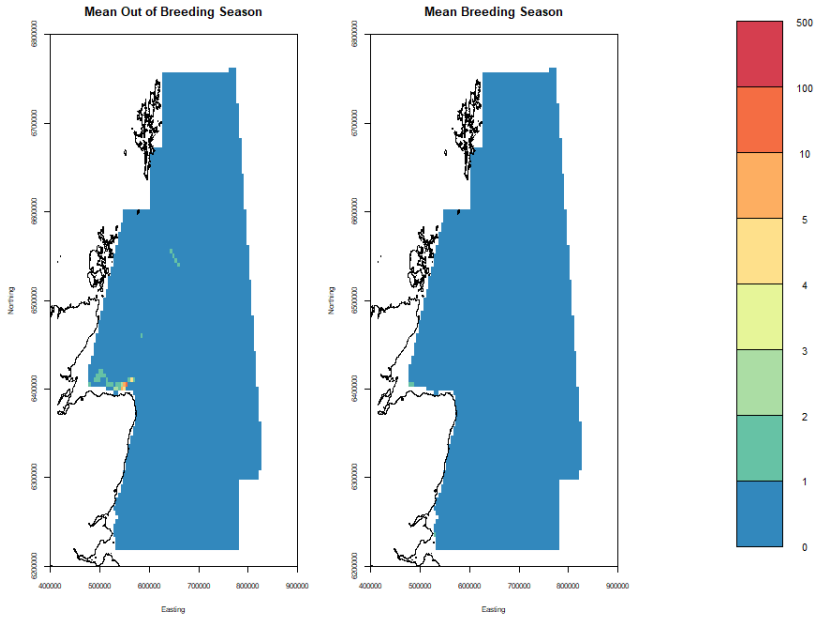

Figure 37. A graph showing mean herring gull density (birds/km^2) surfaces for breeding (April – July) and non-breeding (August – March) seasons.

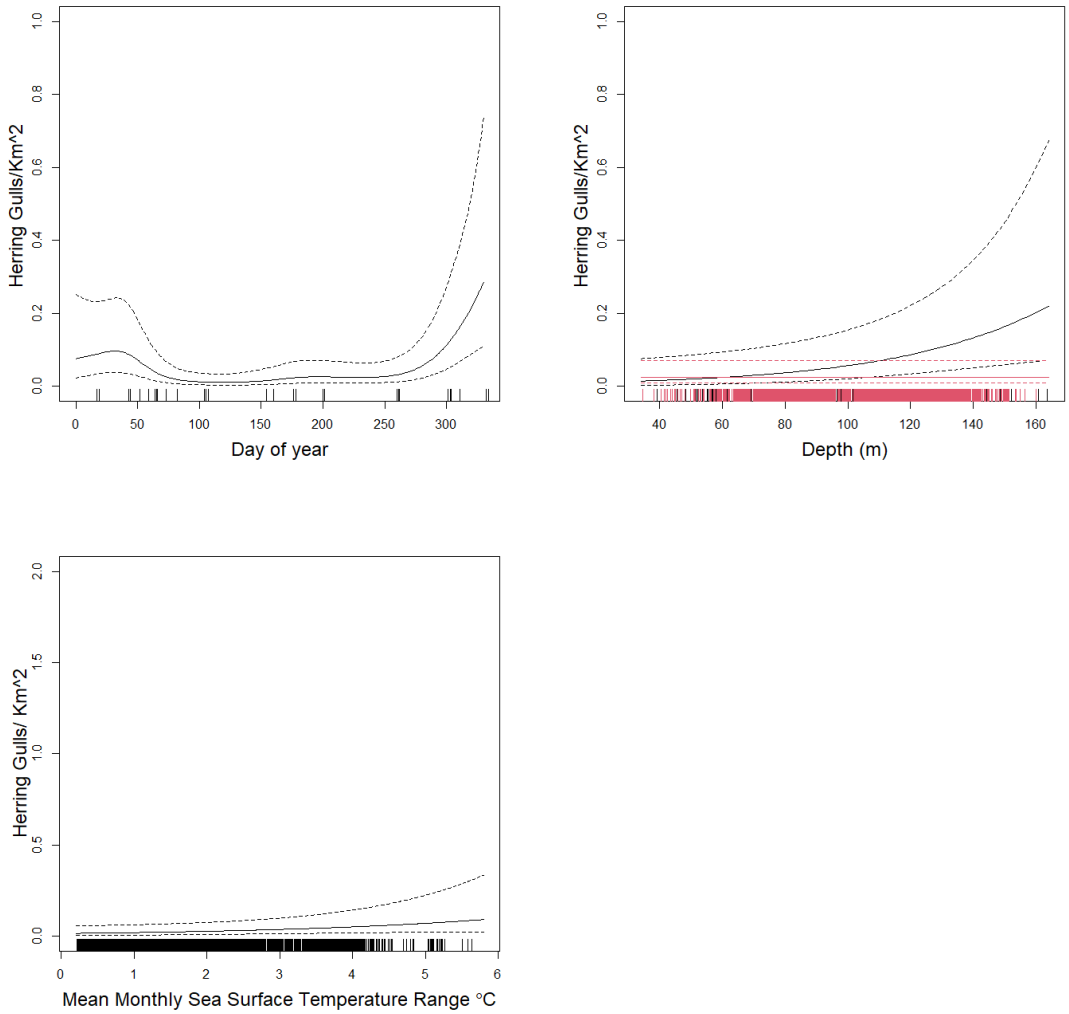

Figure 38. Graphs showing effect of day of year (upper left), depth (upper right) and mean monthly sea surface temperature range (lower left) on herring gull density assuming the middle of survey area outside of the breeding season. The effect of depth differs dependent on whether it is the breeding (red) or non-breeding period (black).

6.3.7 Great Black-backed Gull

The separate fitted models for the breading and non-breeding season are given in Table 8. Estimated numbers through the study period are shown in Figure 39 and indicate relatively low numbers throughout the year but with a small peak between October and January.

Point estimates of gull density for the sampling months along with the confidence bounds are given in Figure 40, Figure 41, and Figure 42. There is high uncertainty in some peripheral regions of the survey region leading to the high upper bounds in Figure 42. Areas with higher densities occur east of Orkney and around the Moray Firth between October and February. The CVs are shown in Figure 43 and are largest at the southern areas of the study site outside the breeding season and in the centre of the study area during the breeding season. The mean point estimates for breeding and non-breeding season in shown in Figure 44. The breeding distribution is further off shore than in the breeding season.

The effect of salinity and seabed roughness in the breeding season model is given in Figure 45. Any salinity effect is weak compared to the effect of greatest seabed roughness. The effect of depth in the non-breeding season model is given in Figure 46 and shows higher densities at greater depths. The relationship with sea surface temperature is difficult to interpret and the model is quite possibly overfitting.

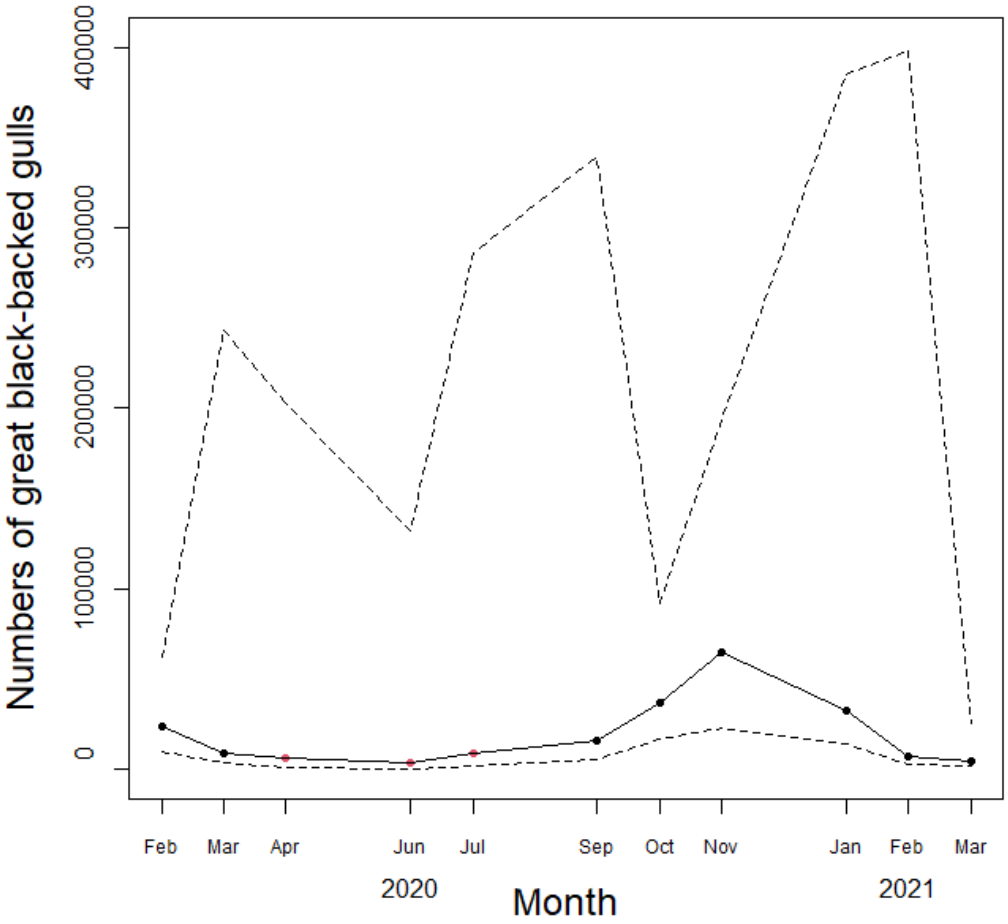

Figure 39. A graph showing estimated numbers of great black-backed gulls over the duration of the study from February 2020 to March 2021. Red points indicate the breeding season (April to July) and the dashed lines represent upper and lower bounds of the 95% confidence intervals. Numbers of gulls peaked in November.

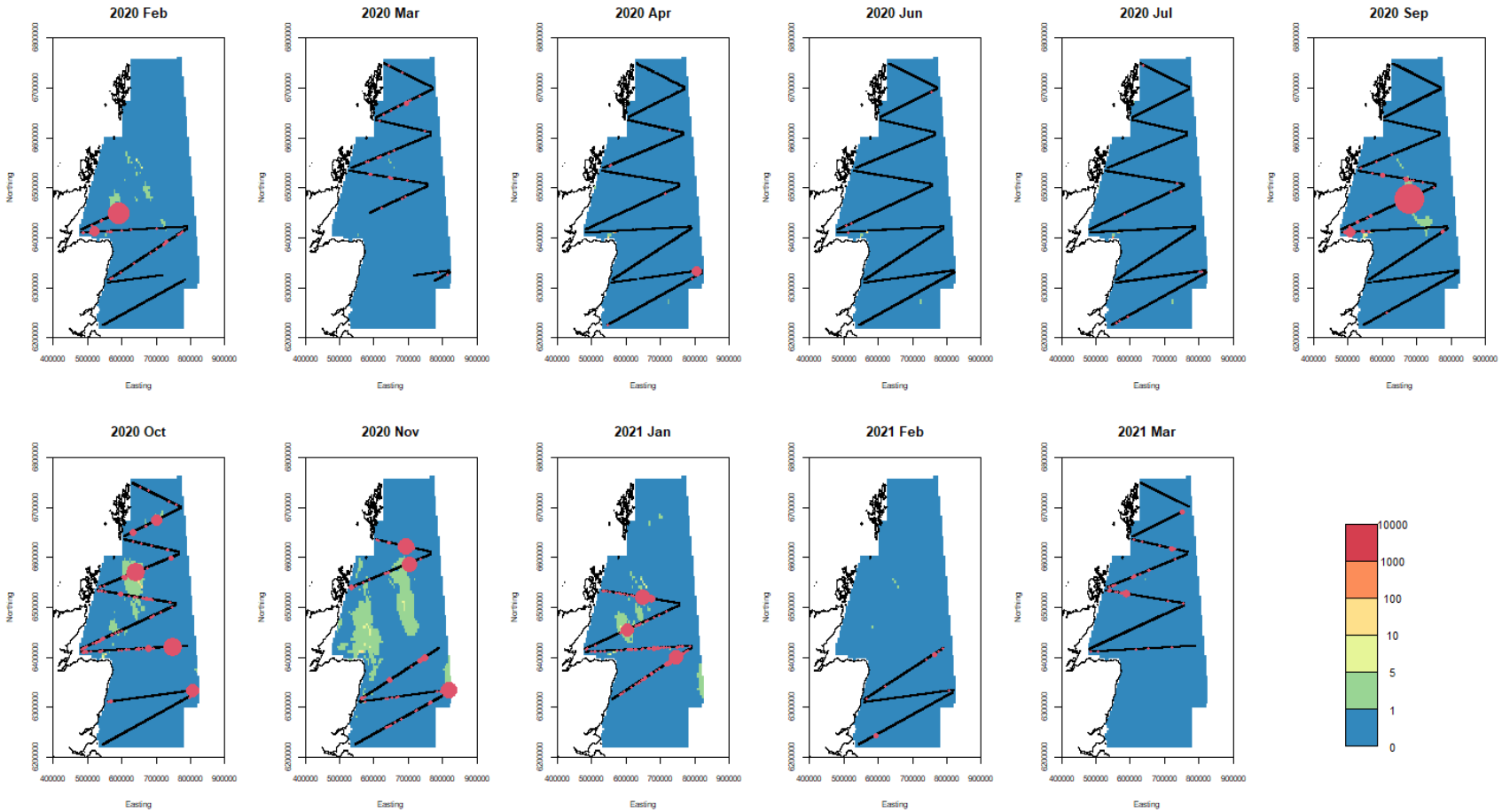

Figure 40. A graph showing point estimates of great black-backed densities for each surveyed month from February 2020 to March 2021. Colours represent estimated densities per km^2. Black lines indicate sampling locations in that month. Red dots indicate observed numbers of birds with size proportional to observed number. Note that scale is matching the following graphs depicting lower and upper confidence intervals.

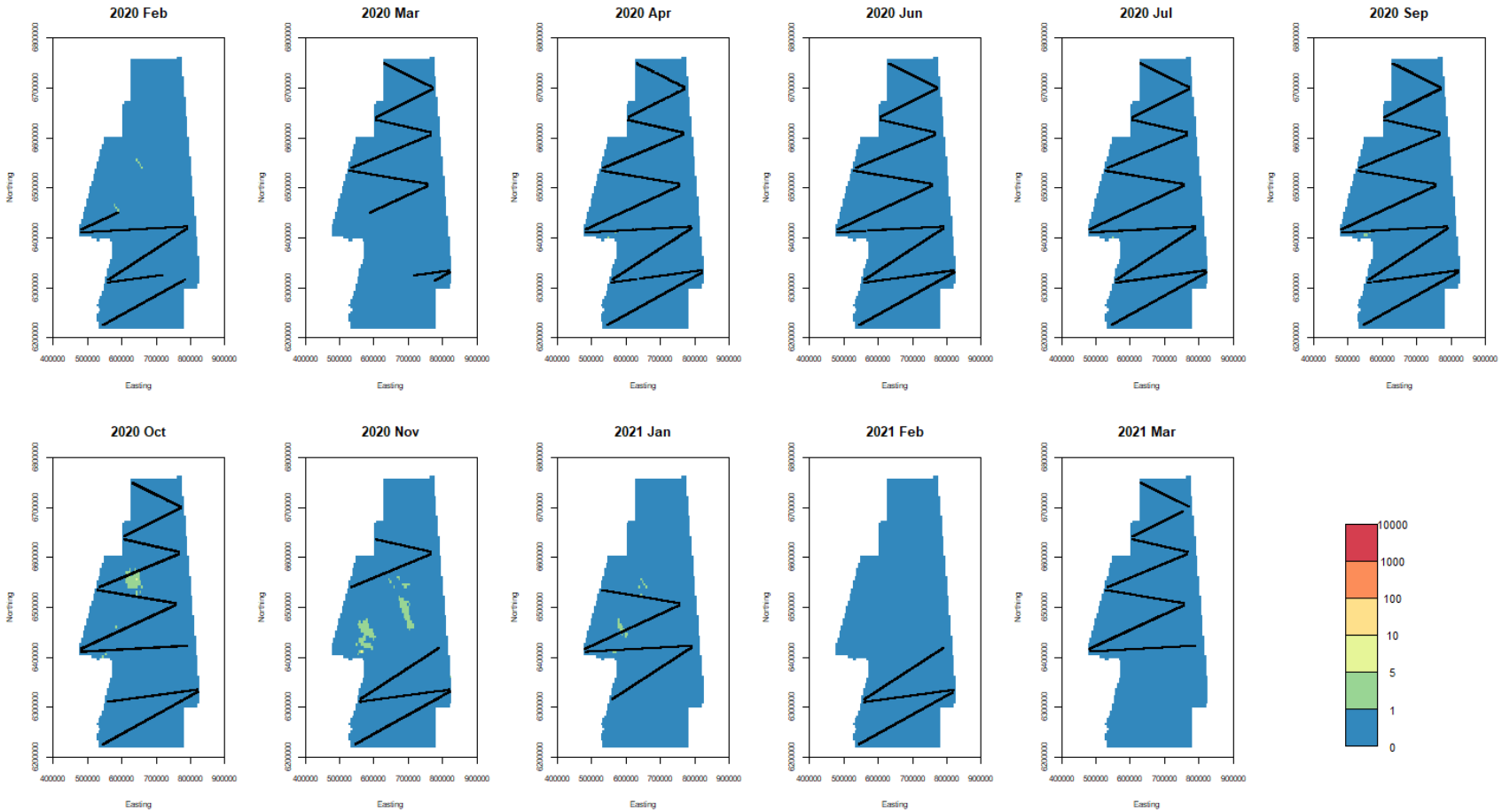

Figure 41. A graph showing lower confidence bound estimates (2.5%) of great black-backed gull densities for each surveyed month from February 2020 to March 2021. Colours represent estimated densities per km^2. Black lines indicate sampling locations in that month. Note that scale is matching the following graphs depicting lower and upper confidence intervals.

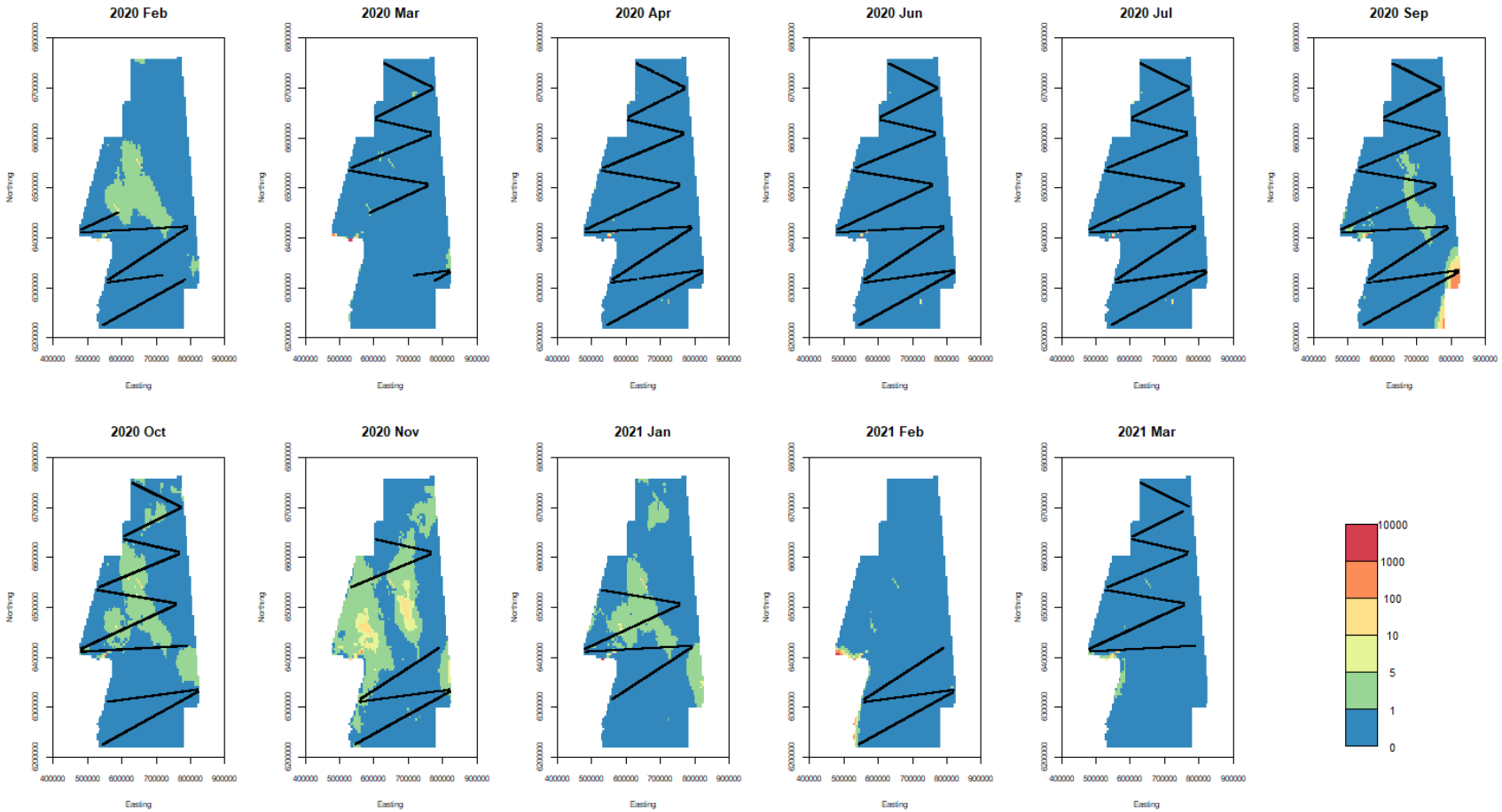

Figure 42. A graph showing upper confidence bound estimates (97.5%) of great black-backed gull densities for each surveyed month from February 2020 to March 2021. Colours represent estimated densities per km^2. Black lines indicate sampling locations in that month.

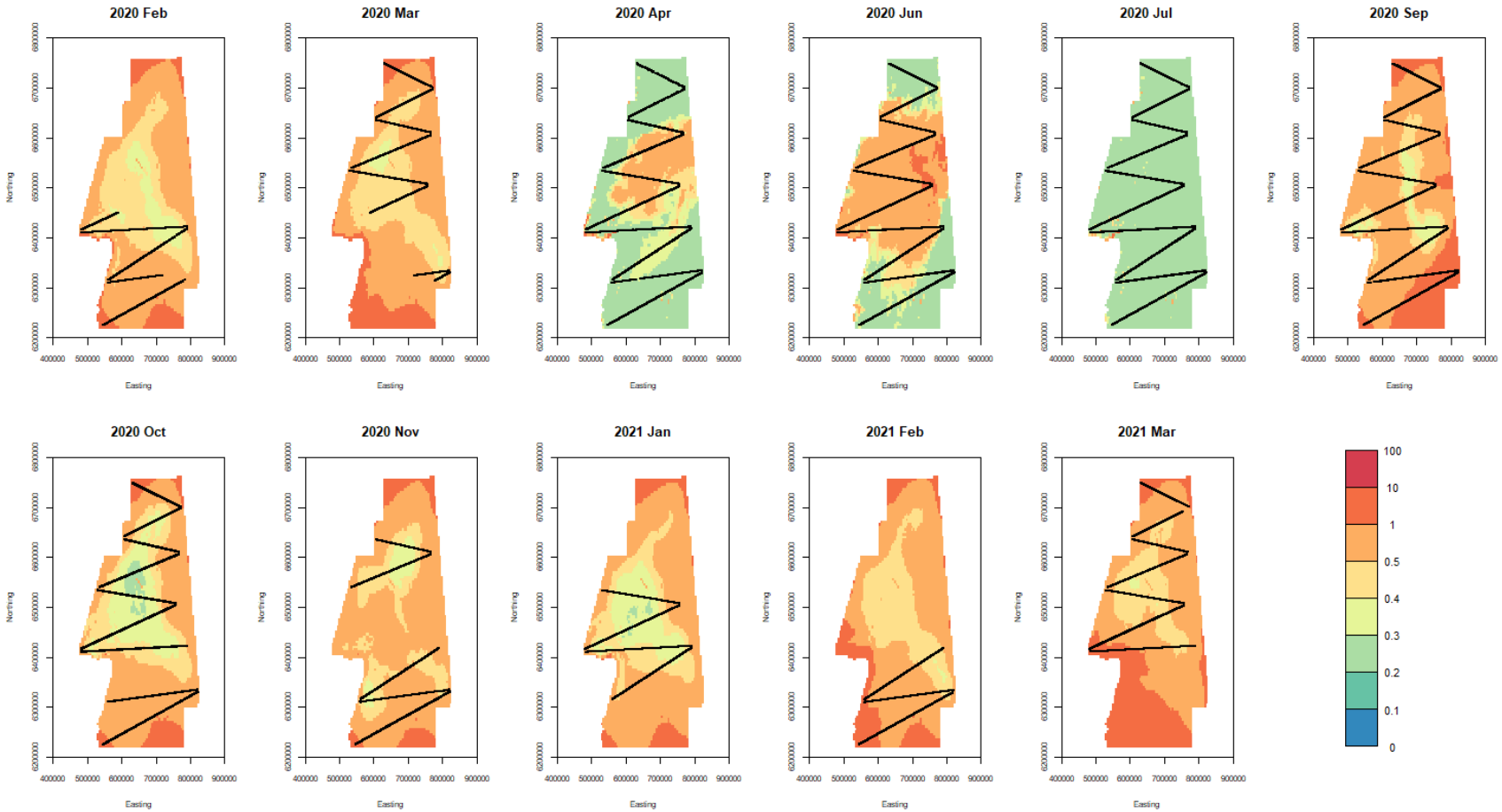

Figure 43. A graph showing great black-backed gull coefficients of variation (CV, in %) in estimated densities of birds for each surveyed month from February 2020 to March 2021. Black lines indicate sampling locations in that month. The largest CVs are at southern part of the study area during non-breeding season and at the centre during the breeding season.

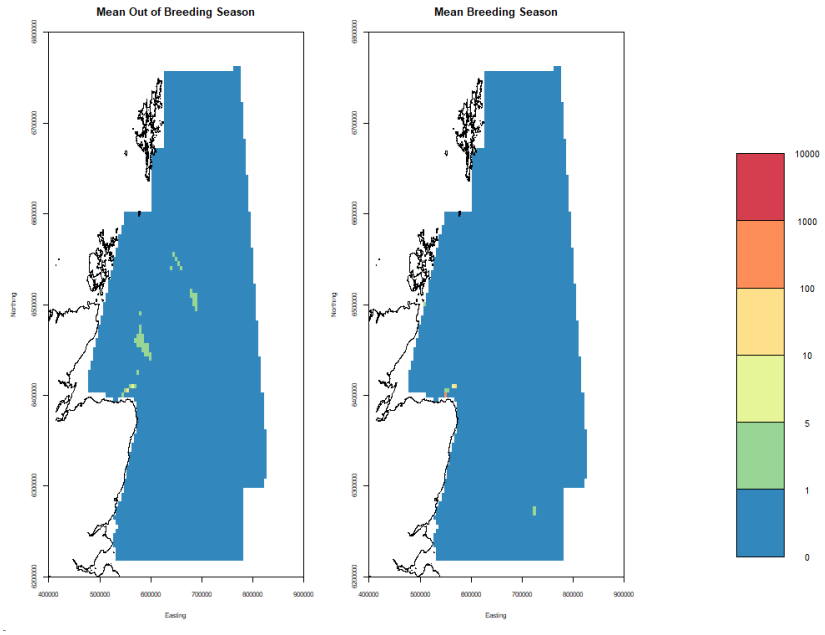

Figure 44, A graph showing mean great black-backed gull density (birds/km^2) surfaces for breeding (April – July) and non-breeding (August – March) seasons.

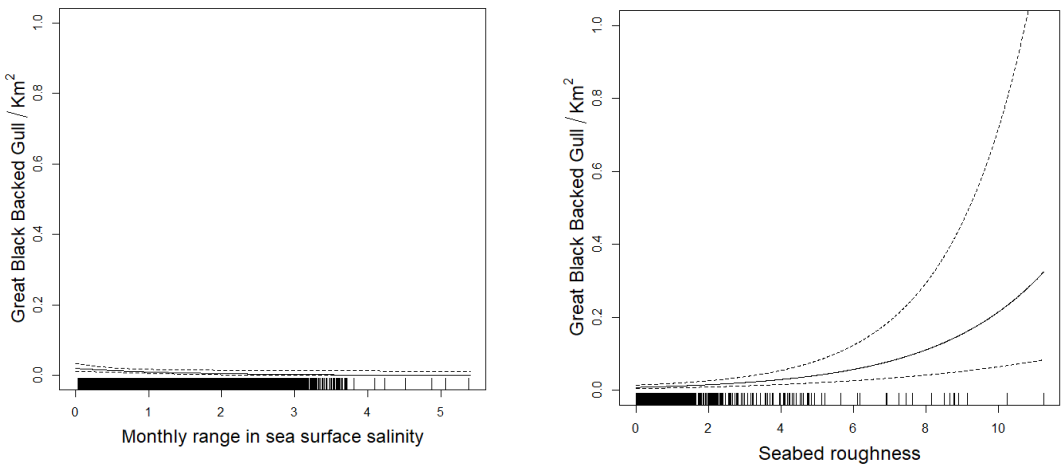

Figure 45. Graphs showing effect of (left) monthly range of salinity and (right)seabed roughness on great black- backed gull observed density assuming the middle of survey area in the breeding season.

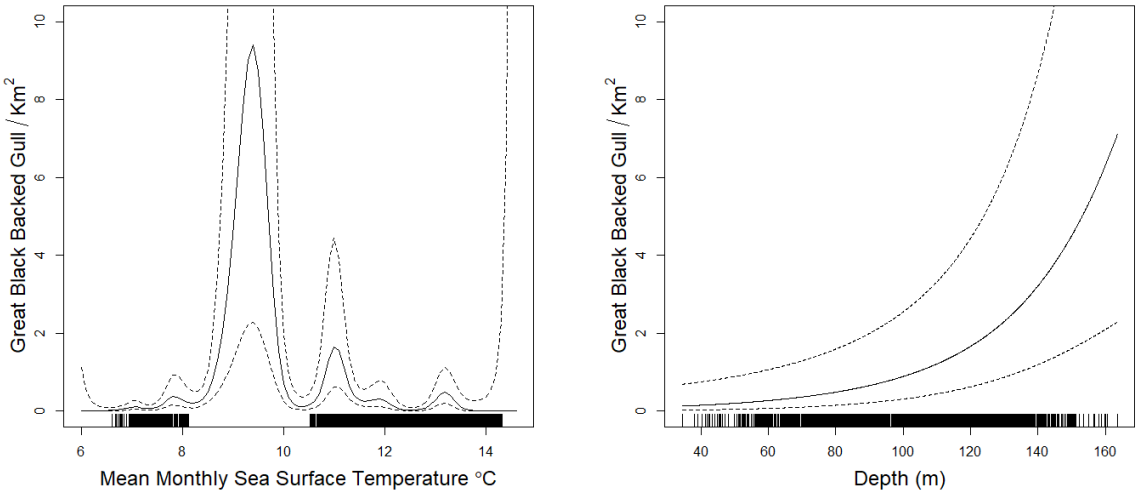

Figure 46. Graphs showing effect of (left) mean monthly sea surface temperature and (right) depth on great black-backed gull observed density assuming the middle of survey area outside of the breeding season.

6.3.8 Black-legged Kittiwake

The model for black-legged kittiwakes is given in Table 8. Estimated abundances of kittiwakes through the study period are given in Figure 47. They show a slight increase during the breeding season (April to July) but little change outside that period.

Point estimates of kittiwake density for the sampling months along with the confidence bounds are given in Figure 48, Figure 49, and Figure 50. They indicate greatest densities nearer to the coast around the Moray Firth and Firth of Forth. The CVs are shown in Figure 51 and are largest at the peripheries of the study site. The mean point estimates for breeding and non-breeding season in shown in Figure 52 and is comparable for these two seasons with highest estimates at the south-western part of the study area.

The effect of monthly mean salinity on kittiwake density is shown in Figure 53 and shows opposite trend for breeding (red) and non-breeding season (black) with increase in kittiwake density with decrease in salinity during the breeding season.

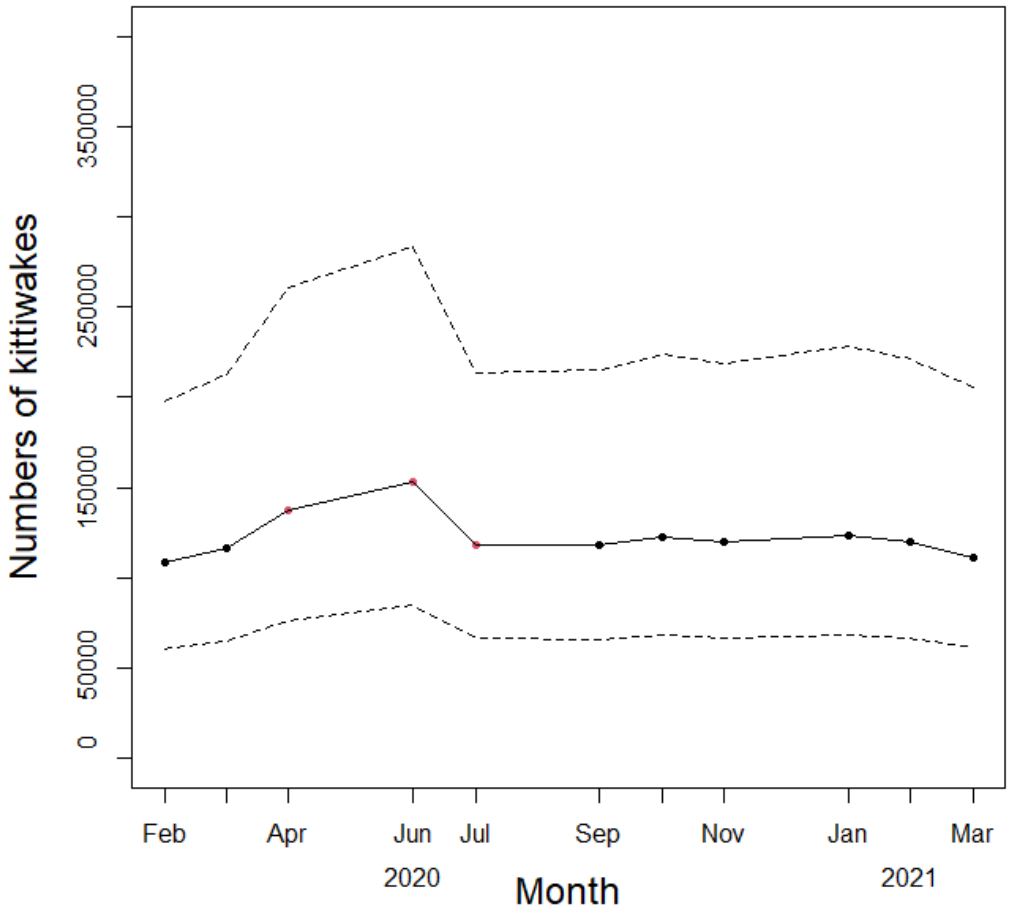

Figure 47. A graph showing estimated numbers of kittiwakes over the duration of the study from February 2020 to March 2021. Red points indicate the breeding season (April to July) and the dashed lines represent upper and lower bounds of the 95% confidence intervals. Numbers of kittiwakes peaked in June.

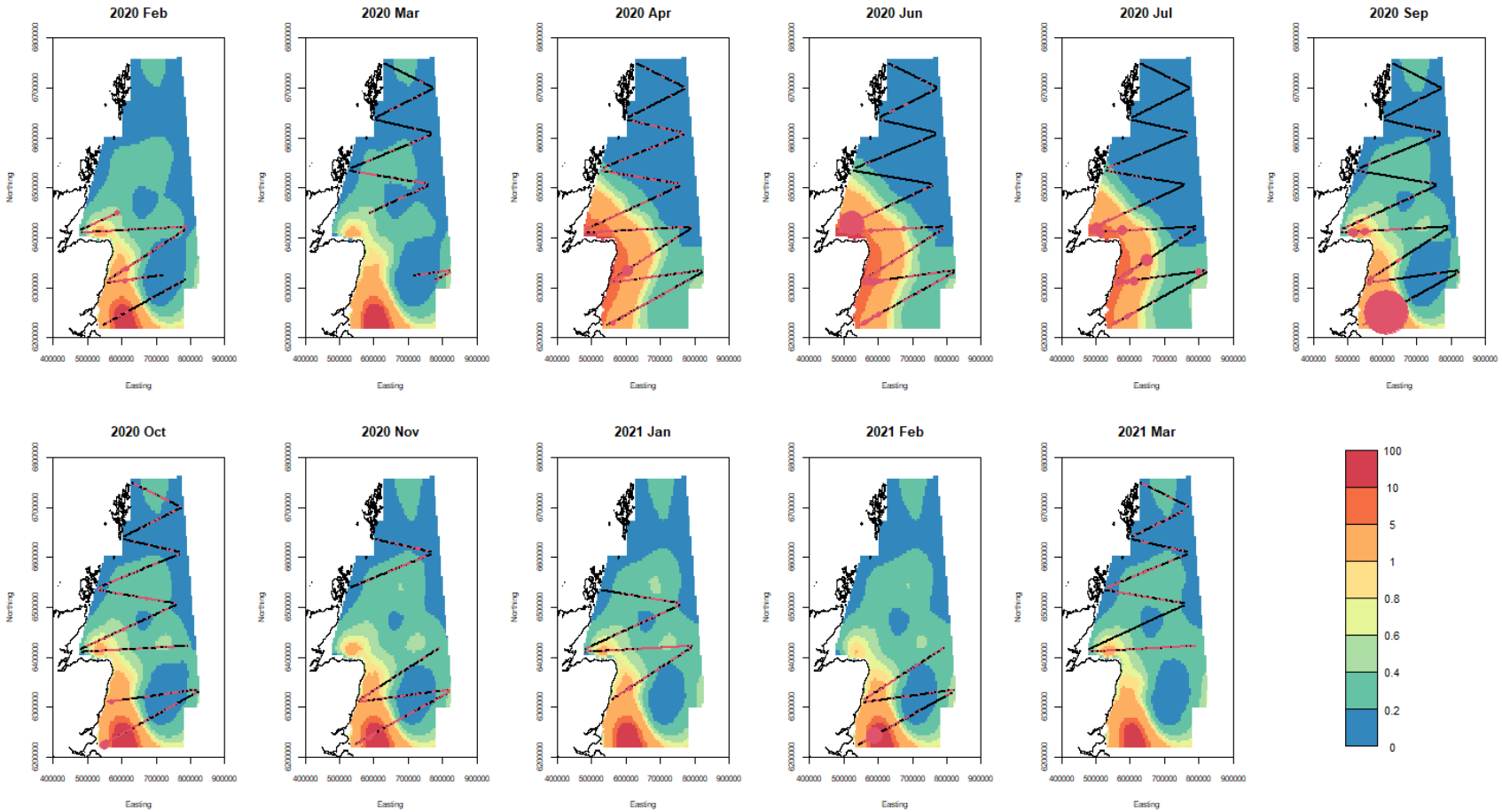

Figure 48. A graph showing point estimates of black-legged kittiwake densities for each surveyed month from February 2020 to March 2021. Colours represent estimated densities per km^2. Black lines indicate sampling locations in that month. Red dots indicate observed numbers of birds with size proportional to observed number. Note that scale is matching the following graphs depicting lower and upper confidence intervals.

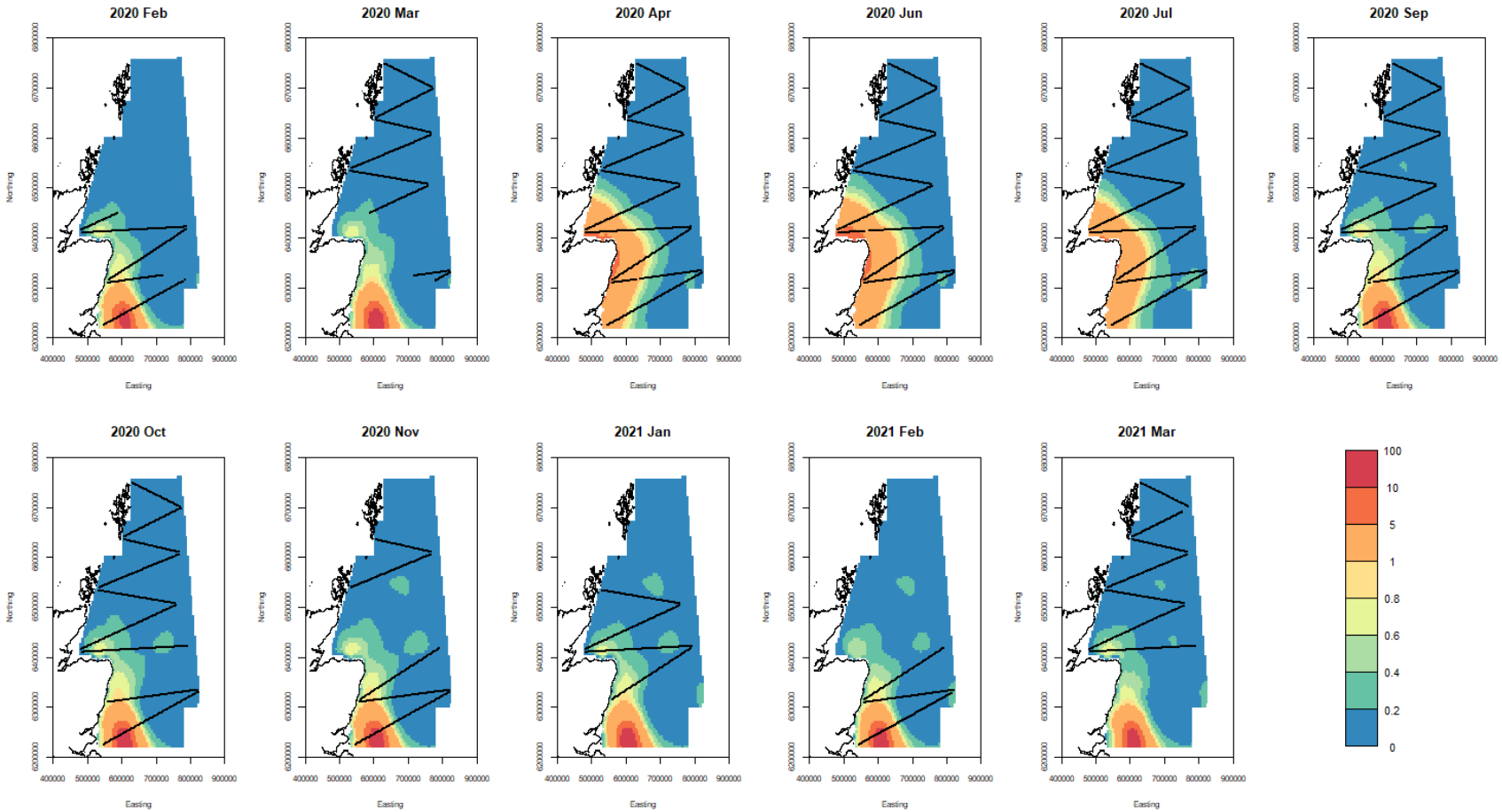

Figure 49. A graph showing lower confidence bound estimates (2.5%) of black-legged kittiwake densities for each surveyed month from February 2020 to March 2021. Colours represent estimated densities per km^2. Black lines indicate sampling locations in that month.

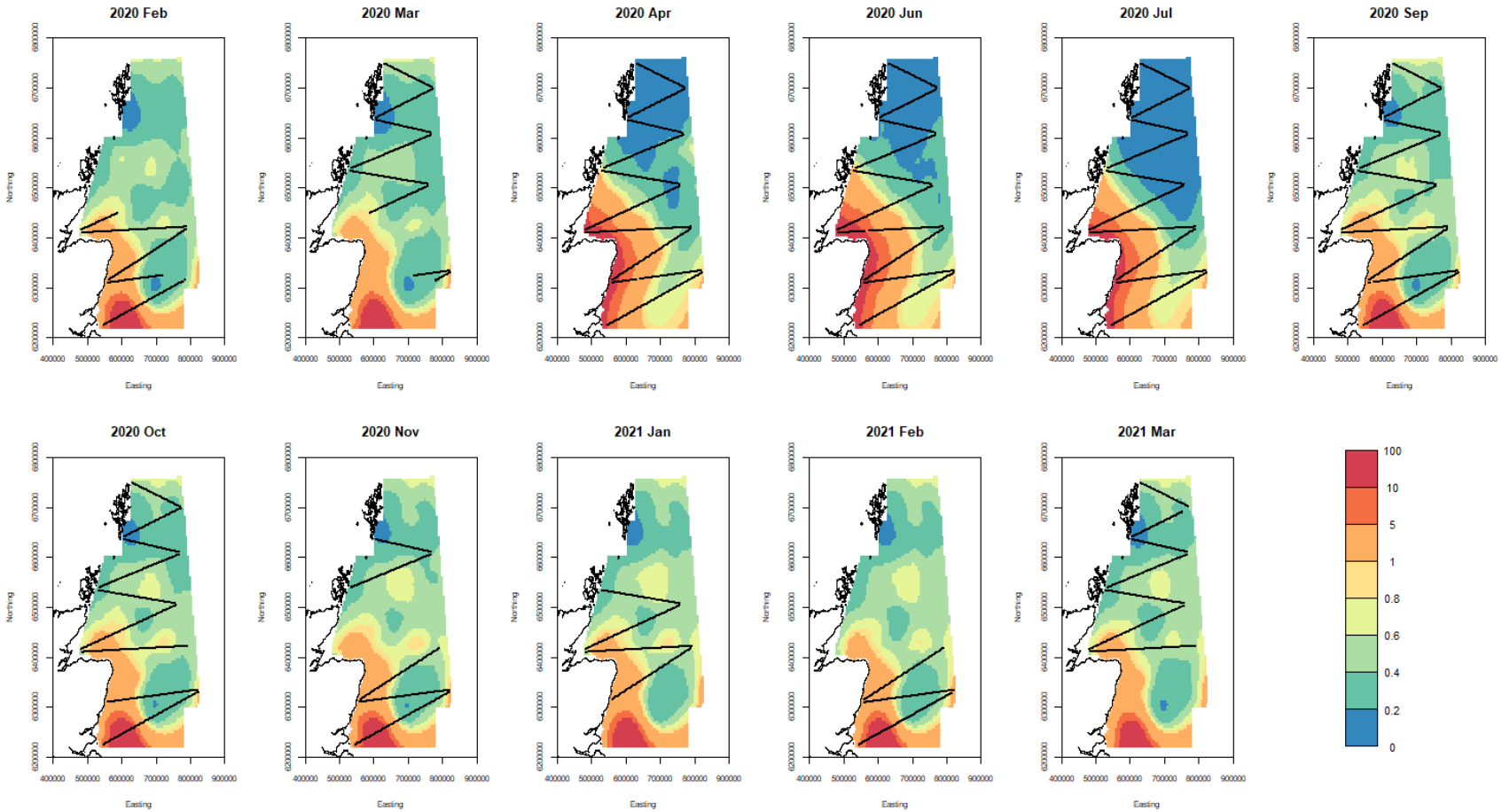

Figure 50. A graph showing upper confidence bound estimates (97.5%) of black-legged kittiwake densities for each surveyed month from February 2020 to March 2021. Colours represent estimated densities per km^2. Black lines indicate sampling locations in that month.

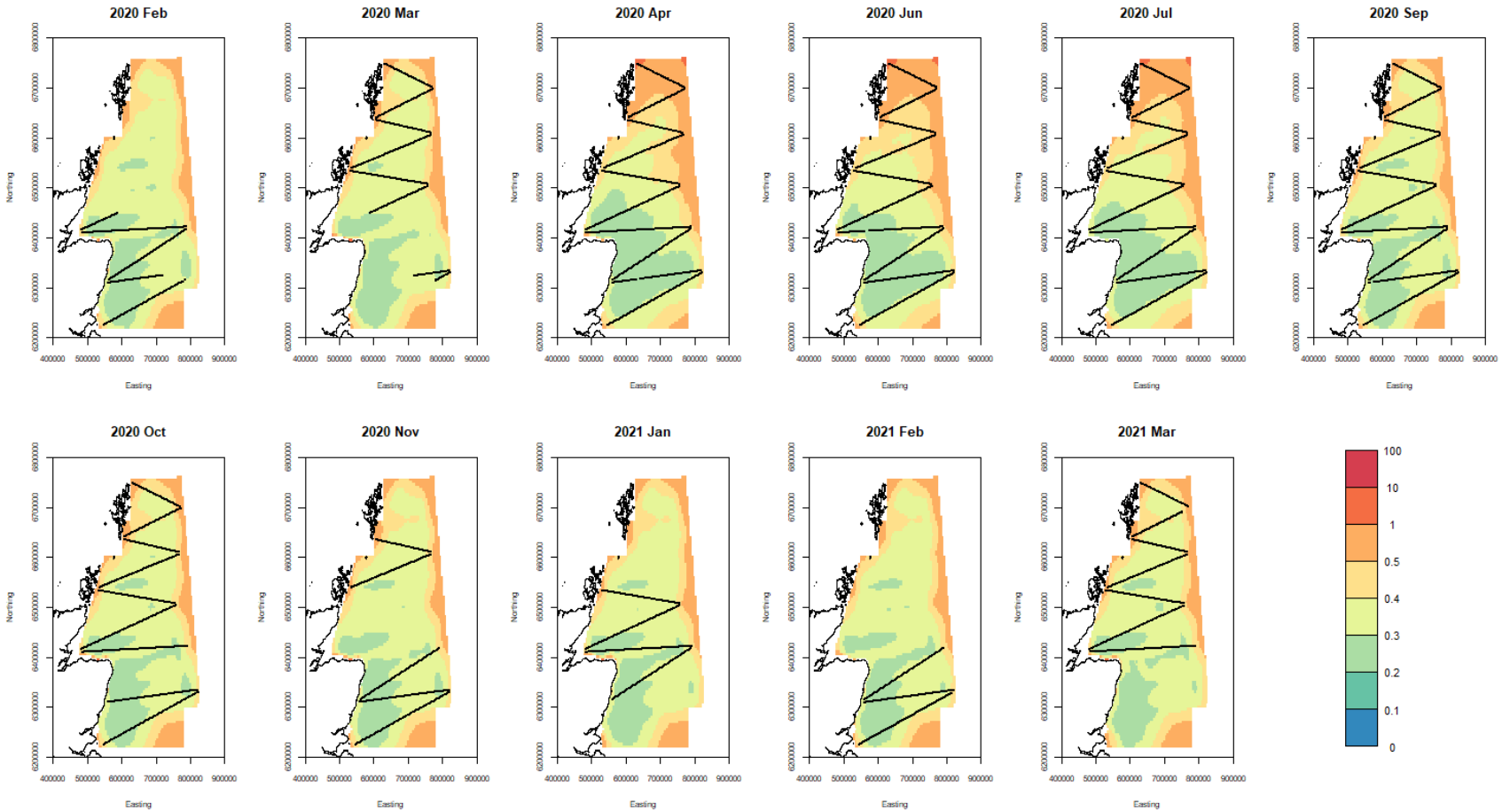

Figure 51. A graph showing kittiwake coefficients of variation (CV, in %) in estimated densities of birds for each surveyed month from February 2020 to March 2021. Black lines indicate sampling locations in that month. The largest CVs are at the peripheries of the study area.

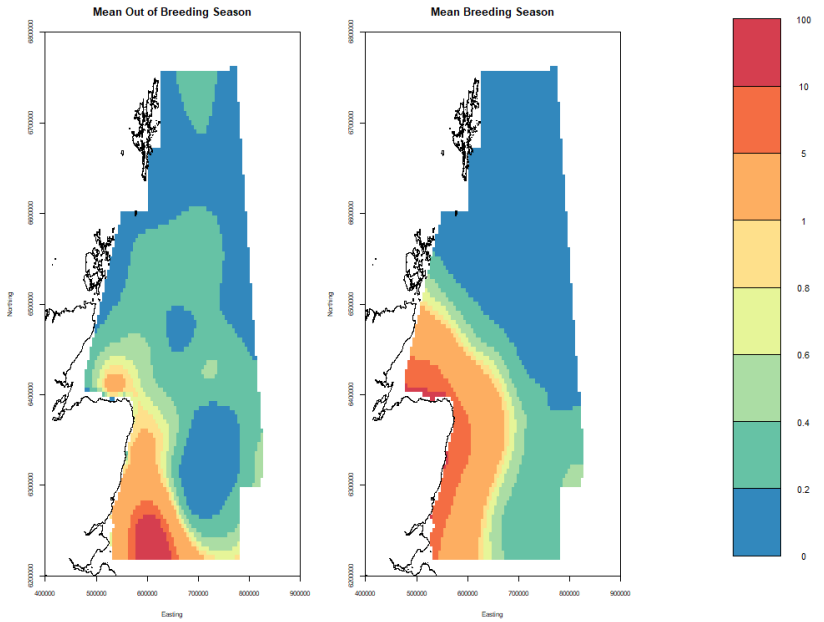

Figure 52. A graph showing mean black-legged kittiwake density (birds/km^2) surfaces for breeding (April – August) and non-breeding (September – March) seasons.

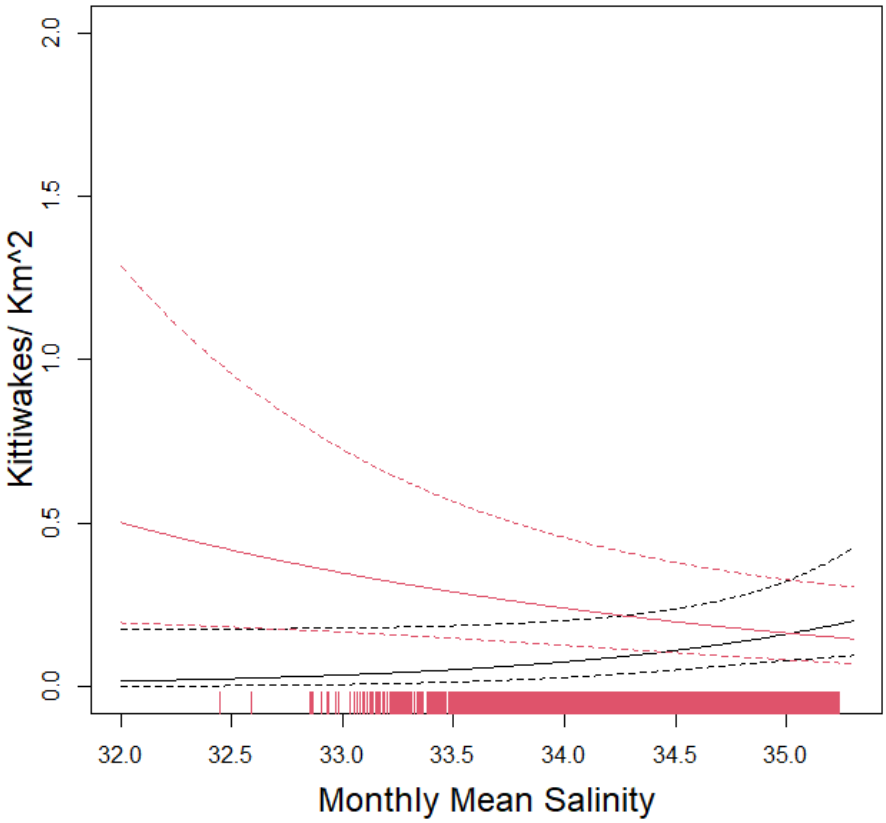

Figure 53. Graph showing effect of monthly mean salinity on black-legged kittiwake observed density assuming the middle of survey area within (red) the breeding season and (black) outside the breeding season. .

6.3.9 Common Guillemot

The single model (i.e. for the full sampling period) based on the amalgamated data is given in Table 8. The predicted numbers over the period of the survey are given in Figure 54. No stable model with a location effect could be found so the model consisted of main environmental effects only.

Point estimates of common guillemot density for the sampling months along with the associated confidence bounds are given in Figure 55, Figure 56, and Figure 57. They show greatest densities nearer to the coast in all months, but particularly between June and September from east of Orkney to the Moray Firth, and down the East Grampian coast as far as the Firth of Forth. The CVs are shown in Figure 58 and are largest at different locations over the study period. The mean point estimates for breeding and non-breeding season in shown in Figure 58. The breeding distribution is closer to the shore than in the non-breeding season.

The effects of the non-location variables are given in Figure 59. Note that these are the effects of these variables in the model given the other variables, so they may be

very different from the actual marginal effect in the absence of the other variables. This is especially the case for SST which is correlated with *Dayofyear* (not shown).

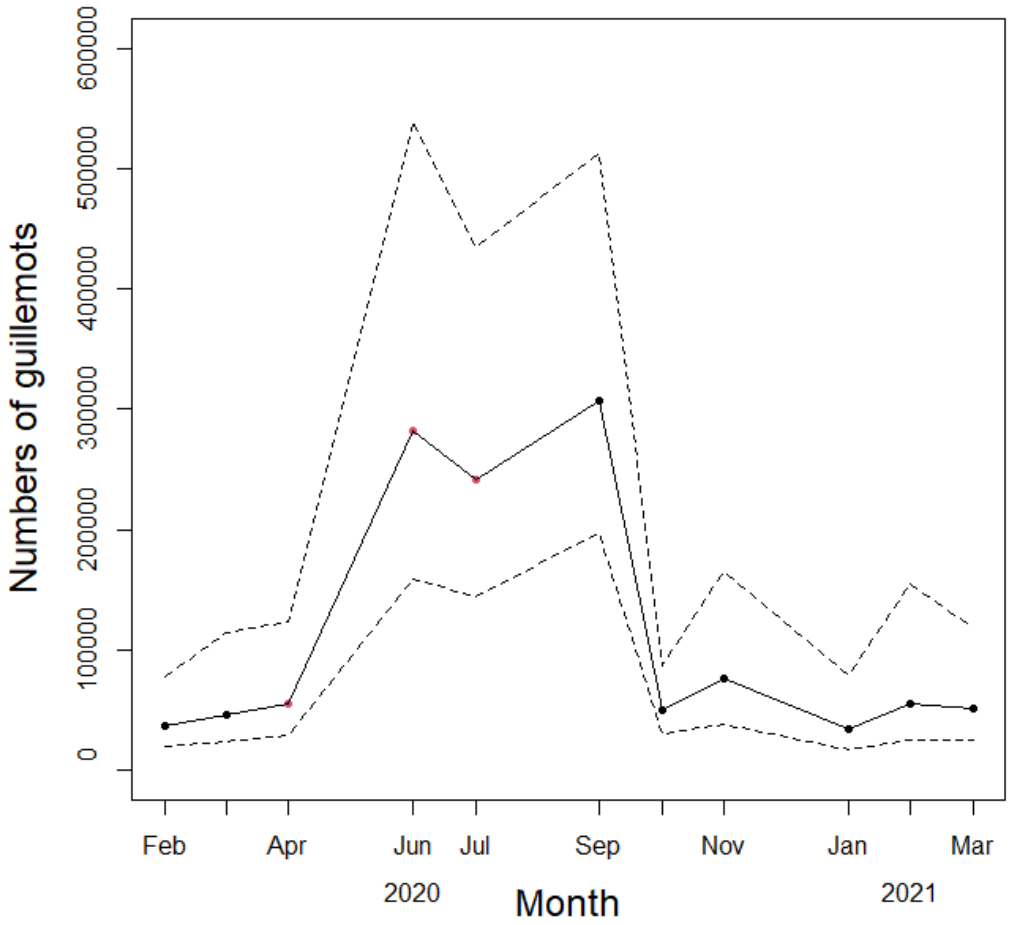

Figure 54. A graph showing estimated numbers of common guillemots over the duration of the study from February 2020 to March 2021. Red points indicate the breeding season (April to July) and the dashed lines represent upper and lower bounds of the 95% confidence intervals. Numbers of guillemots peaked in June-September and had lowest values throughout non-breeding season.

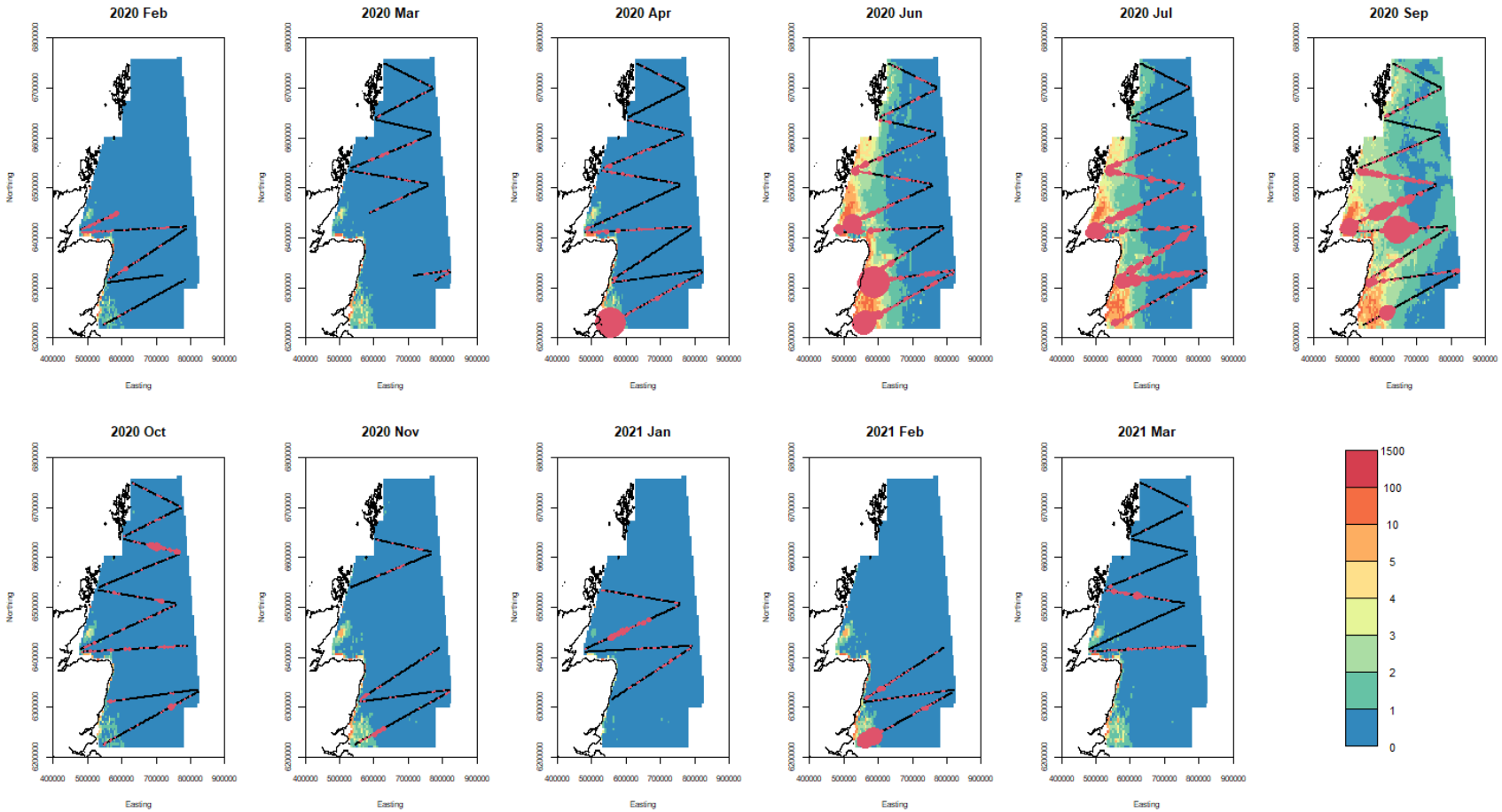

Figure 55. A graph showing point estimates of common guillemot densities for each surveyed month from February 2020 to March 2021. Colours represent estimated densities per km^2. Black lines indicate sampling locations in that month. Red dots indicate observed numbers of birds with size proportional to observed number. Note that scale is matching the following graphs depicting lower and upper confidence intervals.

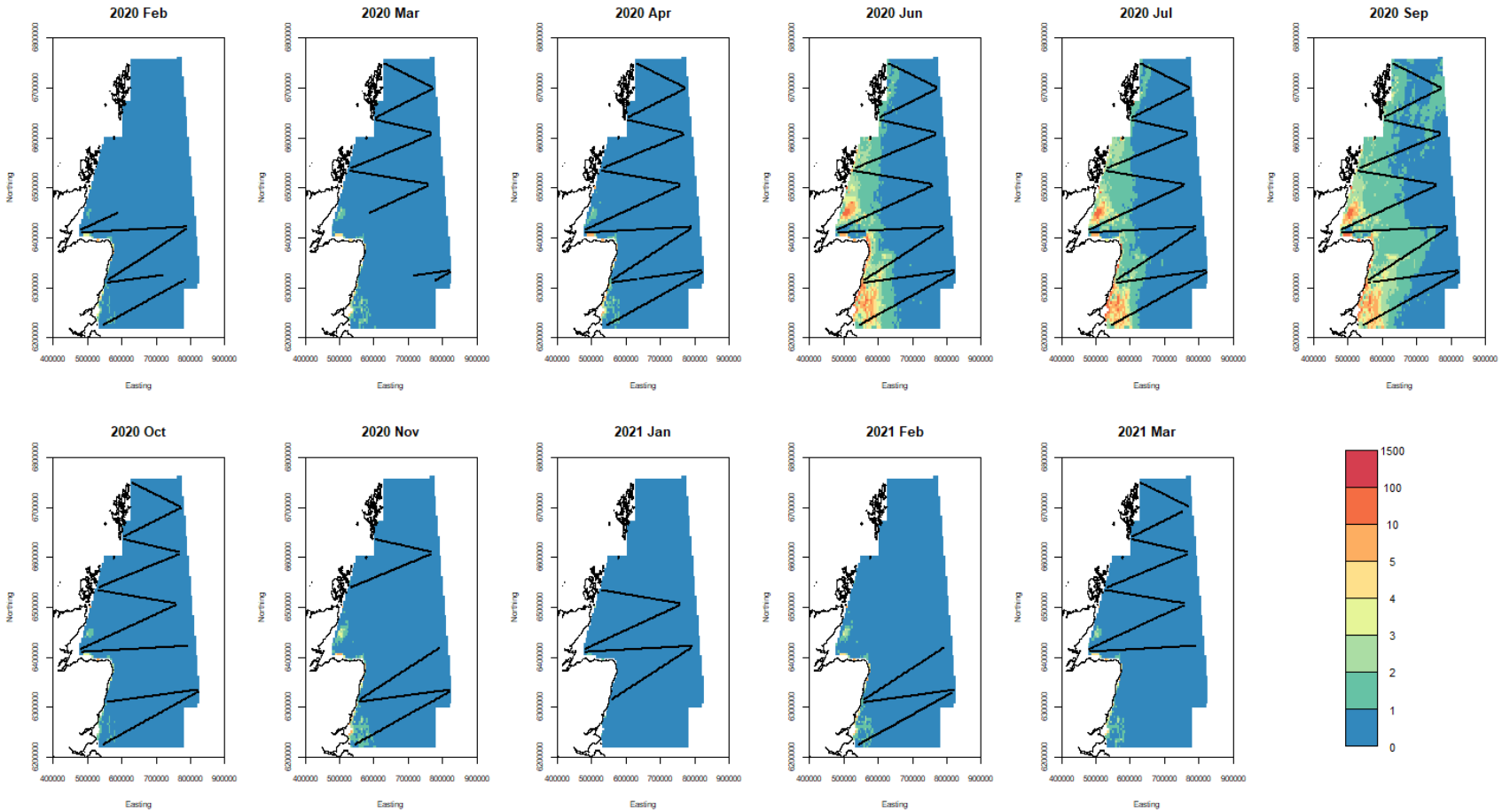

Figure 56. A graph showing lower confidence bound estimates (2.5%) of common guillemot densities for each surveyed month from February 2020 to March 2021. Colours represent estimated densities per km^2. Black lines indicate sampling locations in that month.

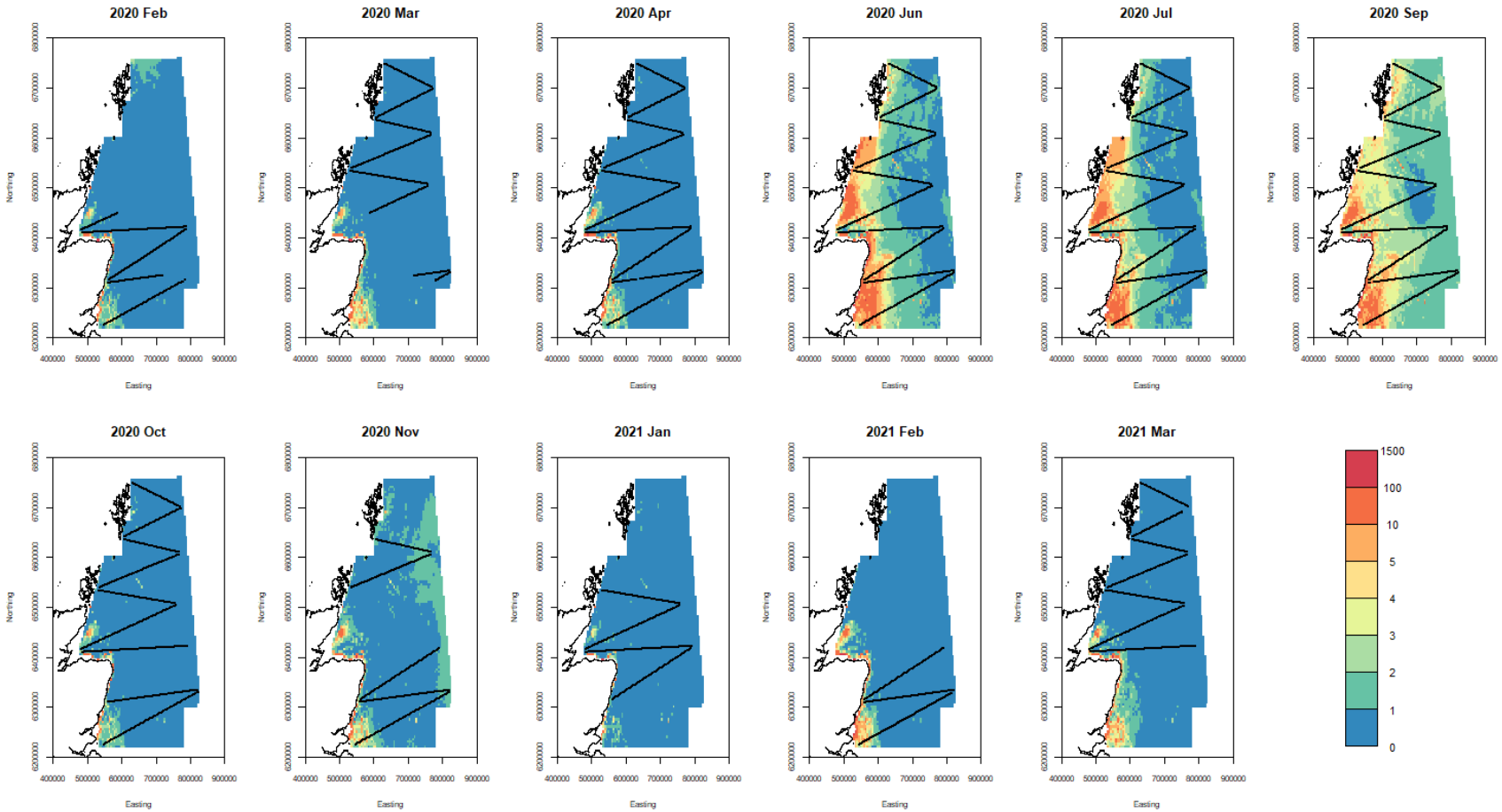

Figure 57. A graph showing upper confidence bound estimates (97.5%) of common guillemot densities for each surveyed month from February 2020 to March 2021. Colours represent estimated densities per km^2. Black lines indicate sampling locations in that month.

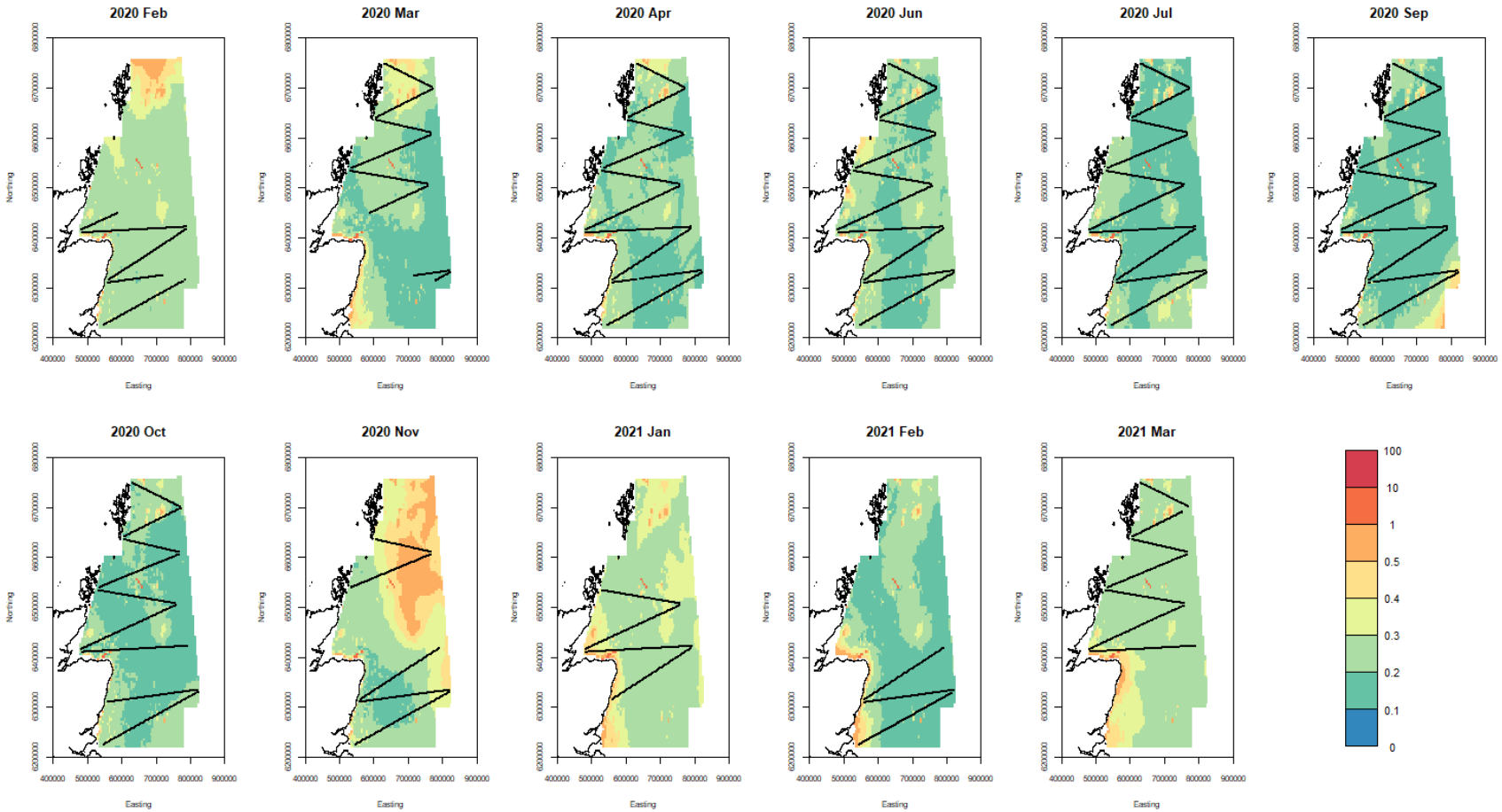

Figure 57. A graph showing common guillemot coefficients of variation (CV, in %) in estimated densities of birds for each surveyed month from February 2020 to March 2021. Black lines indicate sampling locations in that month. The largest CVs are at the north eastern part of the study area.

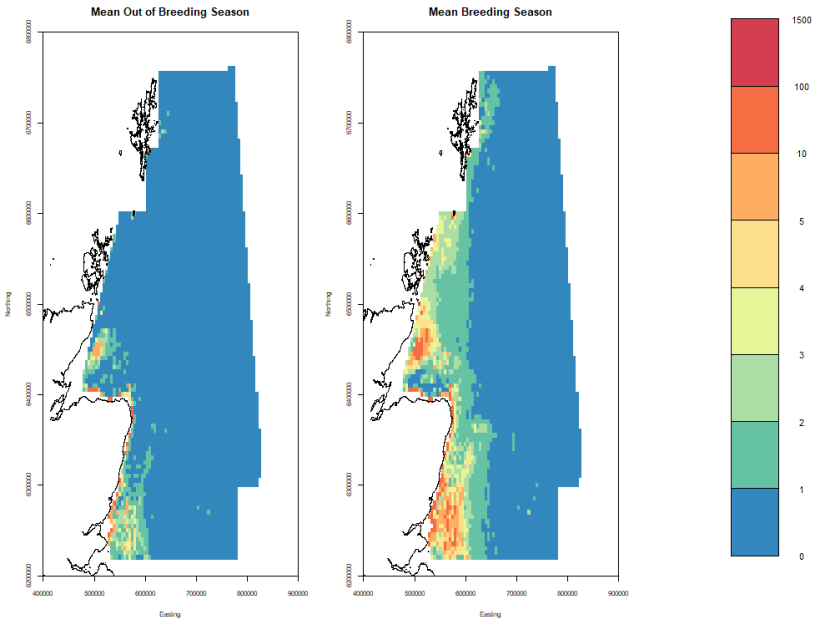

Figure 58. A graph showing mean common guillemot density (birds/km^2) surfaces for breeding (April – July) and non-breeding (August – March) seasons.

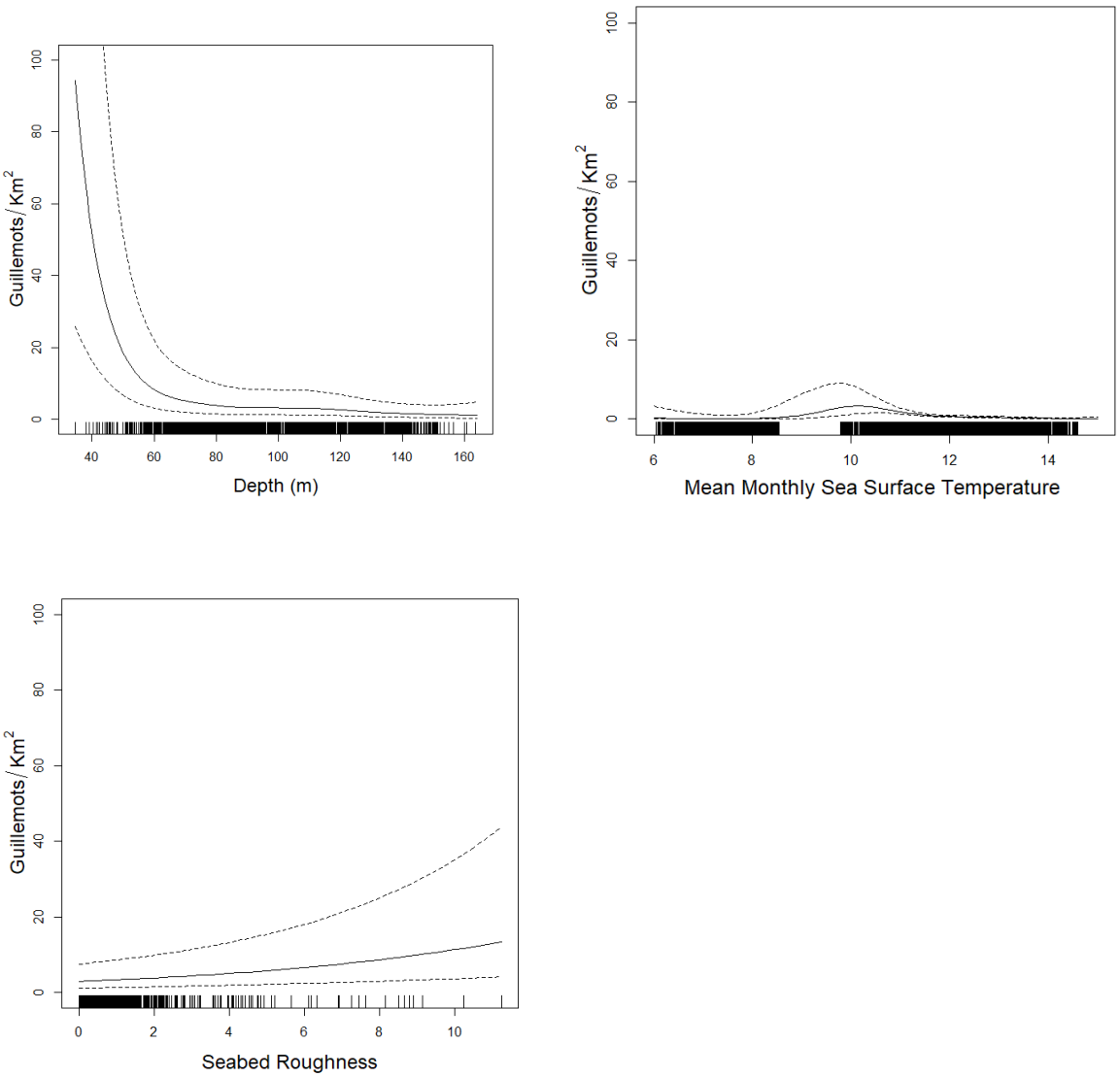

Figure 59. Graphs showing effect of (upper left) depth, (upper right) mean monthly sea surface temperature and (lower left) seabed roughness on common guillemot observed density.

6.3.10 Razorbill

The separate fitted models for breeding and non-breeding season are given in Table 8. The estimated numbers of razorbills in the survey region is given in Figure 60. It shows a strong peak during the breeding season between April and July.

Point estimates of razorbill density for the sampling months along with the confidence bounds are given in Figure 61, Figure 62, and Figure 63. They indicate greatest densities nearer the coast around the Moray Firth, east Grampian region and Firth of Forth, between April and July. There appears to be a hotspot of higher density offshore east of the Moray Firth in late summer and autumn, particularly September and October. The CVs are shown in Figure 64 and are larger in the non-breeding than breeding season. The mean point estimates for breeding and non-breeding season in shown in Figure 65 and shows higher densities in the breeding season at the south western part of the study site.

The effect of monthly mean sea surface temperature (SST) in the breeding season model is given in Figure 66, but note that there may be some overfitting of the model here. The effect of SST, salinity and salinity range in the non-breeding season model, is given in Figure 67. They show little obvious relationships although densities are possibly higher at greater sea surface temperatures and salinities. Note that these are the effects of these variables given the presence of location in the model, so may be very different from the actual biological effect.

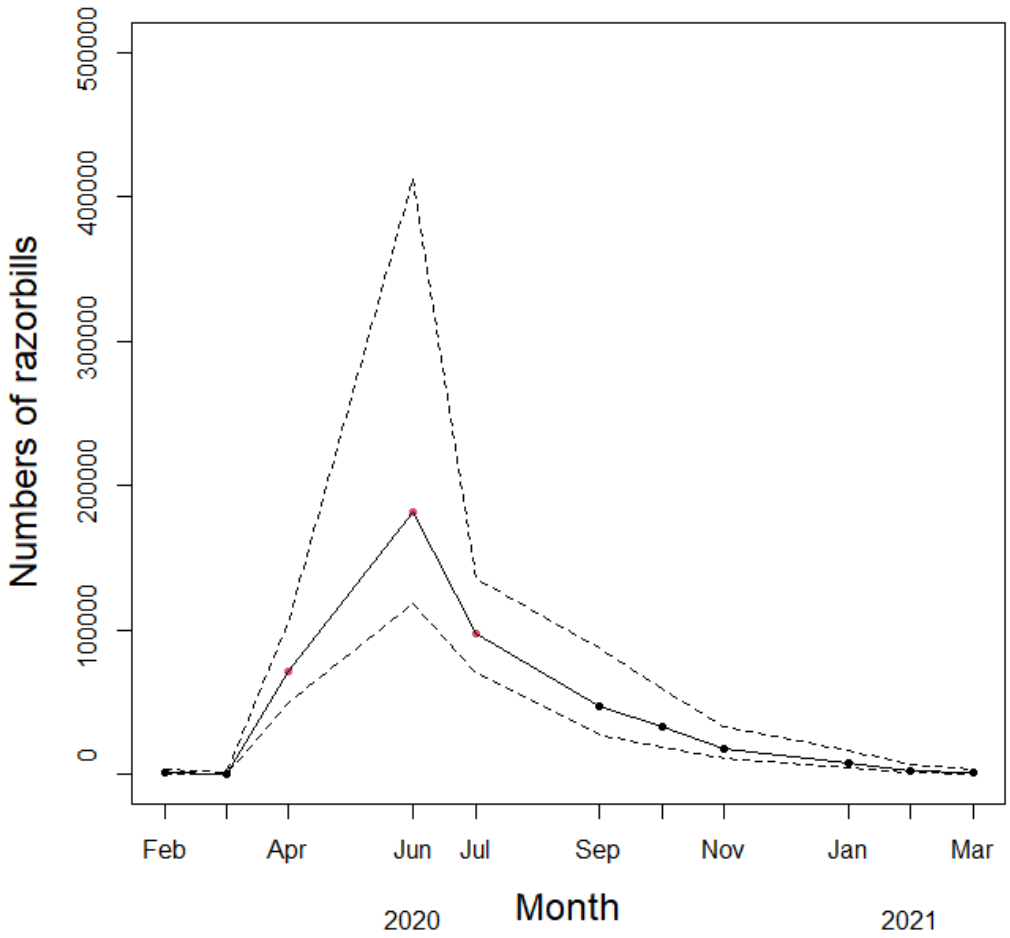

Figure 60. A graph showing estimated numbers of razorbills over the duration of the study from February 2020 to March 2021. Red points indicate the breeding season (April to July) and the dashed lines represent upper and lower bounds of the 95% confidence intervals. Numbers of razorbills peaked in June and had lowest values in winter months (January to March).

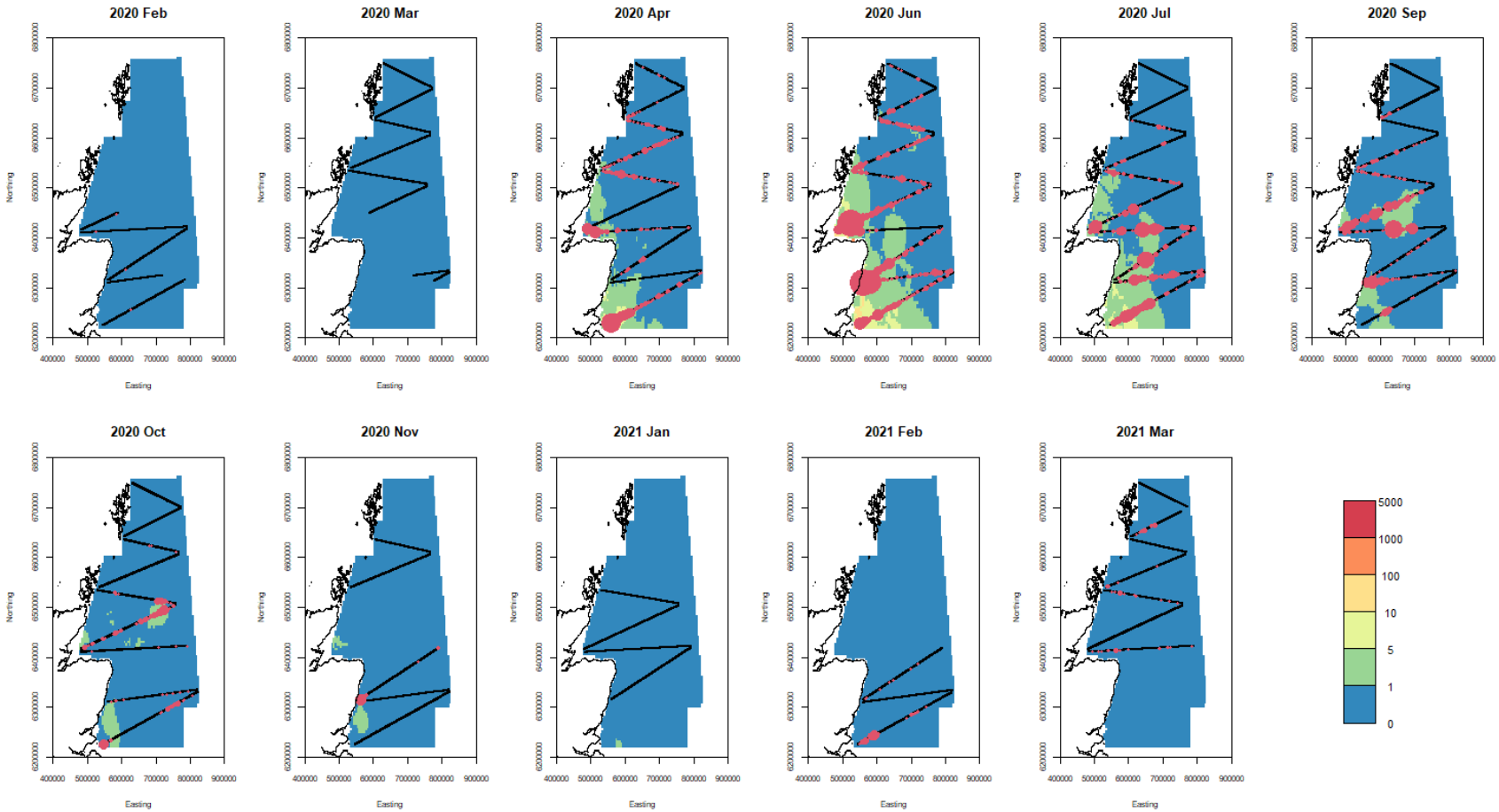

Figure 61. A graph showing point estimates of razorbill densities for each surveyed month from February 2020 to March 2021. Colours represent estimated densities per km^2. Black lines indicate sampling locations in that month. Red dots indicate observed numbers of razorbill with size proportional to observed number. Note that scale is matching the following graphs depicting lower and upper confidence intervals.

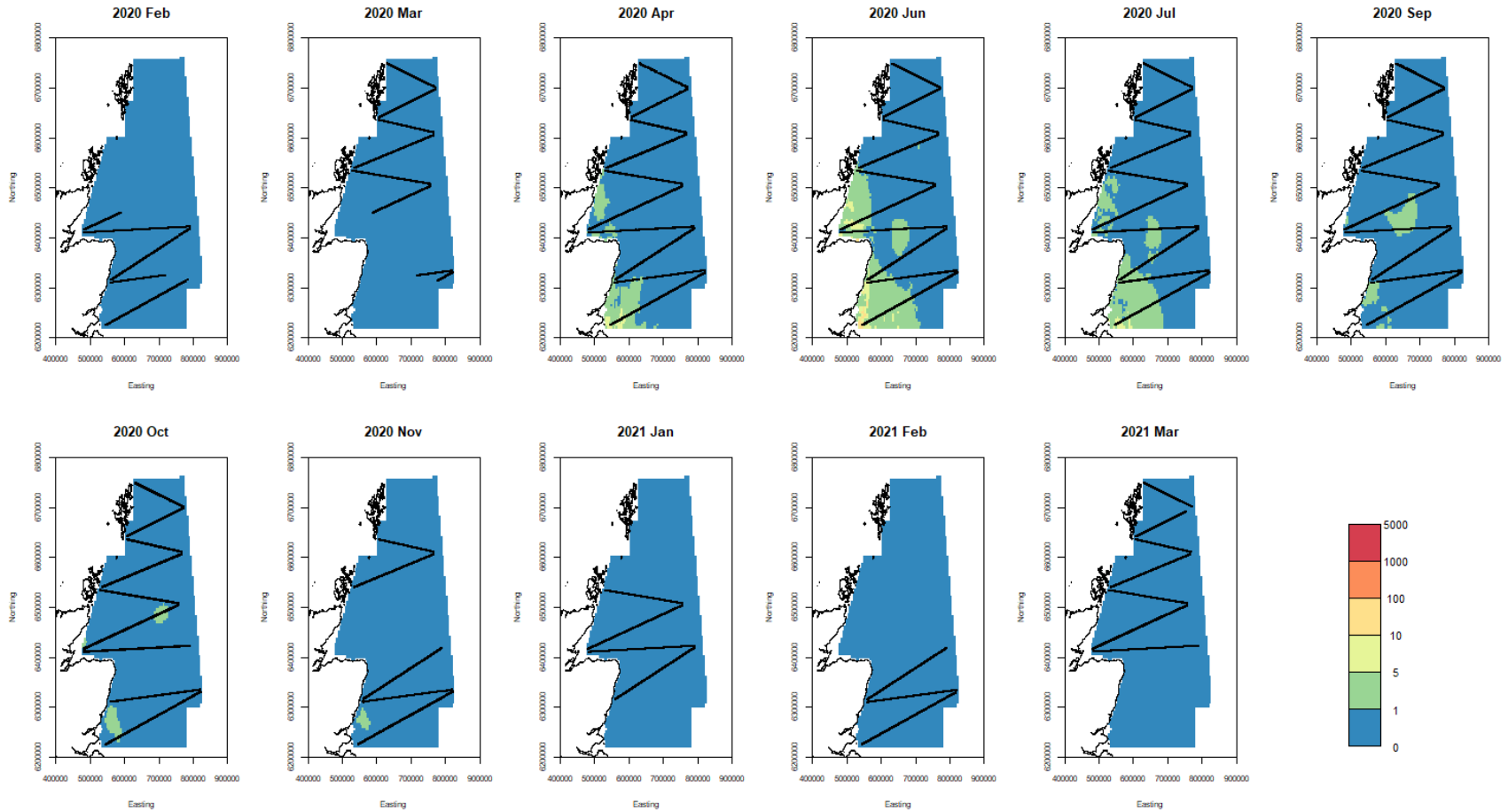

Figure 62. A graph showing lower confidence bound estimates (2.5%) of razorbill densities for each surveyed month from February 2020 to March 2021. Colours represent estimated densities per km^2. Black lines indicate sampling locations in that month.

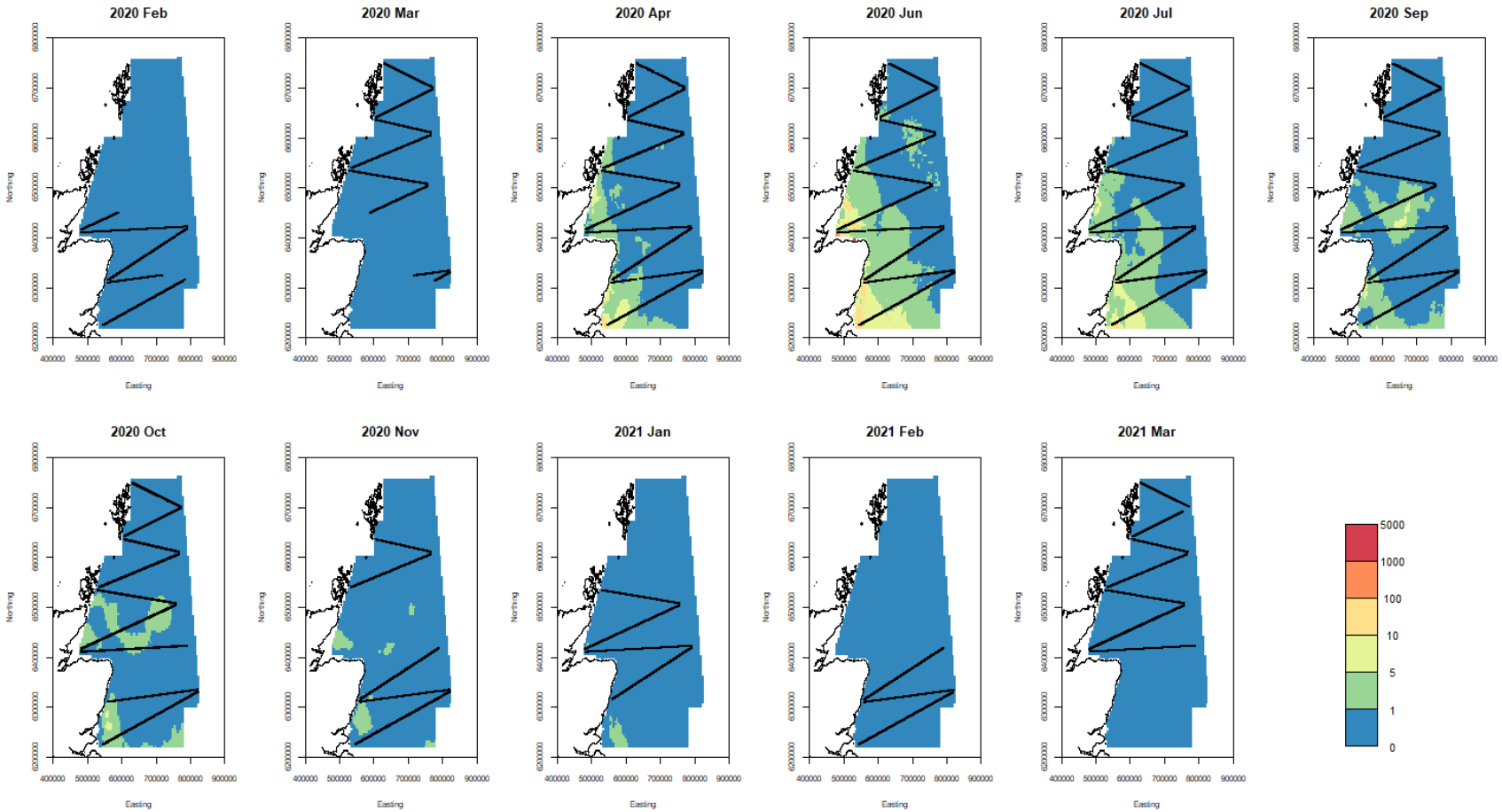

Figure 63. A graph showing upper confidence bound estimates (97.5%) of razorbill densities for each surveyed month from February 2020 to March 2021. Colours represent estimated densities per km^2. Black lines indicate sampling locations in that month.

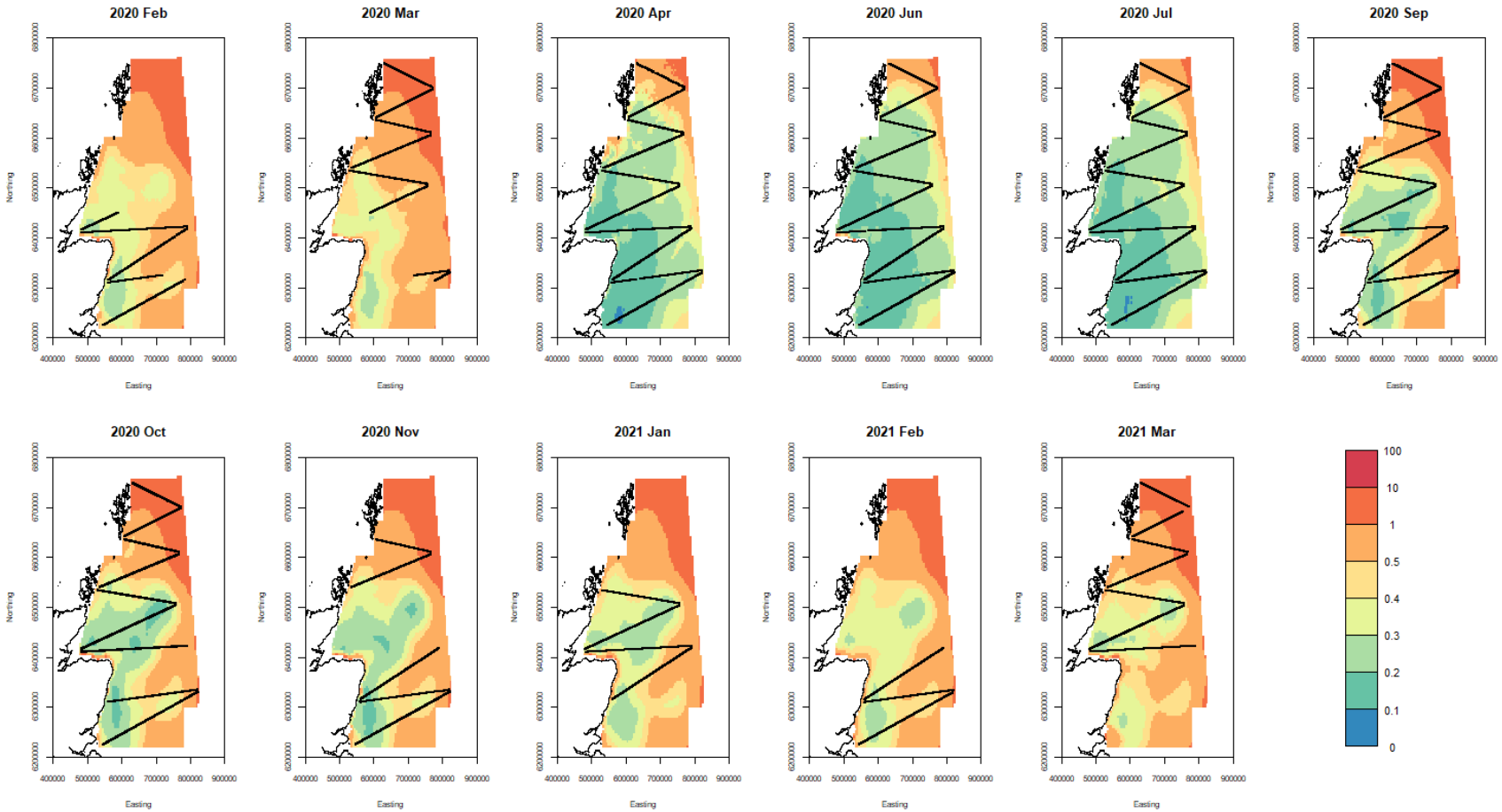

Figure 64. A graph showing razorbill coefficients of variation (CV, in %) in estimated densities of birds for each surveyed month from February 2020 to March 2021. Black lines indicate sampling locations in that month. The largest CVs are at the northern and eastern part the study area.

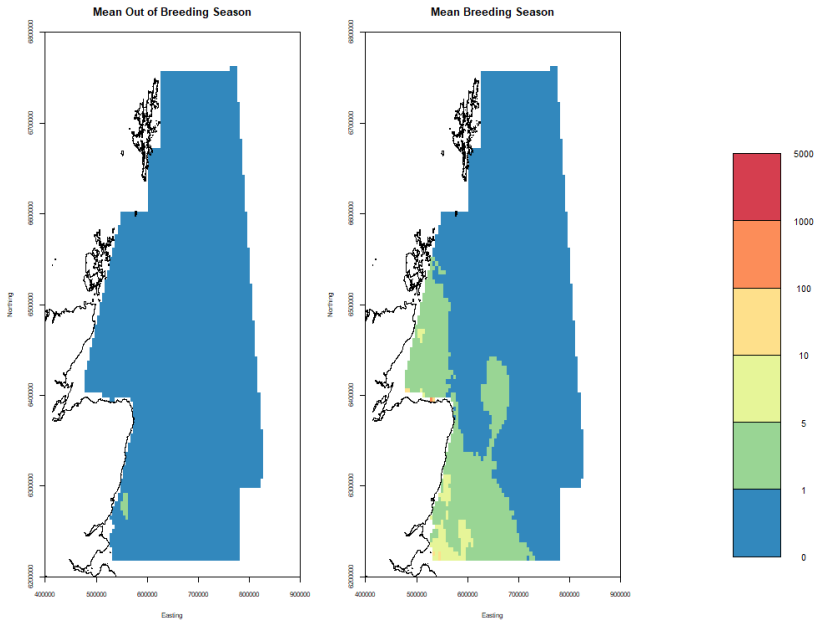

Figure 65. A graph showing mean razorbill density (birds/km^2) surfaces for breeding (April – July) and non-breeding (August – March) seasons.

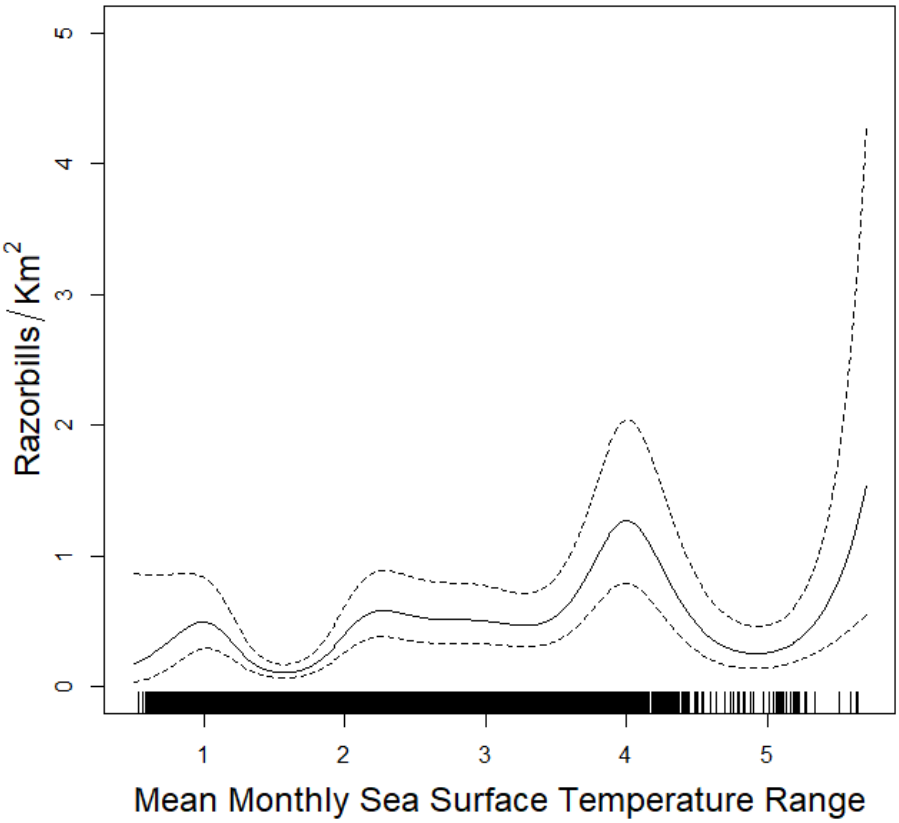

Figure 66. Graph showing effect of mean monthly sea surface temperature range on razorbill observed density assuming the middle of the survey area during the breeding season.

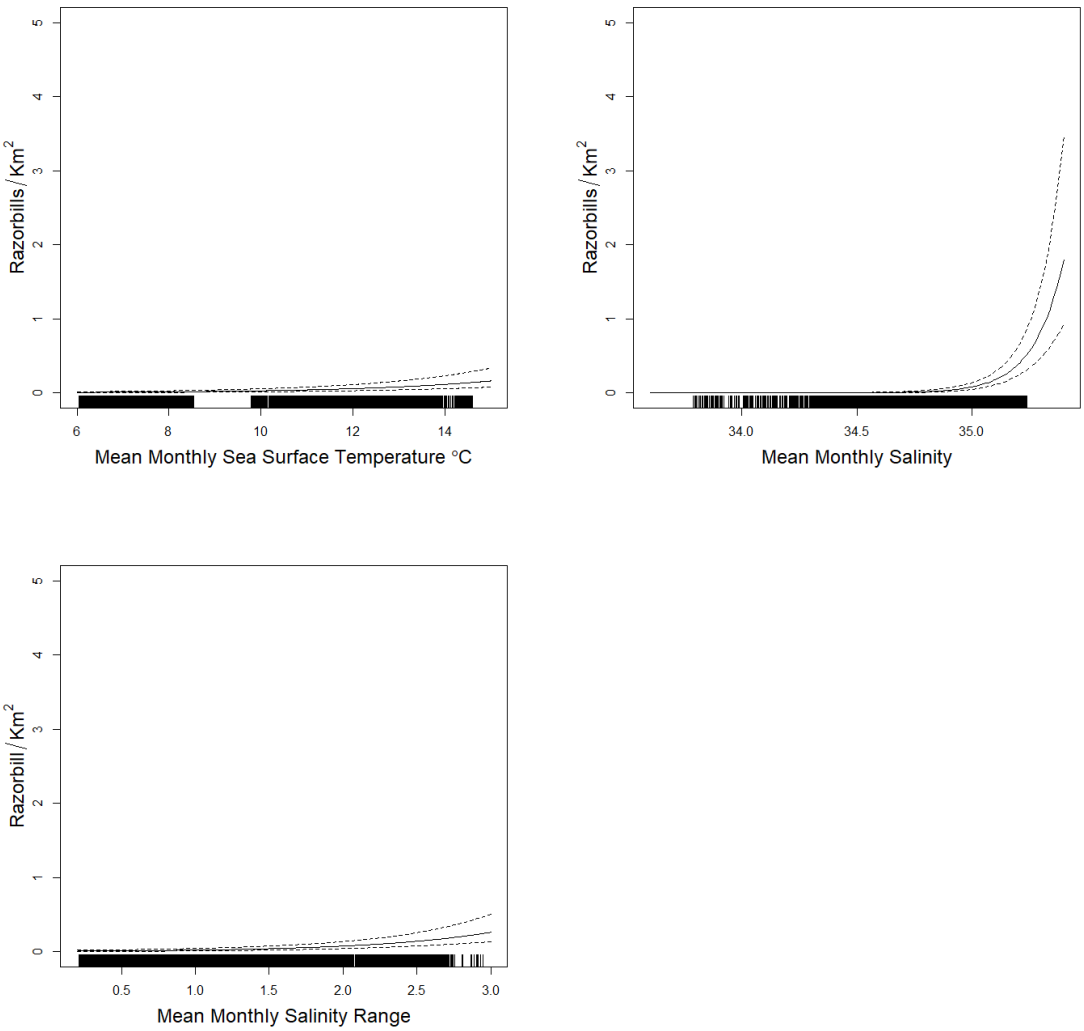

Figure 67. Graphs showing effect of (upper left) monthly sea surface temperature,(upper right) mean monthly salinity and (lower left) mean monthly salinity range on razorbill density assuming the middle of the survey area outside of the breeding season.

6.3.11 Atlantic Puffin

The separate fitted models for breading and non-breeding season are given in Table 8. Estimated numbers through the study period are given in

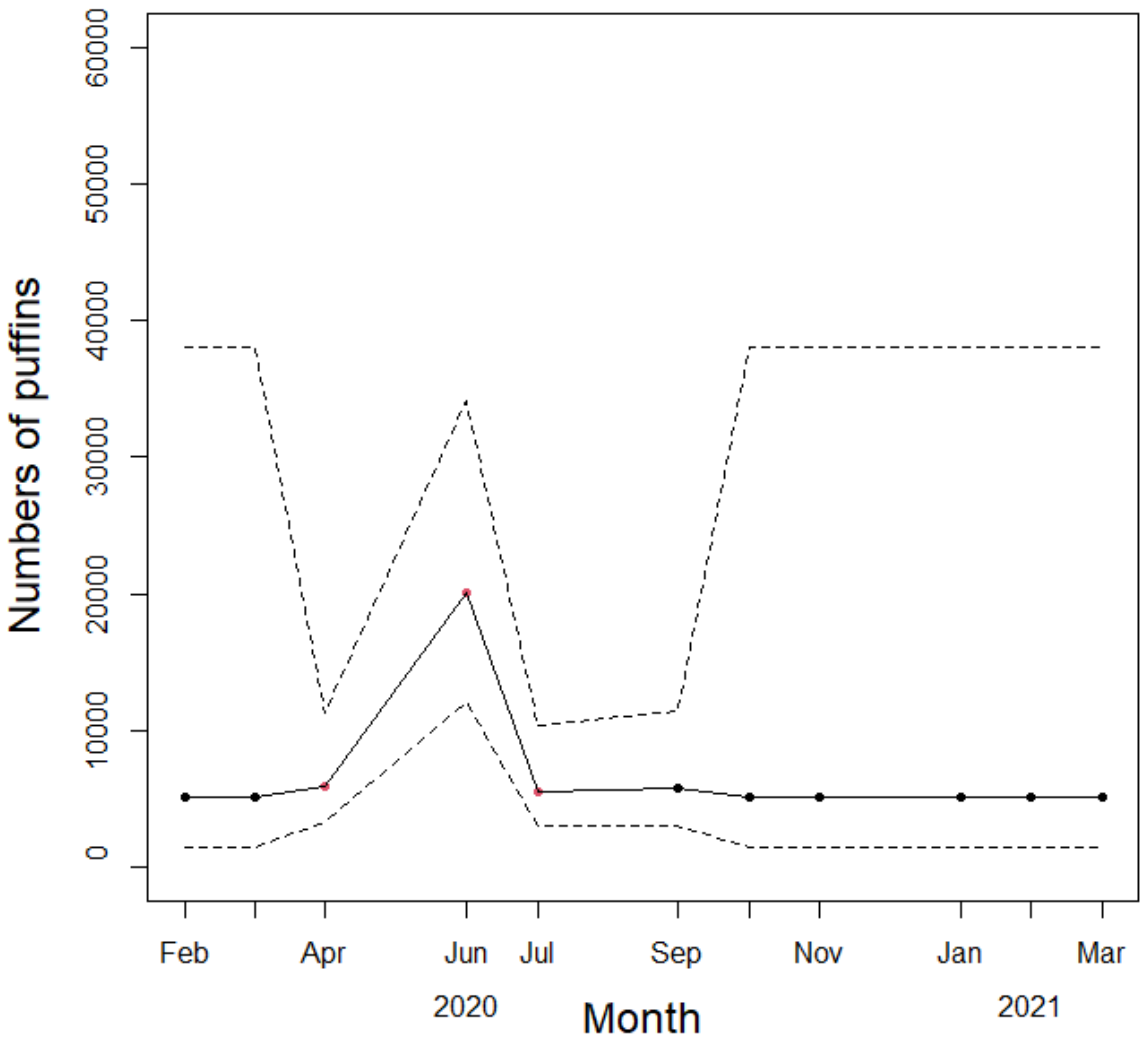

Figure 68. They show a peak during the breeding season between April and July. Point estimates of puffin density for the sampling months along with the confidence bounds are given in the Figure 69, Figure 70 and Figure 71, For this species there were predicted areas of high density near the coast in regions with little survey effort. The CVs are shown in Figure 72 and are higher in breeding than non-breeding season. The mean point estimates for breeding and non-breeding season in shown in Figure 73 and indicate higher densities in the south-western part of the study area during the breeding season.

Greatest densities occurred between April and June particularly in the southern part of the study area, around the Firths of Forth and Tay and east Grampian coast,

although high densities are predicted east of Caithness and the Northern Isles where survey effort was low.

The effect of the non-location variables in the breeding season model is given in Figure 74. The effect of current in the non-breeding season model is given in Figure 75. Note that these are the effects of these variables given the presence of location in the model, so may be very different from the actual biological effect.

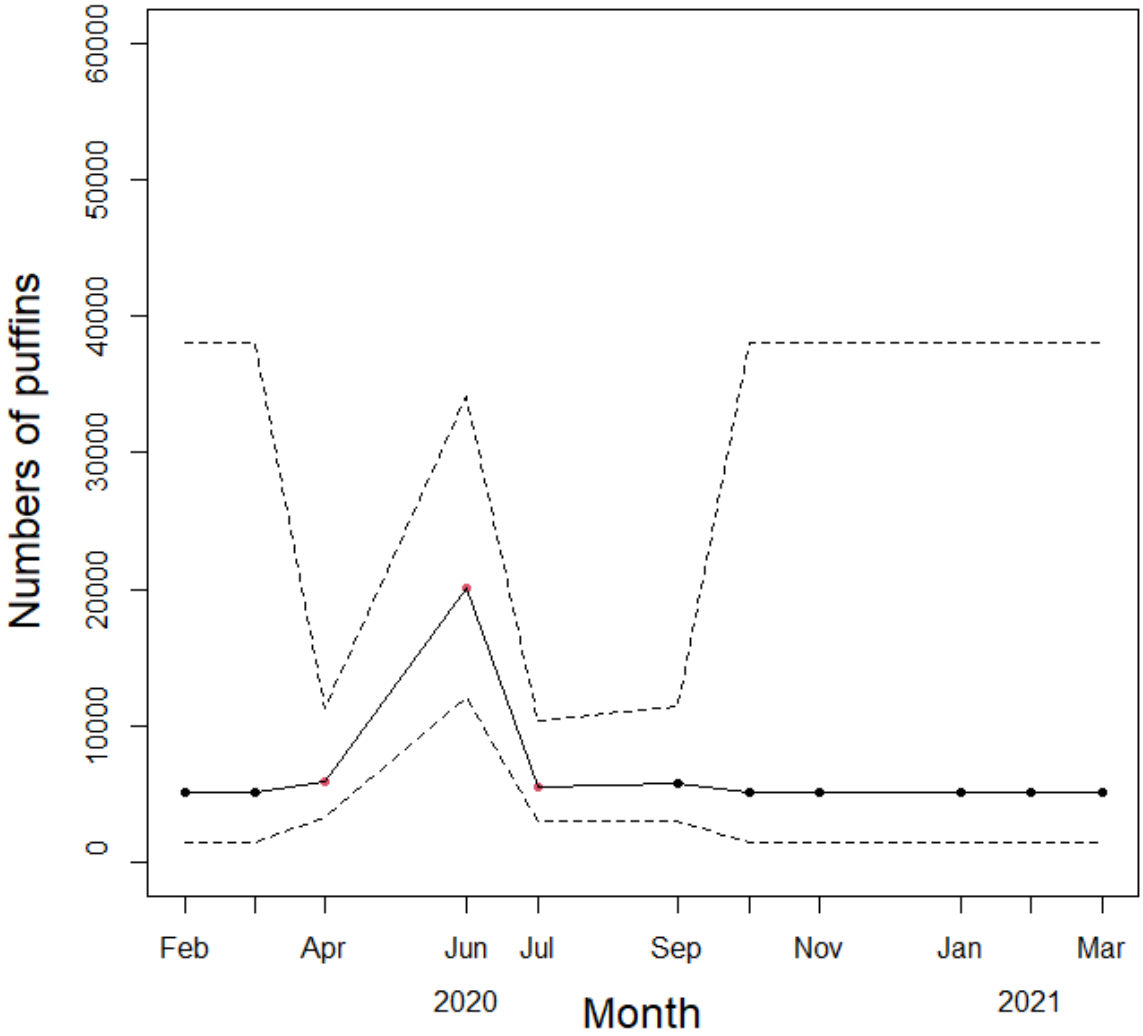

Figure 68. A graph showing estimated numbers of puffins over the duration of the study from February 2020 to March 2021. Red points indicate the breeding season (April to July) and the dashed lines represent upper and lower bounds of the 95% confidence intervals. Numbers of puffins peaked in June. High uncertainty is generated in peripheral regions in the non-breeding season.

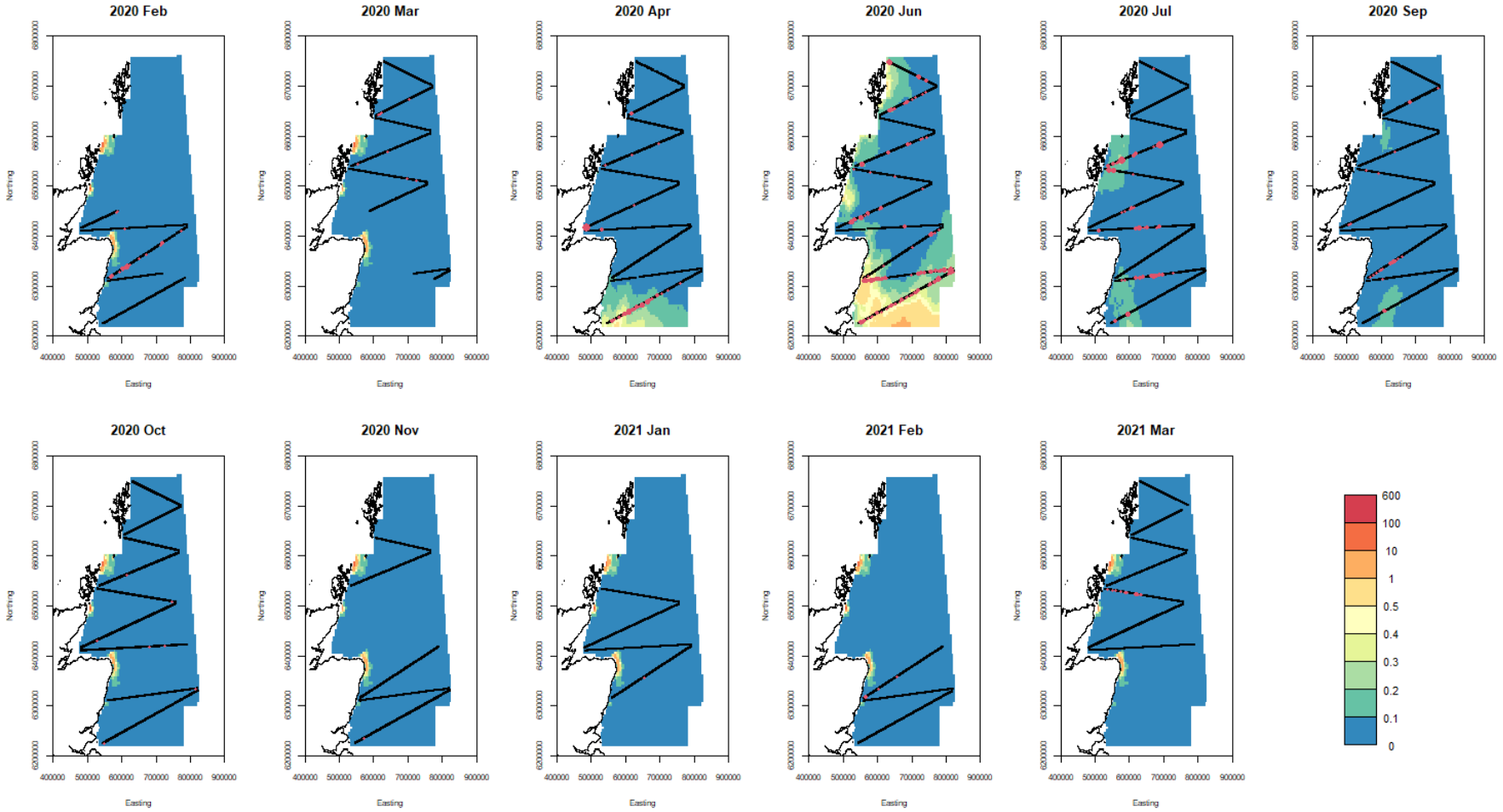

Figure 69. A graph showing point estimates of puffin densities for each surveyed month from February 2020 to March 2021. Colours represent estimated densities per km^2. Black lines indicate sampling locations in that month. Red dots indicate observed numbers of fulmars with size proportional to observed number. Note that scale is matching the following graphs depicting lower and upper confidence intervals

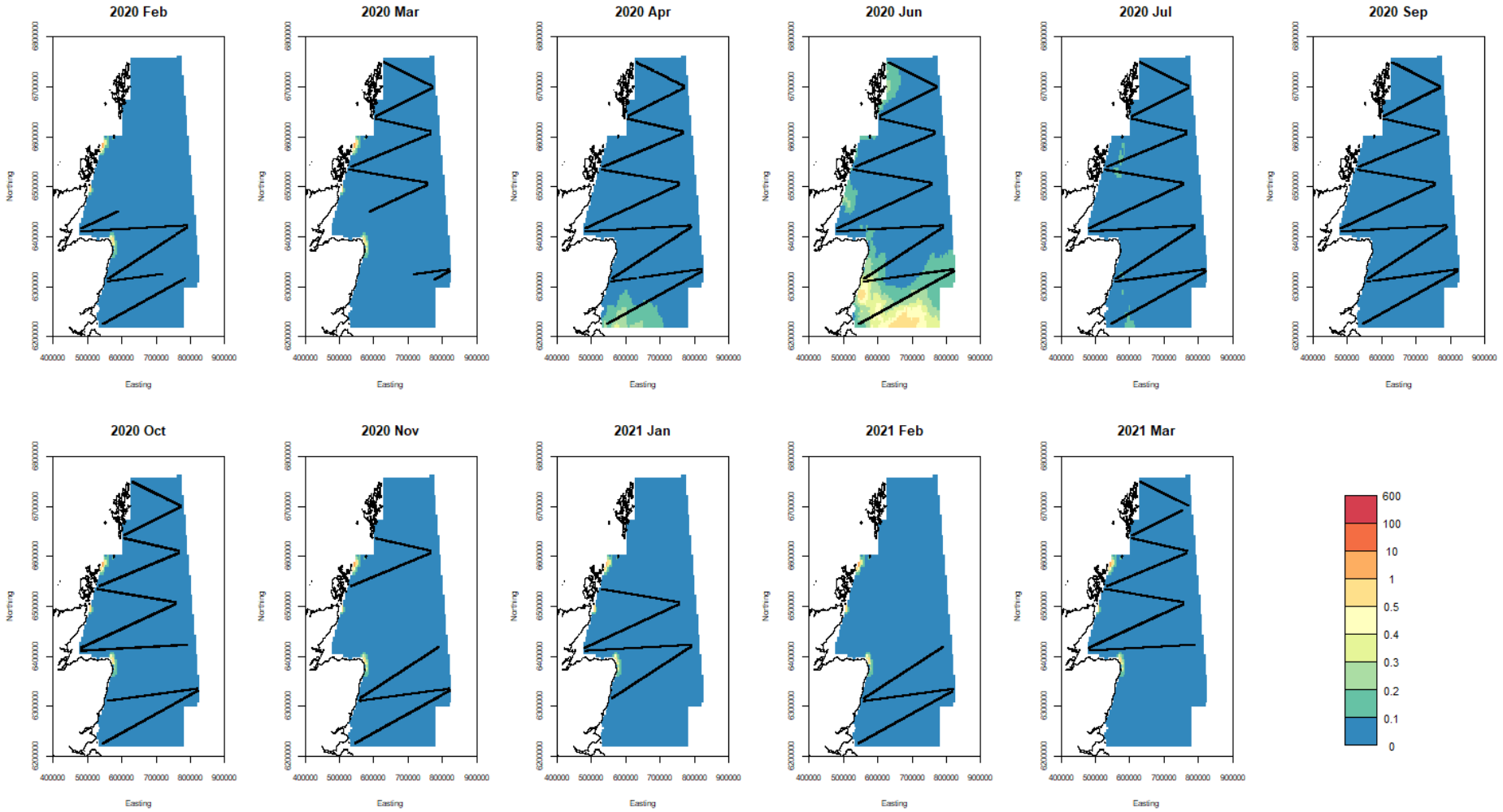

Figure 70. A graph showing lower confidence bound estimates (2.5%) of puffin densities for each surveyed month from February 2020 to March 2021. Colours represent estimated densities per km^2. Black lines indicate sampling locations in that month.

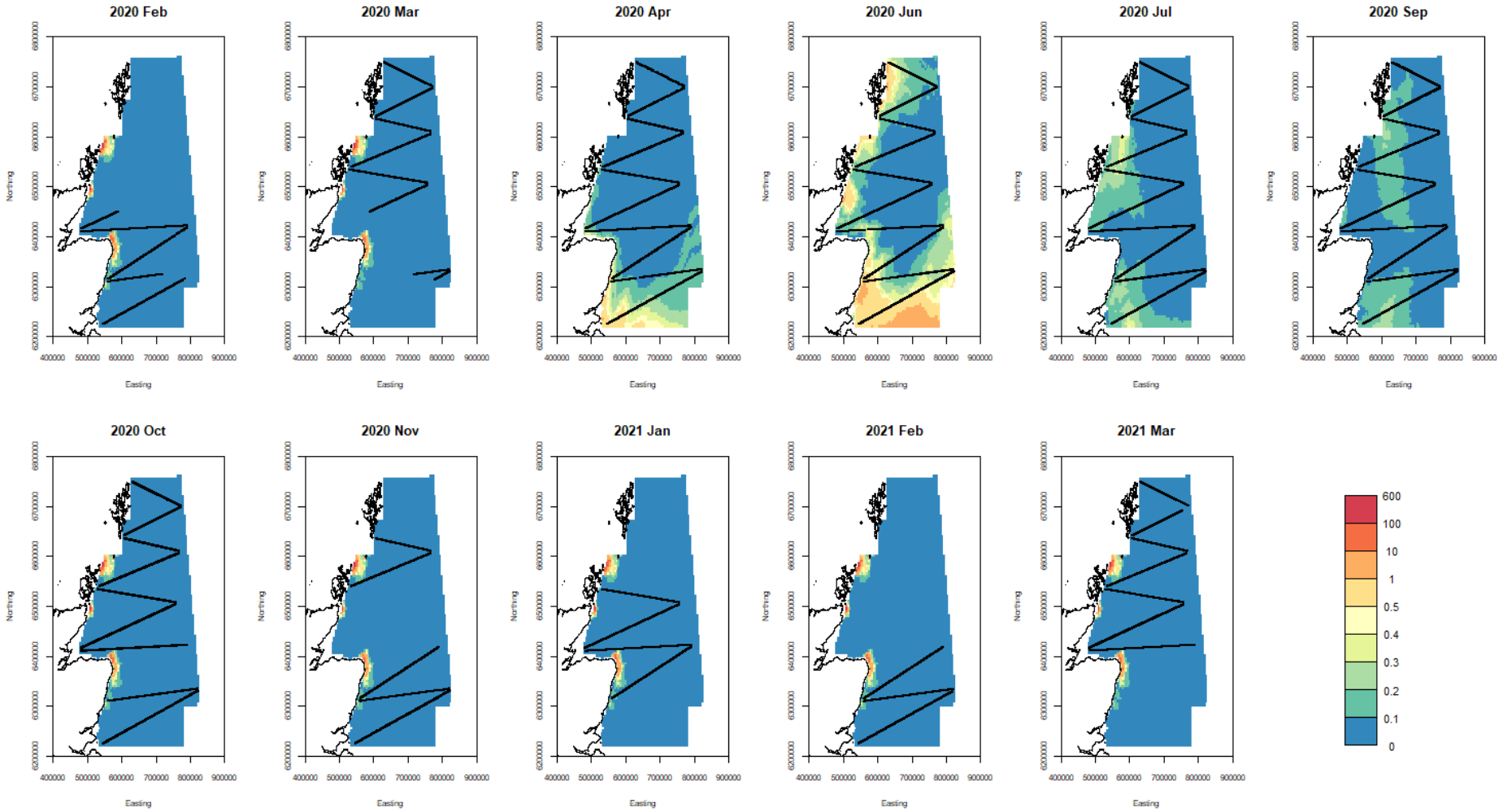

Figure 71. A graph showing upper confidence bound estimates (97.5%) of puffin densities for each surveyed month from February 2020 to March 2021. Colours represent estimated densities per km^2. Black lines indicate sampling locations in that month.

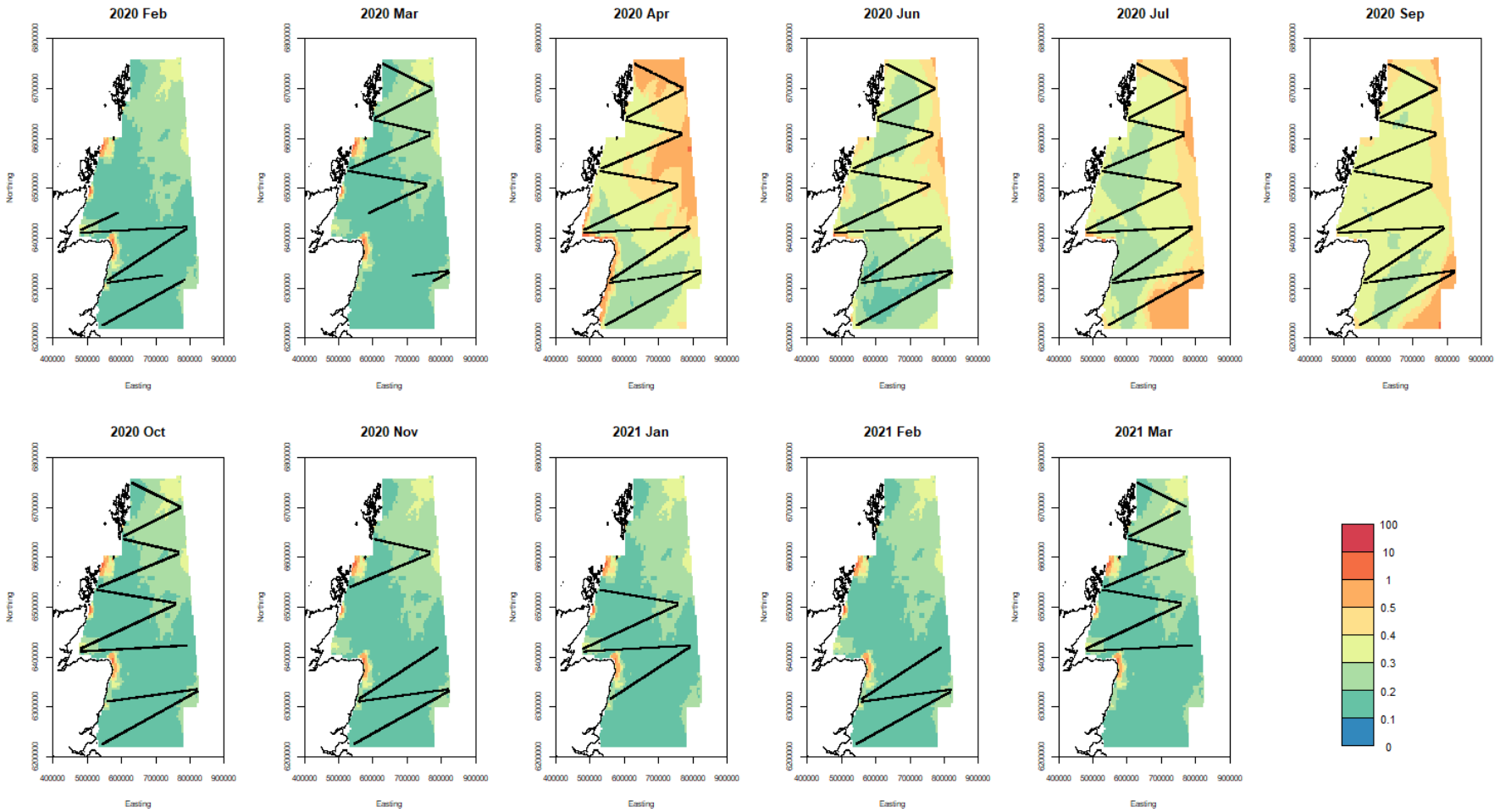

Figure 72. A graph showing Atlantic puffin coefficients of variation (CV, in %) in estimated densities of birds for each surveyed month from February 2020 to March 2021. Black lines indicate sampling locations in that month. The largest CVs are at the northern and eastern of the study area.

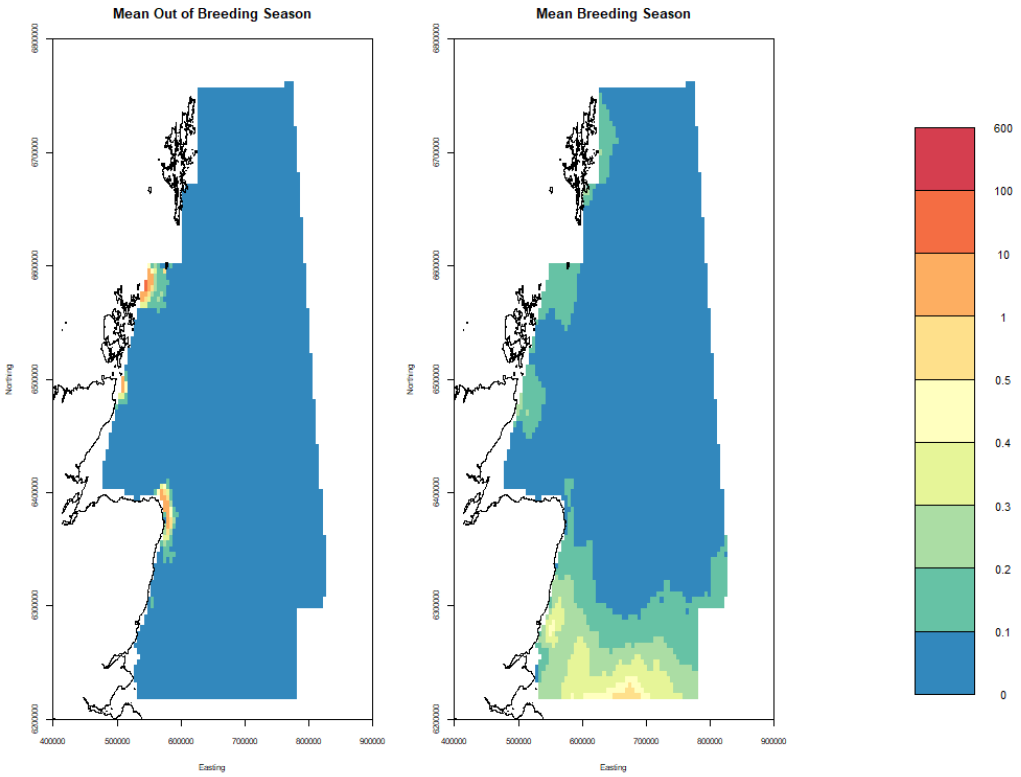

Figure 73. A graph showing mean puffin density (birds/km^2) surfaces for breeding (April – August) and non-breeding (September – March) seasons

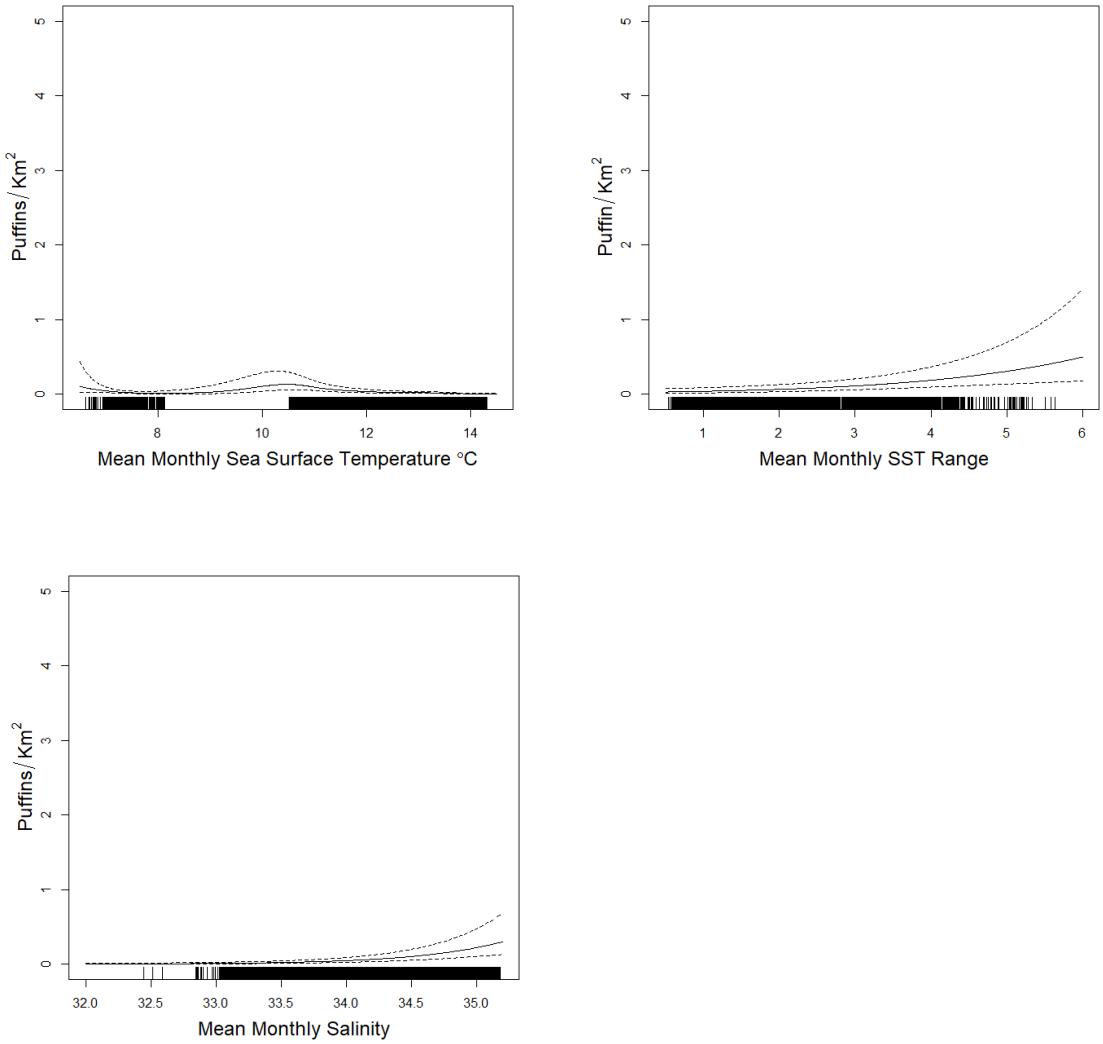

Figure 74. Graphs showing effect of (upper left) monthly sea surface temperature, (upper right) mean monthly SST range and (lower left) mean monthly salinity on Atlantic puffin observed density assuming the middle of survey area during the breeding season.

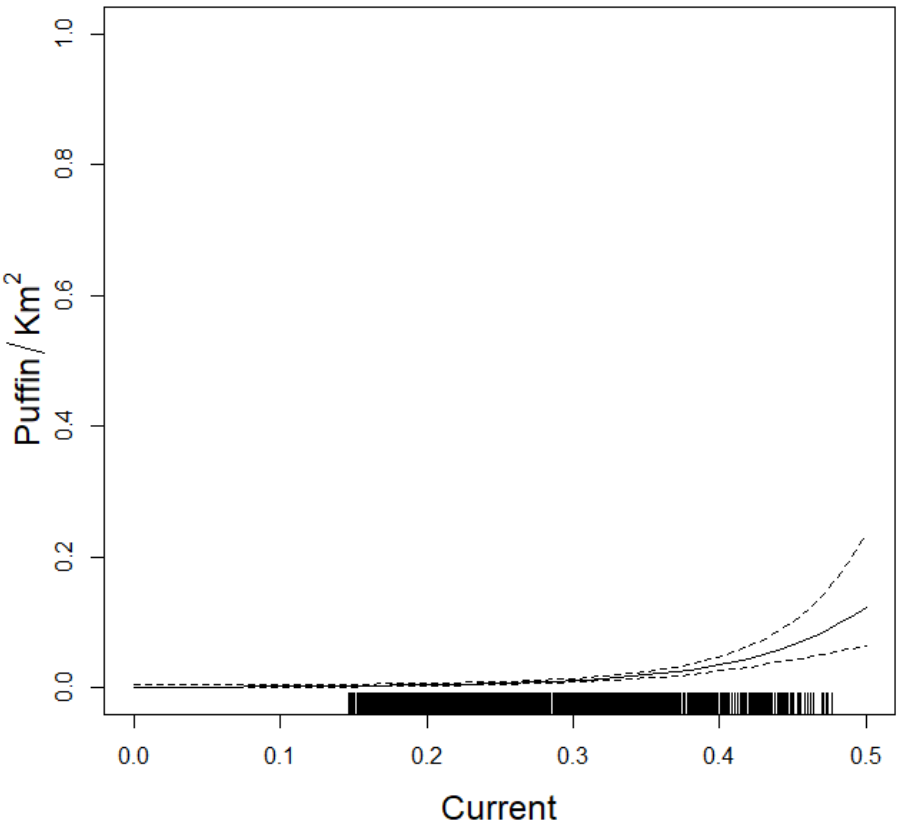

Figure 75. Graph showing effect of current on Atlantic puffin observed density assuming the middle of the survey area outside of the breeding season

6.4 Marine Mammal Species

6.4.1 Minke Whale

There were only 35 datums out of the 5,036 reduced data set locations with minke whale presences, so a number based spatial model could not be fitted. A binomial presence-absence model was fitted and then numbers were estimated based on the mean number seen per presence. This model is not ideal. Availability was estimated at 0.04. Peak numbers occurred in June followed by a steady decline (Figure 76 Table 9).

Point estimates of minke whale density for the sampled months along with the confidence bounds are given in Figure 77, Figure 78, and Figure 79**Error! Reference source not found.**. The higher numbers observed in June occurred in two areas: in the north-western North Sea east of the Grampian region and Firth of Forth, and further east in the middle of the North Sea. No CVs were produced for this species.

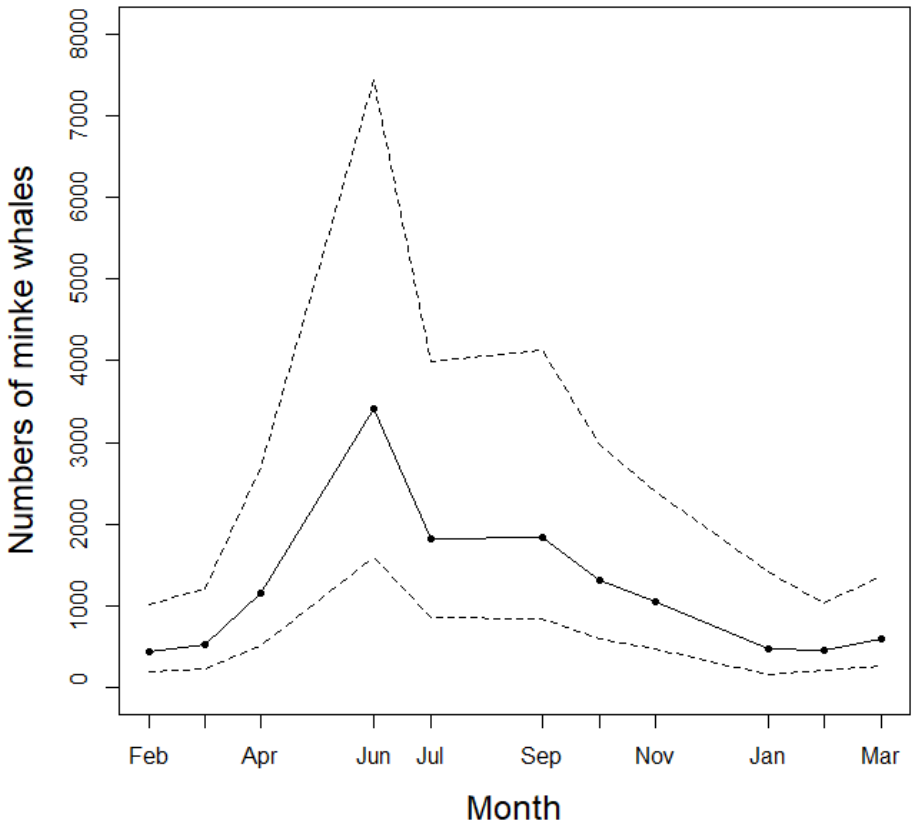

Figure 76. A graph showing estimated numbers of minke whales over the duration of the study from February 2020 to March 2021. Dashed lines represent upper and lower bounds of the 95% confidence intervals. Numbers of minke whales peaked in June.

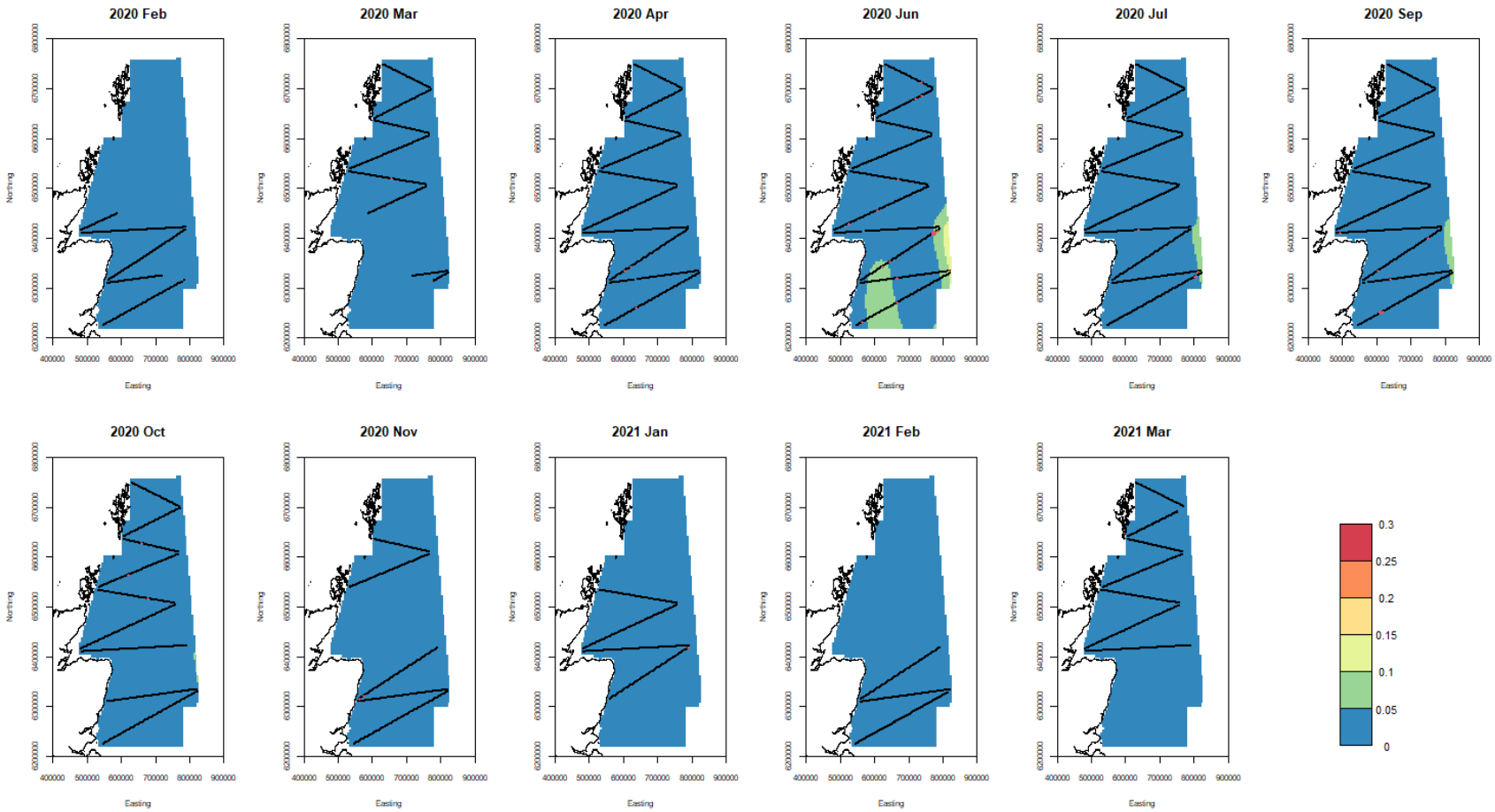

Figure 77. A graph showing point estimates of minke whales densities for each surveyed month from February 2020 to March 2021. Colours represent estimated densities per km^2. Black lines indicate sampling locations in that month. Red dots indicate observed numbers of whales with size proportional to observed number. Note that scale is matching the following graphs depicting lower and upper confidence intervals.

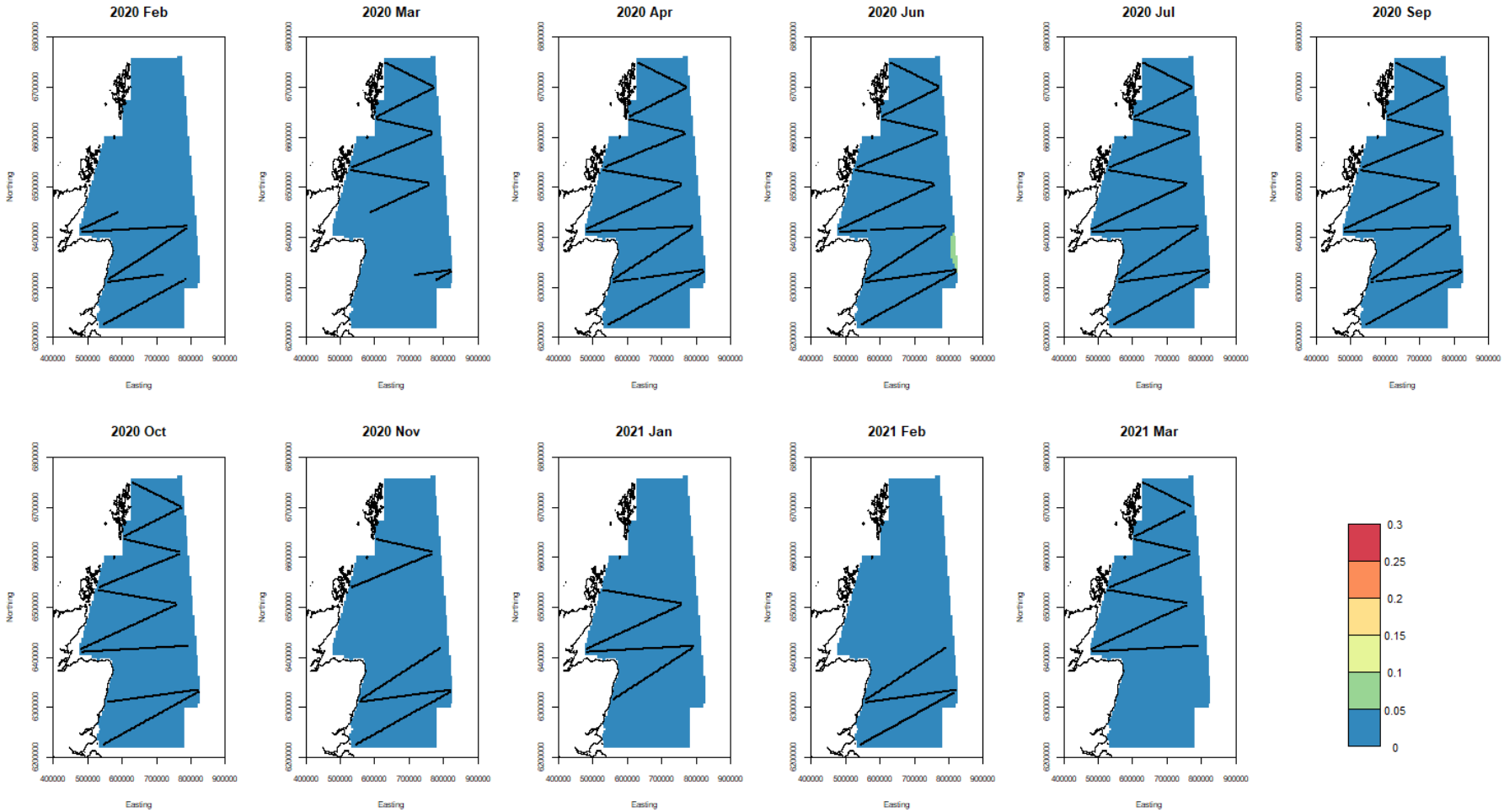

Figure 78. A graph showing lower confidence bound estimates (2.5%) of minke whale densities for each surveyed month from February 2020 to March 2021. Colours represent estimated densities per km^2. Black lines indicate sampling locations in that month.

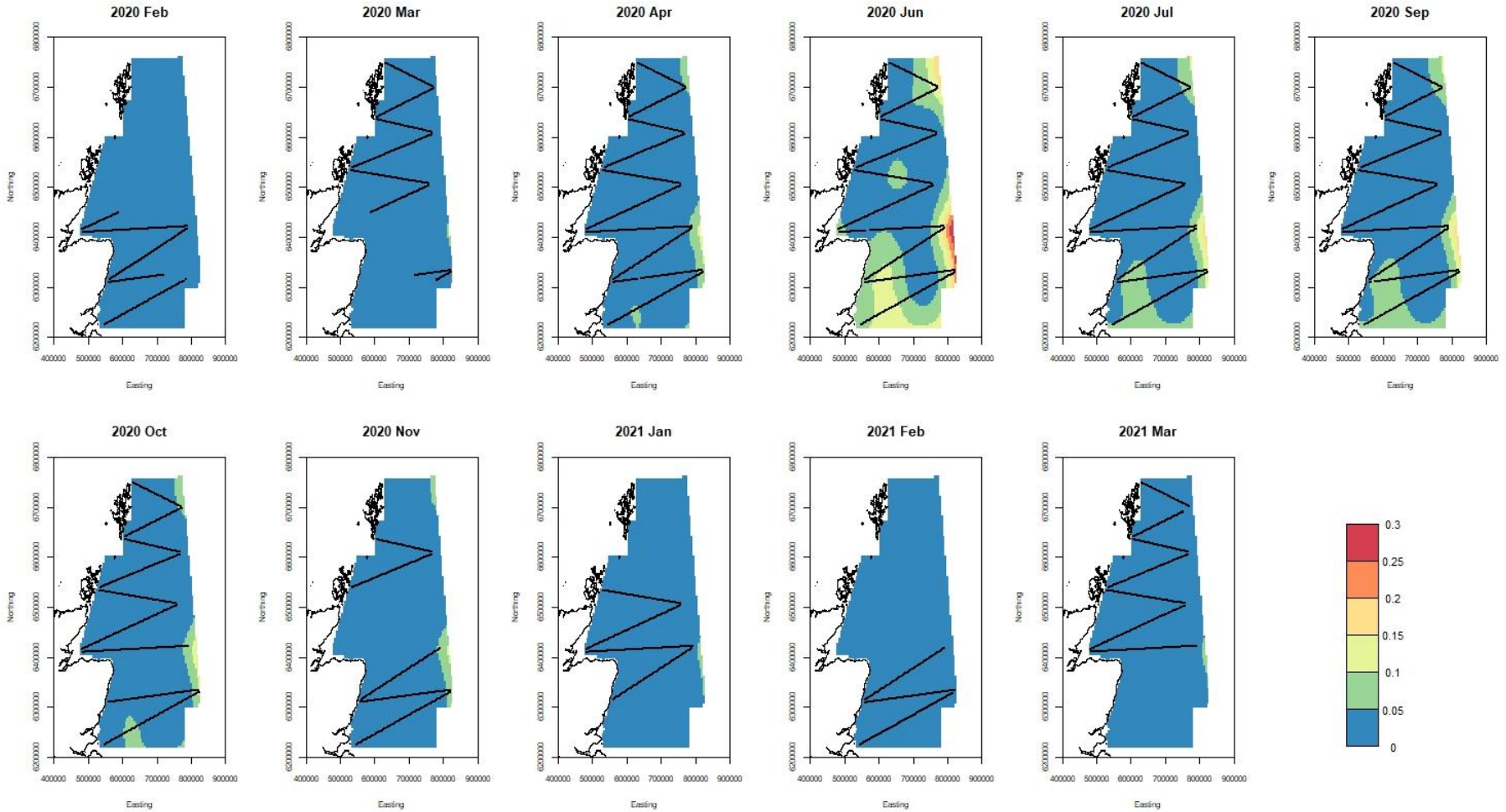

Figure 79. A graph showing upper confidence bound estimates (97.5%) of minke whale densities for each surveyed month from February 2020 to March 2021. Colours represent estimated densities per km^2. Black lines indicate sampling locations in that month.

6.4.2 Common Dolphin

In the case of common dolphins, there were only 18 datums with common dolphin presences. A binomial model of presence was attempted on a reduced dataset from March to July (as no animals were seen outside this time) but no spatial signal could be found (Table 9). The estimates of abundance are therefore 0 outside March to July, otherwise 6170(95% confidence interval 3530 – 10790), assuming an individual availability at the surface of 0.05.

Locations of sightings for common dolphins across the sampled months are given in Figure 80 but no model fits are done. Most sightings occurred in the month of June offshore in the middle of the North Sea although the species was also recorded further north, east of Caithness in March 2020.

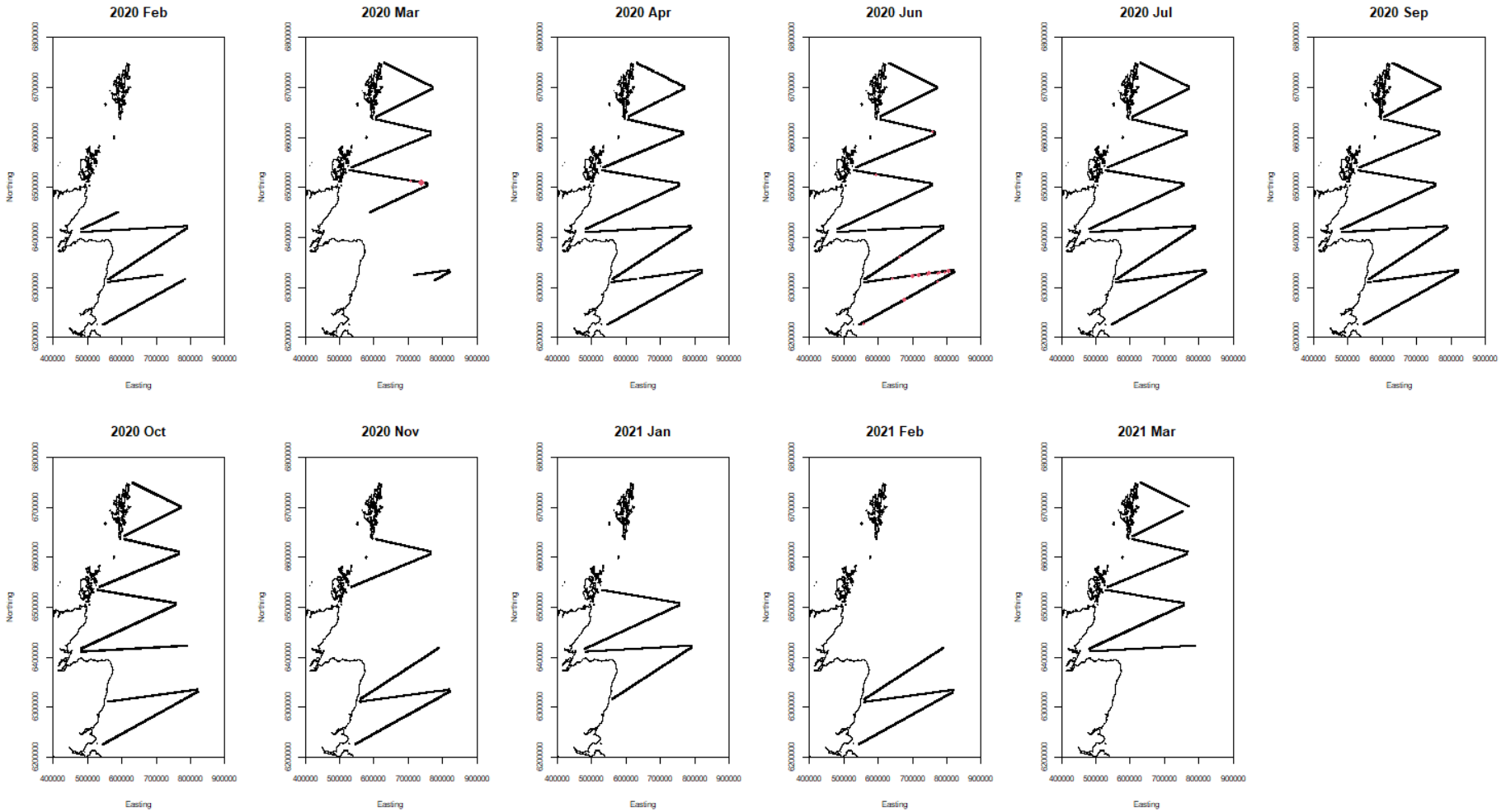

Figure 80. A graph showing locations of sightings of common dolphins. No model was fitted to the data; hence the distribution model outputs are not presented. Black lines indicate sampling locations in that month. Red dots indicate observed numbers of common dolphin with areas proportional to number.

6.4.3 White beaked Dolphin

The fitted model of all data is given in Table 9. A model with *Dayofyear* could not be fitted so instead Month was used as a factor variable. The estimated numbers from the model are given in Figure 81. Although there were sightings in several months of the year, they show a strong seasonal peak in July. Surface availability was assumed to be 0.06.

Point estimates of white-beaked dolphin density for the sampled months along with the confidence bounds and CVs are given in Figures Figure 82, Figure 83, Figure 84, and Figure 85. The models indicate a general distribution across the North Sea with highest densities further offshore.

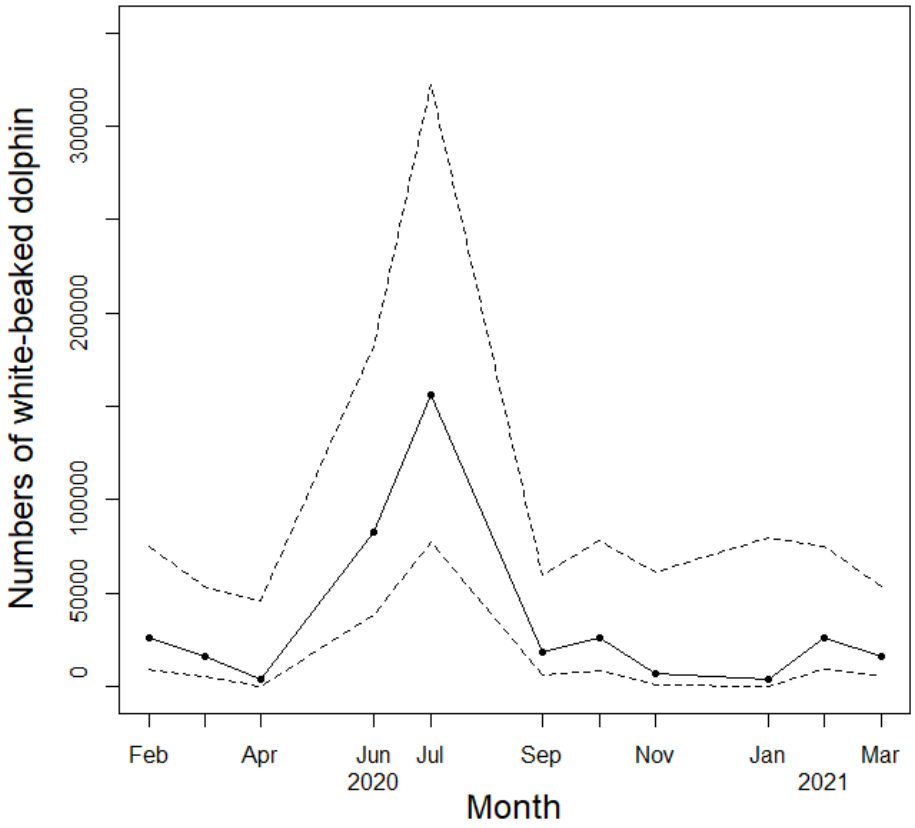

Figure 81. A graph showing estimated numbers of white-baked dolphins over the duration of the study from February 2020 to March 2021. Dashed lines represent upper and lower bounds of the 95% confidence intervals. Numbers of dolphins peaked in July.

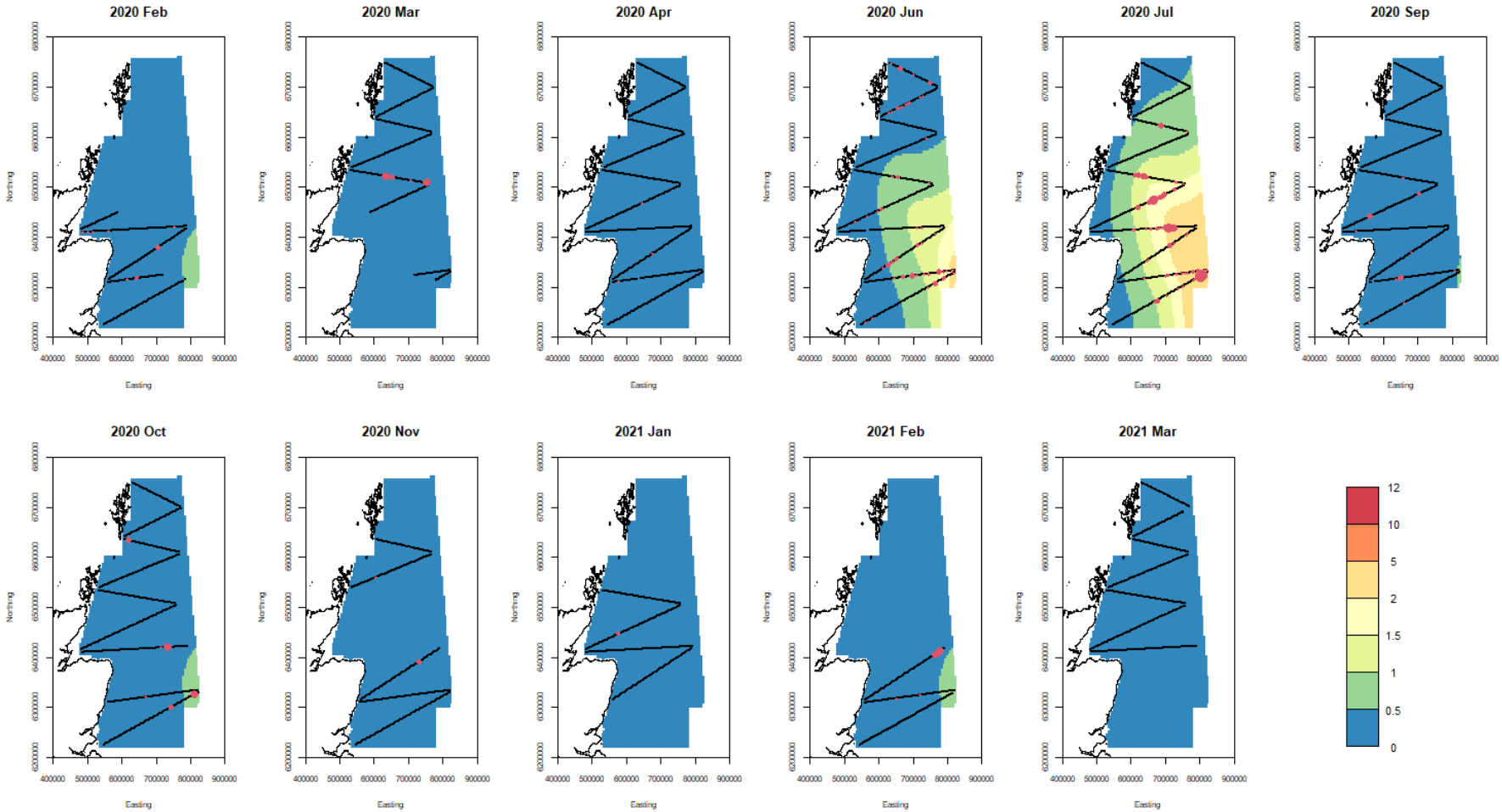

Figure 82. A graph showing point estimates of white-beaked dolphins densities for each surveyed month from February 2020 to March 2021. Colours represent estimated densities per km^2. Black lines indicate sampling locations in that month. Red dots indicate observed numbers of dolphins with size proportional to observed number. Note that scale is matching the following graphs depicting lower and upper confidence intervals

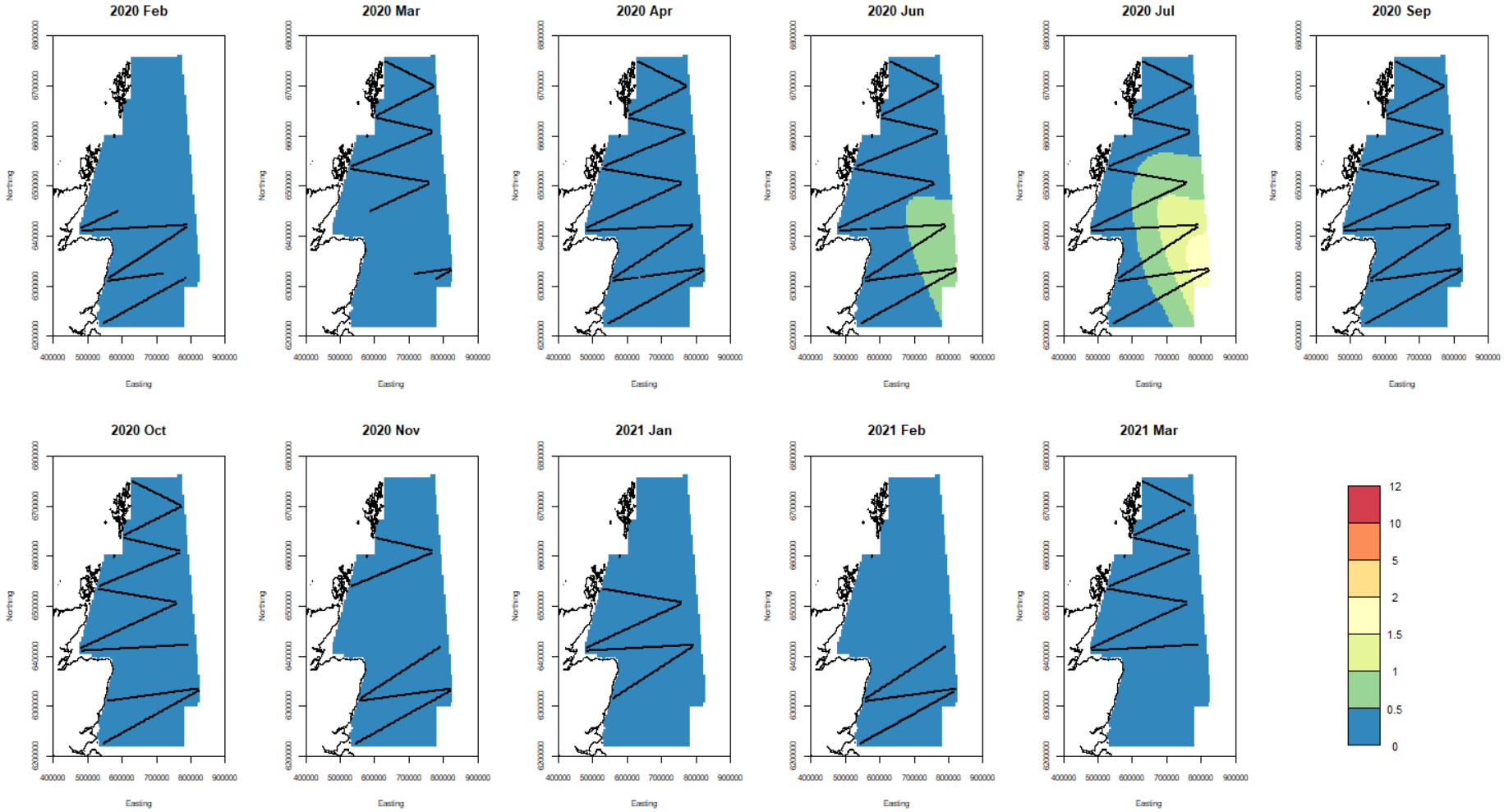

Figure 83. A graph showing lower confidence bound estimates (2.5%) of white-beaked dolphins densities for each surveyed month from February 2020 to March 2021. Colours represent estimated densities per km^2. Black lines indicate sampling locations in that month.

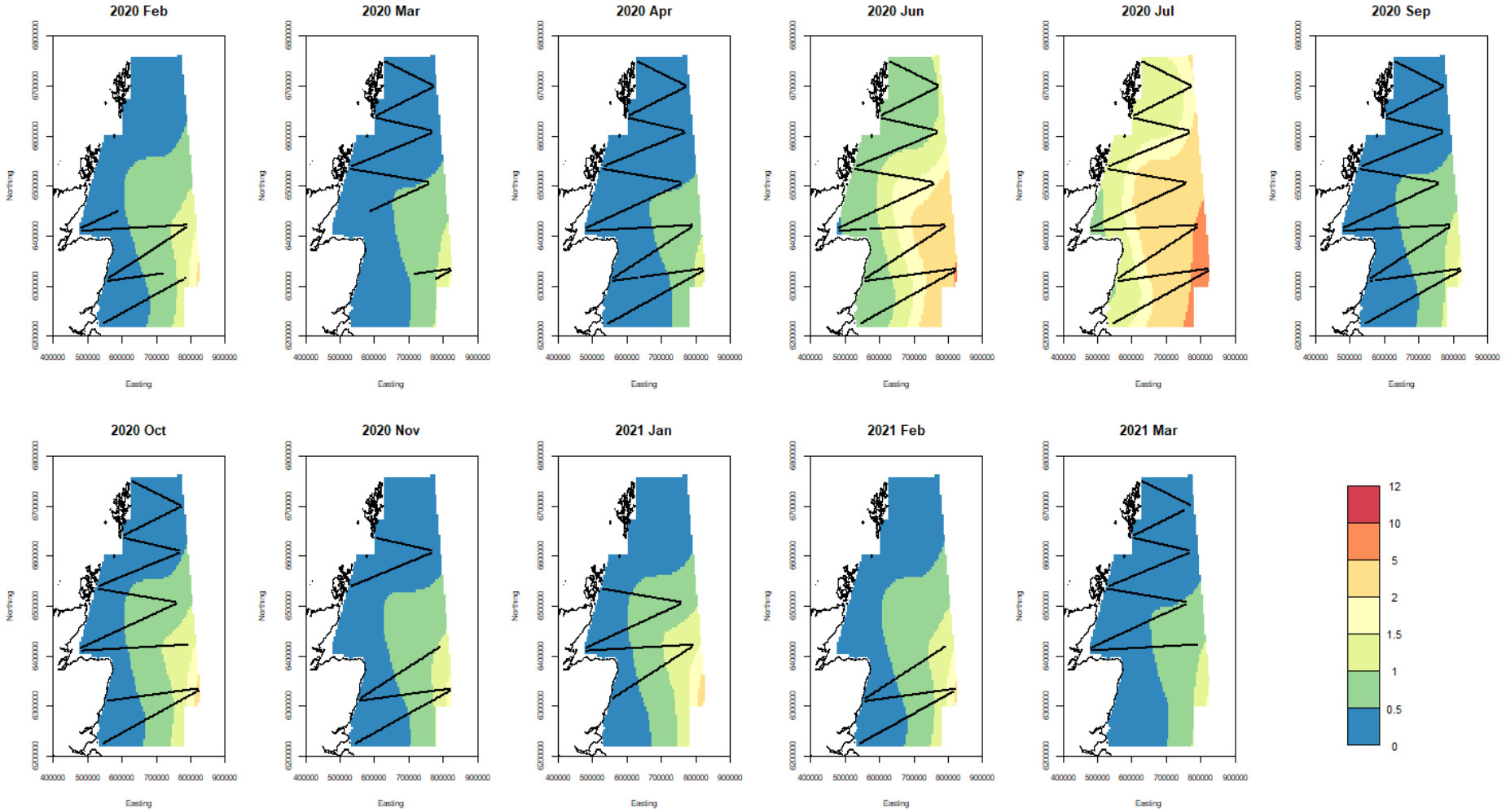

Figure 84. A graph showing upper confidence bound estimates (97.5%) of white-beaked dolphin densities for each surveyed month from February 2020 to March 2021. Colours represent estimated densities per km^2. Black lines indicate sampling locations in that month.

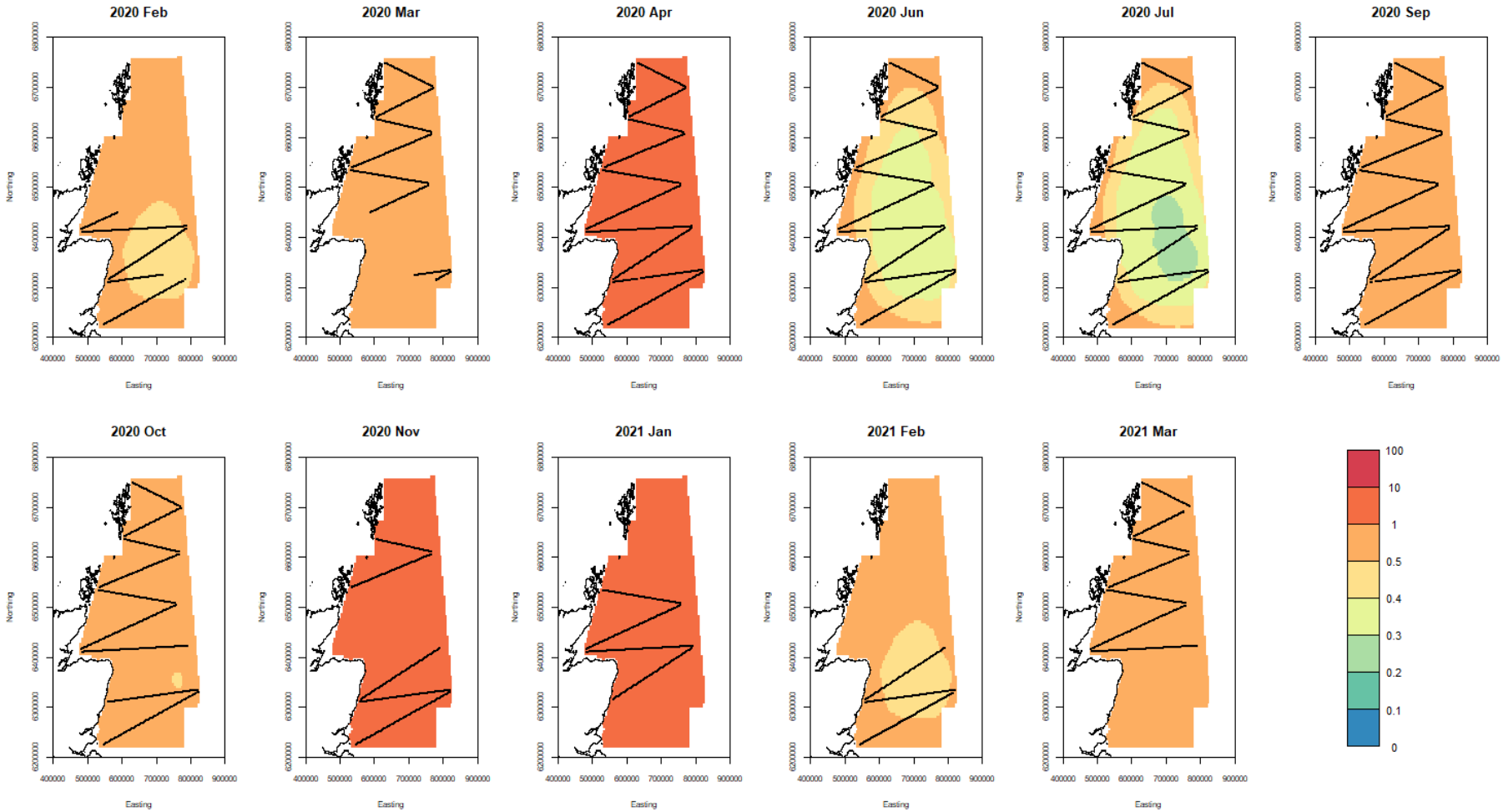

Figure 85. A graph showing white-beaked dolphin coefficients of variation (CV, in %) in estimated densities of dolphins for each surveyed month from February 2020 to March 2021. Black lines indicate sampling locations in that month.

6.4.4 Harbour Porpoise

No model with a correlated error structure could be fitted to the n= 97090 data so the data were further amalgamated into 3-min chunks. This gave a total of 5093 datums. The model is given in Table 9. The predicted numbers over the period of the survey are given in Figure 86. These show broadly similar abundances through the year but with a peak between April and June.

The spatial density surfaces for the sampled months are given in Figure 87, and Figure 89 along with associated uncertainty. They indicate broad distributions for the species in most months, with highest offshore densities east of the Moray Firth and Grampian region.

The effect of salinity on density is given in Figure 91, suggesting there may be higher density where freshwater has a greater influence.

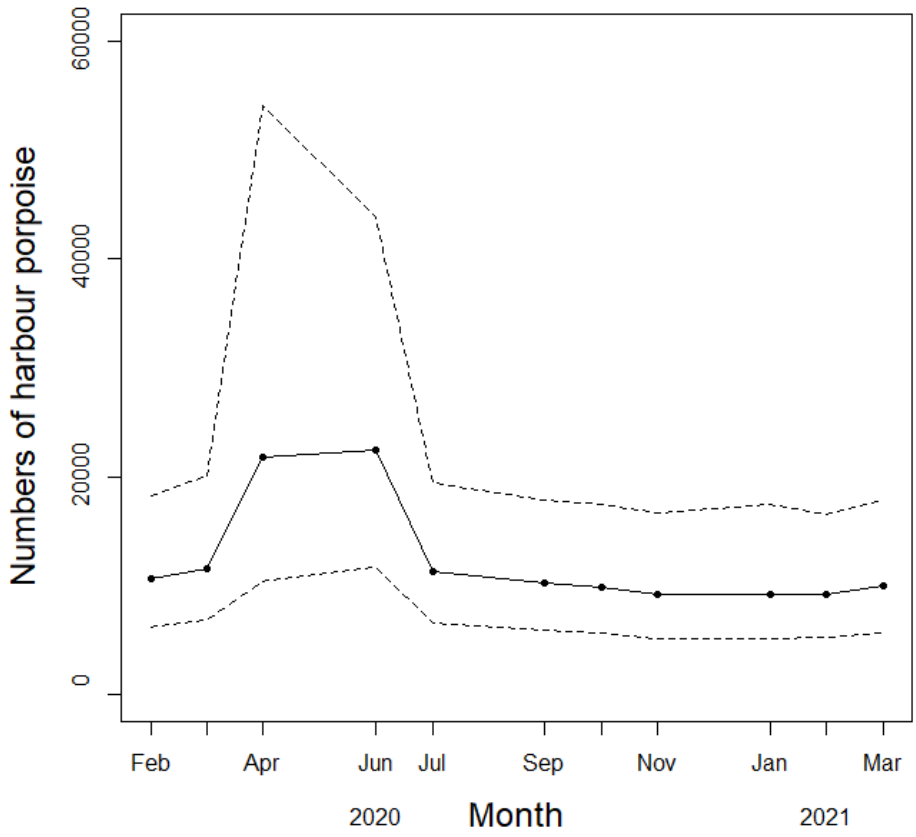

Figure 86. A graph showing estimated numbers of harbour porpoises over the duration of the study from February 2020 to March 2021. The dashed lines represent upper and lower bounds of the 95% confidence intervals. Numbers of porpoises peaked between April and June.

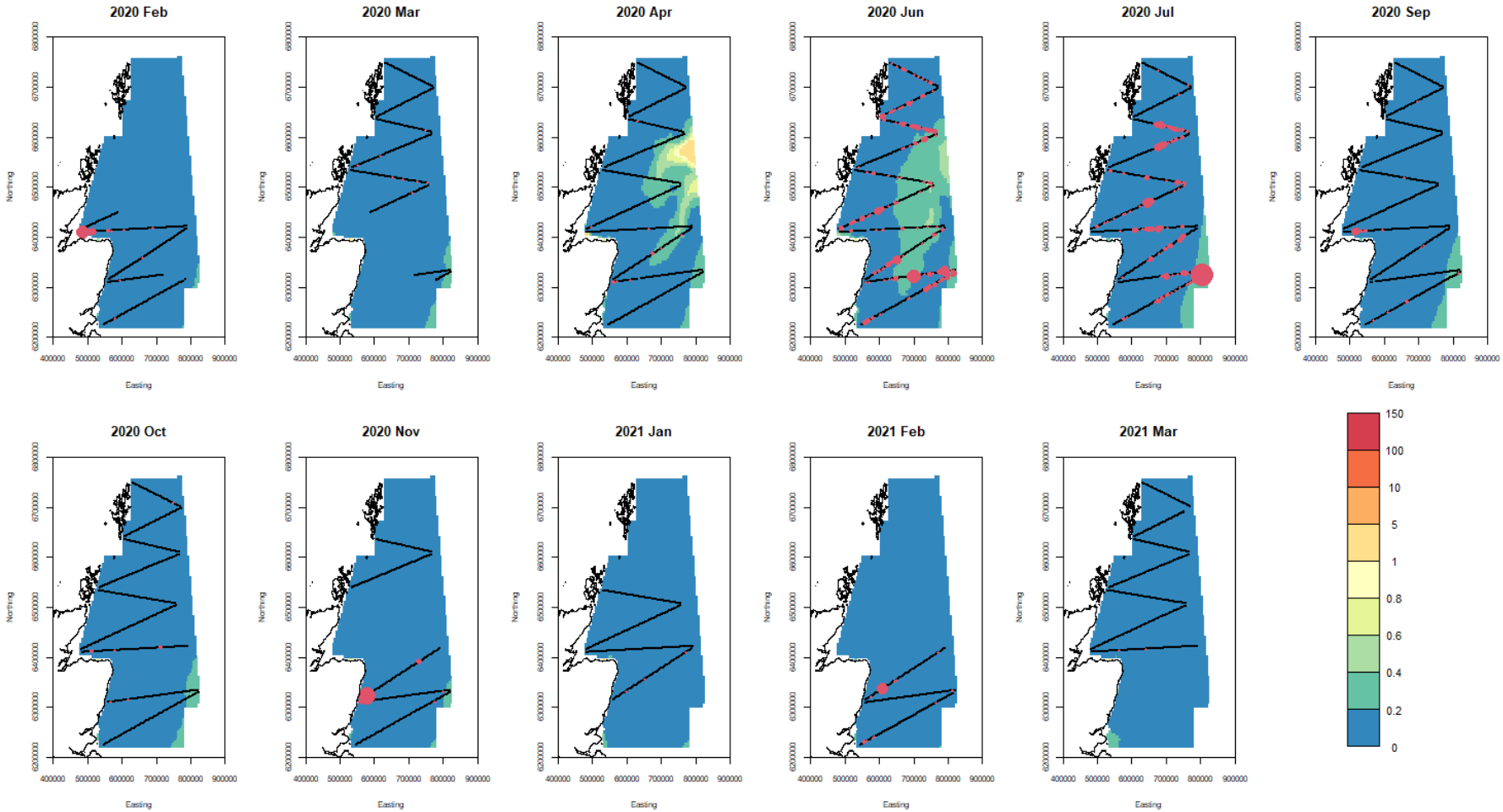

Figure 87. A graph showing point estimates of harbour porpoise densities for each surveyed month from February 2020 to March 2021. Colours represent estimated densities per km^2. Black lines indicate sampling locations in that month. Red dots indicate observed numbers of porpoises with size proportional to observed number. Note that scale is matching the following graphs depicting lower and upper confidence intervals.

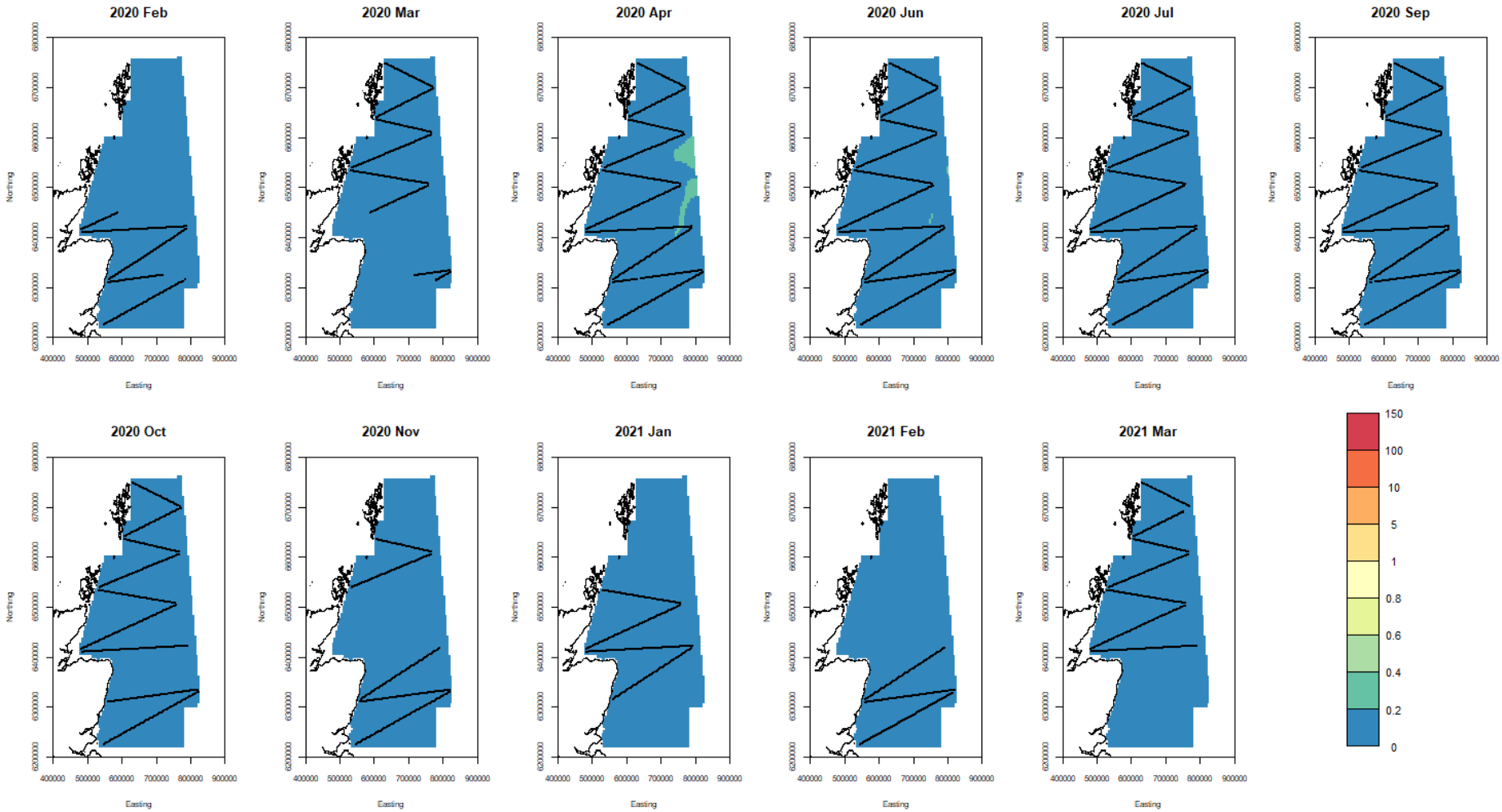

Figure 88. A graph showing lower confidence bound estimates (2.5%) of harbour porpoise densities for each surveyed month from February 2020 to March 2021. Colours represent estimated densities per km^2. Black lines indicate sampling locations in that month.

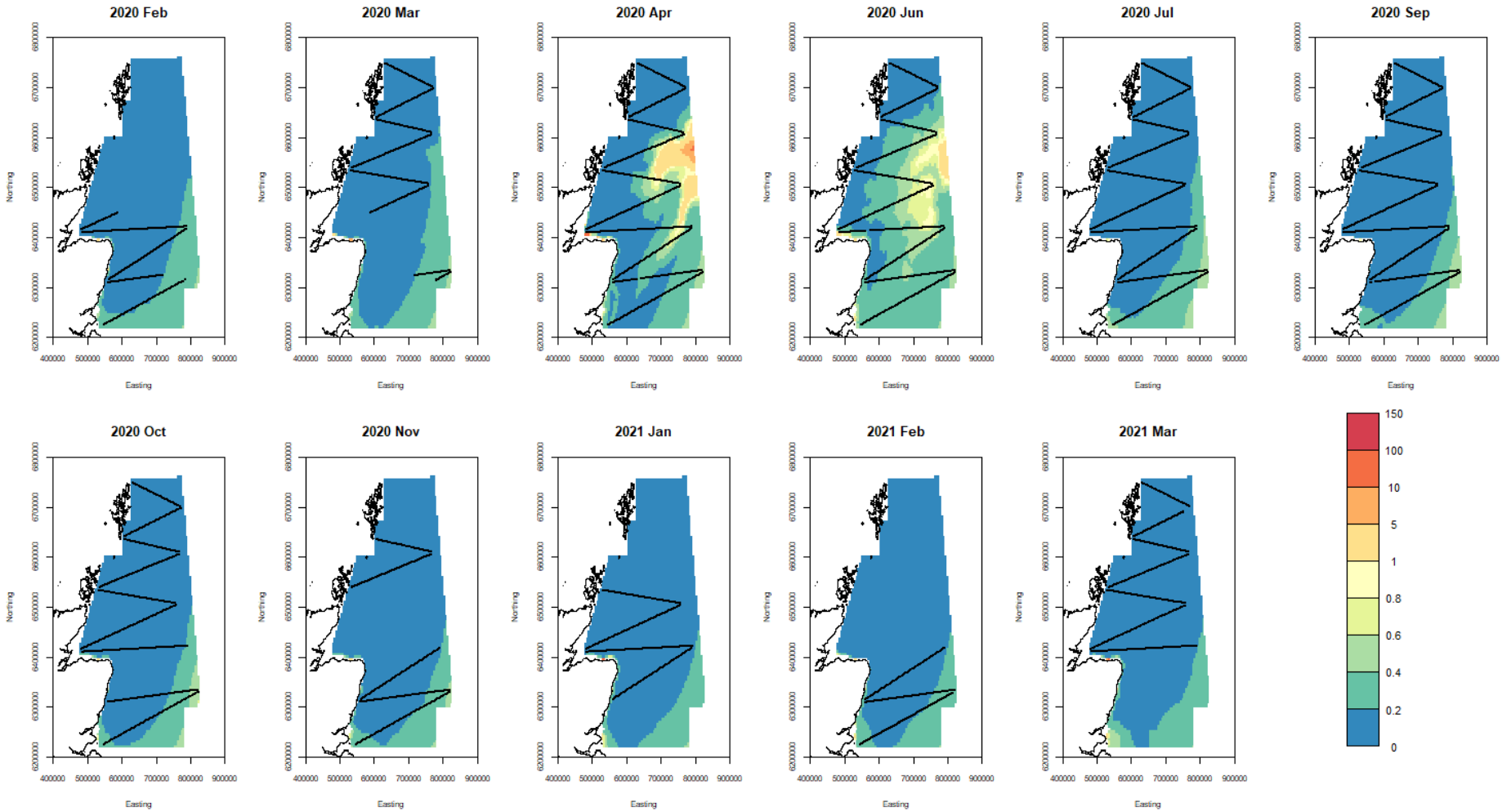

Figure 89. A graph showing upper confidence bound estimates (97.5%) of harbour porpoise densities for each surveyed month from February 2020 to March 2021. Colours represent estimated densities per km^2. Black lines indicate sampling locations in that month.

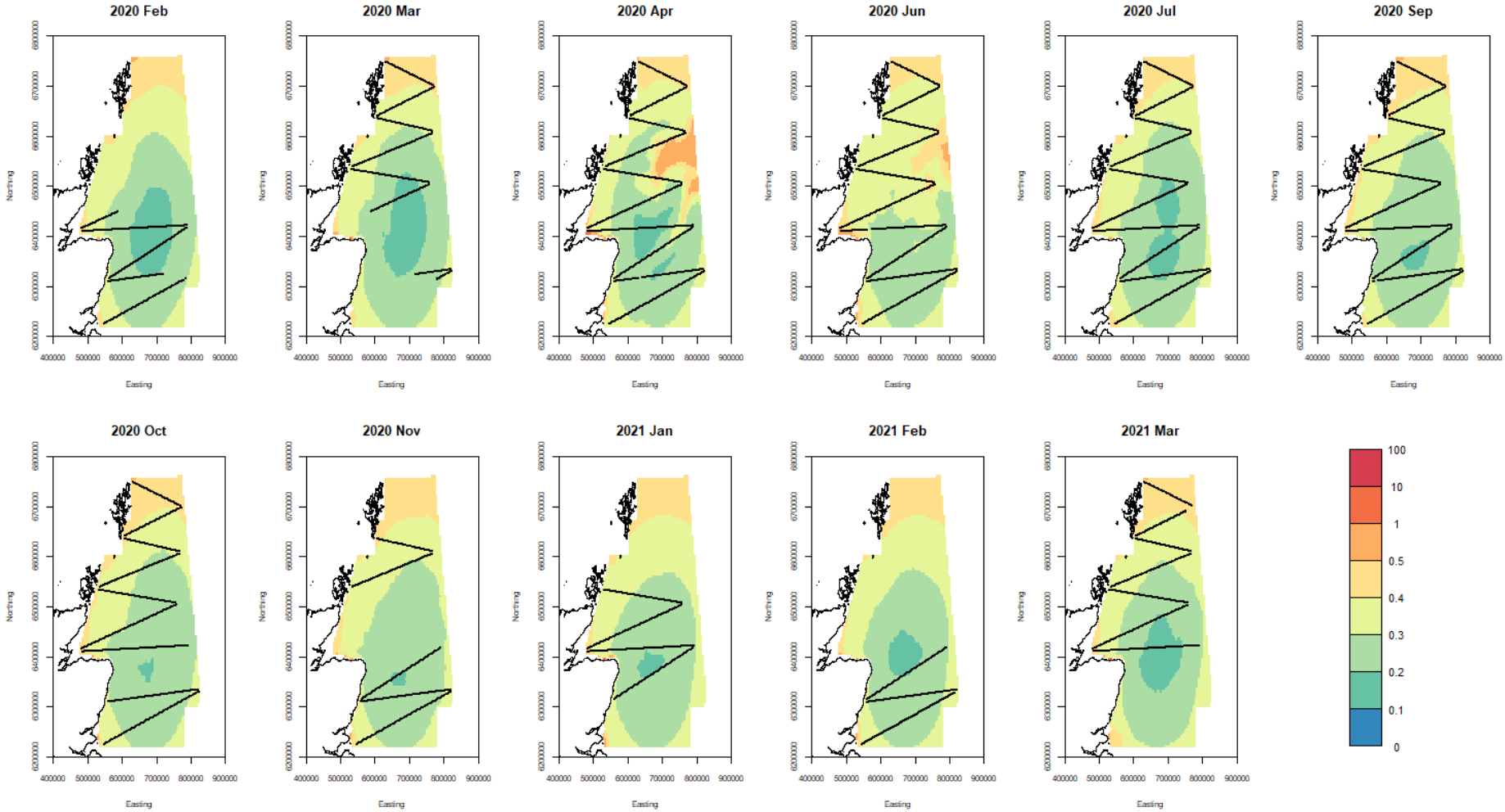

Figure 90. A graph showing harbour porpoise coefficients of variation (CV, in %) in estimated densities of birds for each surveyed month from February 2020 to March 2021. Black lines indicate sampling locations in that month. The largest CVs are at the peripheries of the study area.

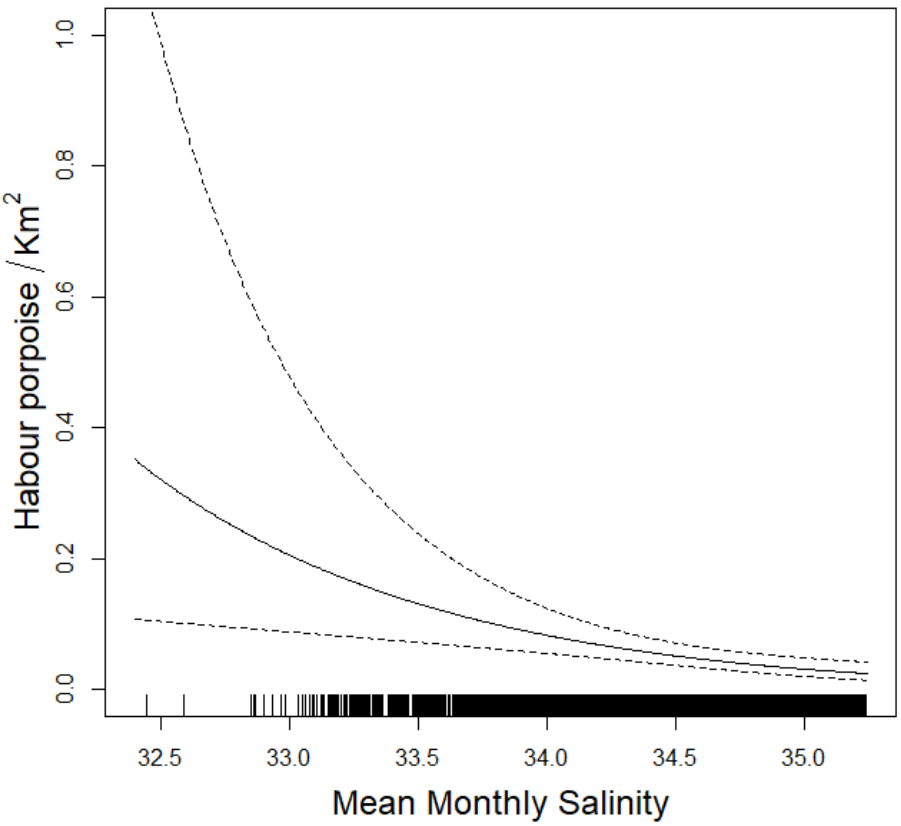

Figure 91. A graph showing effect of mean monthly salinity on surface porpoise observed density assuming the middle of the survey area.

7. DISCUSSION

7.1 General Comments

The results of the aerial surveys highlight some important regions across seabird and cetacean taxa, particularly in summer. These include the area of the North Sea east of Orkney southwards into the Moray Firth extending along the south side of the firth eastwards beyond Fraserburgh, and the Firth of Forth eastwards into the North Sea. North of Orkney in the northernmost North Sea, the coverage is less good but that may also be important. These important regions differed between groups with kittiwakes, guillemots and razorbill having highest abundance in the southeast and fulmar and skuas in the northern part of the study region.

For most species, the estimates of density and abundance derived from analysis of the APEM digital aerial surveys were comparable to those generated from collations of previous survey data which is encouraging. Some of the differences amongst cetaceans may be the result of different corrections applied to account for availability bias. Cetacean species estimated incorporated the availability of the animals at the surface. However uncertainty in surface availability has not been incorporated into the analysis. Some of the availability estimates used in this report are from old studies. More up-to-date estimates based on, for example, telemetry data or our knowledge of relationship between water visibility and species behaviour could be used in the future. A further discussion is also needed on the comparison of accounting for availability based on various methods such as visual and digital survey.

The apportioning of undifferentiated species groups to particular species may lead to error particularly if the proportions of those species has changed over time. Uncertainty associated with this process has not been incorporated into the analysis.

With only eight surveys undertaken across 14 months, it is possible that density distributions may change a lot in the interval between surveys such that the ones used here are unrepresentative. Less common species may also be missed altogether. The following species are known to regularly use the region but were scarcely recorded: amongst cetaceans, these included fin whale, humpback whale, bottlenose dolphin, Atlantic white-sided dolphin, Risso's dolphin. long-finned pilot whale, and killer whale; and amongst seabirds, these included great northern diver, red-throated diver, great cormorant, European shag, European storm petrel, Manx shearwater, velvet scoter, long-tailed duck, common eider, arctic skua, arctic tern, sandwich tern, black guillemot, and little auk. Some of these are predominantly coastal species but others are pelagic. The surveys were targeting offshore areas beyond 12 nm, and so estimates of abundance for the overall region could be significant underestimates for some seabird species, particularly during the breeding season.

Finally, it is worth noting that two significant seabird mortality events have occurred after the survey work was completed. The first of these was a large seabird wreck in late summer of 2021, and the second an outbreak of highly pathogenic avian influenza during the seabird breeding season of 2022. These could lead to significant changes in the at-sea densities of some species.

There are a number of issues to take into account when interpreting the results of the analyses presented here. Inevitably, just eight aerial surveys across a period of 13 months can provide little more than a snapshot of occurrence. Marine mammals and birds are highly mobile, and their distribution and abundance may vary markedly between days so the results on a particular survey day may not be representative for that month. There were also some important spatial and temporal gaps in coverage. The months of May, August and December were not surveyed at all, and coverage was generally more evenly spread in the southern half of the study area than further north around the Northern Isles. Breeding seabirds are central place foragers during the period they are nesting. Unfortunately, there were some survey gaps east of Shetland during the main seabird breeding period (no surveys there between 17 April and 25 June) so birds from the large colonies in that region were not well sampled.

As noted earlier, digital aerial surveys can have their own limitations, mainly related to species identification. The APEM surveys were undertaken at a flight height of 2,000 ft in order to sample a wider area, at a cost of lower image resolution. Besides that issue, species identification may vary between analysts. This was particularly obvious during the first two surveys when no porpoises were specifically identified, and images were classified as porpoise/dolphin, despite the environmental conditions being no different to those on subsequent surveys. And, as noted in the Appendix, reviewing a selection of those images, we found that we could identify to species several of them. Although the relatively high flight height probably exacerbated the situation, aerial surveys inevitably lead to greater problems in differentiating species of similar appearance particularly when the distinguishing features cannot readily be seen from above. Consequently, this remained an issue throughout the survey period with much lower proportions of encounters assigned to a species than would be the case with visual vessel-based surveys. For this reason, we utilised MERP data sets to apply species ratios within species groups, and, for less common species, to improve accuracy of the abundance estimates. Note that some species in the region have predominantly coastal distributions, and so these offshore surveys will not adequately sample them. This applies to bottlenose dolphin amongst cetaceans, and diver, grebe and sea duck species, European shag and great cormorant, arctic skua, black-headed gull, common, arctic and sandwich terns, and black guillemot, amongst birds. Also we did not adjust for any changing ratios of species with time in the MERP data.

Modelling the data here proved challenging especially given the sparsity of some species, nevertheless plausible estimates were obtained. Regions of uncertainty are greatest typically in regions away from the tracklines and on the periphery of the survey region (see cv plots) where there was little effort and perhaps a strange combination of covariates not seen in the actual data.

Below, we first discuss the environmental covariates included in the modelling followed by discussion for each of the main species in the context of our current knowledge of their distribution and abundance. Comparisons are made with the results from previous at-sea surveys and in the case of seabirds with colony counts during the summer breeding season since that relates closely to local densities and abundance at sea. New analyses from updated collations of the MERP dataset were applied, as utilised in a European Commission Bycatch Risk Mapping Project (Evans

et al. 2021) and for the ongoing Phase 2 of the ORJIP Project, led by the Centre of Ecology and Hydrology (CEH) for Marine Scotland.

7.1.1 Environmental Covariates

The modelling approaches used to predict the distribution and densities of animals from observational surveys are broadly divisible into two categories. In a species distribution model (SDM) approach, predictions are based entirely on establishing ecological associations between animal sightings and relevant environmental conditions with the study area, before using these associations to predict the probability of encounters or densities beyond the surveyed area (Elith and Leathwick 2009). For example, measurements of marine animal presence or densities from surveys are often combined with corresponding measurements of sea temperature, establishing which water-masses (e.g., cool, versus warm) are associated with an increased likelihood of encountering animals or higher numbers of animals (Waggitt et al 2020). In the density surface modelling (DSM) approach used here (Miller et al 2013), predictions are more dependent on identifying spatial and geographical descriptors of where animals were sighted, before using these descriptors to predict animal densities beyond the surveyed area. In most applications of DSM, coordinates are used to describe broad-scale aggregations of animals, and environmental conditions are used to describe fine-scale patterns within these aggregations (Gilles et al 2016). Therefore, whilst correlations between animal densities and environmental conditions are presented here, these associations do not necessarily represent habitat preferences of animals, and instead represent geographical descriptions of areas supporting animals. If SDM is going to be performed on this data, a range of additional environmental covariates can be considered such as SST in the previous years or difference from mean SST/salinity across whole area for given time period.

The choice between SDM and DSM depends upon data properties and study objectives. SDM have sometimes been favoured when analysing collations of surveys characterised by heterogeneous coverage, where the distribution of sightings is strongly influenced by effort, and a reliance on spatial and geographical descriptors could cause biased predictions (Waggitt et al 2020, Becker et al 2022). DSM are commonplace when analysing systematic surveys with relatively homogeneous coverage, where variation in effort is less problematic, and a combination of coordinates and geographical descriptors effectively predict areas of aggregations (Hammond et al 2013). Because they attempt to identify habitat preferences of animals, SDM could predict biogeographic ranges within a region well; because they provide a multi-dimensional description of sighting locations, DSM could better predict dense aggregations within this region (Waggitt et al, unpublished analyses). Here, the presence of a systematic survey and emphasis on identifying aggregations meant that DSM approaches were considered more suitable than SDM.

The breeding colony indices (detailed in Waggitt et al 2020) were not retained in seabird models. This is unexpected, as the distribution of seabirds is centred around their breeding colonies in summer months, when animals repeatedly commute between terrestrial nests and marine foraging grounds. Surveys suggest that

densities of animals likely decline exponentially with distance from the breeding colony (Camphuysen 2011), with the highest densities of seabirds occurring <1km from the breeding colony (Gaston et al. 2004). Beyond their immediate vicinity, the location of breeding colonies could primarily influence animal presence rather than animal densities, and this influence likely occurs at a basin (100-1000 km) rather than a regional scale (10-100 km) (Stone et al 1994). Therefore, the absence of surveys <12 nm from coastlines, surveys occurring within foraging ranges of animals breeding within region (see Thaxter et al. 2010), and model focus on animal densities rather than presence may explain the omission of breeding colonies. Alternatively, coordinates could have explained aggregations around breeding colonies better than the breeding colony indices. However, the lack of clear aggregations around breeding colonies in density surfaces suggests that coordinates were not detecting this phenomenon.

7.2 Seabird species

7.2.1 Northern Fulmar

7.2.1.1 Distribution

The northern fulmar has a predominantly high latitude distribution with largest numbers in the Northeast Atlantic breeding in Iceland, the Faroes, Norway (including Svalbard) and northern Scotland (Mitchell et al., 2004). This is reflected in its at-sea distribution in the North Sea where greatest densities and abundance occur off north-east Scotland (Stone et al. 1995, Kober et al. 2010, Waggitt et al. 2020; Searle et al., in prep.). The APEM surveys also showed highest densities offshore in the northernmost part of the North Sea east of the Northern Isles south to the Moray Firth.

There is some seasonal variation in distribution patterns, with lower fulmar densities within the North Sea in winter (between December and March) compared with the rest of the year (Stone et al. 1995, Furness 2015, Waggitt et al. 2020, ORJIP Project unpublished data). In the north-western North Sea, the APEM surveys also showed seasonal variation with peak numbers in September declining through the winter to a low in March just before the start of the breeding season.

Highest densities of fulmars tend to occur near the edge of the continental shelf and around fishing vessels where birds may gather to feed on offal to supplement a diet of zooplankton and small fish (Mitchell et al. 2004). Changes in fishing practice and climate are thought to have influenced the marked changes in both distribution and abundance observed in fulmars over the last hundred years, resulting first in a marked increase and geographical spread, and then, since the mid-1990s, a protracted decline (Mitchell et al. 2004, Daunt & Mitchell 2013, JNCC 2021).

7.2.1.2 Abundance

Point estimates from the APEM surveys indicated 100,000-150,000 fulmars in the study area between January and July increasing to around 400,000 in September before declining again. Highest average densities reached 20 birds/km2 east of

Shetland, Orkney and North-east Scotland, but most areas averaged c. 4 birds/km2 or less.

There are no direct comparisons of abundance. The national census of breeding colonies in 1998-2002 (Mitchell et al. 2004) yielded the following counts of AOS (apparently occupied sites): Shetland (188,544), Orkney (90,846), Caithness (29,957), east coast from Ross & Cromarty south to Aberdeen (8,595), and from Aberdeen south to East Lothian (6,889). Although one cannot derive abundance estimates for the offshore region from these, they highlight the importance of the Northern Isles as a source of fulmars and reflect the lower numbers further south.

JNCC at-sea surveys yielded maximum mean densities of c. 5 birds/km2, mainly in the vicinity of Shetland (Stone et al. 1995). Analysis of the MERP wider data collation gave maximum mean densities of c. 5.5 birds/km^2 occurring in the same region (ORJIP Project Phase 2, unpublished data, using methods from Waggitt et al. 2020).

7.2.2 Northern Gannet

7.2.2.1 Distribution

The northern gannet experienced steady population growth at an overall rate of c. 2% per annum between the late 1960s and end of the twentieth century in the eastern North Atlantic, with several new colonies founded in Britain (Murray & Wanless 1997, Mitchell et al. 2004). Since then, colonies in the Northern Isles and East Scotland have continued to increase, most at annual rates of 3-6% (Murray et al. 2015, JNCC 2021). Greatest numbers breed in Shetland (Hermaness, Noss, Foula and Fair Isle) and the Firth of Forth (Bass Rock) but the density surfaces modelled from the APEM surveys suggest little variation in at-sea density from north to south.

The species forages over wide areas taking a variety of fish including mackerel, sandeel, sprat and herring, and often associating with fishing activities (Hamer et al. 2000, Bodey et al. 2014).

7.2.2.2 Abundance

Point estimates from the APEM surveys indicated a peak of c. 135,000 gannets in the study area across the breeding season (June to October) declining to c. 40,000 gannets for the rest of the year. Average densities ranged from 0 to 2 birds/km2, with densities generally increasing nearer the coast,

The national census of breeding colonies in 1998-2002 (Mitchell et al. 2004) yielded the following counts of AOS (apparently occupied sites): Shetland (26,249), Orkney (5,137), Banff & Buchan (1,085), and East Lothian (44,110). Not all colonies were counted during the Seabird 2000 survey period since there have been separate periodical national censuses. For those colonies not counted, numbers were extrapolated from the 1994-1995 census. By 2019, the number of AOS had increased further in all four regions: Shetland (44,782), Orkney (10,742), Banff & Buchan (4,825), and East Lothian (75,259) (Murray et al. 2015, JNCC 2021). It is

worth noting that, in 2022, an outbreak of Highly Pathogenic Avian Influenza (HPAI) has killed large numbers of gannets from North Sea colonies.

JNCC at-sea surveys yielded maximum mean densities of c. 5 birds/km2 in small gridded areas east of Shetland and in the Firth of Forth between May and October, although most areas had densities of 1.0 bird/km2 or less (Stone et al. 1995). Analysis of the MERP wider data collation gave maximum mean densities of c. 1.5 birds/km2 during the same season but with most densities between 0.5 and 1.0 bird/km2 (Waggitt et al. 2020). Gannet densities in summer were greatest around Shetland and Orkney, and lower throughout the region between November and March (ORJIP Project Phase 2, unpublished data, using methods from Waggitt et al. 2020).

7.2.3 Great Skua

7.2.3.1 Distribution

The great skua is one of Britain's rarest breeding seabirds, with 94% breeding in the Northern Isles, and Scotland accounting for c. 60% of the world population (Mitchell et al. 2004, JNCC 2021). Great skua numbers increased between 1969-70 and 1998-2002, by which time the UK population was estimated to number 9,634 AOT (apparently occupied territories). Since 2000, however, numbers have been decreasing in some areas. In Shetland, for example, three colonies (Hermaness, Noss, and Fair Isle) held 1,476 AOT in 2019, a decrease of 49% since 2007 (JNCC 2021). During 2021 and 2022, there have been outbreaks of Highly Pathogenic Avian Influenza (HPAI) which have caused further significant declines at several great skua breeding colonies, although the full impact is not yet known.

At-sea surveys during the 1980s and 1990s showed highest densities between April and October around the Northern Isles extending southwards into the Moray Firth and off the east coast of Scotland but at lower densities (Stone et al. 1995). Almost no great skuas were present in the study area between November and March (Stone et al. 1995). The more recent MERP collation of survey data generating modelled density distributions highlighted the comparative absence of the species in the region between December and March, with birds primarily recorded in the SW Channel Approaches and south-west of Ireland (Waggitt et al. 2020). However, densities start increasing around the Northern Isles in March, and between June and October are widely spread across the northern North Sea extending southwards as the summer progresses (Waggitt et al. 2020, ORJIP Project Phase 2, unpublished data). Throughout the main breeding season of May to September, highest densities are close to Shetland and Orkney.

The APEM offshore surveys also had highest densities close to Shetland and Orkney between April and October. During this period, there were small numbers of great skua encounters east of the Moray Firth and north-east Grampian coast but none recorded further south. No birds were recorded in the study area during surveys between November and March.

7.2.3.2 Abundance

Point estimates from the APEM surveys increased between April and October, reaching a peak in June of c. 1,800 great skuas in the study area. Care should be taken in interpreting these results because not all the model assumptions were met. Between November and March, numbers were very low, in the order of a few hundred individuals throughout the study area, reflecting the migratory nature of the species with most birds believed move south.

The national census of breeding colonies in 1998-2002 (Mitchell et al. 2004) yielded the following counts of AOT (apparently occupied territories): Shetland (6,846), Orkney (2,209), and Caithness (5), the rest of the UK population breeding in Sutherland, the west coast of Scotland and Hebrides.

Within the study area, JNCC at-sea surveys from the 1980s and 1990s recorded densities between April and June of 1 bird/km2 only in grid cells around Shetland and Orkney, but for the most part, densities were between 0.01 and 0.2 bird/km2 extending south into the Moray Firth (Stone et al. 1995). Between July and October, nearer shore densities in those regions largely ranged between 0.2 and 0.5 bird/km^2, after which birds were generally absent until the following April. Analysis of the MERP data collation yielded maximum predicted densities of c. 1 bird/km^2 close to the coast of Shetland between April and August, whilst further offshore densities averaged c. 0.05 to 0.5 bird/km^2 ((ORJIP Project Phase 2, unpublished data, using methods from Waggitt et al. 2020). Over the wider area to the east and south, densities averaged less than 0.05 bird/km2.

Average offshore densities from the APEM surveys between April and October were greatest east of Shetland mostly ranging from 0.05 to 0.5 bird/km2, with densities generally increasing nearer the coast and being highest in the north. From Orkney southwards and offshore, densities were at all times of the year less than 0.05 bird/km2. These results are very similar to the previous wider-scale survey analyses published.

7.2.4 Common Gull

7.2.4.1 Distribution

The common gull is a coastal and inland breeder largely confined in Britain to Scotland. Greatest numbers of coastal birds breed in Orkney and Shetland, with progressively smaller numbers southwards down the east coast of mainland Scotland (Mitchell et al. 2004). National censuses indicated an increase in the coastal-nesting population from around 13,000 pairs in 1969-70 to c. 15,500 pairs in 1985-88, but with little change in distribution (Cramp et al. 1974, Lloyd et al. 1991). Between 1985-88 and 1998-2002, the population increased by 37% in Orkney but remained fairly constant in Shetland (previously having almost doubled in size since 1969-70) (Mitchell et al. 2004). Over the last 20 years, the coastal common gull population appears to have declined; in 2019, 260 coastal sites held 821 AON, 75% fewer than during the Seabird 2000 census (JNCC 2021).

The APEM offshore surveys indicate a largely nearshore distribution from Orkney to the Firth of Forth between September and March, extending further offshore in a band east of Orkney to the Moray Firth. During April to July, birds are largely absent offshore. Because of its generally coastal and inland distribution, it has not been the focus of attention during analyses of previous at-sea survey collations (Stone et al. 1995, Waggitt et al. 2020, Searle et al., in prep.).

7.2.4.2 Abundance

Point estimates from the APEM surveys show very low numbers offshore during the breeding season (April to July) until September when numbers start to increase, peaking in October at c. 3,500 birds, before declining again through the winter. Density estimates were less than 0.01 bird/km2 throughout the study area between April and July, when birds were breeding. Between September and February, birds were recorded offshore at densities ranging from 0.01 to 1 bird/km2 east of Shetland, Orkney, the outer Moray Firth, and off the east Grampian coast south to the Firth of Forth, with densities highest in the south and nearest the coast.

The national census of breeding colonies in 1998-2002 (Mitchell et al. 2004) yielded the following counts of AON (apparently occupied nests) at coastal sites in the study area: Shetland (2,424), Orkney (11,141), Caithness (468), east coast Sutherland (124), east coast Ross & Cromarty (297), Inverness (135), Aberdeen (280), Kincardine & Deeside (22), Angus (19). They highlight the numerical importance of the Northern Isles for this species.

The numbers recorded at sea around the Northern Isles from the APEM surveys are clearly much lower than those breeding along adjacent coasts. This is probably largely due to a substantial part of the population foraging inland. Following the end of the breeding season, there appears to be a greater tendency for some birds to disperse offshore eastwards and southwards in the North Sea, persisting through the winter.

7.2.5 Lesser Black-backed Gull

7.2.5.1 Distribution

The lesser black-backed gull is a widespread coastal breeder around the British Isles, with at least some of the population migrating south in winter. In the study area, breeding numbers are greatest in Orkney and Shetland, with only small numbers on the east coast of Scotland (Mitchell et al. 2004). The species increased throughout much of its range during most of the twentieth century (Mitchell et al. 2004). Since the 1990s, however, numbers have declined although with some fluctuations (JNCC, 2021). The at-sea distribution of lesser black-backed gulls in the North Sea shows greatest densities and abundance along continental coasts of Germany and the Netherlands, with very low numbers offshore in the APEM survey area (Stone et al. 1995, Kober et al. 2010, Waggitt et al. 2020, ORJIP Project Phase 2, unpublished data).

7.2.5.2 Abundance

The best estimate that could be derived from the APEM offshore surveys was 640 lesser black-backed gulls across the study area, with highest numbers during the breeding season. Average densities were all less than 0.01 birds/km2, the maximum being 0.008 birds/km2 during the survey in June.

The national census of breeding colonies in 1998-2002 (Mitchell et al. 2004) yielded the following counts of AOS (apparently occupied sites): Shetland (341), Orkney (1,045), Caithness and east coast Ross & Cromarty (7), Inverness to Aberdeen (176), Aberdeen to Dundee (80), Dundee to Edinburgh (6,183), and East Lothian (1,470).

JNCC at-sea surveys indicated all densities in the study area were less than 1 bird/km2, but the scales used did not discriminate how much lower they were (Stone et al. 1995). Analysis of the MERP data collation yielded maximum predicted densities of 0.01 birds/km2 close to the Grampian coast between April and July (ORJIP Project Phase 2, unpublished data using methods from Waggitt et al. 2020).

7.2.6 Herring Gull

7.2.6.1 Distribution

Herring gulls are widespread around the coasts of Britain, with some of the largest concentrations breeding in northern and eastern Scotland (Mitchell et al. 2004). In many areas, herring gulls also nest on rooftops. This is particularly the case, for example in the city of Aberdeen where 3,350 apparently occupied nests were counted in 1999-2002 (Mitchell et al. 2004). Since 2000, all trends in numbers from the seabird monitoring programme have shown declines although with some regional variation (JNCC, 2021). This declining trend has been recorded since the first national seabird census in 1969-70, although some of the decline in numbers may have been compensated for by more inland breeding (Mitchell et al. 2004). On a wider scale, the at-sea distribution of herring gulls in the North Sea shows greatest densities and abundance in the south-eastern sector off the coasts of the Netherlands, Germany and Denmark, particularly in winter, with lowest numbers in the northernmost North Sea (Stone et al. 1995, Kober et al. 2010, Waggitt et al. 2020, Searle et al., in prep.).

The APEM surveys indicated highest numbers in the north-western North Sea occurring between Orkney and the Moray Firth from October to February, peaking in November.

7.2.6.2 Abundance

The APEM offshore surveys yielded an overall abundance estimate in the study area of c. 10,000 herring gulls between April and September rising to a peak of c. 55,000 in November before declining through the winter. Average offshore densities were generally between 0 and 1 bird/km2 but in the Moray Firth, during October and November, increased to between 1 and 5 birds/km2.

The national census of breeding colonies in 1998-2002 (Mitchell et al. 2004) yielded the following coastal counts of AON (apparently occupied nests): Shetland (4,027),

Orkney (1,933), east coast Caithness (3,503), east coast Ross & Cromarty (1,345), Inverness to Aberdeen (12,063), Aberdeen to Dundee (5,582), Dundee to Edinburgh (7,579), and East Lothian (3,553). These figures do not include rooftop breeding birds for which a total count had not been made.

JNCC at-sea surveys indicated maximum densities in the study area occurring in the Moray Firth amounting to at least 5 birds/km2, although most grids had densities between 0.01 and 1 bird/km2 (Stone et al. 1995). There was little variation throughout the year. Analysis of the MERP data collation yielded maximum predicted overall densities of c. 1-2 birds/km2 in the Moray Firth and Firth of Forth, also with little variation through the year (ORJIP Project Phase 2, unpublished data using methods from Waggitt et al. 2020).

7.2.7 Great Black-backed Gull

7.2.7.1 Distribution

Most great black-backed gulls in Britain breed on the west coast and in the Northern Isles, with only a few small colonies on the east coast south of the Moray Firth (Mitchell et al. 2004). Although both the UK and Scottish population appeared to increase during the 1990s, since then there has been a prolonged decline (Mitchell et al. 2004, JNCC 2021). Greatest numbers breed in Shetland and Orkney, and this is where localised coastal at-sea densities are highest between April and July (Stone et al. 1995, Waggitt et al. 2020, Searle et al., in prep.).

The APEM offshore surveys indicate low numbers throughout the study area for most of the year although a small peak between October and January may reflect movement into the area, including birds from Fennoscandia (Stone et al. 1995, Furness 2015). Areas with higher densities were east of Orkney and around the Moray Firth, between October and February.

7.2.7.2 Abundance

Point estimates from the APEM offshore surveys indicated a peak of c. 25,000 great black-backed gulls in the study area in October-November declining to between 200 and 1,300 birds from March to July. However, note that high uncertainty in some peripheral regions of the survey region has led to high upper bounds in the confidence limits. Average densities ranged from 0.002 birds/km2 (June) to 0.256 birds/km2 (November).

The national census of breeding colonies in 1998-2002 (Mitchell et al. 2004) yielded the following counts of AOS (apparently occupied sites): Shetland (2,875), Orkney (5,505), Caithness (211), east coast Ross & Cromarty (220), Inverness to Aberdeen (66), Aberdeen to East Lothian (70).

JNCC at-sea densities indicated maximum densities of c. 5 birds/km2 east of Shetland and Orkney in March and April, and in the Moray Firth between August and February (Stone et al. 1995). Analysis of the MERP data collation yielded maximum predicted densities of c. 3.5 birds/km2 close to the coast of Orkney and Shetland between April and July (ORJIP Project Phase 2 unpublished data using methods from Waggitt et al. 2020). In both analyses, however, for most of the north-western

North Sea, estimated great black-backed gull densities offshore were less than 1 bird/km2 (Stone et al. 1995, Waggitt et al. 2020).

7.2.8 Black-legged Kittiwake

7.2.8.1 Distribution

The black-legged kittiwake is believed to be the most abundant species of gull in the world (Mitchell et al. 2004). In Britain, the largest and most numerous colonies are in northwest Scotland, the Northern Isles and east Scotland south to north-east England (Mitchell et al. 2004). Kittiwake numbers in the UK increased by approximately 24% between the late-1960s and mid-1980s but since the early 1990s, have declined rapidly; by 2013, they had decreased to 70% below the 1986 baseline, although numbers may have now stabilised and be slowly increasing in some areas (JNCC 2021).

Kittiwakes in the North Sea are widely distributed, with highest offshore densities between October and March, whereas inshore, numbers are greatest around the major colonies in the north-west between March and September (Stone et al. 1995, Kober et al. 2010, Waggitt et al. 2020).
With improved GPS tracking technology, sample sizes of birds tracked from individual breeding colonies have increased, providing a wealth of individual bird data of known provenance. These have also been used to make predictions of at-sea distributions for some colonial seabird species (Wakefield et al. 2017). From a sample of 464 kittiwakes tracked from 20 colonies, Poisson point habitat use models were developed to predict the species distribution in the waters around Britain and Ireland. In East Scotland, these indicated greater offshore use by foraging kittiwakes with potential high-use areas north of Orkney, east of Caithness, Ross & Cromarty, offshore east of the Grampian Region, in coastal areas of the Scottish Borders, and offshore east of the Firth of Forth (Wakefield et al. 2017). Note that these are derived from breeding birds during a short period of the year; they do not include non-breeders, birds entering the region from populations outside the British Isles, or other periods in the annual cycle of the species.
The APEM surveys showed a slight increase between April and July but little change outside the breeding period. Greatest densities occurred towards the coast around the Moray Firth and Firth of Forth.

7.2.8.2 Abundance

The APEM offshore surveys yielded an overall abundance estimate in the study area of c. 115,000 kittiwakes over much of the year, rising to a peak of c. 150,000 during the main breeding season between March and July. Average offshore densities were greatest between Orkney and the Firth of Forth mostly ranging from 1 to 5 birds/km2, but with densities generally increasing nearer the coast, particularly between April and July.

The national census of breeding colonies in 1998-2002 (Mitchell et al. 2004) yielded the following coastal counts of AON (apparently occupied nests): Shetland (16,732), Orkney (57,668), Caithness (49,533), east coast Ross & Cromarty (749), Moray

(488), Banff & Buchan (30,599), Gordon (3,560), Aberdeen (1,695), Kincardine & Deeside (34,501), Angus (2,926), North East Fife (6,639), Kirkcaldy (3,249), Dunfermline (146), and East Lothian (3,349). These highlight the importance numerically of the Northern Isles and Caithness, Banff & Buchan, and Kincardine & Deeside. JNCC at-sea surveys indicated maximum densities of at least 5 birds/km2 throughout the coastal region of the study area, whereas most offshore grids had densities between 0.01 and 1 bird/km2 (Stone et al. 1995). There was little variation throughout the year. Analysis of the MERP data collation yielded maximum predicted densities of c. 3-5 birds/km2 in the Moray Firth and Firth of Forth areas, throughout the year, with densities offshore rarely below 1 bird/km2 (Seale et al. in prep, using methods from Waggitt et al. 2020).

7.2.9 Common Guillemot

7.2.9.1 Distribution

The common guillemot is the most abundant of the auks in Britain, with the largest colonies in the north and west (Mitchell et al. 2004). National census results show that the UK guillemot population increased by over 130% between the Operation Seafarer (1969-70) and Seabird 2000 (1998–2002) censuses (Mitchell et al. 2004). National census data showed an increase of 82% in the Scottish guillemot breeding population between 1969-70 and 1985-88, with a further increase of 24% up to the time of Seabird 2000. The population trend for guillemot in Scotland was stable during the early 1990s, after which it increased slightly over a few years before levelling off (JNCC 2021). After Seabird 2000 (1998–2002), the index declined and was lower than the 1986 baseline from 2004 to 2016. Since then, it has risen and, in 2019, was 18% above the baseline (JNCC 2021). However, over the last 20 years there has been much regional variation, with study plots in mainland Shetland showing strong declines whereas Fowlsheugh in Kincardine, for example, has increased (JNCC 2021). These varying temporal trends are important to bear in mind when comparing the APEM survey results with previous analyses of at-sea survey data from the region.

Guillemots in the North Sea are widely distributed. Analysis of the ESAS survey data in the 1990s showed high densities particularly nearshore from March through to October, declining between November and February (Stone et al. 1995). A more recent analysis generating modelled density predictions indicated highest densities offshore post-breeding, between July and November, with nearshore densities highest over a wider period between May and September (Waggitt et al. 2020). Areas with greatest densities were between Shetland and Caithness and around the East Grampian coast southward to the Firth of Forth (Waggitt et al. 2020).

Predictions of at-sea distributions in the waters around Britain and Ireland from GPS tracking of 178 breeding guillemots from 12 colonies along with habitat modelling (Wakefield et al. 2017) indicated In East Scotland potential high-use areas around Orkney, east of Caithness, along the south side of the Moray Firth, and around the East Grampian coast southward to the Firth of Forth.

As with the MERP and tracking data, the APEM surveys showed greatest densities in coastal regions, particularly between June and September from east of Orkney to the Moray Firth, and down the East Grampian coast as far as the Firth of Forth. No

surveys were undertaken in May so the seasonal increase in densities may occur earlier coinciding with the start of breeding. During September, densities increase further offshore suggesting a post-breeding dispersal eastwards as indicated also by the MERP data collation.

7.2.9.2 Abundance

The APEM offshore surveys yielded an overall abundance estimate in the study area of somewhere between 200,000 and 300,000 guillemots during summer, peaking in September after the end of the breeding season. Average summer densities were greatest between Orkney and the Moray Firth and down the east Grampian coast to the Firth of Forth mostly ranging from 2 to 10 birds/km2, and generally increasing nearer the coast, exceeding 10 birds/km2 in some localised areas. Between October and March, except for localised areas in the Moray Firth and Firths of Forth and Tay where densities ranged between 1 and 5 birds/km2, densities were generally less than 1 bird/km2.

It should be noted, however, that no correction was made to account for availability bias resulting from guillemots being underwater when the plane flew over. On foraging trips, guillemots rearing small chicks tracked in the North Sea spent 28.8 ±9.5% (mean ±sd) of their time underwater (Thaxter et al. 2010). Dive times averaged 46.4 ±27.4 and 50.4 ±7.4 seconds for guillemots during long and short dives respectively. Dunn et al. (2020) found that guillemots spent on average 4.1 ±0.23 hours per day (i.e. 17%) diving, with proportionately more time underwater during the breeding season than outside this period.

The national census of breeding colonies in 1998-2002 (Mitchell et al. 2004) yielded the following counts of individuals: Shetland (172,681), Orkney (181,026), Caithness (226,254), east coast Ross & Cromarty (1,944), Banff & Buchan (73,970), Gordon (3,345), Aberdeen (395), Kincardine & Deeside (72,179), Angus (1,002), Northeast Fife (28,103), Kirkcaldy (48), and East Lothian (8,266). These emphasise the numerical importance of the Northern Isles and north-east mainland coast of Scotland, although since that census, several colonies in the Northern Isles have suffered declines (JNCC 2021).

JNCC at-sea surveys indicated densities of at least 5 birds/km2 over large parts of the study area between March and October, particularly around Orkney, off the Caithness coast and throughout the Moray Firth, as well as down the East Grampian coast to the Firth of Forth (Stone et al. 1995). These persisted over a large part of the year with grid densities of between 2 and 5 birds/km2 becoming more prevalent off the east coast of mainland Scotland between November and February, when densities around the Northern Isles were around 1 bird/km2 (Stone et al. 1995). Analysis of the MERP data collation showed a similar spatial and seasonal pattern, and indicated densities in some areas (e.g. south Shetland to Caithness and East Grampian) reaching densities of 10-20 birds/km2 between July and September (ORJIP Project Phase 2, unpublished data using methods from Waggitt et al. 2020). However, those analyses used survey data largely collected in the 1990s and/or 2000s since when guillemots in Shetland have experienced declines which may partly explain the relatively low numbers found in that region during the APEM surveys.

7.2.10 Razorbill

7.2.10.1 Distribution

Razorbill numbers in Britain are greatest in Scotland, the largest colonies being in the Hebrides, on Handa island in Sutherland, in the Northern Isles, in east Caithness, Banff and Buchan, and at Fowlsheugh (Kincardine) (Mitchell et al. 2004). Census results showed steady increases in the UK population between 1969-70 and 1998-2002 (Mitchell et al. 2004). Seabird monitoring at sample sites since 2000 indicate major declines in Shetland and Orkney, but increases further south (Fowlsheugh, islands in the Firth of Forth, and St Abbs Head) (JNCC 2021).

At-sea surveys highlight the north-westerly distribution of razorbills within the North Sea, between April and September with distributions more spread out across the southern North Sea between October and March (Stone et al. 1995). The more recent analysis generating modelled density predictions indicated dispersal starting earlier, in July, and remaining over a wider area spanning the central and southern North Sea until March/April (Waggitt et al. 2020). This difference may be due to wider survey coverage of the North Sea region in later years. Areas with greatest densities were between Shetland and Caithness and around the East Grampian coast southward to the Firth of Forth, from May to October (Waggitt et al. 2020, Searle et al., in prep.).

Predictions of at-sea distributions in the waters around Britain and Ireland from GPS tracking of 281 breeding guillemots from 14 colonies along with habitat modelling (Wakefield et al. 2017) indicated In East Scotland potential high-use areas around Orkney, east of Caithness, along the south side of the Moray Firth, off the north Grampian coast and along the coast of the Scottish Borders.

The APEM surveys showed greatest densities in coastal regions, between April and October from east of Orkney to the Moray Firth, and down the East Grampian coast as far as the Firth of Forth. This coincided well with the results from the collated MERP data. During June and July, higher densities extend further offshore in the southern part of the survey area from East Grampian to the Firth of Forth.

7.2.10.2 Abundance

Point estimates from the APEM offshore surveys yielded peak abundance of c. 180,000 razorbills (but with wide upper bounds) in the study area in June, declining thereafter. Average summer densities were greatest between Orkney and the Moray Firth and down the east Grampian coast to the Firth of Forth mostly ranging from 1 to 5 birds/km2, and generally increasing towards the south and nearer the coast, where in the region of the Firth of Forth densities exceeded 10 birds/km2. Between October and March, except for localised areas in and around the Moray Firth and Firths of Forth and Tay where densities ranged between 1 and 5 birds/km2, they were generally less than 1 bird/km2.

As was the case for guillemots, no correction was made to account for availability bias resulting from razorbills being underwater when the plane flew over. On foraging

trips, razorbills rearing small chicks tracked in the North Sea spent 17.5 ±6.6% (mean ±sd) of their time underwater (Thaxter et al. 2010). Dive times averaged 23.1 ±14.9 seconds for razorbills during their dives.

The national census of breeding colonies in 1998-2002 (Mitchell et al. 2004) yielded the following counts of individuals: Shetland (9,492), Orkney (10,194), Caithness (21,657), east coast Ross & Cromarty (251), Banff & Buchan (7,606), Gordon (547), Aberdeen (157), Kincardine & Deeside (9,760), Angus (562), Northeast Fife (4,114), Kirkcaldy and Dunfermline (91), and East Lothian (566). These emphasise the numerical importance of the Northern Isles and north-east mainland coast of Scotland, although as with the guillemot, since that census, several colonies in the Northern Isles have suffered declines (JNCC 2021).

JNCC at-sea surveys indicated densities of at least 5 birds/km2 in coastal areas from Orkney to the Moray Firth, and East Grampian south to the Firth of Tay, particularly between June and September (Stone et al. 1995). Over most of the study area, however, gridded average densities were less than 1 bird/km2. Densities tended to be lower during October to March, with only localised higher values in the inner Moray Firth and in the Firths of Forth and Tay (Stone et al. 1995). Analysis of the MERP data collation showed similar spatial and seasonal patterns, highest densities occurring in coastal areas of east Caithness, east Grampian, and the Firths of Forth and Tay) reaching densities of between 1 and 10 birds/km2 between April and September (ORJIP Project Phase 2, unpublished data using methods from Waggitt et al. 2020). During the breeding season, these were very localised around the main colonies but became more dispersed in August and September at an average density of c. 5 birds/km2 (Waggitt et al. 2020, Searle et al., in prep.).

7.2.11 Atlantic Puffin

7.2.11.1 Distribution

The Atlantic puffin is the second most numerous breeding seabird in Britain, with the largest colonies mainly in the Hebrides, Shetland and Orkney, and around the Firth of Forth (Mitchell et al. 2004). Whereas national censuses indicate that puffin numbers in Britain increased between 1969-70 and 1998-2002, and possibly beyond, there have been marked declines since then in Shetland (for example on Fair Isle), and on the Isle of May (Firth of Forth) (Mitchell et al. 2004, JNCC 2021).

At-sea surveys during the 1980s and 1990s had highest densities of puffins during the breeding season (April to August) in Shetland and Orkney, and the Firth of Forth, after which densities declined reflecting the wide dispersal of puffins during the winter (Stone et al. 1995).

The more recent analysis generating modelled density predictions also indicated highest densities in the north-western sector of the North Sea, particularly between April and September, concentrated around the Northern Isles and east Grampian region, and decreasing further offshore (Waggitt et al 2020, ORJIP Project Phase 2, unpublished data). The results indicated dispersal starting earlier, in July, and remaining over a wider area spanning the central and southern North Sea until March/April (Waggitt et al. 2020, ORJIP Project Phase 2, unpublished data). This

difference may be due to wider survey coverage of the North Sea region in later years. Areas with greatest densities were between Shetland and Caithness and around the East Grampian coast southward to the Firth of Forth, from May to October (Waggitt et al. 2020, Searle et al., in prep.).

The APEM surveys showed greatest densities in coastal regions, between April and June east of Shetland, from east of Orkney to the Moray Firth, and down the East Grampian coast as far as the Firth of Forth. Densities were generally greater further south. From July onwards, puffin densities declined and remained very low from October to March.

7.2.11.2 Abundance

Point estimates from the APEM offshore surveys yielded peak abundance of c. 20,000 puffins in the study area in June, declining thereafter to between 3,000 and 5,000 birds. Average summer densities were greatest east of Shetland, south of Orkney and down the east Grampian coast to the Firth of Forth mostly ranging from 0.2 to 1 bird/km2, and generally increasing towards the south and nearer the coast. From July until March, densities were largely 0.1 bird/km2 or less. In the absence of local surveys it is not known whether or not the apparent persistent winter hotspots close to the coast off north-east Caithness and at the north-east corner of the Grampian coast are genuine.

The national census of breeding colonies in 1998-2002 (Mitchell et al. 2004) yielded the following counts of AOB (apparently occupied burrows): Shetland (107,676), Orkney (61,758), Caithness (1,278), Banff & Buchan (1,026), Gordon (619), Aberdeen (75), Kincardine & Deeside (768), Angus (190), Northeast Fife (42,000), Kirkcaldy and Dunfermline (1,701), Edinburgh (22), and East Lothian (28,412). These highlight the numerical importance of the Northern Isles as well as colonies in and around the Firth of Forth.

At-sea surveys in the 1980s and 1990s showed densities of 5 birds/km2 or more only around known colonies during the breeding season between April and August (Stone et al. 1995). From October to March, densities are low, for the most part less than 1 bird/km2 and spread evenly across the study area (Stone et al. 1995). Analysis of the MERP data collation showed similar patterns, with highest densities of between 1 and 5 birds/km2 occurring in coastal areas around the Northern Isles and East Grampian coast south to the Firth of Forth between April and September (Searle et al, in prep., using methods from Waggitt et al. 2020). Between October and March, densities were for the most part less than 1 bird/km2 (Waggitt et al. 2020, Searle et al., in prep.). Numbers estimated from the APEM surveys across the study area during summer were much lower than one might expect from the neighbouring colony counts. Part of this may be due to recent declines in the region but could also be because Shetland is on the periphery of the prediction region so if there are relatively large numbers there, they were excluded from the overall abundance estimates. On the other hand, there are also lower densities further south than expected from the colony counts, and it may be that not accounting for potential availability bias is the main issue. There is limited telemetry information on puffin dive durations, but birds from the Isle of May spent an average of 7.8h of the day

underwater (Harris & Wanless 2012) whilst birds from Skomer Island spent an average of 4.6h per day with fewer dives but of longer mean dive duration (Shoji e al. 2015).

7.3 Marine mammals

7.3.1 Common Minke Whale

7.3.1.1 Distribution

The North Sea, particularly the north-western sector, has long been known as an important region for minke whales in Europe (Evans 1992, Northridge et al. 1995, Hammond et al. 2002, Reid et al. 2003, Hammond et al. 2013, Paxton et al. 2016, Evans & Waggitt 2020b, Hague et al., 2020, Waggitt et al. 2020, Evans et al. 2021). In the north-western North Sea, whereas some coastal areas around the Northern Isles (Evans & Baines 2010), in the Moray Firth (Robinson et al. 2009), and East Grampian region (Anderwald & Evans 2010) have been identified as local hotspots (see also Paxton et al. 2014), minke whale distribution further offshore has been less well examined, and has relied largely upon synoptic snapshot surveys of abundance such as SCANS (Hammond et al. 2002, 2013, 2021) and the Norwegian minke whale surveys that have extended southwards into the North Sea (Solvang et al. 2015).

Minke whales show general seasonal off-shelf/on-shelf movements, with some evidence of a southwards migration in autumn, returning north in spring (Risch et al. 2014), although a portion of the population remains around the British Isles through the winter (Anderwald & Evans 2007, Waggitt et al. 2020).

The APEM surveys show broadly similar results, with all but the last two surveys (in February and March 2021) having minke whale detections, and most occurring in June. In coastal regions within the study area, peak sighting rates occur in July and August (Evans et al. 2003, Robinson et al. 2009, Anderwald & Evans 2010).

At least in summer, minke whales favour shelf seas, feeding around banks and in areas of upwelling or strong currents around headlands or small islands (Tetley et al. 2008, Robinson et al. 2009, Anderwald et al. 2012).

7.3.1.2 Abundance

The SCANS III survey in July 2016 yielded an estimate of minke whale abundance in the North Sea of around 10,000 animals (Hammond et al. 2021). Within the broad bounds of the APEM survey area, SCANS estimated 2,498 (95% CI: 604-6,791) minke whales in block R east of Grampian region south to east of Tyne & Wear in NE England, 383 (95% CI: 0-1,364) in block S spanning the Moray Firth, Orkney and west of Shetland, and 2,068 (95% CI: 290-6,960) in block T covering the Shetland Isles south to offshore east of the Moray Firth. The boundaries of these blocks do not coincide at all with the APEM survey area so it is not possible to make direct comparisons. In SCANS, minke whale densities per block were estimated at 0.0387/ km2 (block R), 0.0095/km2 (block S), and 0.0316/km2 (block T).

The APEM surveys yielded an overall abundance estimate of a little under 2,000 animals for the survey area in the corresponding month of July with point estimates of densities over the region varying from 0 to 0.1 animal/km2, the areas with higher densities being between 0.05 and 0.1 animal/km2. SCANS surveys used a correction of 0.106 to account for availability bias whereas in this study, the correction applied was 0.04. This discrepancy is due in part to the instantaneous nature of the digital survey. It is based on surfacing rates based on visual shipboard survey which may not be entirely appropriate for a digital survey which dependent on water conditions can see further into the water column.

7.3.2 Common Dolphin

7.3.2.1 Distribution

The common dolphin has a predominantly westerly and southerly distribution around the British Isles, the species being uncommon in the North Sea (Hammond et al. 2002, Reid et al. 2003, Hammond et al. 2013, Paxton et al. 2016, Evans & Waggitt 2020b, Waggitt et al. 2020, Hammond et al. 2021). However, in recent years the species has been seen regularly in small numbers in the northern North Sea, and this has been attributed to the influence of climate change on some of their prey species (Evans & Waggitt 2020a, b).

Common dolphin detections during the APEM surveys occurred on one out of two survey days in March 2020, and three out of four days in June 2020. Most detections were far offshore in the middle of the North Sea. However, the total number of encounters across the eight surveys remains low.

Common dolphins are abundant and widely distributed in the eastern North Atlantic, occurring mainly in oceanic and shelf edge temperate seas from the Iberian Peninsula north to approximately 65°N latitude (though rare north of 62°N), west of Norway and the Faroe Islands (Reid et al. 2003, Murphy et al. 2013). In the offshore North Atlantic it seems to favour waters over 15°C SST and shelf edge features at depths of 400-1,000 m between 49°-55°N, especially between 20°-30°W (Cañadas et al. 2009). In shelf waters off the west coasts of Ireland and Scotland, and in the Irish Sea, common dolphin abundance tends to be greatest in the summer months at depths of 50-150 m (Evans et al. 2003).

7.3.2.2 Abundance

During the SCANS 3 survey in July 2016, there were no encounters with common dolphins in the North Sea and so no abundance estimates for this region. However, the presence of many casual sightings in the region (Evans & Waggitt 2020b) and the APEM aerial survey results support the presence of the species here but in small numbers, and possibly largely seasonally. The point estimate from these surveys is 4,110 common dolphins, assuming an availability at the surface of 0.05. Again, the low availability figure is generated by the instantaneous nature of the digital survey.

7.3.3 White-beaked Dolphin

7.3.3.1 Distribution

The white-beaked dolphin is a cool temperate to arctic species of the North Atlantic, occurring also widely across the North Sea, mainly in the northern and central sectors (Hammond et al. 2002, Reid et al. 2003, Hammond et al. 2013, Paxton et al. 2016, Evans & Waggitt 2020b, Waggitt et al. 2020, Hammond et al. 2021). There is some indication that the species is contracting its range northwards (Lambert et al. 2011, Evans & Waggitt 2020a); during the 1980s and 1990s, the species was common in summer around the north of Scotland and Northern Isles where now it is scarce (Evans & Baines, 2010, Evans & Waggitt 2020a, b).

Most sightings in British waters occur in summer, particularly in July and August (Evans et al. 2003, Evans & Waggitt 2020b), and this applies also to north Scotland (Evans & Baines 2010), and Grampian regions (Anderwald & Evans 2010). The APEM surveys also showed a strong seasonal peak in sightings across the study area in July (there were no surveys in August). No obvious hotspots were identified from these surveys, which was also the conclusion of an earlier wider analysis by Paxton et al. (2014).

White-beaked dolphins occur over a large part of the North-West European continental shelf, mainly in waters of 50–100 m depth, and almost entirely within the 200 m isobath (Reid et al. 2003, Evans et al. 2020b). However, in west Greenland, it can be found in much deeper waters of 300–1000 m (Hansen & Heide-Jørgensen, 2013), and, in the Barents Sea, commonly at 150–200 m and 400 m depths (Fall & Skern-Mauritzen, 2014).

7.3.3.2 Abundance

The SCANS III survey in July 2016 generated an estimate of white-beaked dolphin abundance in the North Sea of around 20,000 animals (Hammond et al. 2021). Within the broad boundaries of the APEM survey area, SCANS estimated 15,694 (95% CI: 3,022-33,340) white-beaked dolphins in block R east of Grampian region south to east of Tyne & Wear in NE England, 868 (95% CI: 0-2,258) in block S spanning the Moray Firth, Orkney and west of Shetland, and 2,417 (95% CI: 593-5,091) in block T covering the Shetland Isles south to offshore east of the Moray Firth. As noted earlier, the boundaries of these blocks do not coincide at all with the APEM survey area so it is difficult to make direct comparisons. In SCANS, white-beaked dolphin densities per block were estimated at 0.243/km2 (block R), 0.021/km2 (block S), and 0.037/km2 (block T).

The APEM surveys yielded an overall abundance estimate of around 150,000 animals for the survey area in the corresponding month of July. Point estimates of densities over the region varied from 0 to 5 animal/km2, with progressively higher densities occurring further offshore. These values are obviously much higher than the SCANS estimates. SCANS surveys used a correction of 0.676 to account for

availability bias whereas in this study the correction applied was 0.06. Again, this was due to the instantaneous nature of the survey.

7.3.4 Harbour Porpoise

7.3.4.1 Distribution

Harbour porpoises are widely distributed throughout the shelf seas of the United Kingdom, with the North Sea a persistent important region for the species in Europe (Evans 1992, Northridge et al. 1995, Hammond et al. 2002, Reid et al. 2003, Hammond et al. 2013, Paxton et al. 2016, Evans & Waggitt 2020b, Waggitt et al. 2020, Hammond et al. 2021). The APEM offshore surveys show highest densities east of the Moray Firth and Grampian region. During the 1990s, numbers around the Northern Isles appear to have been much larger than they are today (Evans et al. 1997, Hammond et al. 2002, 2013), attributed to the marked decline in sandeel stocks in the region over that period (Evans & Borges 1996).

In coastal regions of North and East Scotland, porpoise sighting rates and numbers peak between July and October (Evans et al. 2003, Anderwald & Evans 2010, Evans & Baines 2010). The APEM surveys show an offshore peak in June, which is when most UK porpoises are born (Lockyer 1995), suggesting that some animals may then make a seasonal movement inshore.

Harbour porpoises mainly inhabit temperate and sub-arctic (11-14o C SST) shelf seas in depths of 20-200 metres, although some populations (e.g. West Greenland) may seasonally migrate into deep waters of the central North Atlantic (Nielsen et al. 2018). In coastal regions, the species frequently uses tidal conditions for foraging (Johnston et al. 2005, Pierpoint 2008, Marubini et al. 2009, Isojunno et al. 2012, Jones et al. 2014, Waggitt et al. 2017).

7.3.4.2 Abundance

The SCANS III survey in July 2016 yielded an estimate of harbour porpoise abundance in the North Sea of a little over 300,000 animals (Hammond et al. 2021), with greatest numbers in the central and southern North Sea following a southward shift in the 1990s (Hammond et al. 2002, 2013). Within the broad boundaries of the APEM survey area, SCANS estimated 38,646 (95% CI: 20,584-66,524) porpoises in block R east of Grampian region south to east of Tyne & Wear in NE England, 6,147 (95% CI: 3,401-10,065) in block S spanning the Moray Firth, Orkney and west of Shetland, and 26,309 (95% CI: 14,219-45,280) in block T covering the Shetland Isles south to offshore east of the Moray Firth. Again, the boundaries of these blocks do not coincide at all with the APEM survey area so it is difficult to make direct comparisons. In SCANS, porpoise densities per block were estimated at 0.599/km2 (block R), 0.152/km2 (block S), and 0.402/km2 (block T).

The APEM surveys yielded an overall abundance estimate of around 55,000 animals for the survey area in the corresponding month of July, with a similar number through most of the year except April to June when it increased to c. 120,000 animals. Point estimates of densities over the region varied from 0 to 5 animal/km2, with progressively higher densities occurring in the south of the survey area. We used an instantaneous availability of 0.123.

7.4 Recommendations for monitoring and future data analysis

Due to uncertainties in species identification in many cases from digital aerial images, we used additional information from the survey collation undertaken recently within the NERC/Defra funded Marine Ecosystem Research Programme (MERP) (Waggitt et al. 2020). These included visual survey data both from ships and planes where there was much better species discrimination. This will always be the case where distinguishing features require viewing from the side rather than above. One recommendation for future monitoring therefore would be to include some visual surveys particularly from vessels. Aerial surveys using digital video may also provide useful supplementary information and in some circumstances, is favoured over still imagery alone as a continuous sequence may allow a higher number of identifications at least for marine mammals. The digital aerial surveys were undertaken with relatively low image resolution (high GSD – flight height of 2000 ft) as a trade-off to achieve higher coverage. Consideration should be given on whether to use a lower GSD (i.e. higher image resolution) although only if this will improve species identification rates (e.g. auks & gulls amongst seabirds, and porpoises & dolphins amongst cetaceans). There is another issue of how best to treat subsurface animals, particularly cetaceans, whilst incorporating a correction for availability bias. APEM attempted to identify to species whether or not the animal was at the surface. Unsurprisingly, a higher proportion of species discrimination was made for animals at the surface. However, this will vary according to the levels of turbidity at the time. This was graded 0, 1, 2 or 3 (clear, slightly turbid, moderately turbid, highly turbid). This information may need to be incorporated in future analyses.

The correction for availability for the two dolphin species and the minke whales come from estimates based on visual survey (Table 4). As digital surveys also include animals which are visible beneath the water surface, using corrections based on visual survey may lead to overestimation of the animals. Correction for availability based on telemetry data (as in case for porpoises) would be the most appropriate to use, however to our knowledge, such numbers are not available for the two dolphin species and minke whales.

Some areas and periods of the year were not surveyed. The most important gap was east of Shetland, particularly between mid-April and the end of June, when there are large breeding seabird concentrations in the area as well as marine mammals such as killer whale. This was due to survey interruption arising from restrictions during the early period of the Covid-19 pandemic, and so could not be avoided, but it would beneficial if surveys at those times could take place.

Although the focus was on offshore areas (>12NM from the coast), the modelling would have benefitted from inclusion of results from nearshore surveys to avoid spurious results at the periphery of the target survey area,

The Northern Isles in general would merit more at-sea survey effort. They hold some of the largest populations in Britain of several seabird species and have the richest marine mammal fauna in Britain. They also have experienced significant declines in numbers for several species. And yet this is generally the region of Britain that has been least well surveyed. It would also be advisable to combine the data with those from nearshore surveys in the Northern Isles since depth gradients are more pronounced here than many areas within the North Sea further south off the east

coast. Some species have habitat preferences that are within the 50-metre isobath, and therefore will be poorly sampled by the sawtooth line transect design used for the APEM surveys.

Future work could consider whether given the considerable autocorrelation in the data for almost all species, it could be worth taking photos at greater intervals allowing more widely spaced spatial coverage with little gain in uncertainty.

8. REFERENCES

Anderwald, P. & Evans, P.G.H. 2007. Minke whale populations in the North-Atlantic – an overview with special reference to UK Waters. In: An Integrated Approach to Non-lethal Research on Minke Whales in European Waters (Editors K.P. Robinson, P.T. Stevick and C.D. MacLeod). European Cetacean Society Special Publication Series, 47, 8-13.

Anderwald, P. 2009. Population Genetics and Behavioural Ecology of North Atlantic Minke Whales (Balaenoptera acutorostrata). PhD Thesis, University of Durham, Durham. 216pp.

Anderwald, P. & Evans, P.G.H. 2010. Cetaceans of the East Grampian Region. Final Report to East Grampian Coastal Partnership. Sea Watch Foundation, Bangor, UK. 69pp.

Anderwald, P., Evans, P.G.H., Dyer, R., Dale, A., Wright, P.J., & Hoelzel, A.R., 2012. Spatial scale and environmental determinants in minke whale habitat use and foraging. Marine Ecology Progress Series, 450, 259-274.

Benjamins, S., Dale, A.C., Hastie, G.D., Waggitt, J.J., Lea, M.A., Scott, B., & Wilson, B. 2015. Confusions reigns? A review of marine megafauna interactions with tidal-stream environments. Oceanography and Marine Biology: Annual Review, 53, 1-54.

Becker , E A , Forney , K A , Miller , D L , Barlow , J , Rojas-Bracho , L , Urbán R , J & Moore , J E 2022 , ' Dynamic habitat models reflect interannual movement of cetaceans within the California current ecosystem ' , Frontiers in Marine Science , vol. 9 , 829523

Blake, B.F., Tasker, M.L., Jones, P.H., Dixon, T., Mitchell, R., & Langslow, D.R. 1984. Seabird Distribution in the North Sea. Nature Conservancy Council, Huntingdon.

Bodey, T.W., Jessopp, M.J., Votier, S.C., Gerritsen, H.D., Cleasby, I.R., Hamer, K.C., Patrick, S.C., Wakefield, E.D., & Bearhop, S. 2014. Seabird movement reveals the ecological footprint of fishing vessels. Current Biology, 24(11), R514-515.

Buckland, S.T., Burt, M.L., Rexstad, E.A., Mellor, M., Williams, A.E., & Woodward, R. 2012. Aerial surveys of seabirds: the advent of digital methods. Journal of Applied Ecology, 49, 960-967.

Cañadas, A., Desportes, G., Borchers, D., & Donovan, G. 2009. A short review of the distribution of short-beaked common dolphin (Delphinus delphis) in the central

and eastern North Atlantic with an abundance estimate for part of this area. NAMMCO Scientific Publications, 7, 201-220.

Camphuysen C.J. 2011. Northern gannets *Morus bassanus* in the North Sea: foraging distribution and feeding techniques around the Bass Rock. *British Birds* 104 60–76

Carter, J.C., Williams, J.M., Webb, A., & Tasker, M.L. 1993. Seabird concentrations in the North Sea: An atlas of vulnerability to surface pollutants. Joint Nature Conservation Committee, Peterborough.

Cox, S.L., Embling, C.B., Hosegood, P.J., Votier, S.C., & Ingram, S.N. 2018. Oceanographic drivers of marine mammal and seabird habitat-use across shelf-seas: A guide to key features and recommendations for future research and conservation management. Estuarine, Coastal and Shelf Science, 212, 294-310.

Cramp, S., Bourne, W.R.P., & Saunders, D.R. 1974. The Seabirds of Britain and Ireland. Collins, London.

Daunt, F. & Mitchell, I.M. 2013. Seabirds. MCCIP Annual Report Card 2012-13, MCCIP Science Review 2013: 125-133 (http://www.mccip.org.uk/annual-report-card/2013.aspx)

Donovan, C.R. & Caneco, B.A.R. 2020. Seabird Survey Designs for the East Coast of Scotland. Scottish Marine and Freshwater Science Report Vol 11 No. 19. 78pp.

Dunn, R.E., Wanless, S., Daunt, F., Harris, M..P., & Green, J.A. 2020. A year in the life of a North Atlantic seabird: behavioural and energetic adjustments during the annual cycle. Scientific Reports, 10:5993. https://doi.org/10.1038/s41598-020-62842-x.

Elith, J. & Leathwick, J.R. (2009a) Species distribution models: ecological explanation and prediction across space and time. Annual Review of Ecology, Evolution and Systematics, 40, 677–697

Evans, P.G.H. 1980. Cetaceans in British Waters. Mammal Review, 10: 1-52.

Evans, P.G.H. 1992, Status Review of Cetaceans in British and Irish waters. UK Dept. of the Environment, London. 98pp.

Evans, P.G.H. & Baines, M.E. 2010. Abundance and Behaviour of Cetaceans & Basking Sharks in the Pentland Firth and Orkney waters. Report by Hebog Environmental Ltd & Sea Watch Foundation. Scottish Natural Heritage Commissioned Report No. 419 (iBids and Projects ID 1052). 41pp.

Evans, P.G.H. & Borges, L. 1996. Associations between porpoises, seabirds, and their prey in South-east Shetland, N. Scotland. European Research on Cetaceans, 9, 173-178.

Evans, P.G.H. & Waggitt, J.J. 2020a. Impacts of climate change on marine mammals, relevant to the coastal and marine environment around the UK. MCCIP Science Review 2020, 421–455. doi: 10.14465/2020.arc19.mmm

Evans, P.G.H. & Waggitt, J.J. 2020b. Cetaceans. Pp. 134-184. In: Crawley, D., Coomber, F., Kubasiewicz, L., Harrower, C., Evans, P., Waggitt, J., Smith, B., and Mathews, F. (Editors) Atlas of the Mammals of Great Britain and Northern Ireland. Published for The Mammal Society by Pelagic Publishing, Exeter. 205pp.

Evans, P.G.H. & Wang, J. 2003. Re-Examination of distribution data for the harbour porpoise around Wales and the UK with a view to site selection for this species. Report for the Countryside Council for Wales. Countryside Council for Wales Contract Science Report No: 634, 1-116.

Evans, P.G.H., Anderwald, P., and Baines, M.E. 2003. UK Cetacean Status Review Report to English Nature and the Countryside Council for Wales. Sea Watch Foundation, Oxford. 160pp.

Evans, P.G.H., Carrington, C., & Waggitt, J. 2021. Risk Assessment of Bycatch of Protected Species in Fishing Activities. European Commission, Brussels. 213pp. https://ec.europa.eu/environment/nature/natura2000/marine/docs/RISK MAPPING REPORT.pdf

Evans, P.G.H., Harding, S., Tyler, G. & Hall, S. 1986 Analysis of Cetacean Sightings in the British Isles, 1958-1985. Nature Conservancy Council, Peterborough. 71pp.

Evans, P.G.H., Weir, C.R., & Nice, H.E. 1997. Temporal and spatial distribution of harbour porpoises in Shetland waters, 1990-95. European Research on Cetaceans, 10: 233-237.

Fall, J. & Skern-Mauritzen, M. 2014 White-beaked dolphin distribution and association with prey in the Barents Sea. Marine Biology Research, 10, 957–971.

Furness, R.L. 2015. Non-breeding season populations of seabirds in UK waters. Population Sizes for Biologically Defined Minimum Population Scales (BDMPS). Natural England Commissioned Report NECR164, 389pp.

Gaston, A.J. 2004. Seabirds. A Natural History. T .& A.D.. Poyser, London.

Gilles, A., Viquerat, S., Becker, E. A., Forney, K. A., Geelhoed, S. C. V., Haelters, J., Aarts, G. (2016). Seasonal habitat-based density mod -els for a marine top predator, the harbour porpoise, in a dynamic environment. Ecosphere, 7(6), e013

Hague, E.L., Sinclair, R.R., & Sparling, C.E. 2020. Regional baselines for marine mammal knowledge across the North Sea and Atlantic areas of Scottish waters. Scottish Marine and Freshwater Science, 11(12).

Hamer, K.C., Phillips, R.A., Wanless, S., Harris, M.P., & Wood, A.G. 2000. Foraging ranges, diets and feeding locations of gannets Morus bassanus in the North Sea: evidence from satellite telemetry. Marine Ecology Progress Series, 200, 257-264.

Hammond, P.S., Berggren, P., Benke, H., Borchers, D.L. Collet, A, Heide-Jørgensen, M. P., Heimlich, S., Hiby, A.R., Leopold, M.F., & Øien, N. 2002. Abundance of harbour porpoise and other cetaceans in the North Sea and adjacent waters. Journal of Applied Ecology, 39, 361-376.

Hammond, P.S., Lacey, C., Gilles, A., Viquerat, S., Börjesson, P., Herr, H., Macleod, K., Ridoux, V., Santos, M.B., Scheidat, M., Teilmann, J., Vingada, J., & Øien, N. 2021. Estimates of cetacean abundance in European Atlantic waters in summer 2016 from the SCANS-III aerial and shipboard surveys - revised June 2021. https://synergy.st-andrews.ac.uk/scans3/files/2017/05/SCANS-III-design-based-estimates-2017-05-12-final-revised.pdf

Hammond, P.S., Macleod, K., Berggren, P., Borchers, D.L., Burt, M.L., Cañadas, A., Desportes, G., Donovan, G.P., Gilles, A., Gillespie, D. et al. 2013. Cetacean

abundance and distribution in European Atlantic shelf waters to inform conservation and management. Biological Conservation, 164, 107-122.

Hansen, R.G. & Heide-Jørgensen, M.P. 2013. Spatial trends in abundance of long-finned pilot whales, white-beaked dolphins and harbour porpoises in West Greenland. Marine Biology, 160, 2929–2941.

Harris, M.P. & Wanless, S. 2012. The Puffin. T. & A.D. Poyser, London.

Hedley, S.L. 2000. Modelling Heterogeneity in Cetacean Surveys. Ph.D Thesis, University of St Andrews.

Hedley, S.L. & Buckland, S.T. 2004. Spatial Models for line transect sampling. Journal of Agricultural, Biological and Environmental Statistics, 9, 181-199.

Hedley, S.L., Buckland, S.T., & Borchers. D.L. 2004. Spatial distance sampling models. In: Buckland, S.T., D.R. Anderson, D.R. Burnham, K.P. Laake, D.L. Borchers & L. Thomas (eds). Advanced Distance Sampling. Oxford: Oxford University Press, pp. 48-70.

Isojunno, S., Matthiopoulos, J., & Evans, P.G.H. 2012. Harbour porpoise habitat preferences: Robust spatio-temporal inferences from opportunistic data. Marine Ecology Progress Series, 448, 155-170.

Johnston, A., Thaxter, C.B., Austin, G.E., Cook, A.S.C.P., Humphreys, E.M., Still, D.A., Mackay, A., Irvine, R., Webb, A., & Burton, N.H.K. 2015. Modelling the abundance and distribution of marine birds accounting for uncertain species identification. Journal of Applied Ecology, 52, 150-160.

Joyce, G.G., Øien, N., Calambokidis, J., & Cubbage, J. C. 1989. Surfacing Rates of Minke Whales in Norwegian waters. Report of the International Whaling Commission 39, 431 – 434.

JNCC. 2016. Seabird Oil Sensitivity Index. https://hub.jncc.gov.uk/assets/b2925741-a119-4b65-aec7-515df973c93b

JNCC. 2021. Seabird Monitoring Programme Report 1986-2019. https://jncc.gov.uk/our-work/smp-report-1986-2019/

Johnston, D.W., Westgate, A.J., & Read, A.J. 2005. Effects of fine-scale oceanographic features on the distribution and movements of harbour porpoises Phocoena phocoena in the Bay of Fundy. Marine Ecology Progress Series, 295: 279–293. http://www.int-res.com/abstracts/meps/v295/p279-293/.

Jones, A.R., Hosegood, P., Wynn, R.B., De Boer, M.N., Butler-Cowdry, S., & Embling, C. B. 2014. Fine-scale hydrodynamics influence the spatio-temporal distribution of harbour porpoises at a coastal hotspot. Progress in Oceanography, 128, 30–48. http://www.sciencedirect.com/science/article/pii/S0079661114001256.

Kober, K., Webb, A., Win, I., Lewis, M., O'Brien, S., Wilson, L.J., & Reid, J.B. 2010. An analysis of the numbers and distribution of seabirds within the British Fishery Limit aimed at identifying areas that qualify as possible marine SPAs. JNCC report No. 431. 83pp.

Lambert, E., MacLeod, C.D., Hall, K., Brereton, T., Dunn, T.E., Wall, D., Jepson, P.D., Deaville, R. and Pierce, G.J. 2011. Quantifying likely cetacean range shifts in

response to global climate change: implications for conservation strategies in a changing world. Endangered Species Research, 15, 205-222.

Lloyd, C.S., Tasker, M.L., & Partridge, K. 1991. The status of seabirds in Britain and Ireland. T. & A.D. Poyser, Calton.

Lockyer, C. 1995. Investigations of aspects of the life history of the harbour porpoise, Phocoena phocoena, in British waters. Report of the International Whaling Commission, (Special Issue 14), 189-197.

Lockyer, C. & Morris, R. 1986. The history and behaviour of a wild sociable bottlenose dolphin (Tursiops truncatus) off the north coast of Cornwall. Aquatic Mammals 13(1), 3–16.

Lockyer, C. & Morris, R. 1987. Observation on Diving Behaviour and Swimming Speeds in a Wild Juvenile Tursiops truncatus. Aquatic Mammals 13, 31–35.

Marubini, F., Gimona, A., Evans, P.G.H., Wright, P.J., & Pierce, G.J. 2009. Habitat preferences and interannual variability in occurrence of the harbour porpoise Phocoena phocoena in the north-west of Scotland. Marine Ecology Progress Series, 381: 297-310.

Miller, D.L.; Burt, M.L.; Rexstad, A.E.; Thomas, L. Spatial models for distance sampling data: Recent developments and future directions. Methods Ecol. Evol. 2013, 4, 1001–101

Mitchell, I., Daunt, F., Frederiksen, M., & Wade, K. 2020. Impacts of climate change on seabirds, relevant to the coastal and marine environment around the UK. In: MCCIP science review 2020. Lowestoft, Marine Climate Change Impacts Partnership, 382-399. http://nora.nerc.ac.uk/id/eprint/527055/

Mitchell, P.I., Newton, S.F., Ratcliffe, N., & Dunn, T.E. 2004. Seabird Populations of Britain and Ireland. T. & A.D. Poyser, London. 511pp.

Murphy, S., Pinn, E.H., & Jepson, P.D. 2013. The short-beaked common dolphin (Delphinus delphis) in the north-eastern Atlantic: distribution, ecology, management and conservation status. Oceanography and Marine Biology: An Annual Review, 51, 193-280.

Murray, S. & Wanless, S. 1997. The status of the gannet in Scotland in 1994-1995. Scottish Birds, 19, 10-27.

Murray, S., Harris, M.P., & Wanless, S. 2015. The status of the gannet in Scotland in 2013-14. Scottish Birds, 35, 3-18.

Nielsen, N.H., Teilmann, J., Sveegaard, S., Hansen, R.G., Sinding, M.H.S., Dietz, R., & Heide-Jørgensen, M.P., 2018. Oceanic movements, site fidelity and deep diving in harbour porpoises from Greenland show limited similarities to animals from the North Sea. Marine Ecology Progress Series 597, 259-272.

Northridge, S., Tasker, M.L., Webb, A., & Williams, J.M. 1995. Seasonal distribution and relative abundance of harbour porpoises Phocoena phocoena (L.), white-beaked dolphins Lagenorhynchus albirostris (Gray) and minke whales Balaenoptera acutorostrata (Lacepède) in the waters around the British Isles. ICES Journal of Marine Science, 52, 55-66.

Paxton, C.G.M., Scott-Hayward, L.A.S., & Rexstad, E. 2014. Statistical approaches to aid the identification of Marine Protected Areas for minke whale, Risso's dolphin, white-beaked dolphin and basking shark. Scottish Natural Heritage Commissioned Report No. 594.

Paxton, C.G.M., Scott-Hayward, L., Mackenzie, M., Rexstad, E., & Thomas, L. 2016 Revised Phase III Data Analysis of Joint Cetacean Protocol Data Resource. JNCC Report No. 517, JNCC, Peterborough, ISSN 0963-8091.

Pierpoint, C. 2008. Harbour porpoise (Phocoena phocoena) foraging strategy at a high energy, near-shore site in south-west Wales, UK. Journal of the Marine Biological Association UK, 88, 1167–1173.

Pollock, C.M., Mavor, R., Weir, C.R., Reid, A., White, R.W., Tasker, M.L., Webb, A., & Reid, J.B. 2000. The distribution of seabirds and marine mammals in the Atlantic Frontier, north and west of Scotland. Joint Nature Conservation Committee, Aberdeen.

Potiek, A., N. Vanermen, N, Middelveld, R.P., de Jong, J., Stienen, E.W.M., & Fijn, R.C. 2019. Spatial and temporal distribution of different age classes of seabirds in the North Sea. Analysis of ESAS database. Bureau Waardenburg report 19-129. Bureau Waardenburg, Culemborg.

R Core Team. 2021. R: A Language and Environment for Statistical Computing. R Foundation for Statistical Computing, Vienna, Austria. URL: https://www.R-project.org/.

Reid, J.B., Evans, P.G.H. & Northridge, S.P. 2003. Atlas of Cetacean Distribution in North-west European Waters. Joint Nature Conservation Committee, Peterborough. 76pp.

Risch, D., Castellote, M., Clark, C. W., Davis, G.E., Dugan, P.J., Hodge, L.E.W., Kumar, A., Lucke, K., Mellinger, D.K., Nieukirk, S.L., Popescu, C.M., Ramp, C., Read, A.J., Rice, A.N., Silva, M.A., Siebert, U., Stafford, K.M., Verdaat, H., & Van Parijs, S.M. 2014. Seasonal migrations of North Atlantic minke whales: novel insights from large-scale passive acoustic monitoring networks. Movement Ecology 2, 24. http://www.movementecologyjournal.com/content/2/1/24

Robinson, K.P., Tetley, M.J., & Mitchelson-Jacob, E.G., 2009. The distribution and habitat preference of coastally occurring minke whales (Balaenoptera acutorostrata) in the outer southern Moray Firth, northeast Scotland. Journal of Coastal Conservation, 13(1), 39-48.

Scott, B.E., Sharples, J., Ross, O.N., Wang, J., Pierce, G.J., & Camphuysen, C.J. 2010. Sub-surface hotspots in shallow seas: fine-scale limited locations of top predator foraging habitat indicated by tidal mixing and sub-surface chlorophyll. Marine Ecology Progress Series, 408, 207-222.

Searle, K.R., Mobbs, D.C., Waggitt, J., Evans, P.G.H., Bogdanova, M., Jones, E., Bolton, M., Wilson, L., Cleasby, I., Cook, A., Thaxter, C., Donovan, C., Caneco, B., Matthiopoulos, J., Daunt, F. & A Butler, A. Further development of the seabird sensitivity mapping tool. Report to Offshore Renewables Joint Industry Programme (ORJIP) for Offshore Wind. In prep.

Searle, K.R., Waggitt, J.J., Evans. P.G.H., Bogdanova, M., Daunt, F., & Butler, A. 2022. Study to examine the impact of climate change on seabird species off the east coast of Scotland and potential implications for environmental assessments. Scottish Government. 79pp. https://www.gov.scot/publications/study-examine-impact-climate-change-seabird-species-east-coast-scotland-potential-implications-environmental-assessments/

Shoji, A., Elliott, K., Fayet, A., Boyle, D., Perrins, C., & Guilford, T. 2015. Foraging behaviour of sympatric razorbills and guillemots. Marine Ecology Progress Series, 520, 257-267.

Solvang, H.K., Skaug, H.J., & Øien, N. 2015. Abundance estimates of common minke whales in the Northeast Atlantic based on survey data collected over the period 2008 and 2013. IWC SC/66a/RMP/8. 10pp.

Stone, C.J., Webb, A., Barton, C., Ratcliffe, N., Reed, T.C., Tasker, M.L., Camphuysen, C.J. & Pienkowski, M.W. 1995. An atlas of seabird distribution in north-west European waters, JNCC, Peterborough, ISBN 1 873701 94 2. https://hub.jncc.gov.uk/assets/c132752f-827c-41fc-b617-e681db21eaf5

Tasker, M.L., Webb, A., Hall, A.J., Pienkowski, M.W., & Langslow, D.R. 1987. Seabirds in the North Sea. Nature Conservancy Council, Peterborough.

Tetley, M.J., Mitchelson-Jacob, E.G. & Robinson, K.P. 2008. The summer distribution of coastal minke whales (Balaenoptera acutorostrata) in the southern outer Moray Firth, NE Scotland, in relation to co-occurring mesoscale oceanographic features. Remote Sensing of Environment, 112(8), 3449-3454.

Teilmann, J., Christiansen, C.T., Kjellerup, S., Dietz, R. and Nachman, G. (2013), Geographic, seasonal, and diurnal surface behavior of harbor porpoises. Mar Mam Sci, 29: E60-E76. https://doi.org/10.1111/j.1748-7692.2012.00597.x

Thaxter, C.B. & Burton, N.H.K. 2009. High Definition Imagery for Surveying Seabirds and Marine Mammals: A Review of Recent Trials and Development of Protocols. British Trust for Ornithology Report Commissioned by Cowrie Ltd. 40pp.

Thaxter, C.B., Wanless, S. Daunt, F., Harris, M.P., Benvenuti, S., Watanuki, Y., Gremillet, D., & Hamer, K.C. 2010. Influence of wing loading on the trade-off between pursuit-diving and flight in common guillemots and razorbills. Journal of Experimental Biology, 213,1018-1025.

Thaxter CB, Lascelles B, Sugar K, Cook ASCP, Roos S, Bolton M, Langston RHW, Burton NHK. 2012. Seabird foraging ranges as a preliminarytool for identifying candidate Marine Protected Areas. Biological Conservation156:53–61

Waggitt, J.J., Evans, P.G.H. Andrade, J. Banks, A.N. Boisseau, O. Bolton, M., Bradbury, G. Brereton, T., Camphuysen, C.J., Durinck, J. Felce, T., Fijn, R.C. Garcia-Baron,I., Garthe, S., Geelhoed, S.C.V. Gilles, A. Goodall, M. Haelters, J., Hamilton, S. Hartny-Mills, L. Hodgins, N. James, K. Jessopp, M. Kavanagh, A.S., Leopold, M. Lohrengel, K. Louzao, M. Markones, N. Martinez-Cediera, J. O'Cadhla, O., Perry,S. L. Pierce, G. J. V. Ridoux, V. Robinson, K. P.Santos, M.B., Saavedra, C., Skov, H. Stienen, W. M., Sveegaard, S., Thompson P., Vanermen, N., Wall, D., Webb, A., Wilson, J. Wanless, S., & Hiddink, J. G. 2020. Distribution maps of

cetacean and seabird populations in the North-East Atlantic. Journal of Applied Ecology, 57, 253 -269.

Wakefield, E.D., Owen E., Baer, J., Carroll, M.J., Daunt, F., Dodd, S.G., Green, J.A., Guilford, T., Mavor, R.A., Miller, P.I., Newell, M.A., Newton, S.F., Robertson, G.S., Shoji, A., Soanes, L.M., Votier, S.C., Wanless, S., & Bolton, M. 2017. Breeding density, fine-scale tracking, and large-scale modelling reveal the regional distribution of four seabird species. Ecological Applications, 27(7), 2074-2091.

Wood, S. 2017. Generalized Additive Models. Chapman & Hall. London.

Zydelis, R., Dorsch, M., Heinänen, S., Nehls, G., & Weiss, F. 2019. Comparison of digital video surveys with visual aerial surveys for bird monitoring at sea. Journal of Ornithology, 160, 567-580.

9. APPENDIX 1. Review of sample images used by APEM for marine mammal and seabird identification from digital aerial surveys off East Scotland

9.1 Background

The aim of this exercise was to review a selection of digital images to check species identifications. The motivation for this was as a validation procedure for species occurring out of their normal range / habitat, and to better understand the reasons why there was large variation in the proportions of sightings ascribed to species (e.g. harbour porpoise) vs species group (porpoise/dolphin). Taking that example, the first two aerial surveys had no porpoises recorded but 51 and 13 porpoise/dolphin species groups respectively. Although there were several instances where we would recommend a change in ID, we did no updates for the analysis. This would have necessitated a complete new evaluation involving going through many thousands of images.

9.2 Results

Species out of normal habitat Three cases were examined: 1) a black guillemot recorded far offshore in the northern North Sea on 6 Mar 2021 (@12:21). This species is normally very coastal; 2) a red-throated diver also recorded far offshore on 17 Sep 2020 and 3) a red-throated diver recorded far offshore on 29 Oct 2020. This species tends to occupy shallow waters, estuaries and bays. In all three cases, the species identification could be correct although we would have been more cautious for the latter two, and assigned them as diver sp. we checked also black guillemot images from more coastal areas, and agreed that they were of this species.

Species out of normal range Images identified as common dolphin were examined for 4 Mar 2020, 14 Apr 2020, 2 Jun 2020 (multiple sightings), 8 Jun 2020, and 24 Jun 2020. This species is rare in the North Sea but occasionally enters the northern

sector (presumably from the Atlantic – it occurs regularly in the Hebrides). Images from each of those surveys were examined. Very few images were unambiguously common dolphin, but most were probably so. Of 22 images, we agreed with ten, disagreed with three, and were uncertain for nine.

Another species that is rare in the North Sea (south of Caithness) is the Risso's dolphin. There was one record of five animals some distance offshore due east of the Firth of Forth on 2 June 2020. On checking, we confirmed these as Risso's dolphins.

White-beaked Dolphin vs Atlantic White-sided Dolphin The main dolphin species inhabiting the North Sea, particularly offshore, is the white-beaked dolphin. However, in northern Scotland (Caithness to the Northern Isles), in recent years white-beaked dolphins have become scarce and the main dolphin species recorded there is Atlantic white-sided dolphin. In the APEM data set, no Atlantic white-sided dolphins are recorded. These two species can be confused although they should be easier from the air due to the conspicuous white area over the back behind the dorsal fin in the white-beaked dolphin. Atlantic white-sided dolphins tend to occur in large groups (numbering 25 to a few hundred) whereas white-beaked dolphin average group size is <10. Checking the larger groups recorded as white-beaked dolphins, all images were confirmed as that species, and no definite white-sided dolphins were identified.

Harbour Porpoise vs Porpoise/Dolphin There are thousands of images in one or other of these two categories. We therefore concentrated upon one of the first two surveys, on 2 June 2020. A total of 242 images assigned to Porpoise/Dolphin were reviewed. Of those, two images were identified as white-beaked dolphins, 122 were classified as harbour porpoise, and 118 were of indeterminate species. Condition of light and sea state were no worse on those two first surveys compared with subsequent ones, suggesting that perhaps the person going through the images had not yet got their eye in to differentiating porpoises (NB they have a characteristic body shape: blunt head, rotund body tapering to a narrow tail stock but relatively wide tail fluke). When animals are below a certain depth in the water or visibility underwater is poor, it is not possible to be confident in determining body shape because it becomes distorted. This will always account for a proportion of animals. It is quite likely that the great majority of the 118 images unassigned to species, were in fact porpoises but we cannot be sure.

Other species Some random checks were made on other species / species groups (e.g. minke whale, whale sp., marine mammal sp., small gull sp., razorbill/guillemot, razorbill, guillemot). There were no cases where there was disagreement on the identification but there were some which would be better downgraded to a species group. For other species, there were none from within a species group that could confidently be assigned to a species. Some of the whale sp. looked as if they were minke whales and one appeared to be a possible fin whale but without knowing the sizes, it was impossible to confirm.

9.3 Conclusions

There was general agreement over the species identification assigned to the images reviewed. In some cases, however, more caution would have been applied leading to downgrading of species ID. On the other hand, for porpoise/dolphin, one could more confidently separate porpoises, at least for the early surveys and probably to a lesser extent for all surveys. Clearly, this project could not go through everything again in that latter category, re-assign those, and re-calculate numbers and densities. One option might be to consider all porpoises/dolphins as porpoises and use that as the upper bound for estimates since the great majority of encounters will be of that species.

This publication is available at **www.gov.scot**

Any enquiries regarding this publication should be sent to us at

The Scottish Government
St Andrew's House
Edinburgh
EH1 3DG

ISBN: 978-1-80435-938-9 (web only)

Published by The Scottish Government, November 2022

Produced for The Scottish Government by APS Group Scotland, 21 Tennant Street, Edinburgh EH6 5NA
PPDAS1154482 (11/22)

w w w . g o v . s c o t